Mechanisms of 3-Dimensional Organisation of the Human Genome

Susan Gilchrist

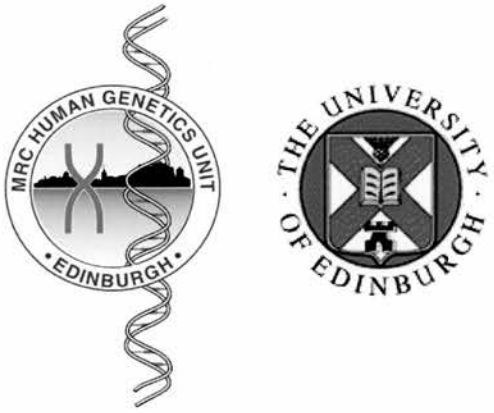

PhD
University of Edinburgh
2003

DECLARATION

I declare that this thesis has been composed by me, and all of the work is my own unless stated otherwise.

Susan Gilchrist
October 2003

'Seididh gaoth is dearrsaidh grian,
Tro mheas nan craobhan, lin gu lin,
Ach thig an la is thig an t-am,
Airson an ubhal as airde
Air a' chraobh a bhuain.'

- R and C MacDonald.

For Dylan.

ACKNOWLEDGEMENTS

First thanks go to Wendy as without her fascination for all things nuclear this PhD thesis would not be here. I'm forever grateful for being introduced to the wonderful world of chromosomes and nuclei, who'd have thought anything so small could be so exquisitely complicated?

Shelagh and Paul ('PP') have been indispensable. Not only for fixing all the expensive imaging equipment and processing software when I'd pushed one button too many, but also for their daily chat, numerous car trips (home-relocation and otherwise) and tea-making abilities. Without Paul's analysis scripts and Shelagh's experimental guidance very little of this data here would be here to discuss.

Nick ('The Boy') and Heidi ('Heid the Ba') have continuously provided me with protocols and are fountains of scientific information and humorous chat. Huge thanks also goes to the previous members of the lab for their help and friendship; Nic ('The Girl'), Muriel ('Mad Old Bag') Lee, Graham ('Dellaire, PhD') and Jonathan ('Show Us Your Belly'). I can't forget the current Bickmore lab members who have shared some of my time at the MRC - Steph, Severine, Elodie, Inga and Anne. The Bickmore lab members past and present have unrivalled culinary abilities and renowned partying skills.

There are more HGU colleagues that should be acknowledged. Thanks to Mary 'T' for her vast scientific knowledge, friendly banter and generally keeping all the trouble-makers in line. Jeremy (and Severine too!) rarely have days in the lab when there isn't a smile or a joke to share with you and its appreciated. Sandy and Douglas in photography have shared many jokes and Freehand secrets in the past few months, and let's not forget all the posters I've had made too, thanks guys! Andrew Carruthers helped me a lot with the statistics and gave another side to every analysis.

My good friends Gill, Steph, Jane and Kate have kept me sane. Steph, Gill (and Sapna) and Kate have even saved me from homelessness! We've had a whole lot of laughs, indulgent dinners, the odd gin and bit of dancing along the way.

I doubt I could have got this far without Nathan ('Geek Boy'). In these past years, I've been introduced to camping, car rallying and Winchester Cathedral. He also deserves a special mention for his encouragement, entertainment, interested-in-science questions, and of course my computing facilities!

Last, but no means least, thanks to my family. My parents have encouraged and supported me throughout my academic life. Without their food parcels and sly fivers, I would have been forced to get a proper job ages ago! My brother, David, didn't quite understand the appeal of another four years as an impoverished student and will forever think of me as the mad scientist. Mad? Who, me?

ABSTRACT

In many ways the (near) complete human genome sequence is only the beginning. We have still much to learn of the packaging and spatial organisation of nearly 2 metres of DNA within each cell nucleus. In recent years we have become increasingly aware that many important cellular factors are compartmentalised within the nucleus, and this is also true of chromatin.

The nuclear position of chromosome territories can be correlated to the DNA sequence – the overall gene density. Previous work has shown that chromosomes have a radial arrangement, gene-poor chromosomes are situated at or near the nuclear periphery, while more gene-rich chromosomes are in the centre of the nucleus at least in lymphoblast and fibroblast cells. It was not known if this pattern of chromosome territory organisation is particular to these cells and hence, I have investigated the nuclear distribution of chromosomes in a variety of different primary and transformed cell lines. I have also performed FISH and chromosome position analysis on histological tissue sections. The data suggest that the nuclear organisation in cultured cells reflects that of the nuclei in human somatic cells *in vivo*.

It is possible that chromatin composition, especially histone modifications, is involved in the maintenance of chromosome spatial organisation. Using chemical inhibition of histone deacetylation with the drug Trichostatin-A (TSA), endogenous levels of histone acetylation in the nucleus were disrupted. I have then analysed the position of centromeres and chromosomes in cells treated with TSA. I found no detectable rearrangement of chromatin under these conditions. This suggests that histone acetylation does not play a vital role in influencing the spatial organisation of chromatin.

Many nuclear membrane and lamina components have chromatin binding domains and are capable of binding chromatin and/or associated proteins *in vitro*. Interest in the nuclear lamina and a role in spatial organisation of chromatin has recently increased with the discovery of human 'laminopathies', syndromes caused by mutations in lamin A or emerin. Experiments have shown that the spatial organisation of chromosomes is not altered in lymphoblast cells that carry a null mutation of emerin. I have generated stable cell lines over-expressing disease-associated mutations of lamin A protein. Some peripheral chromosomes are no longer present at the nuclear periphery in cells over-expressing lamin A. I also followed the interphase dynamics of different lamin A disease-associated mutants and some mutant proteins are more mobile than the wild-type lamin A in FRAP studies.

Many different cells types of the human body arrange the genome in a radial fashion, including lymphoblasts and fibroblasts. My observations would suggest that chromatin composition, specifically core histone acetylation, is not the most influential factor on this radial arrangement in fibroblasts; what is perhaps more significant is the relative levels of nuclear lamina components.

CONTENTS PAGE

LIST OF FIGURES PAGE

CHAPTER 1

CHAPTER 3

CHAPTER4

Chapter 5

LIST OF TABLES PAGE

LIST OF TEXT BOXES PAGE

ABBREVIATIONS

2-D	Two-dimensional
3-D	Three-dimensional
A	adenine (purine)
(AD/X)EDMD	(Autosomal dominant/X-linked) Emery-Dreifus Muscular Dystrophy
Arabidopsis	Arabidopsis thaliana
ATP	adenosine triphosphate
ATRX	α-thalassemia/mental retardation syndrome, X-linked
BRCA-1	breast cancer associated gene-1
BrdU	5-bromo-2-deoxyuridine
BSA	bovine serum albumin
C	cytosine (pyrimidine)
CCD	charged couple device camera
CENP	centromere protein
CFP	
CFP	cyan fluorescent protein
CHO	chinese hamster ovary cells
Chromodomain	chromatin organiser modifier
CM	Cardiomyopathy
CpG	cytosine and guanine
CREST	calcinosis, Rayauds' phenomenon, esophageal dysmotility, sclerodactyly, telangiectasia
C-terminal	carboxy-terminal
DAPI	4,6-diamidino-2-phenylindole
dATP	deoxyadenosine triphosphate
dCTP	deoxycytosine triphosphate
dGTP	deoxyguanine triphosphate
DMEM	Dulbecco's modified Eagle's medium

DMSO	dimethyl sulphoxide
DNA	deoxyribonucleic acid
DNase	deoxyribonuclease
Dnmt	DNA methyltransferase
dNTP	deoxynucleoside triphosphate
Drosophila	*Drosophila melanogastor*
dTTP	deoxythymine triphosphate
dUTP	deoxyuridine triphosphate
EM	electron microscopy
ER	endoplasmic reticulum
FACS	flow-assisted cell sorting
FCS	fetal calf serum
FISH	fluorescence in situ hybridisation
FITC	fluorescein isothiocyanate fluorochrome
FLIP	fluorescence loss in photobleaching
FPLD	Dunnigan-type Familial Lipodystrophy
FRAP	fluorescence recovery after photobleaching
G	guanine (purine)
g	gravities
G1	growth phase 1 of the cell cycle (pre-replication)
G2	growth phase 2 of the cell cycle (post-replication)
G-band	chromosome pattern produced by Giemsa staining
GC	guanine and cytosine
GFP	green fluorescent protein
(Phospho) H3-S10	(phosphorylated) histone H3 serine 10
HAT	histone acetyltransferase
HCl	hydrochloric acid
HDAC	histone deacetylase
HGPS	Hutchinson-Gilford Progeria Syndrome

HMT	histone methyltransferase
HP1	heterochromatin protein
HSA	human autosome
ICD	interchromatin domain
ICF	immundeficiency-centromeric instability-facial anomalies syndrome
IF	immunofluorescence
INM	inner nuclear membrane
ISWI	imitation switch
K	lysine
(Ac)K5-H4	(acetylated) lysine 5 histone H4
(Ac)K9-H3	(acetylated) lysine 9 histone H3
kb	kilobase pairs of DNA
KCl	potassium chloride
kDa	kilo Daltons (molecular weight/10^3)
L	leucine
LacI	lactose inducer
LacO	lactose operator
LBR	Lamin B receptor
LCR	locus control region
LEM	LAP, Emerin, MAN
LGMD	Limb Girdle Muscular Dystrophy
LM	light microscopy
M	molar
MAA	methanol, acetic acid
MAD	Mandibuloacral Dysplasia
Mb	megabase pairs of DNA
MBD	methyl binding domain
MeCP	methyl binding protein
Met_2/Met_3K9-H3	dimethyl/trimethyl lysine 9 histone H3
mRNA	messenger RNA

N	asparagine
NaCl	sodium chloride
NOR	nuclear organising regions
NPC	nuclear pore complex
N-terminal	amino-terminal
OD	optical density
p	chromosome short arm
P	proline
PAGE	polyacrylamide gel electrophoresis
PBS	phosphate buffered saline
PcG	polycomb group
PCNA	proliferating cell nuclear antigen
PCR	polymerase chain reaction
PEV	position effect variation
pFa	paraformaldehyde
pFa	paraformaldehyde
PML	promyelocytic leukaemia
q	chromosome long arm
R	arginine
R-band	chromosome pattern produced by reverse Giemsa staining
rDNA	rRNA encoding DNA
RNA	ribonucleic acid
RNase	ribonuclease
ROI	region of interest
rRNA	ribosomal RNA
S	serine
S.cerevisiae	Saccaromyces cerevisiae
S.Pombe	Schizosaccharomyces pombe
S/MAR	scaffold/matrix attachment region
SAGA	spt-Ada-Gcn5 acetyltransferase
SAHA	suberoylanilide hydroxamic acid

SDS	sodium dodecyl sulphate
SEM	standard error of the mean
SMC	structural maintenance of chromosomes
S-phase	synthesis phase of the cell cycle
SSC	standard saline citrate (1x: 150mM NaCl, 15mM tri-Na citrate, pH 7.4)
SWI/SNF	mating type switching/sucrose non-fermenting
T	thymine (pyrimidine)
t½	half-life
TAE	Tris, EDTA acetic acid buffer (1x: 90mM Tris-HCl, 90mM glacial acetic acid, 2mM EDTA pH8.0)
T-band	Telomeric band (extreme form of R band)
TE	Tris, EDTA buffer (10mM Tris, 1mM EDTA, pH8.0)
TEM	transmission electron microscopy
TF	transcription factors
Topo-II	topoisomerase-II
trxG	trithorax group
TSA	trichostatin-A
UV	ultraviolet
W	tryptophan
Xenopus	Xenopus laevis
Xi	inactive X
YFP	yellow fluorescent protein

CHAPTER 1

INTRODUCTION

The complete linear sequence of human DNA is a powerful resource for researchers across the world, but we still understand very little of the contextual relevance of the nucleotide combinations. The linear DNA sequence is central to the functional macromolecular units of inheritance, the chromosomes. In humans, the genome consists of approximately 6.6 x 10^9 base pairs of DNA unequally divided into 46 chromosomes (Figure 1.1). It is still unclear which mechanisms are responsible for packaging the 2 metres of DNA into each cell nucleus, 5-15 microns in diameter.

In the early 1970s it was shown that RNA polymerases do not actively transcribe naked DNA and hence, the biologically active form of DNA was not the naked molecule itself, but a nucleoprotein complex, chromatin (Parker and Roeder, 1977; Jaehning and Roeder, 1977). Through hierarchical stages of DNA-protein and protein-protein interactions the linear DNA molecule is twisted and condensed into the chromatin fibre. The structure and composition of the chromatin fibre, in concert with many transcription factors, is linked to the orchestrated expression of ~23, 000 protein-encoding genes of the human genome (Ensembl Release 16.33.1, July 2003).

This introduction summarises what is currently known of the mechanisms of chromatin packaging and the interphase organisation of the genome. I will also explore the existing evidence for the mechanisms mediating the condensation and compartmentalisation of the genome.

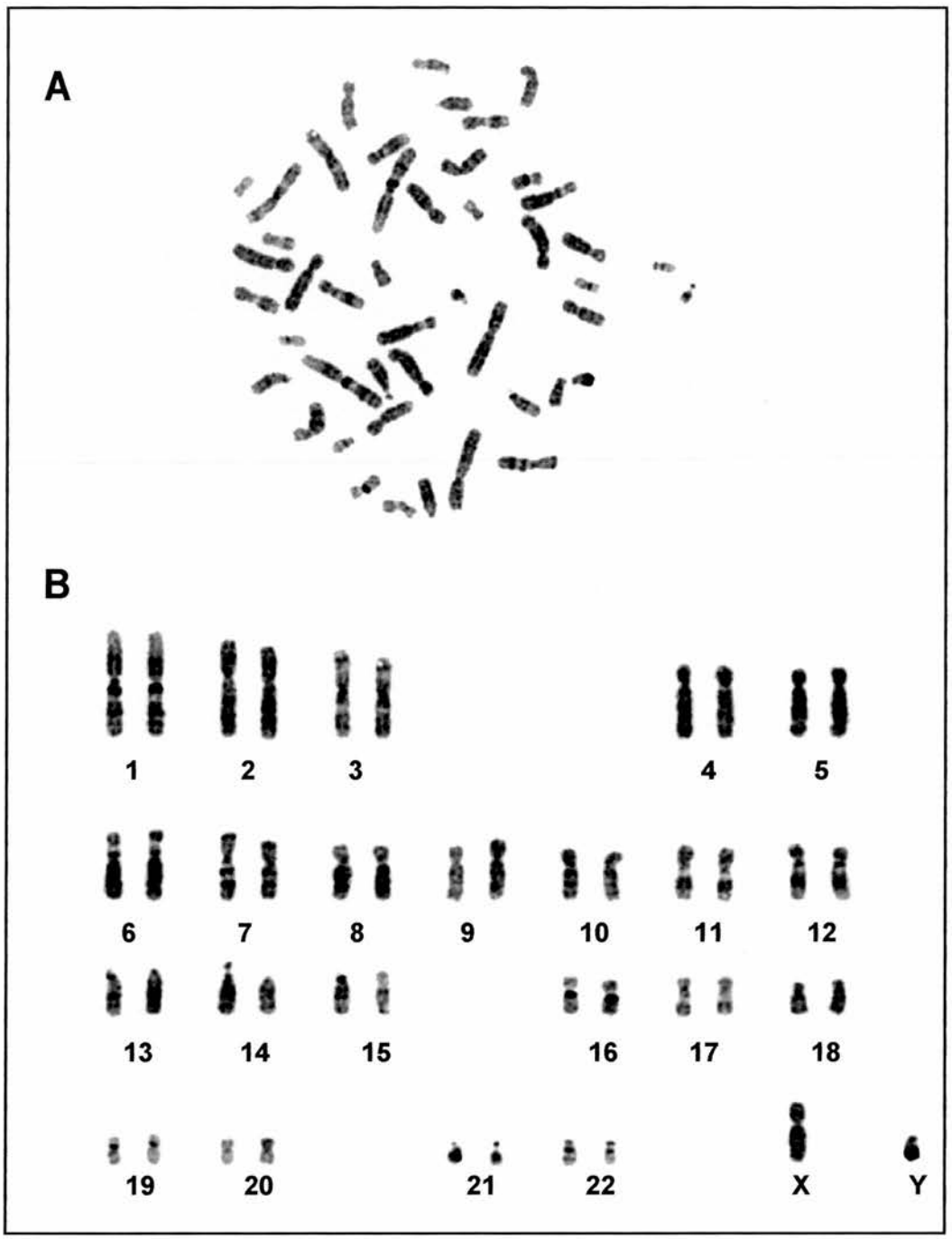

Figure 1.1 The human chromosome complement.
Metaphase chromosome spread of 3:1 MAA fixed chromosomes from a male human lymphocyte stained with DAPI (**A,** negative image). Karyotype analysis of the metaphase chromosome spread (**B**).
Image from S. Boyle.

1.1 CHROMATIN STRUCTURE

Chromatin is composed of positively-charged histone and non-histone proteins binding negatively charged DNA. The basis of chromatin architecture which is responsible for the first level of DNA packaging is the nucleosome (Kornberg and Lorch, 1999). Each nucleosome consists of approximately 2 turns of the 146bp of the linear DNA molecule around a core histone octamer (2 molecules each of H2A, H2B, H3 and H4; reviewed in Belmont et al., 1999). All eukaryotes package their genome using histone proteins and the four core histones are among the most evolutionarily conserved proteins described (Wolffe, 1995).

Studies of interphase chromatin suggest that arrays of nucleosomes along a molecule of DNA are folded into a single fibre 30nm in diameter (see section 1.1.5; van Holde and Zlatanova, 1996). We are still gaining insight into the complexity of this chromatin condensation and the higher levels of condensation between the 30nm fibre and the metaphase chromosomes. Nucleosomes and chromatin fibres are not structurally inert, but undergo conformational change, and this is thought to contribute to transcriptional control. These changes can be related to modifications of chromatin structure evident at the level of both DNA and histones.

1.1.1 DNA methylation

CpG dinucleotides within the DNA duplexes can be modified at cytosine bases by the addition of a methyl group (Figure 1.2A). This modification has been shown to be involved in the control of gene expression and is essential for mammalian development (Okano et al., 1999). In the adult vertebrate genome, 60-90% of all CpG dinucleotides are methylated. The remaining non-methylated CpGs (~15% in humans) are predominately found within CpG islands. These genomic regions include functional promoters and are predominantly found in the early replicating (R-bands) of the genome (Craig and Bickmore, 1994).

DNA methylation is normally associated with gene silencing (Bird and Wolffe, 1999) and is involved in X-inactivation (see section 1.3.2) and genomic imprinting (Ng and Bird, 1999). Three DNA methyltransferases (DNMT1, -3a, and –3b) have been identified (Bestor, 2000; Okano et al., 1998); these enzymes catalyse the addition of methyl groups onto cytosine bases. Cytosine methylation marks can be copied after DNA replication and are hence considered an epigenetic mark that results in heritable changes to chromatin structures.

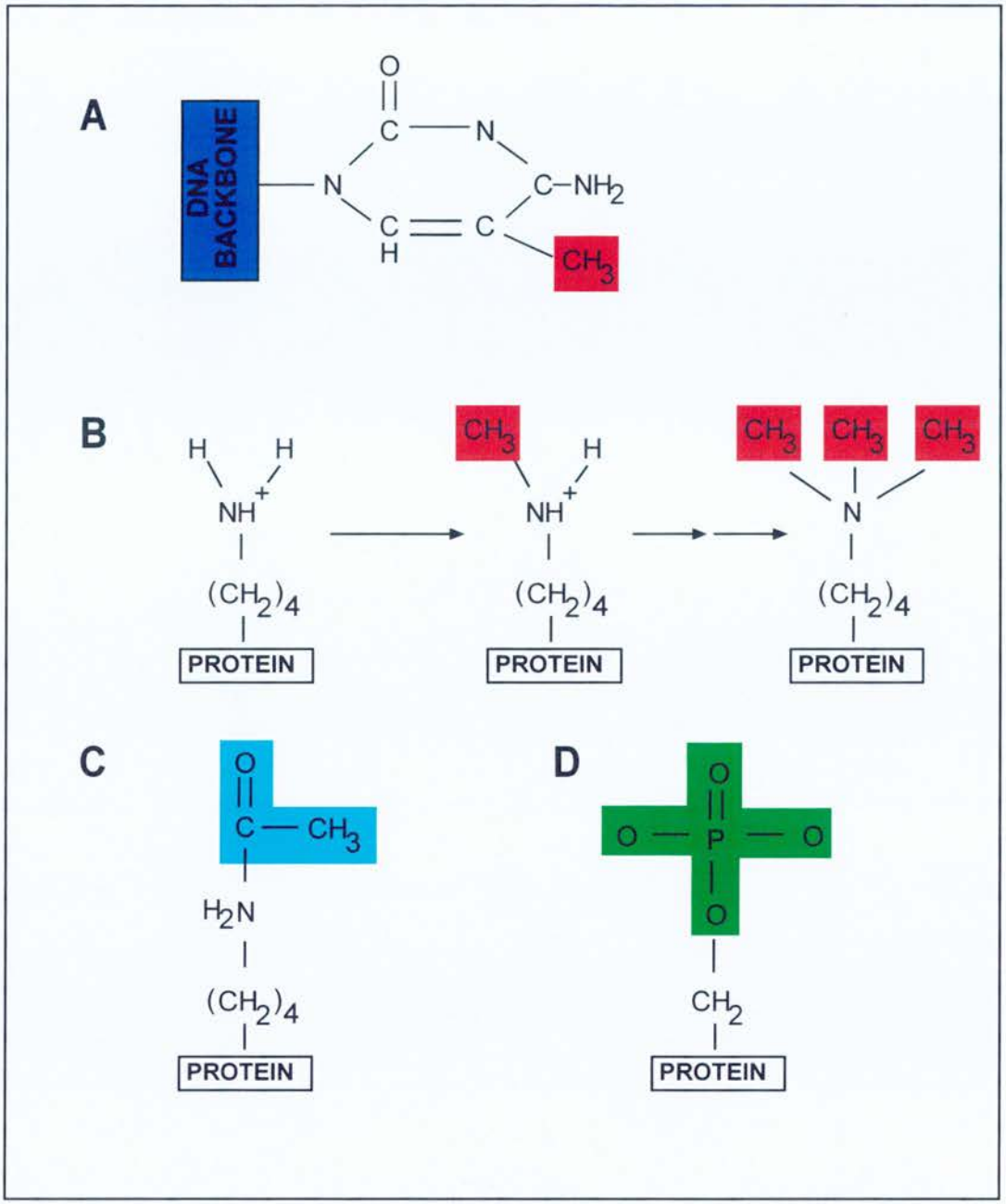

Figure 1.2 Chemical modifications of DNA and histones. The cytosine bases of DNA can be modified by the addition of a methyl group (red) and this reaction is catalysed by DNA methyltransferases (**A**). Lysine sidechains of histone proteins can be modified by methylation, this is catalysed by histone methyltransferase (HMT) activity. Unmodified lysine (left) can accept up to three methyl groups (red, right) becoming tri-methylated (**B**). Lysine sidechains can also be modified by the addition of an acetyl group (blue) by histone acetylases (HATs, **C**). Serine residues can be phosphorylated (green, **D**) and this is catalysed by serine/threonine kinases.

The direct molecular mechanisms by which DNA methylation might influence gene expression have yet to be determined. There are two main possible mechanisms, either DNA methylation can influence gene expression/genome packaging by directly modifying chromatin structures or, methylation could create binding sites for repressor proteins. Highly methylated DNA is transcriptionally inactive and is thought to have a more compact conformation which is evident as nuclease resistance (Antequera et al., 1989; Antequera et al., 1990). In addition, identification of the methyl CpG binding proteins MeCP1 and –2 suggests that methylated DNA recruits protein factors capable of repressing transcription, for example histone deacetylase enzymes (see section 1.1.3.1; Meehan et al., 1989; Meehan et al., 1992; Lewis et al., 1992). Experiments in model organisms closely link DNA methylation to histone modifications. In *Neurospora*, the H3-K9 histone methyltransferase (HMT) protein, dim-5, is required for DNA methylation (Tamaru and Selker, 2001). HMT activity is also involved in maintenance of DNA methylation in *Arabidopsis* through the enzymatic activity of protein KRYPTONITE (Jackson et al., 2002). This suggests a hierarchical relationship between chromatin/DNA modifications and gene expression.

A family of methyl-CpG binding proteins (including MeCP1 and –2) has been identified which are thought to mediate the biological consequences of DNA methylation (Hendrich and Bird, 1998). Each family member contains a methyl-binding domain (MBD). The founder member of this family, MeCP2, is a transcriptional repressor and can act remotely from a gene promoter. This protein recruits repression complexes containing histone deacetylases (see section 1.2.2.3; Jones et al., 1998; Nan et al., 1998) which subsequently inhibit gene expression by blocking initiation. As MeCP2 is mutated in Rett Syndrome (Hendrich and Bickmore, 2001) the correct interpretation of methyl-DNA signals appears significant to development.

1.1.2 Core histones

Histones are small (11-16kDa), positively-charged, lysine and arginine rich proteins that interact with the linear DNA molecule via non-covalent forces. In all eukaryotes H2A, H2B, H3 and H4 are the four subunits that interact to make the nucleosome and the crystal structure of the core nucleosome particle (146bp of DNA wrapped around a histone octamer; (Luger et al., 1997). All histones have a common protein structure of a charged amino (N-) terminus which contains the bulk of the lysine residues and an extended histone fold domain at the carboxy (C) terminus (Arents et al., 1991).

1.1.3 Core histone modifications

The chromatin fibre is dynamic; localised decondensation and remodelling is thought to influence the accessibility of the fibre to protein factors involved in transcription, replication and DNA repair. In the nucleus, the N-terminal tails of the core histone proteins are subject to post-translational modifications including acetylation, methylation and phosphorylation (Figure 1.2 and 1.3) while ubiquitination occurs mainly on C-terminal tails. These modifications are thought to influence the structure of the chromatin fibre by altering the electrostatic charge of the histones and/or through creating binding sites for non-histone chromatin-associated proteins, although the direct structural consequences of histone modifications and associated proteins are not well understood.

The discovery of histone tail modifications lead to the hypothesis that they may provide a basis for epigenetic marks for gene activity (Turner, 1998). This later lead to the proposal of the 'histone code hypothesis' which suggests combinations or sequences of histone modifications result in signalling specific downstream transcriptional events by recruiting transcriptional inducers or repressors (Strahl and Allis, 2000). Recently, Allis and co-workers have extended the histone code hypothesis to suggest that groups of particular histone tail modifications, rather than individual modifications, provide chromatin signals which permit gene expression and chromatin condensation (Fischle et al., 2003b). It is proposed that the most significant role for histone modifications in not alteration of nucleosome or chromatin structure directly but more that they permit or inhibit protein-protein interactions that in turn influence structure and hence DNA accessibility.

1.1.3.1 Histone acetylation

Acetylation of histone N-terminal tails has a major influence on chromatin structure and gene activity (Allfrey, 1964). Within the nucleus, several lysine residues of histone tails, particularly H3 and H4, can be acetylated (Figure 1.2C). There is a constant cellular turnover of histone acetylation, mediated by histone acetyltransferase enzymes (HATs) that add acetyl groups and histone deacetylases (HDACs) which remove them. During S phase, *de novo* synthesised histones H3 and H4 are acetylated and these acetylated histones are used to assemble nascent chromatin (Ruiz-Carrillo et al., 1975). Following their incorporation into newly synthesised chromatin, H3 and H4 molecules are rapidly deacetylated (Jackson et al., 1976).

The first protein described with histone acetyltransferase activity was Gcn5, identified as the catalytic subunit of two yeast HAT complexes Ada (Ada-containing HAT complex) and SAGA (Spt-Ada-Gcn5-acetyltransferase; (Brownell et al., 1996; Grant et al., 1997). Distinct HAT protein families have been described and there is a high degree of sequence similarity between members of each of the families (Kuo and Allis, 1998). HATs share two common protein domains, the acetyltransferase domain and bromodomain. Bromodomains are highly conserved protein domains of ~110 amino acids and these domains bind acetyl-lysine residues (Dhalluin et al., 1999; Marmorstein, 2001).

The overall level of histone tail acetylation within the cell is determined by an equilibrium between histone acetyltransferase and the deacetylase activity of histone deacetylases class I and II (Heinzel et al., 1997; Alland et al., 1997). There are at least 9 HDACs in humans, and HDACs 1, 2 and 3 being members of class I (homologous to Rpd3 of *S. cerevisiae*) while HDACs 4, 5 and 6 being class II members (homologous to Hda1 *S. cerevisiae;* (Leipe and Landsman, 1997; Fischle et al., 1999; Grozinger et al., 1999). When histone H4 has 3 or more acetylated lysine residues it is termed hyperacetylated, while this protein with one or two acetylated histones is termed hypoacetylated (Figure 1.3; Turner and Fellows, 1989; Zhang et al., 2002).

In general, high levels of acetylation correlate with transcriptional activity while decreased acetylation correlates with transcriptional repression. The first molecular link between transcription and histone acetylation was provided by the discovery of acetyltransferase activity of Gcn5, originally identified as a transcriptional regulator (Brownell et al., 1996). There is also a key role for acetylation in maintaining transcriptional repression of the inactive X chromosome of female cells (see section 1.3.2). Subsequently, many more transcriptional activators or repressors have been linked to HAT or HDAC activity respectively (Marmorstein, 2001). Recently, the acetylation pattern for specific histone tails and their relation to gene activity has been described for the mouse β–globin gene (Bulger et al., 2003) and references therein), mouse insulin gene (Chakrabarti et al., 2003) and the human interferon-beta gene (IFN-β; (Agalioti et al., 2002).

Following the identification of the first yeast HAT, Gcn5, several human HATs have been described, including p300/CBP, TAF250 and the Gcn5 homologue, PCAF,. These proteins appear to act locally at gene promoters and are components of multi-subunit complexes, which modulate transcription on a gene-by-gene basis. Bromodomains target HATs and

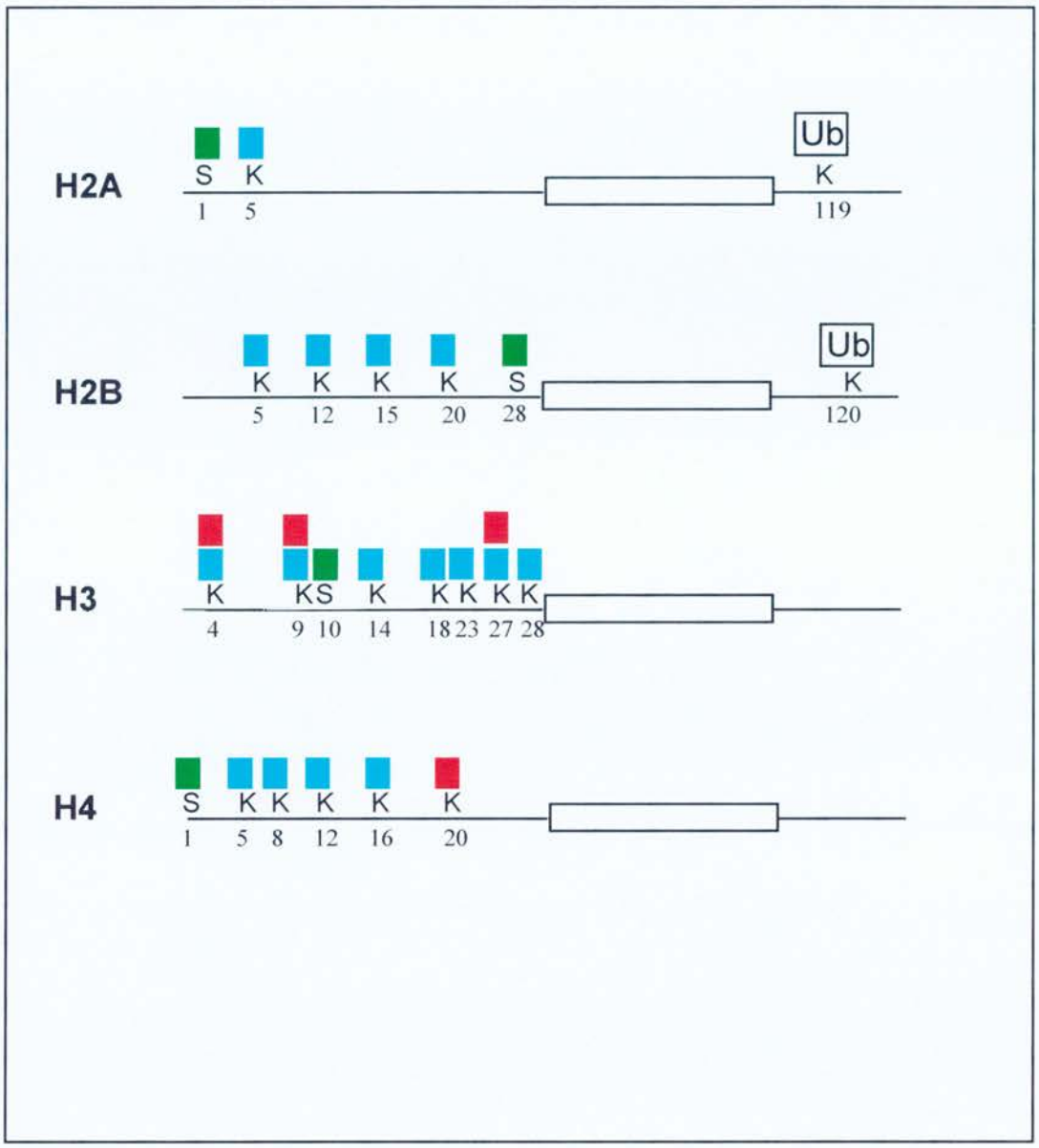

Figure 1.3 Histone Modifications
The N- and C-terminal tails of histones can be chemically modified by methylation (red box), acetylation (blue box), phosphorylation (green box) or ubiquitination (Ub) at several residues along the length of the protein. Each histone protein consists of the N- and C-terminal tails and a central globular domain (white box). When nucleosomes assemble, the globular domains are masked by the protein/DNA interactions and the tail regions protrude outwards from the nucleosome particle. This schematic highlights some of the residues known to be targeted by histone modifications for each of the four core histones, H2A, H2B, H3 and H4. Some residues, for example lysine 4 of histone H3, can be modified by both acetylation and methylation, however, this has not been demonstrated on the same histone protein simultaneously. H = histone protein, K = lysine, S = serine.

transcription factors to histones that are acetylated on specific lysine residues (Winston and Allis, 1999; Dhalluin et al., 1999; Owen et al., 2000; Jacobson et al., 2000).

It is not clear how histone acetylation specifically alters or influences the biophysical properties of chromatin fibres, however, there is some evidence that acetylation of N-terminal histone tails results in a weakened interaction with the DNA backbone (McGhee et al., 1983). This compromised interaction could facilitate the interaction of transcription factors with their target binding site (Wolffe and Hayes, 1999). There is some contradictory evidence to suggest histone tail acetylation does not have this predicted weakening effect on DNA-histone interaction (Marmorstein, 2001). Instead acetylation may be required more for maintenance of an active chromatin state rather than its establishment (Cavalli and Paro, 1999) and this may be achieved through acetylated histones creating binding sites for bromodomain-containing transcription factors (Fischle et al., 2003a).

1.1.3.2 Histone methylation

Core histones can be methylated at lysine residues and the functional consequences of this modification are not clearly defined. There is interplay between lysine methylation and acetylation and these modifications can influence transcription, for example, histone H3 can be either acetylated or methylated at lysine 4, 9 and 27. Acetylation and methylation modifications are considered mutually exclusive at H3 lysine 9; a single H3 molecule has not been identified with both modifications at the same time.

Histones can be modified by methyltransferases and each lysine residue can accept up to three methyl groups (Figure 1.2B). Specific cellular HMTs have only recently been identified and the significance of this modification in downstream events is only beginning to become apparent. Unlike acetylation, methylation exchange on histones tails appears somewhat irreversible (Byvoet, 1971) and to date no proteins with demethylase activity have been identified. It is possible that the only way to demethylate chromatin is by histone exchange, where methylated histones are removed from a nucleosome and replaced by unmethylated histones. HMT activity is directed by the SET (*S*u[var]3-9, *E*nhancer of zeste, *T*rithorax) protein domain and a subset of the Su(var) group proteins with a C-terminal SET domain are implicated in targeting chromatin regions for formation of heterochromatic structures resulting in inhibition of gene transcription from these regions. Many recent experiments link human and mouse homologues (both termed SUV39H1) of the *Drosophila* Su(var)3-9 protein with methyltransferase activity, which can then influence histone

deacetylation and DNA methylation activities (Macaluso et al., 2003; Vaute et al., 2002; Fuks et al., 2003)

A direct role for histone methylation in transcriptional regulation has been outlined. The nuclear receptor coactivator-associated protein, CARM1, has H3-specific arginine methyltransferase activity (Chen et al., 1999). In addition, the human and *S. pombe* homologues of *Drosophila* heterochromatin protein Su(var)3-9 (SUV39H1 and Clr4 respectively) are characterised H3-specific lysine methyltransferases (Rea et al., 2000; Zhang and Reinberg, 2001; Rice and Allis, 2001). Humans have additional SET domain proteins including SET7 (Wang et al., 2001) and SET9 (Nishioka et al., 2002), however, the direct role, if any, of these proteins in transcriptional control is not yet known.

Histone methylation can induce divergent transcriptional outputs, depending on the modification and its context. The Su(var)3-9 protein family (including Su[var]3-9, SUV39H1 and Clr4, see above) and the protein G9a mediate transcriptional silencing as they target H3-lysine 9 (H3-K9) for methylation. Methylated H3-K9 is a binding site for heterochromatin protein 1 (HP1, section 1.2.2.1; Rea et al., 2000). The HMT protein, Dot1 (Disruptor of telomeric silencing-1; (van Leeuwen et al., 2002) is specifically involved in silencing at telomeres, the mating-type locus and rDNA in budding yeast; however, this protein does not contain a SET domain and it specifically targets H3-K79 for methylation, a residue distal from the N-terminal tail. The human homologue of the *Drosophila* ESC-E(Z) complex, EED-EZH2, has been identified as the complex that catalyses H3-K27 methylation (Cao et al., 2002). H3-K27 has been associated with transcriptional silencing of the *HOX* gene cluster in *Drosophila* (Muller et al., 2002) and human cells (Cao et al., 2002). In contrast, methylation of H3-lysine 4 (H3-K4) has been correlated with transcriptional activity of genes in *S. cerevisiae* (Santos-Rosa et al., 2002) and *Tetrahymena* (Strahl et al., 1999). Immunofluorescence studies using antibodies detecting di- and tri-methylated H3-K4 suggest that tri-methylation is specific for active transcription while di-methylation is present at both active and repressed genes (Santos-Rosa et al., 2002).

Emerging evidence suggests the influence of histone methylation on transcription might not only be different dependent on the residue targeted, but also by the number of times it is methylated. Methylated histones are specifically bound by the chromatin associated proteins HP1 (Rea et al., 2000) and polycomb group proteins (Cao et al., 2002; Muller et al., 2002) and this links methylation of H3-K9 and H3-K27 with transcriptional repression.

1.1.3.3 Histone phosphorylation

Many histone residues are also subject to post-translational phosphorylation (including serine 10 of histone H3 and serine 1 of both histone H2A and H4) and are targeted for this modification by serine/threonine kinases (Figure 1.2D and Figure 1.3). The significance of this modification is less well understood than acetylation and methylation, however, it has been implicated in many diverse cellular processes including transcription, DNA repair, apoptosis and mitotic chromosome condensation (reviewed in Cheung et al., 2000). These cellular processes may appear conflicting but histone phosphorylation might utilise a common mechanism in all of them; opening of the chromatin fibre to allow access to downstream factors. These factors may then serve to further condense or decondense chromatin.

Histone H3 is phosphorylated at serine 10 by aurora kinase B during mitosis (Hsu et al., 2000; De Souza et al., 2000) and antibody detection of this modification is commonly used as a biological marker for cell division. Many of the phosphorylation sites in histone tails are adjacent to residues targeted by acetylation and/or methylation e.g. serine 10 of H3, neighbouring lysine 9. It is hence possible that some phosphorylation events may prevent particular methylated or acetylated residues being used as protein docking sites (Prigent and Dimitrov, 2003). This molecular mechanism has been demonstrated in mammalian cells as HP1 can no longer bind methylated lysine 9 of histone H3 when the adjacent serine residue is phosphorylated (Rea et al., 2000).

1.1.4 Histone variants

Histones are part of a multi-gene family. Within this family of proteins there are the four core histones and several core histone variants. These variants are thought to confer specialised properties to nucleosomes and are differentially expressed during development (Romano, 1992; Wolffe, 1995). A subset of histone variants appears to be involved in the process of spermatogenesis and indeed their expression is restricted to short time windows (e.g. H3.3B during meiotic prophase only; (Bramlage et al., 1997). Variant histones can be larger (e.g. macro H2A; (Pehrson and Fried, 1992), modified to a greater extent (e.g. H2A.X) or share a high degree of sequence similarity to core histones (CENPA and H3; (Sullivan et al., 1994).

Histone H2A has several variants with specialised functions (reviewed in Redon et al., 2002). Most of the molecular details of specialised histone variant functions have been

described for the H2A.X and H2A.Z. H2A.X has a conserved motif from yeast to man, the SQ motif, which is phosphorylated in response to double-strand breaks induced by ionizing radiation (Rogakou et al., 1999). Phosphorylated H2A.X can be seen as nuclear foci and this histone variant colocalises with DNA repair proteins including BRCA1, Rad50 and Rad51 (Paull et al., 2000), however the functional details of these associations are unclear. A second variant of H2A, H2A.Z, has been associated with transcriptional control as deletion mutants in yeast exhibit slower growth patterns (Santisteban et al., 2000; Carr et al., 1994) and it is not evenly distributed through the genome, as seen with IF studies of *Drosophila* polytene chromosomes (Leach et al., 2000).

One of the best studied histone variants, CENP-A, has significant sequence similarity to H3, can be incorporated into nucleosomes and dimerises with H4 (Sullivan et al., 1994). CENP-A is targeted to centromere sequences by its histone-fold domain, and this importantly raises the idea that histone variants may well associate with particular DNA sequences. There is some evidence to suggest that CENP-A incorporation may result in specialised nucleosome structure at centromeres (Smith, 2002). It is tempting to consider that many of the histone variants could have a similar effect on nucleosome, and indeed, chromatin structure. A second H3 variant is H3.3 and has two sub-types, A and B, which are differentially expressed during development (Bramlage et al., 1997).

1.1.5 The 30nm chromatin fibre

Electron microscopy (EM) techniques are limited in their resolution of chromatin fibres and, with the exception of lampbrush and polytene chromosomes (see section 1.3.1), higher order chromatin structures have not been resolved. Nucleosomal arrays adopt a 10nm diameter conformation *in vitro* and can condense into a compact 30nm fibre depending on the ionic strength of the reaction buffer. From these studies, two principle theories for 30nm chromatin fibre condensation were developed; the solenoid model where linker DNA and nucleosomes supercoil, and the zigzag model where the linker crosses the fibre (Widom, 1998; Zlatanova et al., 1999; Thomas, 1999); Figure 1.4).

It was originally proposed that 30nm chromatin fibre folding was mediated by inter-nucleosome bridging by linker histone H1. However, H1-deficient chromatin will still condense (Carruthers et al., 1998) and *Xenopus* extracts are capable of normal chromosome condensation and nuclear assembly in the absence of linker histones (Dasso et al., 1994; Ohsumi et al., 1993). These data argue that H1 is not essential for formation of the 30nm

fibre. It is becoming more apparent that histone modifications (see section 1.1.3), and indeed incorporation of core histone variants (see section 1.1.4), into chromatin may be more influential on fibre architecture. It is not clear how the 30nm chromatin fibre is packaged into the nucleus and microscope observations reveal that there is heterogeneity in chromatin structure.

1.2 THE CELLULAR CHROMATIN ENVIRONMENT

As the cell progresses through the cell cycle the 2m of cellular DNA is transcribed, replicated and subsequently divided between two daughter cells. The individual chromosomes are only visible between early prophase and late telophase, hence much of our knowledge is limited to mitotic chromosome structure. It has been calculated that interphase chromatin is condensed up to 200-250 times to form mitotic chromosomes compared to only two fold in *S. pombe* (Umesono et al., 1983).

1.2.1 Euchromatin and heterochromatin

Microscopic observations of interphase nuclei and metaphase chromosomes reveal two distinct types of chromatin, heterochromatin and euchromatin revealed by EM observations (Figure 1.5A). Using DNA dyes such as DAPI, heterochromatin stains brightly and can be distinguished from euchromatin (Figure 1.5B). For many years, this characteristic has been exploited in chromosome banding cytogenetic techniques. Heterochromatin and euchromatin are also thought to have different physical properties; heterochromatin is highly condensed while euchromatin has a more open conformation. Constitutive heterochromatin (i.e. that which is always condensed) can be stained using heat treatment (C-banding). It is considered genetically inert and traditionally defined as the region of the chromosome that remains condensed throughout the cell cycle. Karyotypes of C-banded metaphase chromosomes show that regions of constitutive heterochromatin are found on and around the centromeres of all chromosomes and at the telomeric ends of the Y chromosome (Sumner et al., 1990). Formation and/or maintenance of constitutive heterochromatin is clearly influenced by DNA sequence and methylation as treatment of cells with either distamycin (an AT-binding drug; (Radic et al., 1987) or 5-azacytidine (a DNA

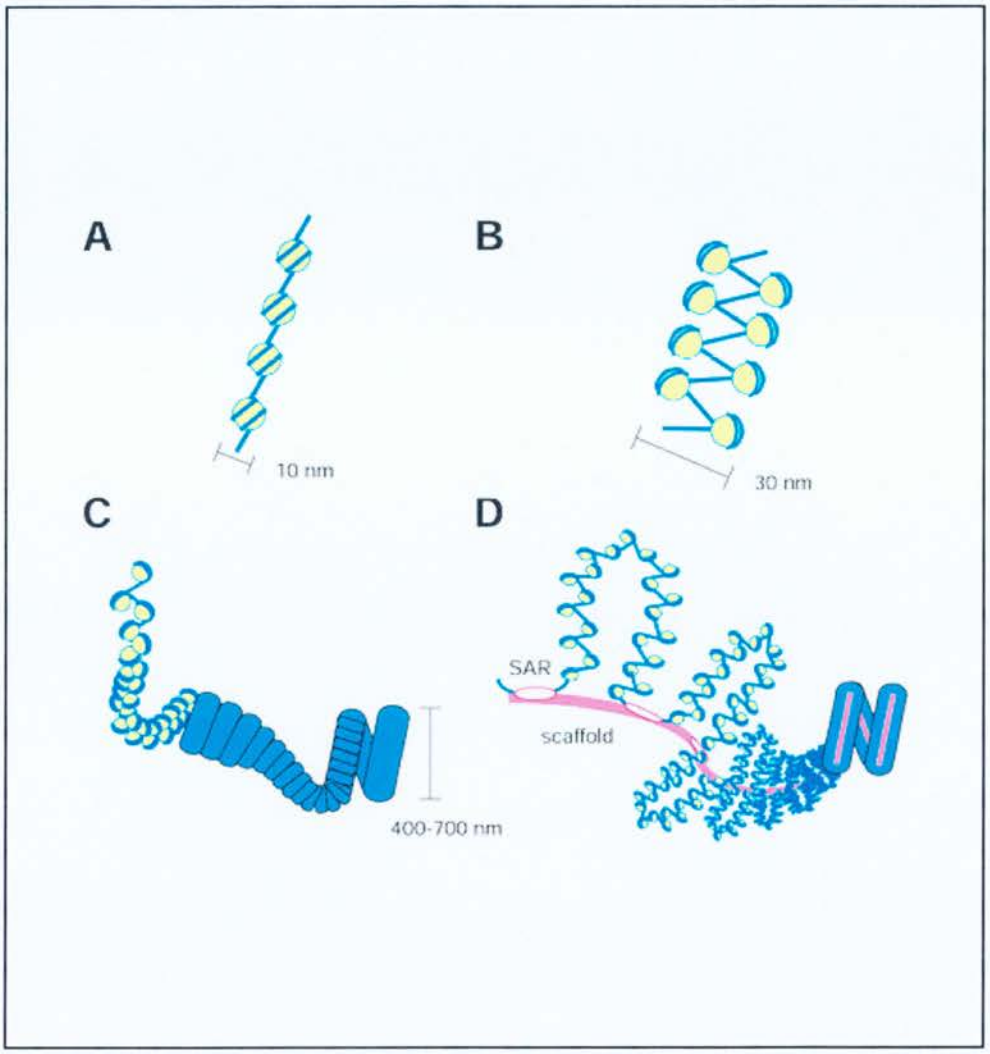

Figure1.4 Models of mitotic chromosome condensation

Several models exist for the folding and condensation of mitotic chromosomes. Each of these models agree that the DNA strand is firstly wrapped twice around an octamer of histone proteins(yellow circle), the nucleosome (A). These linear fibres are folded in a zig-zag or crossover fashion to produce the 30nm solenoid fibre (B). Progressive folding and/or coiling of the solenoid fibre would allow for larger chromatin fibres to be formed (C). These larger fibres could then loop and further condense (D). Looping may be mediated in a non-random way and influenced by chromosome scaffold proteins and regulatory SAR sequences (see text).

Adapted from Swedlow and Hirano. 2003

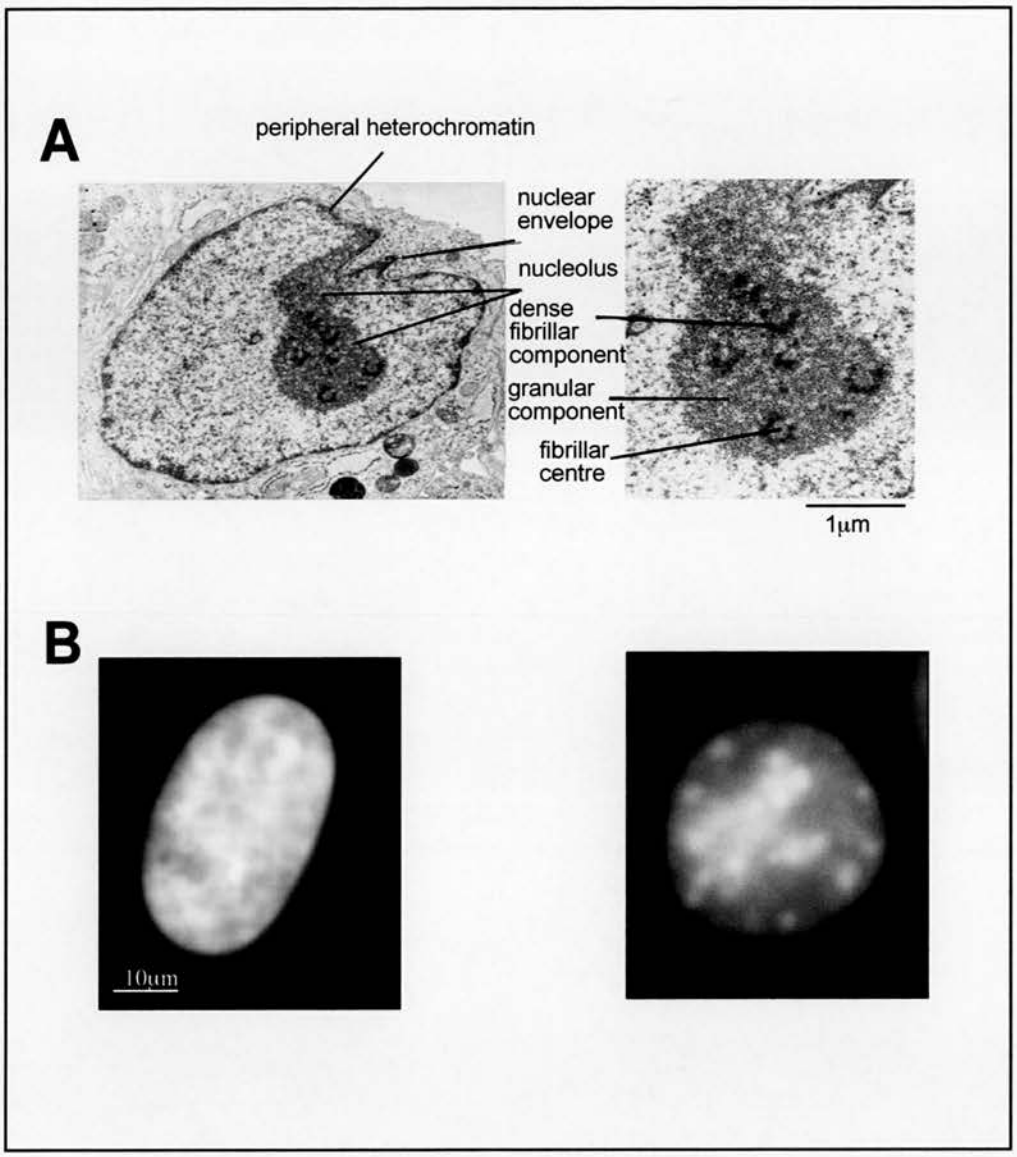

Figure 1.5 The cellular chromatin environment.
(**A**) Electron micrographs of the nucleus (left) and nucleolus (right) of a human primary fibroblast. Areas of dark, condensed heterochromatin can be seen adjacent to the nuclear envelope. The nucleolus contains three distinct regions, the dense fibrillar component, granular component and fibrillar centre. ***Taken from Alberts et al., Molecular Biology of the Cell (Third Edition).*** (**B**) Fluorescent light micrographs of the nuclei of human (left) and mouse (right) cells stained with DAPI. Heterochromatin is clearly visible as DAPI bright spots in the mouse nucleus and these typically represent the location of centromeric heterochromatin. Heterochromatic regions are less readily visible by this technique in human nuclei.

methylation inhibitor, (Joseph et al., 1989) result in decondensation of centromeric heterochromatin. In addition to this, a human genetic disease, Immunodeficiency-centromeric instability-facial anomalies syndrome (ICF), is caused by mutations in the *DNMT3B* gene (DNA methylase 3B) and patient cells show destabilisation of centromeric heterochromatin (Xu et al., 1999). Facultative heterochromatin is euchromatin that will adopt heterochromatic properties in a developmentally controlled manner. This suggests temporal silencing of regions of the genome. The classical example of this phenomenon is the inactive X chromosomes of females (see section 1.3.2).

Euchromatin, while distinct from heterochromatin, is not homogenous in its response to staining and hence can be differentiated by metaphase chromosome banding techniques. Quinacrine (Q) mustard banding was the first technique used to produce a differential staining pattern along the length of metaphase chromosomes to allow for karyotype analysis of the human chromosome complement (Caspersson et al., 1968) and Q-bands are considered to be AT-rich (Sumner et al., 1990). Giemsa banding (G-banding) of mitotic chromosome is routinely used to show reproducible light and dark bands along the length of chromosomes (Sumner et al., 1971). G-bands are late-replicating, AT-rich, gene-poor chromosomal regions, while G-negative 'R-Bands' are early-replicating, GC-rich, and gene-rich regions (Bickmore and Sumner, 1989; Craig and Bickmore, 1993). Constitutive heterochromatin bands can be visualised by C-banding or T-banding, techniques requiring heat treatment before Giemsa staining. In humans, C-bands are evident on chromosomes 1, 9, 16 and Y, and centromeres are also readily observed using C-banding (Sumner et al., 1990).

In position effect variegation (PEV), euchromatic genes can be silenced by being brought into close proximity to heterochromatin following chromosomal rearrangement or translocation. This phenomenon was first described in *Drosophila* and has been described in mammalian cells and implicated in human disease, for example Aniridia, where patients are born with characteristic eye malformations (Kleinjan and van, V, 1998). Genetic screens in yeast and *Drosophila* identified proteins capable of modifying PEV and many of these proteins are involved in chromatin dynamics.

At the molecular level, heterochromatic regions are rich in repetitive DNA sequences, have a low gene density and regularly spaced nucleosomes. In contrast to this, nucleosomes within euchromatin can be irregularly spaced or more mobile and may be replaced by different

DNA-binding proteins, e.g. transcription factors. In addition to characteristic nucleosome spacing, heterochromatin can generally be associated with particular histone modification patterns and associated proteins (reviewed in Richards and Elgin, 2002). In general, heterochromatin is marked by histone hypoacetylation, H3-K9 methylation and cytosine methylation of the DNA. Contrasting this, euchromatin is enriched with acetylated histones and has lower levels of cytosine and histone methylation.

1.2.2 Chromatin remodelling

As chromatin influences many cellular processes, it is anticipated that cellular chromatin has a dynamic, heterogeneous structure (van Holde and Zlatanova, 1996; Zlatanova et al., 1999). As discussed above, DNA and histone modifications serve to 'mark' genomic regions and signal for downstream mechanistic events: this is achieved through hierarchical DNA-protein and/or protein-protein interactions. Several of these layers of interaction are associated with enzymatic activity that can modify the chromatin fibre to influence the next step in the interaction pathway. Many different 'chromatin remodelling' activities have now been described which direct a range of structural transitions that occur during gene regulation and these are thought to control the accessibility of the DNA sequence to the transcriptional machinery.

1.2.2.1 Heterochromatin protein-1

There are three isoforms (α, β and γ) of HP1 proteins expressed in mammals (Singh et al., 1991; Saunders et al., 1993; Ye and Worman, 1996) and they each contain a chromodomain and a chromoshadow domain. HP1 was originally termed 'heterochromatin protein' as in IF experiments it was seen to localise to heterochromatic regions in *Drosophila* (James and Elgin, 1986). HP1 binds to H3-K9 via the chromodomain of the protein in fission yeast (Bannister et al., 2001; Lachner et al., 2001; Nielsen et al., 2001b). The three isoforms of HP1 have different localisations through the cell cycle, HP1α and β are found predominantly at the pericentromeric heterochromatin while HP1γ is found on euchromatic sites (Minc et al., 2000; Nielsen et al., 2001a). HP1s can interact with many proteins, e.g. transcription factors (TIF1β, KAP-1, Ryan 1999), SUV39H1 (Aagaard et al., 1999) and lamin B receptor (Ye et al., 1997).

1.2.2.2 Polycomb group proteins

The Polycomb (PcG) group of transcriptional repressors were first identified in *Drosophila* as proteins required for repression of homeotic gene expression during development. These

proteins work antagonistically with a group of activation proteins, the trithorax proteins (trxg, members of the SWI/SNF protein family; see section 1.2.2.2), to orchestrate the temporal and spatial expression of the Hox genes during development (reviewed in Simon and Tamkun, 2002). This partnership of proteins is conserved from *Drosophila* through to mammals and homeotic transformations have been described in mutant mice (Akasaka et al., 2001). PcG and trxg proteins are present *in vivo* as members of multi-subunit protein complexes and the first PcG complex to be purified (Polycomb recessive complex-1 - PRC1) was isolated from *Drosophila* embryos (Shao et al., 1999). A series of *in vitro* experiments using this complex suggest that its mechanism of action leaves chromatin regions inaccessible to ATP-dependent chromatin remodelling complexes (e.g. SWI/SNF; section 1.2.2.5). Indeed, a recombinant complex consisting of four core components (Polycomb, Posterior sex combs, Polyhomeotic and RING1) is capable of blocking SWI/SNF remodelling in *in vitro* assays (Francis et al., 2001). A second polycomb group complex is the extra sex combs-enhancer of zeste (ESC-E[Z]) complex containing ESC, E(Z), SU(var)12 and Pleiohomeotic (PHO, homologue of the mammalian YY1 transcription regulator (Cao et al., 2002; Czermin et al., 2002; Muller et al., 2002).

The current model for the mechanism by which on or off transcription states are maintained is based on opposing pathways for repressive PcG and activating trxg (Simon and Tamkun, 2002; Orlando, 2003). PcG complexes are linked to histone methylation, and the first example of this activity is the extra sex combs-enhancer of zeste (ESC-E[Z]) complex targeting H3-K9 and –K27 residues (Cao et al., 2002; Czermin et al., 2002). Antagonistically, trxg complexes associate with histone acetylation activity through the TAC1 complex (trithorax acetyltransferase complex 1; (Petruk et al., 2001). The trxg proteins TRX and ASH1 are also HMTs, however, they specifically target H3-K4 for methylation and this modification is generally associated with active transcription (Beisel C et al., 2002; Cao et al., 2002).

It is not clear how PcG and trxg target specific chromatin regions for remodelling in mammals. PcG proteins in general, do not have characterised DNA-binding domains and it is therefore proposed that their specificity be influenced by interactions with DNA-binding proteins and transcription factors. However, ESC(EZ) complex could be targeted to DNA via the PHO subunit as this has DNA binding properties (Mohd-Sarip et al., 2002). Previous work in *Drosophila* identified specialised DNA regions termed polycomb response elements

to which PcG proteins bind to control activity downstream of genes (PREs; (Lyko and Paro, 1999) however, such elements have yet to be described in mammals.

1.2.2.3 ATP-dependent chromatin remodelling

A sub-set of nuclear proteins have been characterised which harness ATP hydrolysis to reposition or modify the structure of nucleosome particles within the chromatin fibre (reviewed by Tsukiyama, 2002). To date, four classes of ATP-dependent remodelling factors have been described based on the ATPase subunits in the complexes – the SWI/SNF (mating type switching/sucrose non-fermenting), ISWI (imitation switch), CHD (chromodomain ATPase) and IN080 classes.

The founding member of the SWI/SNF family is the Swi2/Snf2 complex first identified in budding yeast genetic screens (Stern et al., 1984; Neigeborn and Carlson, 1984). Further work proved a link between SWI/SNF mutations and alterations in chromatin structure at the promoter regions of target genes. Open chromatin structure of, and hence gene transcription from, the promoter region of the sucrose hydrolysing enzyme gene, SUC2, requires SWI/SNF (Hirschhorn et al., 1992). This is also true for the promoter regions of the homothallic switching gene (HO) where it has been shown that chromatin opening is associated with recruitment of SAGA (the Spt-Ada-Gcn5-acetyltransferase complex; (Krebs et al., 1999). In mammalian cells there are two characterised Swi2/Snf2-like ATPases – BRM (related to *Drosophila* brahma SWI/SNF complex) and BRG1 (brahma-related gene 1). $BRM^{-/-}$ mice are viable and develop normally, although they show increased levels of cell proliferation and fibroblast lines from null mice fail to trigger cell cycle arrest in response to DNA damage or culture confluence (Reyes et al., 1998). Interestingly, $BRG^{-/-}$ homozygote mice are embryonic lethal, and heterozygotes are susceptible to tumour growth (Bultman et al., 2000). Both BRM and BRG proteins can associate with tumour suppressor proteins retinoblastoma protein (pRB), breast cancer associated gene-1 (BRCA1) and have also been isolated in several tissue and/or cell-type specific complexes (reviewed in Tsukiyama, 2002). The human genetic disease, α-thalassemia/mental retardation syndrome, X-linked (ATRX) is caused by mutations in the *ATRX* gene. ATRX protein is an ATP-dependent type II class SNF2 helicase (Picketts et al., 1996). Taken together these findings implicate SWI/SNF remodelling in tumourigenesis, differentiation and development.

The ISWI (imitation switch) family of remodelling complexes was originally described following the identification of a *Drosophila* protein with ATPase domain homology to brahma. Family members include NURF (nucleosome remodelling factor), ACF (ATP-utilizing chromatin assembly and remodelling factor) and CHRAC (chromatin-accessibility complex; reviewed in Varga-Weisz and Becker, 1998). Yeast (Isw1 and Isw2) and human (hSNFL and SNF2H) homologues of ISWI have been identified and are currently being characterised. Initial studies on yeast Isw2 mutants have shown that this complex is involved in control of meiotic growth genes and is required for formation of nuclease-resistant chromatin structures (Goldmark et al., 2000). This suggests that ISWI family proteins have opposing functions to that of SWI/SNF proteins as one family induces closed chromatin conformations while the other promotes chromatin opening.

Much less is presently known about the *in vivo* functions of the CHD and IN080 classes of ATP-dependent chromatin remodelling complexes. The CHD class of proteins is generally thought to play a role in transcriptional repression. This is due to the characterisation of one family member, Mi-2, and its interaction with HDACs and putative methyl-DNA binding proteins (Zhang et al., 1998; Wade et al., 1999). IN080 was first described as a protein required for transcriptional activation of the *IN01* gene, transcribed in the absence of inositol (Ebbert et al., 1999). The molecular mechanisms of chromatin remodelling used by this newly identified complex remain to be outlined.

There is still much to learn of the direct mechanisms of ATP-dependent chromatin remodelling *in vivo*. There is some evidence for the direct action of SWI/SNF complexes on chromatin structure at specific gene promoters, although the mechanistic details are unclear. Two models have been proposed: nucleosomes would slide along a DNA strand or alternatively the DNA itself writhes/twists around a nucleosome. Either of these models propose a means by which novel regions of contact between the nucleosome and downstream DNA sequences are made (reviewed in Flaus and Owen-Hughes, 2001).

1.2.3 Locus control regions and insulators

Two specialised DNA sequences have been characterised that act *in cis* to influence chromatin structure: insulators and locus control regions (LCRs; Figure 1.6). These specialised genomic regions are often characterised by DNase I hypersensitive sites.

Insulator sequences (also termed boundary elements) are thought to act as barriers to the linear progression or 'spreading' of chromatin remodelling factors along an individual chromatin fibre, and hence play a role in delineating a regional chromatin conformation. While many insulators were first described in *Drosophila*, they are also found in vertebrates (Bell and Felsenfeld, 2000) and can be an integral part of LCRs. LCRs and insulators are characterised in two simple assays where their ability to (1) prevent an enhancer working on a promoter is followed or (2) prevent the propagation of condensed (i.e. silenced) chromatin (reviewed in Burgess-Beusse et al., 2002). A number of groups have characterised insulators at specific genomic locations; the *Drosophila* hsp70 locus (Kellum and Schedl, 1991), the chicken β-globin locus (Hebbes et al., 1994), the H19 locus in mouse (Bell and Felsenfeld, 2000; Hark et al., 2000) and the T-cell receptor locus in humans (Zhong and Krangel, 1997). With the application of sophisticated experimental techniques such as 'chromosome conformation capture' and RNA TRAP (tagging and recovery of associated proteins), there is clear evidence that the β-globin LCR can facilitate chromatin looping (Tolhuis et al., 2002; Carter et al., 2002). However, it is not clear if the observed looping is transient or perhaps a more permanent feature. There is some contention in the field that this looping is transient, and will merely recruit histone modifying proteins and chromatin remodellers which will control the insulating activity.

LCRs are defined as chromatin regions that allow the expression of linked genes in a temporal or tissue specific fashion (reviewed in Li et al., 2002). The first LCR was identified as a region 5' of the human β-globin locus in transgenic mice studies (Grosveld et al., 1987). LCRs can function in a position-independent manner and their influence on gene expression levels is copy number-dependent. There appears to be no consensus between the molecular details of LCR function at different genomic locations, however, the establishment of 'open' chromatin structure is common. In support of this, LCR sequences of genes have been linked to changes in histone modifications (Forsberg et al., 2000; Bulger et al., 2003) and DNA methylation status (Santoso et al., 2000).

There are two main theories as to the mode of action of insulator sequences (Figure 1.6). In the first, the insulators are seen as a physical boundary that prevents spreading or progression of chromatin modifiers along a gene region (Figure 1.6A). This is supported by the identification of interactions between insulator binding proteins and chromatin remodelling proteins, for example the relationship between Su(Hw) and trithorax group protein Mod(mgd4) (Gerasimova and Corces, 1998). Secondly, it is considered that insulators are

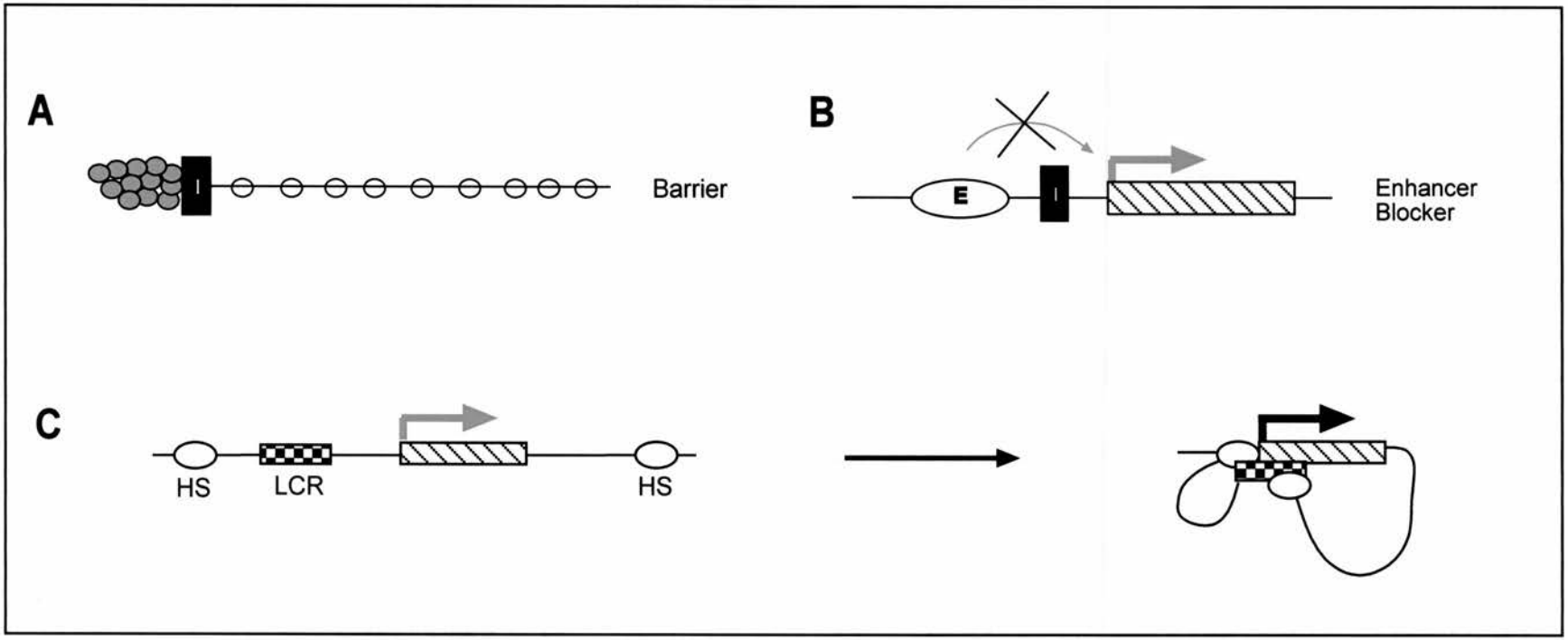

Figure 1.6 Models of insulator and locus control region function.
Insulator sequences can influence gene transcription. Some insulator sequences (I) may function as barriers or boundary elements which act to prevent the spread of chromatin condensation (**A**). Other insulators may act as enhancer-blocking elements which disrupt enhancer action when placed between enhancers and gene promoters (**B**). Enhancer-blocking elements only affect gene transcription when positioned between enhancers and promoters and not when they are found at other genomic sites. Locus control regions are known to cause chromatin looping to bring distal DNaseI hypersensitive sites (white circles), LCRs (checked box) and gene sequences (hatched box) into close proximity and drive gene expression (**C**).

capable of self-association and might drive local looping of the chromatin fibre restricting promoter and enhancer interactions (Figure 1.6B).

Proteins have been identified that specifically bind insulator sequences, these include Supressor of Hairy Wing (Su[Hw], (Gerasimova and Corces, 1998) and CCCTC binding factor (CTCF; (Bell et al., 1999), which may play a role in mediating this looping.

1.2.4 The role of RNA

There is a significant role for non-coding RNAs in epigenetic regulation of transcription, and hence chromatin structures, for a subset of genes. The importance of transcribed, but not translated, RNA molecules was first identified with isolation of transcripts from the mammalian *Xist* gene which are involved in initiation of X-inactivation in female cells (see section 1.3.2). *Xist* transcripts coat the X chromosome which is being inactivated (Clemson et al., 1996). Further non-coding RNAs are known to be involved with imprinting at genomic loci, including *Air* transcripts from the *Igf2r/Slc22a2/Slc22a3* cluster (Sleutels et al., 2002; Sleutels et al., 2003).

The study of post-translational gene silencing (PTGS) in plants has highlighted the presence of an additional mechanism by which non-coding RNAs influence chromatin structure. In 1999, Hamilton and Baulcombe identified short RNA species of 21-25 nucleotides (nt) in plants exhibiting PTGS which specifically target endogenous genes for transcriptional silencing. This work suggested a mechanism for RNA interference (RNAi) where double strand RNA (dsRNA) molecules can target mRNA for degradation forcing 'knock-down' of protein expression (Elbashir et al., 2001). Further work in this field has shown that endogenous non-coding RNA molecules exist which are processed by the RNAi machinery to generate siRNAs that will promote chromatin modifications at centromeres and gene loci in fission yeast (Hall et al., 2002; Volpe et al., 2002), *Tetrahymena* (Taverna et al., 2002), *Drosophila* (Pal-Bhadra et al., 2002), *Arabidopsis* (Zilberman et al., 2003) and mammalian cells (Maison et al., 2002). Recent experiments in fission yeast have shown that long terminal repeats (LTRs) in the genome also effect chromatin-based silencing of nearby genes in an RNAi-dependent manner (Schramke and Allshire, 2003). With the existence of many non-coding RNAs there is the possibility that several regions of constitutive or indeed facultative heterochromatin may be maintained by this mechanism.

1.2.5 Metaphase chromosomes

Many of the initial studies of chromosome architecture focussed on the easily observed and isolated mitotic, metaphase chromosomes. Metaphase chromosomes stained with various dyes reveal that each one has a particular composition that allows identification of individual chromosomes (Figure 1.1, section 1.2.1). Regions of early-replicating DNA, known as Giemsa-light (G-light, also termed R-bands) alternate with G-dark bands (mid- to late-replicating DNA) along the length of any given mitotic chromosome. Within the R-bands, there is a subset, known are the T-bands, which correspond to the regions of highest gene density (Craig and Bickmore, 1994).

As described above, we are becoming increasingly aware of the molecular mechanisms that underpin the folding and condensation of chromatin fibres. EM analysis of extracted metaphase chromosomes (from which most chromosomal proteins have been biochemically extracted) reveals an underlying skeletal structure (Paulson and Laemmli, 1977). Studying the metaphase chromosomes at higher resolution using X-ray scattering indicates that they exhibit diffraction features characteristic of 30nm, suggesting that they are produced by further folding of the 30nm fibre (Langmore and Paulson, 1983; Paulson and Langmore, 1983). Loops of DNA ranging from 50-100kb radiate outwards from an internal scaffold, which is predicted to consist of chromosomal proteins. In this model, scaffold proteins Sc-I (topoisomerase-II) and -II are thought to anchor the DNA loops, serving a role in maintaining metaphase chromosome structure (Earnshaw et al., 1985; Earnshaw and Heck, 1985; Gasser et al., 1986; Saitoh et al., 1994).

Topoisomerase-II is an ATP-dependent enzyme which decatenates (untangles) DNA strands (Wang, 2002). Two isoforms (α and β) of topoisomerase II (Topo-II) have been identified in vertebrates. These isoforms show identical catalytic activities *in vitro* but have different localisation patterns *in vivo*; Topo-IIα is concentrated on mitotic chromosomes while Topo-IIβ is not (Earnshaw and Heck, 1985; Christensen et al., 2002). The distribution of Topo-II protein on mitotic chromosomes is thought to be related to DNA-sequence, as the protein co-localises with AT-rich sequences (Saitoh and Laemmli, 1994) termed scaffold attachment regions (SARs, see below; (Hart and Laemmli, 1998). Recent studies on the interphase mobility properties of Topo-II have shown that GFP-tagged molecules are mobile, and this suggests that chromosome condensation is a dynamic process (Christensen et al., 2002).

SMC2 (structural maintenance of chromosomes, or Sc-II) is a subunit of a condensin complex, and is essential for chromosome condensation *in vitro* in *Xenopus* extracts (Hirano and Mitchison, 1994). *In vitro* assays have demonstrated that condensin is capable of inducing superhelical tension in DNA molecules in an ATP-dependent manner (Kimura and Hirano, 1997; Kimura et al., 1999). The process has recently been visualised using electron spectroscopic imaging (ESI, (Bazett-Jones et al., 2002), however it is not clear if this supercoiling activity is present *in vivo* where the substrate is chromatin and not naked DNA. Genetic studies of condensin subunits have shown that SMC4 is not required for condensation of metaphase chromosomes but is involved more in the anaphase separation of sister chromatids in *Drosophila* (Steffensen et al., 2001). A recent report of a conditional knockout of the SMC2 condensin subunit in chicken cells details delayed, but eventually normal levels of mitotic chromosome condensation (Hudson et al., 2003). Furthermore, chicken cells lacking SMC2 show loss of additional proteins thought to contribute to the metaphase chromosome scaffold, e.g. Topo-II and INCENP (a centromere component; (Hudson et al., 2003).

Several other factors are thought to be involved in metaphase chromosome condensation, including titin (Machado et al., 1998). Titin, an extremely large muscle protein, was identified as a metaphase chromosome component by IF studies using scleroderma antisera (Machado et al., 1998). *Drosophila* titin mutants show muscle defects and problems with chromosome condensation, suggesting that the presence of titin on metaphase chromosomes may indeed have a functional significance (Machado and Andrew, 2000). Intriguingly, the human and mouse titin mutants do not phenocopy the *Drosophila* mutants and therefore the role of titin in metaphase chromosome condensation in mammals is difficult to reconcile (Hackman et al., 2002; Gerull et al., 2002; Garvey et al., 2002).

Specific regions of DNA within the human genome that co-localise with the metaphase scaffold were identified by FISH on extracted metaphase chromosomes (Bickmore and Oghene, 1996). Furthermore, DNA sequences corresponding to matrix/scaffold attachment regions (SAR/MARs) were used as FISH probes illustrating that these sequences are unevenly distributed throughout the human genome (Craig et al., 1997). Some SAR/MARs are thought to be permanent structural features of the genome while others, for example those contained within transcribed DNA sequences, may make transient associations with nuclear structures to facilitate a more dynamic chromatin structure. However, recent work from Belmont and co-workers has demonstrated that chromatin condensation is not

necessarily influenced by primary DNA sequences as different vector compositions show comparable levels of condensation when stably maintained in CHO cells (Strukov et al., 2003).

Although controversial, the above data all point towards the existence of a metaphase chromosome scaffold or skeleton. Several models exist to propose the mechanisms and interactions underlying the chromatin condensation mechanisms that generate metaphase chromosomes (reviewed in Swedlow and Hirano, 2003). However, progress is this field is limited by current experimental techniques as we do not have the capacity to accurately visualise the DNA fibre compaction at this resolution *in vivo*. Importantly, we also know little of how the activities of Topo-II and condensin are orchestrated to bring about mitotic chromosome condensation. Clearly, this process will be intrinsically linked to other cellular events such as DNA replication, cell cycle checkpoints and gene activity.

1.2.6 Interphase chromosomes

By observing metaphase chromosomes, we are only considering chromatin structures within a small snapshot of the cell cycle. The largest proportion of a cell's life is spent in interphase and many of the chromatin-dependent cellular processes take place during interphase (DNA replication, DNA repair and gene transcription). How does the metaphase chromosome skeleton and 'banding' translate to the interphase chromosomes?

There is evidence to suggest the presence of an underlying chromosome/nuclear skeleton during interphase. Cells grown on microscope coverslip glass are treated with detergent (to remove the cell membranes), washed in increasing salt concentrations (removing soluble proteins and histones) and then visualised (Vogelstein et al., 1980). This results in a residual nuclear matrix with a surrounding 'halo' of loops of DNA. Interphase DNA extraction experiments suggest different attachments to the nuclear matrix or nuclear domains such as the nucleolus or nuclear lamina between chromosomes. Chromosome 18 is released into the DNA halo at high salt concentrations while chromosome 19 is always retained in the residual nucleus (Croft et al., 1999). This may be attributed to the sequence differences between these chromosomes – they do not show the same distribution pattern for SAR/MARs when observed by FISH (Craig et al., 1997). Alternatively, association between the nuclear matrix and chromosomes has been linked to activity (Berezney et al., 1996) and as chromosome 18 and 19 have contrasting gene activities they may also have different interactions with the nuclear matrix.

There is additional data to support the idea that metaphase chromosome banding characteristics translate to interphase. Human genome compartmentalisation into early- or late-replicating sequences (the R- and G-bands) during interphase had previously been demonstrated (Kill et al., 1991). There is further evidence to suggest that the very earliest replicating sequences (replication foci) occupy an internal nuclear position, while later replicating sequences are more dispersed and peripheral (Kennedy et al., 2000; Sadoni et al., 1999).

1.2.7 Models of large-scale chromatin folding

At the molecular level, we are learning of the intricate and dynamic balance between histone modifications, chromatin remodellers and their associated protein complexes (see above). However, due to problems with visual resolution, we still have limited understanding of how chromatin packaging manifests *in vivo*. There are several models proposing how chromatin fibres might be packaged into mitotic and interphase chromosomes. Each of these models considers the requirement of a dynamic chromatin fibre, poised to respond to cellular cues. There are caveats with the models mentioned here, it is likely that *in vivo* chromatin fibre folding draws parallels from some aspects of each.

1.2.7.1 The radial array model

This chromosome-folding model was originally proposed for mitotic chromosome structure (Paulson and Laemmli, 1977) and later extended to interphase (Manuelidis and Chen, 1990). Its basis is the 30nm fibre, which would arrange as paired loops approximately 30kb in length radiating outwards from a central axis. Importantly, this model predicts that the different degrees of condensation observed as G- and R-band regions during metaphase would translate into regions of more or less condensed interphase chromatin regions (Yokota et al., 1995). Ten 30kb loops (a radial array) are predicted to be subject to degrees of coiling which would directly influence chromatin fibre accessibility. A recent study of chromatin condensation of transgenic sequences in CHO cells reveals that the distribution of human β-globin SAR sequences is inconsistent with radial loop arrays of chromatin (Strukov et al., 2003).

1.2.7.2 The random loop/giant walk model

This model is based on the assumption that each chromosome consists of randomly folded flexible loops several megabases long (Sachs et al., 1995; Yokota et al., 1995). These loops would protrude out from a malleable chromosome backbone, which would itself be randomly folded into loops of varying sizes to make up the interphase chromosome structure. This model does not support the idea that chromosomes are composed of non-random sub-domains such as early- and late-replicating sequences. This modelling would involve a degree of chromatin domain overlap and suggests no maintenance of interchromosomal channels (Yokota et al., 1997)

1.2.7.3 The folded 'chromonema' model

In 1978, Sedat and Manuelidis proposed a model of chromosome folding where successive coiling of 10nm chromatin fibres would give rise to metaphase chromatids (Sedat and Manuelidis, 1978; Strukov et al., 2003). Modifications to this initial model were made following light microscopy and transmission electron microscopy (TEM) studies of chromosome intermediates at the transition phases before and after mitosis (Belmont and Bruce, 1994; Li et al., 1998). Folding of 10 and 30nm fibres would produce a ~100nm 'chromonema' fibre. This chromonema would then fold into a 200-300nm prophase chromatid which itself coils to produce a metaphase chromosome. In this model there is no role for a central chromosome protein axis to anchor DNA loops. It is postulated that chromatin organisation would be achieved through interaction with nuclear scaffold proteins, or by inter-fibre interactions which would possibly be modulated by histone modifications.

1.2.7.4 The multi-loop subcompartment model

In a computer simulation, interphase chromosomes can be modelled as flexible fibres of rosette-like subcompartments that correspond in size to observed subchromosomal foci of early- and late-replicating DNA (Munkel et al., 1999). This model predicts that a 'spring-like' structure of anchoring proteins maintains 120kb loops, and higher-level folding of these loops into rosettes, in a random manner. Again, this does not allow for any functional compartmentalisation of regions of chromatin fibres.

1.3 THE ROLE OF LARGE-SCALE CHROMATIN STRUCTURE IN REGULATION OF TRANSCRIPTION

1.3.1 Model chromosomes

Observations of special interphase chromosomes provided preliminary evidence that chromatin structure influences gene expression *in vivo*. Studies of lampbrush chromosomes in meiotic nuclei and polytene chromosomes of many Dipterans have demonstrated that interphase chromosomes consist of functional large-scale domains. These chromosomes can be isolated in physiologically ionic conditions and contain DNA that is very transcriptionally active.

Lampbrush chromosomes have an obvious central axis of two chromatin strands from which loops of highly transcribed DNA radiate (Figure 1.7A; Callan, 1986). Lampbrush chromosome studies have provided much of the experimental data upon which the radial array model (section 1.2.7.1) of chromosome folding is based. Loops of DNA are coated in several RNA polymerase molecules and their nascent transcripts give DNA loops a brush-like appearance. DNaseI digestion experiments lead to the discovery that the axis of lampbrush chromosomes consists of two DNA duplexes while each protruding loop involves only one DNA duplex (Callan, 1986). Furthermore, DNA loops range up to 100kb in length and particular DNA sequences are contained within different loops (Callan et al., 1987). Interspersed between the DNA loops are stretches of inactive chromatin which condense to form bead-like structures termed chromomeres, and several of these compact DNA domains can aggregate to form larger higher order structures. Antibody studies on lampbrush chromosomes have shown that histones, actin and RNA binding proteins co- localise with the high levels of RNA transcription within the DNA loops (Roth and Gall, 1987).

Polytene chromosomes are of particular interest as they are giant chromosomes commonly found in highly active secretory cells of many insect larvae. Each polytene chromosome is thousands of homologous pairs of chromosomes that align to form a single macro chromosome. Light microscopy identified interphase banding and transient decondensed 'puffs' along the length of polytene chromosomes (Figure 1.7B). Later, EM studies of the Balbiani ring gene cluster in *Chironomus tentans* showed that each transcribed gene is located within decondensed puffs and that these puffs are generally associated with high transcriptional activity (Bjorkroth et al., 1988; Ericsson et al., 1989). Many studies have

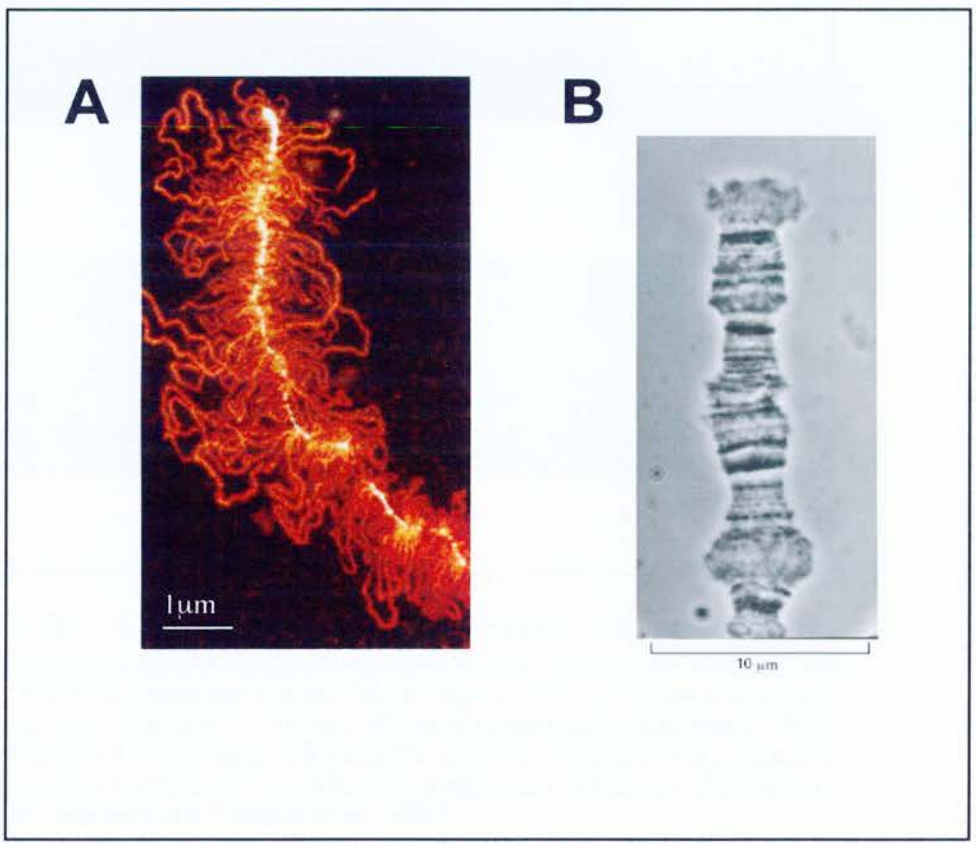

Figure 1.7 The structure of model chromosomes. (**A**) A meiotic lampbrush chromosome of the salamander *Notophthalmus viridescens*. Extended DNA (white) loops out and is transcribed into RNA (red).
Taken from Gilbert. Developmental Biology (Sixth Edition).
(**B**) Light micrograph of a portion of polytene chromosome from the salivary gland of *Drosophila.* Distinct patterns of decondensed 'puffs' of chromatin are clearly visible interspersed between highly condensed dark bands.
Taken from Alberts et al., Molecular Cell Biology (Third Edition).

used polytene chromosomes to map the involvement of particular linker histones (Mohr et al., 1989), histone modifications (for example, (Turner et al., 1990; Turner et al., 1992) and PcG proteins (Zink and Paro, 1989); (DeCamillis et al., 1992) in transcription.

1.3.2 X-inactivation

Chromatin structure has been correlated with gene expression control during X-inactivation during dosage compensation in nematodes and female mammals (reviewed in Plath et al., 2002). The inactive X (Xi) is visualised as a heterochromatic region, known as the Barr Body at the nuclear periphery of female cells (Lyon, 1961).

Inactivation is initiated by *Xist* (Xi-specific transcript) non-coding RNA produced at the *X-inactivation centre* (XIC) and these transcripts act *in cis,* to coat the length of the Xi (Clemson et al., 1996). *Xist* RNA has been found to be necessary and sufficient for chromosome-wide silencing in mouse inducible transgene studies where silencing spreads from the insertion site to nearby autosomal regions (Wutz and Jaenisch, 2000). Interestingly, many experiments have documented that there is only a narrow window during which *Xist* exerts its effects as expression of transcripts in cells other than embryonic stem cells (ES) does not target chromatin for silencing (Plath et al., 2002).

Many years of X inactivation research have documented several characteristic molecular marks that appear to be required for maintaining the inactive chromatin state. The Xi is late replicating (Takagi, 1974), methylated at CpG island promoters (Wolf et al., 1984) and has hypoacetylated histones (Jeppesen and Turner, 1993; Belyaev et al., 1996). Recent work has shown that the Xi also has high levels of methylation at H3-K27 and decreased levels for H3-K4 (Boggs et al., 2002; Heard et al., 2001; Peters et al., 2002; Silva et al., 2003; Gilbert et al., 2003).

In addition to these heterochromatic characteristics, the variant histone macroH2A has been located to the Xi (Costanzi and Pehrson, 1998) and its recruitment appears to depend on *Xist* RNA (Csankovszki et al., 2001; Beletskii et al., 2001). It is not yet clear what role this histone variant (and its isoforms) may play in maintaining the silenced chromatin structure. Another interesting relationship between BRCA-1 and the Xi has been described. BRCA-1 localises on the Xi of female somatic cells and is linked to *Xist* RNA through the BRCA-1 binding partner, BARD-1 (Ganesan et al., 2002). The authors also show that BRCA-$1^{-/-}$ cells fail to establish X inactivation, however, the molecular basis for this is not clear and it is not

known if disrupting this association is directly involved in tumourigenesis (Ganesan et al., 2002).

1.3.3 Effect of transcriptional activation on chromatin structure

For many years, particular chromatin structures have been associated with transcriptional activity and repression; open (decondensed) chromatin is considered transcriptionally competent, while closed (condensed) structures are associated with transcriptional repression. Early biochemical experiments using nucleases suggested that actively transcribing genes are more susceptible to enzyme digestion and the first nucleosomes released are acetylated. There is also evidence that actively transcribing chromatin is deficient in H1 and more readily exchanges histones H2A and H2B (reviewed in Wolffe, 1995).

To understand more of the molecular requirements/effects of transcriptional activation, the cascade of chromatin modifications that contribute to activation of a specific gene are now being followed. The techniques of chromatin immunoprecipitation (ChIP) and real time PCR, together with nuclease sensitivity assays, have demonstrated *in vivo* that gene activation results in molecular changes associated with chromatin remodelling (increased histone acetylation and SWI/SNF recruitment;(Litt et al., 2001; Agalioti et al., 2002; Chakrabarti et al., 2003). It is generally considered that increased nuclease sensitivity corresponds to regions of more open or decondensed chromatin (marked by enriched histone acetylation and H3-K4 dimethylation). A recent report from Groudine and co-workers has suggested that there may be more than one level of structural change resulting in gene expression (Bulger et al., 2003). Their experiments analysing the mouse β-globin locus detail that perceived chromatin 'openness' (marked by nuclease sensitivity) does not necessarily map to the same regions as histone modifications associated with transcriptional activity (high histone acetylation).

Due to the limitations in visualising chromatin fibres *in vivo*, there is still much to learn of the topology of the structural changes induced by gene activation. However, experiments following the fate of fluorescently tagged chromatin fibres can begin to address this. The viral transcription factor VP16 has been shown to cause large-scale unfolding of a heterochromatic domain in mammalian cells (Tumbar et al., 1999). However further work is required to determine whether this is true of endogenous genes rather than an observation for a transgenic heterochromatic construct with many integrated copies.

1.4 THE INTERPHASE LOCATION OF CHROMOSOME TERRITORIES

1.4.1 Model organisms

In the 1880s it was proposed by Rabl and Boveri that chromosomes retained a specific structure and distribution pattern throughout the cell cycle (Rabl, 1885; Boveri T, 1909). The classical 'Rabl' configuration, first described *in vivo* in *Salamandra maculata* and plant meristem cells, suggests that nuclei have a degree of polarity. In these polarised cells, the chromosomes retain their anaphase-telophase orientations and decondense on entering interphase. This gives rise to a nucleus with centromeres clustered at one pole and telomeres at the opposite pole. The Rabl configuration of chromosome arrangement has been observed in nuclei of both yeast (Jin et al., 2000) and *Drosophila* (Hochstrasser et al., 1986; Marshall et al., 1996). However, this organisation can be modulated during development as *Drosophila* embryos show nuclear polarity while larval imaginal disks do not (Csink and Henikoff, 1996). Centromeres can be arranged at one nuclear pole and telomeres at the other in the cells of some organisms (Rabl, 1885; Boveri T, 1909; Funabiki et al., 1993).

1.4.2 Chromosome territories

In the early 1980s, cell biologists returned to the interphase nucleus and became increasingly aware of the spatial organisation of chromosomes. Preliminary experiments demonstrated that interphase chromosomes were indeed the discrete entities modelled by Rabl and Boveri (Cremer et al., 1982a). The first experiments suggesting that chromosomes were arranged into territories involved micro-irradiation of Chinese Hamster Ovary cells. This showed that any DNA-damage induced by micro-irradiation during interphase was restricted to only a few chromosomes at mitosis suggesting that there might be a discrete 3-D organisation of interphase chromatin (Cremer et al., 1982b). In addition to this, particular nuclear locations for the DNA sequence of one chromosome (termed a chromosome territory) were visualised by FISH (Manuelidis, 1985) and multiple FISH chromosome paints can be used in tandem to highlight the distribution of many chromosomes in a cell (Figure 1.8A). Direct *in vivo* labelling of whole chromosomes has also been achieved (Zink et al., 1998) although this technique is somewhat limited as chromosome labelling is random.

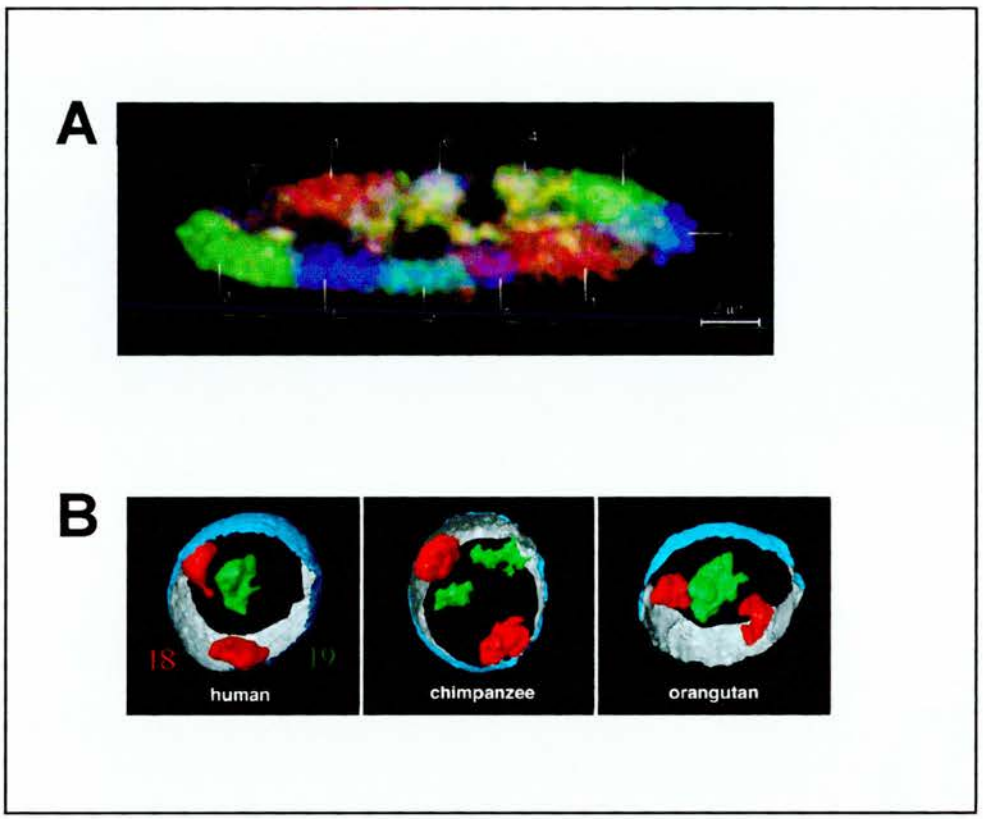

Figure 1.8 Chromosome territories in evolution. (**A**) In the chicken, mutually exclusive chromosome territories are evident with multicolour FISH in fibroblast nuclei. Homologous chromosomes are seen at separate nuclear locations. ***Taken from Cremer and Cremer, 2001.*** (**B**) Chromosomes HSA18 and –19 (and the sytenic sequences) are found in comparable nuclear locations in peripheral lymphocytes of human, chimpanzee and orangutan. ***Taken from Tanabe et al., 2001***

Another significant conclusion was drawn from observations of replication domains by S-phase incorporation of fluorescently-tagged dNTP analogues (Ferreira et al., 1997; Sadoni et al., 1999). Gene-rich sequences (R-bands, early-replicating) are towards the nuclear interior and gene-poor sequences (G/C-bands, late-replicating) are towards the nuclear edge. This organisation is evident within the territory of one chromosome, suggesting a polar orientation (Sadoni et al., 1999).

1.4.3 A radial distribution of chromosome territories

Preferred nuclear locations for chromosomes were initially suggested by the discovery that some human autosomes preferentially associate with the nucleolus. In humans, these are the rDNA-containing, acrocentric chromosomes 13, 14, 15, 21 and 22 (Bobrow and Heritage, 1980). Following this, Croft *et al.*, (1999) provided direct evidence for preferential location of non-rDNA containing chromosomes. Two human chromosomes (HSA18 and HSA19) were selected as they are of similar physical size in base pair length (77 and 63 Mbp respectively, Ensembl Release 16.33.1, July 2003) yet have contrasting gene densities and functional characteristics. HSA18 is gene-poor (~4.3 genes per Mbp) while HSA19 is gene-rich (22.7 genes per Mbp; (Craig and Bickmore, 1994). These two chromosomes, when visualised by FISH in interphase nuclei, have very different positions – HSA18 is observed near the nuclear periphery while HSA19 occupies a more internal location (Croft et al., 1999). Intriguingly, translocated chromosomes containing sequences from both HSA18 and –19 appear to target the respective regions of the derived chromosome to the expected nuclear locations. This would suggest the DNA sequence and/or associated proteins are involved in targeting the chromosome territories to their nuclear locations. Boyle *et al.,* (2001) went on to analyse the territory positions of the entire chromosome complement in primary human fibroblasts and a human lymphoblastoid cell line. This data set provides a reproducible chromosome territory map for these cells and shows that there are few striking differences in chromosome location between these two cell types.

Previous work has suggested that nuclear position of chromosomes is a direct consequence of their size in megabases, with the smallest chromosomes being more internal (Sun et al., 2000). The experimental evidence of Croft *et al.*, (1999) and Boyle *et al.,* (2001) contradict this, suggesting that relative gene density rather than actual number of base pairs is more influential on chromosome location. FISH studies suggest that gene-rich chromosomes (e.g. HSA17, -19 and -22) are concentrated towards the centre of the nucleus with more gene-poor chromosomes (e.g. HSA4, -13 and -18) around the periphery and this is confirmed by

analyses of chromosome translocation frequencies (Bickmore and Teague, 2002; Cornforth et al., 2002). It appears that this 'radial arrangement' of chromosomes is conserved through evolution (Haberma et al., 2001). Studies in higher primate lymphoblasts indicate that sequences syntenic to that of HSA18 and –19 occupy peripheral and internal nuclear locations respectively (Figure 1.8; Tanabe et al., 2002). This pattern of interphase organisation is also consistent with that of the chicken genome as the gene-rich microchromosomes are internal in chicken fibroblast and neuron nuclei while the gene-poor macrochromosomes are peripheral (Habermann et al., 2001).

The radial model of chromosome territory organisation does not necessitate that each chromosome has a strict address or neighbour. It has been proposed that chromosome territories are arranged with respect to their neighbours and particular chromosome pairing events have been described (reviewed in Parada and Misteli, 2002). This is based on observations of mitotic rosettes in human cells, where it has been reported that homologous chromosomes are diametrically opposed (Nagele et al., 1995). This pattern of organisation was later described in quiescent interphase nuclei for HSA7, -8 and-16 (Nagele et al., 1999). However, there are conflicting reports describing chromosomes positioned randomly with respect to each other during mitosis (Allison and Nestor, 1999) and during interphase (Habermann et al., 2001; Cornforth et al., 2002). It has been shown that chromosome neighbourhoods change during the cell cycle (Walter et al., 2003) and the translocation analyses performed in (Cornforth et al., 2002) shows no evidence for precise chromosome positions.

In order to consolidate a model of chromosome territory organisation, there is increasing interest in the inheritance of any spatial organisation through cell division. If chromosomes were arranged with respect to one another and if this position is heritable then the spatial organisation of mother and daughter nuclei is predicted to be comparable. Two recent studies have followed the fate of maternal nuclear organisation patterns into daughter cells using cell lines ectopically expressing fluorescent histone H2B. Walter and co-workers conclude that, as only 40% of daughter nuclei resemble mother nuclei, there is one significant change to chromosome territory organisation during HeLa cell mitosis (Walter et al., 2003). In contrast to these findings, a second inheritance study concluded that organisation transmits from one generation to the next in rat NRK cells (Gerlich et al., 2003).

1.5 NUCLEAR COMPARTMENTS AND THEIR ROLE IN CHROMATIN ORGANISATION

There is growing evidence that the chromosomes are not the only nuclear components subject to functional compartmentalisation. Nuclear proteins involved in DNA replication, repair, transcription, ribosome biosynthesis and splicing also concentrate within particular domains (Figure 1.9; Belmont, 2003). While these compartments are not delineated by membranes they are spatially distinct, morphologically identified by light and electron microscopy. GFP-fusion technology has made a significant contribution to our understanding of the dynamics and behaviour of many of these nuclear compartments (reviewed in Dundr and Misteli, 2001). Many groups have shown through Fluorescence Recovery After Photobleaching (FRAP, see section 1.7) experiments that there is a high degree of protein turnover and exchange in many of the nuclear protein domains. These dynamics suggest a situation where there is constant maintenance and perhaps modulation of any interphase nucleus spatial organisation, this could facilitate cellular responses to the physiological environment.

1.5.1 The nucleolus

The nucleolus is the most conspicuous nuclear substructure. It contains three morphological components when visualised by EM: the fibrillar centre, dense fibrillar component and the granular component (Figure 1.5A). It is responsible for the transcription and processing of ribosomal DNA (rDNA) and pre-ribosome assembly. In human cells the nucleolus assembles around rDNA gene clusters (active and inactive) on the p arms of acrocentric chromosomes HSA13, -14, -15, -21 and -22 (Sullivan et al., 2001; Hernandez-Verdun D. et al., 2002). This nuclear component has also been implicated in cell cycle control, with a role in sequestration of important proteins such as Mdm2, a regulator of p53 activity (Visintin and Amon, 2000).

The nucleolus is linked to chromosome territory organisation through its associations with the acrocentric chromosomes (Hernandez-Verdun D. et al., 2002) and these rDNA-containing chromosomes co-localise with the nucleolus in a transcription-independent fashion (Sullivan et al., 2001). As a cell divides, the small nucleoli on the rDNA genes (nucleolar organiser regions - NORs) on each acrocentric chromosome fuse to create one or more mature nucleoli (Hernandez-Verdun D. et al., 2002).

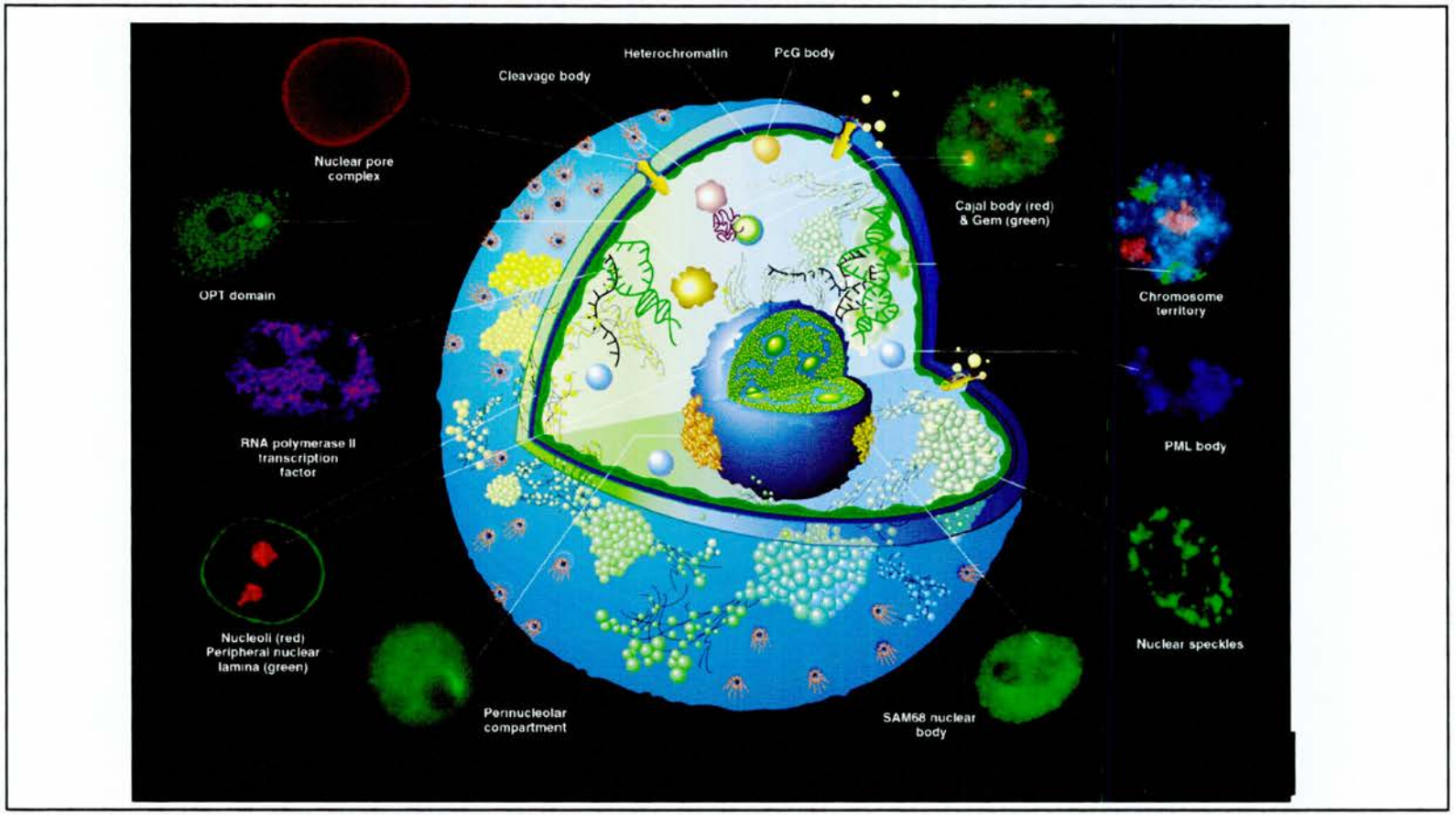

Figure 1.9 Compartmentalisation in the interphase nucleus.
Many nuclear proteins exist in discrete protein domains that can be observed by light microscopy. These include Cajal bodies (containing TFIIF and –H proteins), PML bodies (Sp100 and others), splicing speckles (Sc-35 protein), SAM68 bodies, the perinucleolar compartment, nucleolus (fibrillarin and Ki67), RNA polymerase II domains and OPT (Oct-1 and PTF protein) domains. ***Taken from Spector, 2001.***

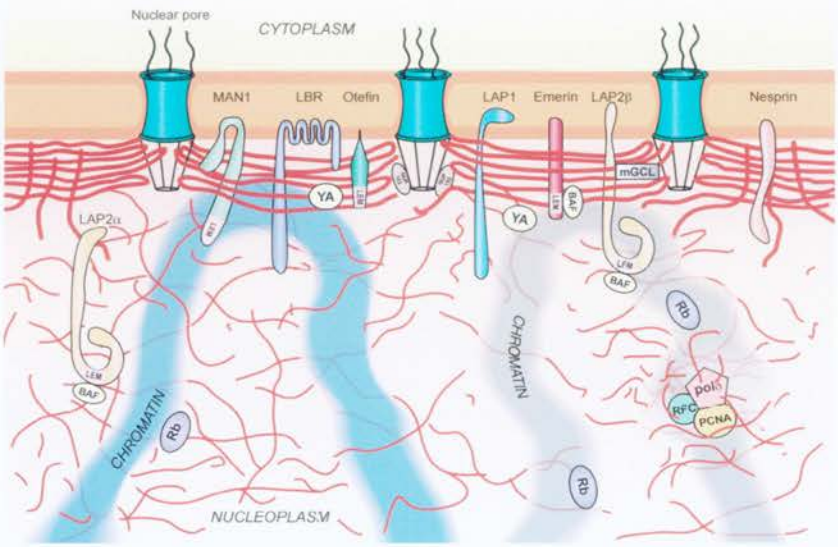

Figure 1.10 The nuclear periphery: nuclear membrane and lamina. Proposed interactions of lamins with inner nuclear membrane proteins, nuclear pores, and other nucleoplasmic factors (see text). The lamins predominantly located as a filamentous network (thick red lines) adjacent to the inner nuclear membrane, and are also thought to be distributed throughout the nucleoplasm (thinner red lines). Some known LEM domain proteins are shown binding lamins. LAPs 2α and 2β, MAN1, otefin, and emerin are depicted. Also shown are other factors that are thought to interact directly or indirectly with the lamins, including YA, BAF, Rb, LBR, LAP 1, mGCL, and nesprin. The possible association between lamins and nuclear pore complexes, perhaps through NUP 153 is indicated. Two interphase chromosome domains are also shown. One contains a DNA replication center containing a higher concentration of nucleoplasmic lamins, RFC, PCNA, and DNA polymerase . For details, see text. ***Taken from Goldman et al., 2002.***

The satellite sequences of HSA1 and the Y chromosome are positioned within the nucleolus during G1 (Bridger et al., 1998) and the internal chromosome territories of HSA 17 and -19 are in very close proximity to the nucleolus (Bridger et al., 2000). It may also be significant that HSA18 is not seen to localise to the nuclear periphery until the nucleolus is formed in proliferating fibroblasts (Bridger et al., 2000).

1.5.2 The nuclear lamina

The nuclear periphery of mammalian cells consists of the nuclear lamin (Goldman et al., 2002) and the nuclear membrane (see section 1.5.3). The ultrastructure of the nuclear lamina was originally described, following EM analysis of *Xenopus* oocytes and rat hepatocytes, as a filamentous layer 20-50nm thick (Dwyer and Blobel, 1976; Aebi et al., 1986). It is a meshwork of type V intermediate filaments, the lamin proteins (Fuchs and Weber, 1994) anchored to the inner nuclear membrane (INM, Figure 1.10; see section 1.5.4). The lamin family of filaments is conserved through evolution, although not present in yeast or plants (Benavente and Krohne, 1986; Doring and Stick, 1990) and lamins are classified as type A or B based on amino acid sequence, expression profile and behaviour during mitosis (Stuurman et al., 1998). They are subject to post-translational farnesylation and carboxymethylation at the C-terminus and these modifications are thought to be responsible for targeting to the nuclear membrane (Vorburger et al., 1989; Weber et al., 1989). Type B lamins have a ubiquitous expression pattern while type-A proteins are expressed only in differentiated cells (Stick and Hausen, 1985; Rober et al., 1989; Lehner et al., 1987). Type-A lamins include lamins A and C, alternatively spliced products of the same gene (Figure 5.1; McKeon et al., 1986; Fisher et al., 1986). The first 566 amino acids are identical between the two proteins, with lamin C 98 amino acids shorter than lamin A. This truncation removes a CaaX motif (C, cysteine; a, aliphatic; X, any amino acid) which is targeted by post-translational modification. Pre-lamin A is proteolytically cleaved after incorporation into the lamina to yield mature lamin A (lacking 15 amino acids at the C-terminal tail; (Weber et al., 1989; Sinensky et al., 1994; Sasseville and Raymond, 1995).

Lamins assemble into filaments through hierarchical interactions forming dimers and eventually protofilaments (Stuurman et al., 1998). Many of the interactions are controlled by phosphorylation/dephosphorylation events, and the kinases/phosphatases responsible link lamina assembly and break down to the cell cycle machinery (Moir et al., 1995; Dyer et al., 1997; Moir et al., 2000).

The nuclear lamina has been implicated in many important cellular events including maintenance of nuclear size, spacing of nuclear pores, determining nuclear shape and transcription and replication (reviewed in Hutchison, 2002). Immunodepletion of lamina in cell extracts results in nuclei of smaller size (Meier et al., 1991; Newport et al., 1990); this is also observed in experiments using dominant negative lamins (Spann et al., 1997; Ellis et al., 1997). There is a role for lamins in the nuclear pore spacing as nuclear pores aggregate in D*rosophila* knockouts of *lamin* Dm_0 (Lenz-Bohme et al., 1997).

That lamins influencing nuclear shape is suggested by the discovery of germ cell specific lamins which are thought to be responsible for the hooked shape of mouse sperm nuclei (Furukawa and Hotta, 1993). In addition to this, RNAi of lamin gene *lmn-1* in *C.elegans* results in changed nuclear morphology in treated worms (Liu et al., 2000). The phenotypes of lamin null mammals are discussed in chapter 5.

Lamins are known to be a network of intertwined filaments attached to the INM, but they have also been identified in internal nuclear aggregates that associate with condensed chromatin and PCNA (Goldman et al., 1992; Bridger et al., 1993; Moir et al., 1994; Fricker et al., 1997). This suggests that they may have additional functions as nuclear matrix components or mediators of replication and transcription. In the immunodepletion experiments mentioned above, DNA replication is functionally (Meier et al., 1991) or physically (Newport et al., 1990) disrupted as nuclei fail to organise replicon clusters and initiate replication. Further experiments using dominant negative lamin proteins have attempted to clarify which phase of replication lamins are involved in, however, the results so far are inconclusive (reviewed in Hutchison, 2002). It has not yet been explicitly demonstrated whether lamins specifically influence the initiation or elongation of DNA replication. There is evidence to suggest that lamin proteins also influence gene expression because they are predominately located at the nuclear edge, a location associated with silencing. In *Xenopus* eggs dominant-negative lamin A disrupts RNA polymerase II foci, splicing speckles and inhibits mRNA synthesis (Spann et al., 2002). Interactions have also been described between lamins, their associated proteins (see section 1.5.3) and transcription factors Oct-1 (Imai et al., 2000), mouse Germ cell-less and E2F-associated proteins (via LAP2β; (Nili et al., 2001).

1.5.3 The nuclear membrane

The nuclear membrane is an important cellular structure as it presents a physical barrier between transcription and translation. It is a double membrane consisting of two sides, one adjacent to the nucleoplasm (the inner nuclear membrane, INM) and one adjacent to the cytoplasm (the outer nuclear membrane, ONM). The lumen between these two membrane surfaces is continuous with that of the endoplasmic reticulum (ER). The nuclear membrane is perforated by large protein assemblies, the nuclear pore complexes (NPCs), that facilitate macromolecule exchange (both active and passive) between the nucleoplasm and cytoplasm (reviewed in Suntharalingam and Wente, 2003). NPCs are implicated in interphase chromatin organisation in yeast. The NPC components Nup2 and Sir proteins are involved in tethering heterochromatin and telomeres to the nuclear edge (Hediger et al., 2002; Ishii and Laemmli, 2003). The protein Esc1 has been identified as a binding partner of Sir proteins in yeast and is also involved in tethering chromatin to the nuclear edge (Andrulis et al., 2002).

INM proteins are synthesised in the rough ER and diffuse through the membrane to the nuclear membrane where they become anchored by interactions with the nuclear lamina (section 1.5.3, Table 1.1; Burke and Stewart, 2002). These include Man-1, emerin, and many isoforms of lamin associated proteins 1 and 2 (LAP-1, -2; (Foisner and Gerace, 1993). Proteins such as Lamin B receptor (LBR; (Worman et al., 1988) and LAP-2β (Foisner and Gerace, 1993; Furukawa et al., 1998) also show binding affinity for lamin B in *in vitro* assays. LAP-2α and all LAP-1 isoforms bind only lamin A while emerin show no preference and binds to both A and B type proteins (Dechat et al., 2000). Another family of proteins, the nesprins have been located to the INM (Zhang et al., 2001a), including nesprin-1 (=Syne-1=Myne-1; (Apel et al., 2000) and nesprin-2 (=Syne-2; (Mislow et al., 2002b). Nesprin-1α has been shown to bind both emerin and lamin A (Mislow et al., 2002a). In *Drosophila*, the INM proteins otefin and young arrest (YA) interact directly with lamin D_m, however, there are no documented mammalian homologues for these proteins as yet (Ashery-Padan et al., 1997 ; Goldberg et al., 1998).

It is proposed that the lamina acts a bridge between chromatin and the nuclear envelope and is therefore involved in anchoring certain chromatin regions to the edge of the nucleus (Figure 1.10). Several INM proteins contain a ~40 amino acid LEM domain (*L*AP, *E*merin, *M*AN) which can bind DNA and chromatin *in vitro* (Foisner and Gerace, 1993; Ye and Worman, 1996; Dechat et al., 2000). This LEM domain can also bind Barrier against Auto-integration Factor (BAF) protein (Lee et al., 2001). As BAF is a DNA-binding chromatin-

associated protein, this binding partnership further links the lamina and chromatin (Lee and Craigie, 1998; Segura-Totten et al., 2002). Additional interactions include LAP-2β and LBR binding HA95, another chromatin associated protein (Martins et al., 2003).

1.6 NUCLEAR LOCATION AND CONTROL OF GENE ACTIVITY

The linear human genome contains both widely expressed housekeeping genes and genes that are expressed under temporal and/or tissue-specific control. The non-random arrangement of chromatin domains gives weight to the idea that chromosomes adopt a structured organisation in order to influence this orchestrated gene expression (Leitch, 2000). It has also been shown that highly expressed genes are clustered together along the length of the chromosomes (Caron et al., 2001; Versteeg et al., 2003).

Location and context are known to be important to gene expression in model organisms, however, we know less of the significance of this in human cells. Study of this phenomenon can focus at two distinct levels: that of the actual 3-D nuclear position of a gene locus or of the relative locus position within its associated chromosome territory. An increasing body of evidence shows that transcriptional control may well be influenced by both of these relationships.

1.6.1 The nuclear periphery and silencing

The nuclear periphery is a region classically associated with inhibition of gene expression in model organisms. Transcriptional repression can be reimposed at a crippled mating-type locus (Andrulis et al., 1998) or a telomeric reporter gene when known silencer *RAP1* is mutated (Andrulis et al., 2002) when these loci are artificially tethered to the nuclear periphery. Gene silencing at the mating type locus and telomeric genes is dependent on recruitment of Sir proteins and formation of heterochromatin at these loci (Gartenberg, 2000). Sir proteins were subsequently shown to be involved in targeting these silenced sequences to the nuclear periphery (Andrulis et al., 1998). The proteins yKu (Galy et al., 2000), Mlps (Strambio-de-Castillia et al., 1999) and Esc (Andrulis et al., 2002) have been shown to play a role in tethering silent loci to the nuclear membrane. Mlp1 and Mlp2 (myosin-like proteins) are extensions of the nuclear pore complex that interact with Yku70, a telomere-associated protein (Galy et al., 2000).

Protein	Binding Domain	Protein Interactions
Lamin Associated Protein (LAP) 1A	Unknown	A/B-type lamins
LAP1B*	Unknown	A/B-type lamins
LAP1C*	Unknown	A/B-type lamins
LAPB2β	LEM domain	B-type lamins, chromatin proteins BAF and HA95
LAP2ε, δ, γ+	LEM domain	Binding partners yet to be determined
Lamin B Receptor (LBR)	LEM domain	B-type lamins, chromatin proteins HP1 and HA95
Emerin	LEM domain	A-type lamins, chromatin protein BAF
Nurim	Unknown	Unknown
MAN1	LEM domain	Binding partners yet to be determined
Syne1 (Myne1, Nesprin1)	Unknown	A-type lamins and emerin Possible self-association
Syne2 (Nesprin2)	Unknown	Unknown Several splice variants

Table 1.1 Human Inner Nuclear Membrane Protein Interactions.

Several INM proteins are known to bind lamina components and some of the interaction domains have been characterised.

Adapted from (Burke and Stewart, 2002). *splice variant of LAP1A, +splice variants of LAPB2β

This protein interaction was considered to dock telomeres to the nuclear periphery, leading to repression of gene transcription. However, a recent report from S. Gasser and co-workers has demonstrated that there are two partially redundant mechanisms involved in tethering sequences at the nuclear periphery in yeast (Hediger et al., 2002). In their model, yKu is responsible for anchoring sequences at the nuclear edge in G1 in an Mlp-independent manner and during S phase, tethering is mediated by Sir proteins including Esc1. The association of particular loci with the nuclear periphery has also been described in *Drosophila.* In FISH experiments histone genes and satellite sequences are located at or near the nuclear envelope (Marshall et al., 1996). The human chromosomes with the lowest gene densities are located at, or near, the nuclear periphery (see section 1.4.3).

However, there is no evidence to support the hypothesis that each peripheral chromosome is transcriptionally inactive as a direct result of its localisation. Transcription is not limited to the centre of the nucleus as labelled nascent RNAs are distributed throughout the nucleoplasm (Verschure et al., 1999).

1.6.2 The nuclear interior and transcription

S-phase labelling of DNA with fluorescent nucleotides revealed that early-replicating DNA (the gene-rich R-bands) are preferentially located in the nuclear interior (Sadoni et al., 1999) and this is consistent with the clustering of gene-rich chromosomes there (Habermann et al., 2001; Boyle et al., 2001).

Movement of small chromatin domains in response to the cell cycle and gene activation has now been shown *in vivo* by a GFP-tagged gene locus in Chinese Hamster Ovary cells (Robinett et al., 1996; Tumbar et al., 1999). When a transgene is not transcribed, it is located near the nuclear membrane. On induction of transcription, the transgene shifts position and can be observed at a more internal nuclear site. A change in nuclear position in response to transcriptional state in these experiments may be a feature of large 'heterochromatic' arrays of exogenous sequence, and not a true reflection of the normal situation (Robinett et al., 1996). However, nuclear relocation has also been demonstrated for an endogenous locus in lymphocyte differentiation (Kosak et al., 2002).

1.6.3 Centromeric heterochromatin

Chromatin condensation is thought to play a role in control of gene expression and regions of heterochromatin are usually transcriptionally inactive. In D*rosophila*, transgenic insertion of centromeric repeats into the euchromatic *brown* gene leads to position-effect variegation (PEV) of gene expression and recruitment of this locus to endogenous heterochromatin (Csink and Henikoff, 1996; Dernburg et al., 1996). There is also evidence to support centromeric recruitment of silent chromatin in mammalian cells. Studies in murine B-lymphocytes that show inactive genes co-localise with Ikaros protein and centromeric heterochromatin during proliferation (Brown et al., 1997; Brown et al., 1999). However, these findings are disputed by experiments that indicate it is Ikaros-binding, rather than centromeric recruitment, that influences gene activity in B-lymphocytes (Sabbattini et al., 2001) by recruiting chromatin remodelling factors (Kim et al., 1999; O'Neill et al., 2000).

It is appealing to consider centromeric heterochromatin as a transcriptionally silent domain, with recruitment of a locus to this region ultimately controlling its expression. However, studies of adipogenesis suggest that recruitment to heterochromatin maybe a consequence of silencing rather than causative. CAAT/enhancer proteins (C/EBPs) regulate white adipose tissue differentiation (reviewed in Isogai and Tjian, 2003). Recruitment of C/EBPβ and –δ to pericentromeric heterochromatin potentiates increased histone acetylation (Zhang et al., 2001b) and TATA-box-binding protein targeting (Schaufele et al., 2001). This suggests that association with heterochromatin is not sufficient to silence gene expression in every situation (reviewed in Dillon and Festenstein, 2002)

1.6.4 Positioning relative to nuclear bodies

Several links have now been made between gene/chromosome loci and nuclear domains, the first of which was the association of the rDNA genes and the nucleolus (see section 1.5.2). A growing body of evidence suggests that nuclear organisation consists of many such 'preferred' associations. Although, it is not immediately evident if the close proximity between loci and protein domains has functional relevance or is merely a consequence of the limited available space in the nucleoplasm (reviewed in Lamond and Earnshaw, 1998; Dundr and Misteli, 2001).

The histone and U2 small nuclear RNA genes have been localised proximal to coiled (Cajal) bodies (Frey et al., 1999). In another study, promyelocytic leukaemia protein (PML) bodies were shown to associate with the major histocompatability (MHC) locus in primary human fibroblasts using immuno-FISH techniques (Shiels et al., 2001). There is some evidence to suggest that transcriptional activity of some genes may also influence interactions with particular nuclear protein domains. Nuclear speckles (containing pre-mRNA splicing factors such as SC-35) preferentially interact with actively transcribed genes, and contain their mRNA transcripts, in muscle fibres (e.g. myosin heavy chain; (Smith et al., 1999) and fibroblasts (collagen 1α1 and β-actin; (Xing et al., 1995). However, this is not perceived to be the case for every transcribed gene as dystrophin RNA does not appear to be synthesised proximal to Sc-35 domains (Smith et al., 1999). Recent work has suggested that large euchromatic regions (R-bands) and active genes within them, cluster proximal to particular Sc-35 domains (Shopland et al., 2003). The authors propose a model where Sc-35 domains create local euchromatic 'neighbourhoods'.

The true function of proximity relationships is poorly understood. There is evidence to suggest that associations between genes and protein domains influences transcription as in $PML^{-/-}$ mouse cell lines, the MHC I protein is downregulated (Zheng et al., 1998). However, this is contradicted by the recent discovery that in RNAi knockdown experiments or in the presence of mutant PML protein, MHC I expression levels are unaffected in human cells (Bruno et al., 2003).

1.6.5 Transcription and the chromosome territory

In recent years, much effort has focussed on the location of active transcription in the context of the entire nucleus. However, interest is also growing into how transcription might be organised within an individual chromosome territory.

The size of a chromosome territory is thought to be influenced by its gene density. Comparing the relative areas of the territories of HSA18 and –19 shows that the more gene-rich chromosome, HSA19, has a larger and, by inference, more decondensed territory (Croft et al., 1999). This is a logical extension of the models of chromatin fibre composition where a 'permissive'/active chromatin fibre is less condensed than heterochromatic regions. However, there is increasing support for the idea that heterochromatin is not as inaccessible to transcription factors as was first thought (Dillon and Festenstein, 2002).

1.6.5.1 Chromosome territory structure: The'modified' ICD model

In order to understand what influence a chromosome territory might have on gene activity it is essential to have an indication of how they are structured. The most up-to-date model of chromosome territory structure proposes that the nuclear volume consists of distinct chromosome territories of variable shapes and structural complexities (the chromosome-terriory-interchromatin-compartment-model [CT-ID], Figure 1.11; Cremer et al., 2000; Cremer and Cremer, 2001).

Chromosome territories are thought to consist of 'open' chromatin domains containing active genes and 'closed' domains containing inactive genes. Neighbouring chromosome territories are imagined to be discrete entities separated by a network of chromatin-free channels or spaces – the interchromatin domain (ICD). The ICD would be contiguous with the nuclear pores and weave between the individual territories to end between chromatin branches of 1Mb-100kb in length. These channels are thought to contain the macromolecular machinery required for transcription, RNA splicing and transport. Genes in 'open' chromatin domains

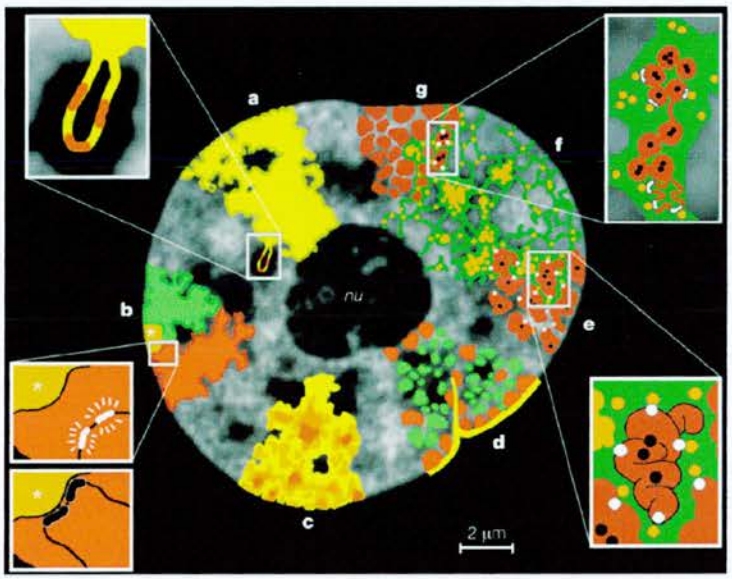

Figure 1.11 Modelling interphase nucleus architecture. Summary of experimental evidence supporting the CT-ID model, drawn approximately to scale on an optical section through a HeLa cell. (**A**) Chromosome territories (CTs) have complex folded surfaces, with some regions that loop out from the main body of the territory into the interchromatin space (IC). (**B**) CTs contain distinct domains for the centromeric domains (asterisks), short (p) and long (q) chromosome arms. Inset: transcribed genes (white) are remote from centromeric chromatin while recruitment of the same genes to centromeric heterochromatin leads to silencing (black). (**C**) CTs have variable chromatin density (high density = dark brown; low density = light yellow). (**D**) CTs consist of early- (green) and late-replicating (red) domains. Gene-poor chromatin is preferrentially located at the nuclear periphery and in close contact with the nuclear lamina (yellow) and the nucleolus (nu). Gene-rich chromatin (green) is located between the gene-poor compartments. (**E**) Higher order chromatin structures. Inset: topological view of gene regulation where active genes (white) are on the surface of chromatin fibres. Silenced genes (black) may be located towards the interior. (**F**) The CT-ID model predicts the IC (green) contains complexes (orange) for transcription, splicing and DNA repair. Inset: relationship between active genes (white) at the surface and inactive genes (black) in the interior. ***Taken from Cremer and Cremer, 2001.***

would therefore have access to transcription and splicing factors more readily than those situated within 'closed' domains. However, many FRAP experiments have shown that nuclear proteins can be very dynamic (reviewed in Dundr and Misteli, 2001) and recent work has shown that proteins such as HP1 are not permenantly bound to heterochromatic regions (Cheutin et al., 2003; Festenstein et al., 2003).

1.6.5.2 Positioning of active vs. inactive genes within territories

A number of studies using FISH techniques directly support the ICD model of territory organisation. They suggest that inactive genes are positioned towards the interior of chromosome territories while active genes are on the surface of the territory, adjacent to the ICD space (Dietzel et al., 1999; Nogami et al., 2000; Volpi et al., 2000). However, this contradicts studies describing the interphase distribution of early- and late-replicating DNA (Visser et al., 1998) and G-C rich sequences (Tajbakhsh et al., 2000) as they are found throughout the volume of territories.

The initial reports showing active gene transcription on the surface of chromosome territories focussed on individual selected loci. The authors of Mahy *et al.,* (2002) chose to determine the position of genes, both active and in-active, along the length of a contiguous chromatin fibre (HSA11 p arm; (Mahy et al., 2002b). They found that active genes were not always on the surface of the territory and expression is possible when a locus is inside the bulk of a chromosome territory. Interestingly, it was also found that at the scale of BAC/YACs (or gene by gene) the topology of chromosome territories is conserved; the mouse genomic region syntenic to the human region studied had the same pattern of territory localisation (Mahy et al., 2002b).

It has now been suggested that the structure of territories is influenced by the relative gene densities of chromosomal regions along a chromatin fibre reinforcing the idea that metaphase chromosome composition translates into interphase arrangement of chromatin. Several gene-dense regions of HSA11, -21 and –22 are predominantly extruded from their chromosome territories in FISH studies (Mahy et al., 2002a), along with other genomic regions, for example the MHC locus (Volpi et al., 2000) and the EDC locus (Williams et al., 2002). Treating cells with drugs which inhibit transcription, Actinomycin-D (ActD) and 5,6-dichloro-b-ribofuranosylbenzimidazole (DRB), reduced the percentage of loci visualised outside the territory (Mahy et al., 2002a). This would suggest that chromatin looping is influenced, but not driven, by transcriptional status.

The findings of gene signals outside of territories detected by chromosome paints shows the limitations of the techniques currently available to study chromosome territory topology. Current chromosome territory paints cannot outline the whole domain of a chromosome, and highlight only the most condensed regions. As recent studies have shown, some chromatin loops extruded from their chromosome territory are not detected by whole chromosome paint (for example, (Williams et al., 2002; Mahy et al., 2002b). Higher resolution analyses are required to understand the relationship between linear chromatin fibres and chromosome territory structure. Genetic loci are known to protrude from the body of chromosome territories yet we have little knowledge of whether they have a preferred nucleoplasmic destination or the molecular details of the neighbourhood they find themselves in. Some researchers have described relationships between loci and nuclear domains, although no clear function has been ascribed (see section 1.6.4). It is possible that genes that are regulated in a temporal or developmental manner may aggregate in nucleoplasmic domains to aid orchestrated expression or repression. EM analysis suggests that while interchromatin spaces are observed, decondensed chromatin from neighbouring territories can be seen in contact (Visser et al., 2000).

1.7 Dynamics of large-scale chromatin organisation

Much of what we know of the structure of chromosomes during both interphase and metaphase comes from microscopy of fixed cellular material in 2- or 3-dimensions. Advances in FISH and IF protocols now enable us to observe chromosomes or subdomains in 3-dimensions. Therefore they are simply a representation of the nuclear situation at the exact time of fixation, and there may also be the problem of experimental artefacts.

As the interphase nucleus is an organelle of a living cell it is important to consider the 4th dimension of observation, time. In order to transcribe genes, grow and divide, the nucleus needs to be dynamic and poised to respond to its environment. Information can be gathered on protein dynamics by studying the mobilities of fluorescently tagged fusion proteins in live cell assays such as FRAP or FLIP (fluorescence loss in photobleaching, Figure 1.12; Lippincott-Schwartz et al., 2003). In FRAP analyses, a cell expressing fluorescent protein is imaged at low level laser intensity, and then a region of the cell is photo-bleached at high laser intensity (Figure 1.12A). The whole cell is imaged during the recovery period and the

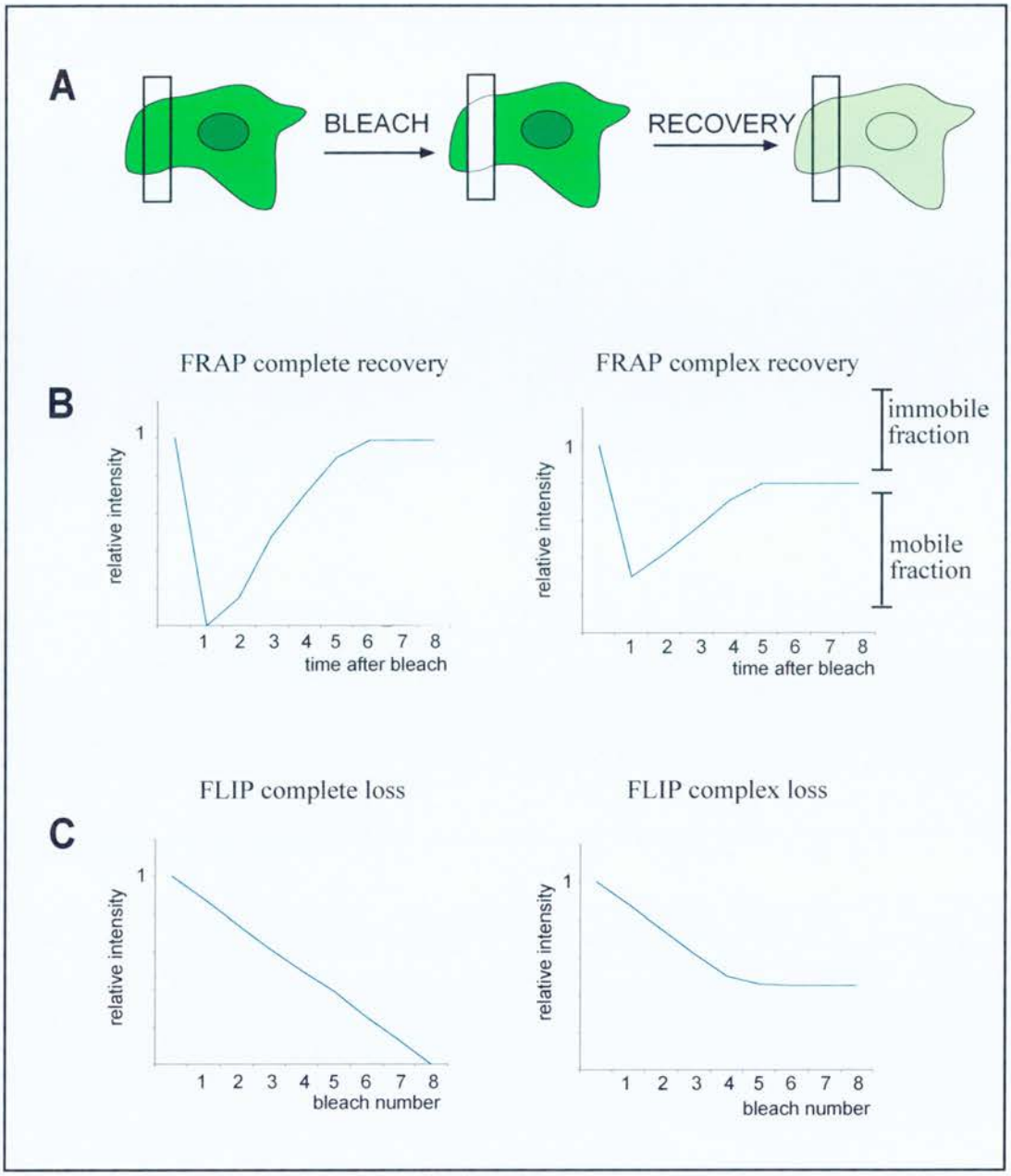

Figure 1.12 The principles of photobleaching techniques.
A cell expressing fluorescent proteins is imaged at low laser power before and after photobleaching inside the region of interest (ROI, black outline, **A**). In fluorescence recovery after photobleaching experiments (FRAP) the relative intensity of the ROI is measured over a period of time following a single bleach event (**B**). An unbound protein or highly mobile protein will completely recover 100% of the pre-bleach intensity rapidly (left). When a full recovery is not evident following FRAP, the percentage of the protein population that is immobile or mobile protein can be calculated (right). In fluorescence loss in photobleaching experiments (FLIP) an ROI is repeatedly bleached and the relative intesity of the bleach region decreases over time. Measuring the fluorescence intensity of a region adjacent or distant from the bleach regions allows the diffusion rates of the fluorescent protein to be calculated (**C**). When a protein can freely diffuse between the bleach ROI and other cell compartments a straight line is recorded (left), when there is a percentage of immobile proteins or complex protein dynamics a hyperbola is recorded (right).

percentage of fluorescence recovery is recorded (Figure 1.12B). Mobile proteins will recover pre-bleach fluorescence intensity levels while proteins with an immobile fraction will only be capable of recovering a percentage of the pre-bleach intensity. FLIP analysis is an application of photobleaching techniques that allows for the relationships between cell compartments to be addressed. A small region of a cell is continually bleached for successive rounds in FLIP analyses, and the fluorescence of adjacent and remote regions of the cells is then measured following the bleaching rounds. Gradual loss of fluorescence within a region adjacent to the bleach suggests lateral diffusion between this region and the bleached region (Figure 1.12C).

Data from FRAP studies support the idea that the interphase nucleus is anything but static (Dundr and Misteli, 2001; Spector, 2003). Live cell microscope observations highlight that the nuclei of cells are subject to movement and can be seen to rotate around every axis of symmetry and alter their relative positions within the cytoplasm. As movement is possible at this scale, it is more than reasonable to expect that smaller scale movements of particular chromosomes or chromatin fibres within the nucleus are also commonplace.

1.7.1 Chromatin motion in living cells

It was initially thought that during interphase, chromatin and chromosomes were immobile. Early studies of chromatin location over short periods of time (~2 hours) indicated that there were only very localised Brownian motions rather than defined movements (Abney et al., 1997; Zink et al., 1998; Manders et al., 1999). Time-lapse microscopy of HeLa cells transfected with GFP-cenpB protein showed very small centromere movements in this time scale (7-10μm/h; Shelby et al., 1996). Fluorescence recovery after photo-bleaching (FRAP) *in vivo* supported this as only constrained chromatin movements were visualised over short periods of time (Abney et al., 1997).

Microinjection of fluorescent nucleotides enables chromatin domains to be followed in living cells. Using a thymidine analogue Cy3 conjugate it is possible to visualise complete chromosome territories (Zink et al., 1998) in living cells. Studies using this labelling technique suggest that individual territories can change shape and rearrange sub-chromosomal foci within these territories over time (Zink et al., 1998). Recent experiments using GFP-H2B show that there is little large-scale chromatin movement during G1 using GFP-H2B FRAP (Walter et al., 2003).

By combining genetic manipulation and GFP technology we can begin to address the structure and behaviour of specific chromosome regions in living cells. Chromosomal integration of tandem arrays of the bacterial Lac operator sequence can be visualised with GFP-lac repressor proteins (Robinett et al., 1996). A bright GFP spot corresponding to the integration site can then be seen on the chromosome and observed in response to cellular events and environmental stimuli. This approach has now been applied to yeast (Li et al., 1998; Marshall et al., 1997), *Drosophila* (Vazquez et al., 2001), Chinese Hamster Ovary (Robinett et al., 1996) and human cells (Chubb et al., 2002). This technique has highlighted that the mobility of a genetic locus can be influenced by its interaction with and/or proximity to nuclear compartments. Comparison between loci at different 3-D interphase locations reveals that proximity to the nucleolus or nuclear periphery can restrict movement (Chubb et al., 2002). A nucleoplasmic GFP tagged-locus has a maximum range of movement of 1.5μm, while a nucleolar or peripheral locus is restricted to movements of 0.9 μm. These findings echo the situation described for budding yeast where telomeres move within a relatively small domain of the nuclear volume in comparison with loci distal from the telomeres of chromosome IV and XIV (Heun et al., 2001).

Studies in *Drosophila* and human cells suggest that the mobility of chromatin loci is due to Brownian motion (Zink et al., 1998; Bornfleth et al., 1999; Chubb et al., 2002). In contrast to this, motion was found to be active in budding yeast as the use of ATPase inhibitors reduced overall mobility of GFP-tagged loci in G1 (Heun et al., 2001). The authors propose that observed movements are therefore mediated by ATP-dependent chromatin remodelling factors (see section 1.2.2.2). In addition, this paper reports that DNA motion is restricted by the assembly of DNA replication complexes on chromatin fibres, as yeast strains with mutated replication origins showed increased locus movements.

It is also considered that chromatin motion may be a direct result of transcriptional activity (reviewed in Iborra and Cook, 2002). This model proposes that the transcriptional machinery aggregates in relatively immobile protein complexes, termed transcriptional factories. These factories are thought to be immobile, and in order for transcription to progress the chromatin fibre is actively pulled through the stationary factory and the DNA template is progressively scanned. The mobility studies in yeast support this model as during S phase there is a higher degree of chromatin motion (Heun et al., 2001), however the *Drosophila* and human studies suggest that chromatin motion is more passive than active. It is difficult to reconcile the contrasting observations in yeast, *Drosophila* and human cells. It

may be that the experimental techniques used in larger nuclei of flies and mammals are not sensitive enough to detect energy-dependent chromatin movements due to complications with ATPase inhibitor mechanisms or limits in microscopy resolution.

1.7.2 Cell cycle changes, quiescence and senescence

In contrast to few or restricted chromatin movements over a short space of time, chromatin domains and indeed whole chromosomes are capable of obvious relocation over periods of time equivalent to the cell cycle (reviewed in Leitch, 2000). Quiescent cells are no longer dividing and do not synthesise DNA, however they are capable of transcription and translation. Stimulating quiescent fibroblasts (GO) to return to the cell cycle (G1) induces movement of whole chromosomes. Chromosome 18 is located in the centre of the nucleus in quiescent cells (Bridger et al., 2000) and when these cells re-enter the cell cycle this chromosome moves from its internal position to the nuclear periphery. Early G1 has been identified as a period of dynamic chromatin movements (see section 1.7.1; Bridger et al., 2000; Walter et al., 2003). G1 was first identified as a period of increased chromatin motion where early- and late-replicating domains of CHO nuclei were differentially labelled using the thymine analogues 5-chloro-2'-deoxyuridine (CldU) and 5-iodo-2'deoxyuridine (IdU) in pulse-chase experiments (Dimitrova and Gilbert, 1999). In these experiments, the nuclear positions of early- and late- replicating sequences are established early in G1 in CHO cells, and this establishment of nuclear organisation can be supported by *Xenopus* cellular extracts *in vitro*.

B-lymphocytes have also been observed rearranging their chromatin when progressing from quiescence to cell division (Brown et al., 1999). During quiescence, inactive genes are distributed throughout the nuclear volume. When the cells are then stimulated to divide, these loci move towards centromeric heterochromatin domains and co-localise with the DNA-binding factor Ikaros. A change in the nuclear location of the centromere of HSA11 has also been described during peripheral lymphocyte activation (Tagawa et al., 1997).

In CHO cells, GFP-tagged heterochromatin of the HSR (homogeneously staining region) decondenses in mid- to late S phase, preceding the onset of DNA replication for this locus (Li et al., 1998). The authors document that this decondensation was concurrent with a movement of this locus from the nuclear periphery to the nuclear interior. It is perhaps expected that chromatin would relocate to some degree during S phase. At this time the

chromatin content is doubling and the nucleus is increasing in size, so some movements will be required to allow progression of the replication machinery.

There is an on-going debate whether cellular ageing (cellular senescence) may be responsible for changes in nuclear organisation. In support of this hypothesis there are reports of reactivation, and hence implied decondensation, of the Xi in mice (Wareham et al., 1987).

1.7.3 Differentiation

Terminal differentiation results in a specific gene expression pattern in a cell lineage which is faithfully inherited through any subsequent cell divisions. Multi-cellular organisms are comprised of many different cell types, the majority of which are terminally differentiated and quiescent. Does the nuclear organisation of chromatin influence the differentiation process or its inheritance?

Changes in the pattern of heterochromatin are evident in the differentiation of many cell types. During mouse oogenesis, four characteristic stages of ovarian follicle development are evident by the distribution of heterochromatin (Mattson and Albertini, 1990). There is evidence that differentiation into particular cell lineages requires condensation of peripheral heterochromatin (mediated by myeloid and erythroid nuclear termination stage-specific protein, MENT) in haemotopoetic cells (Grigoryev et al., 1999). In addition, *in vitro* differentiation of myoblasts (Chaly and Munro, 1996) and neurons (Choh and De Boni, 1996) results in the redistribution of centromeric heterochromatin to the nuclear periphery.

The spatial organisation of chromosomes within the nucleus has been observed in fibroblast and lymphoblast cells (Boyle et al., 2001). While the territory locations are broadly similar in both these cell-types there are differences in the positions of HSA8 and -21. It is not known if these discrepancies in territory arrangement are significant to the gene expression profiles of fibroblasts or lymphoblasts. Quiescent human fibroblasts have been shown to have altered distribution of HSA18 as in proliferating nuclei it is at the nuclear periphery while in quiescent cells it is in the nuclear interior (see section 1.7.2).

Several studies have suggested that the ultrastructure of chromosome territories changes in response to changes in gene expression. Volpi *et al.,* (2000), reported a difference in the extrusion of the MHC locus from the bulk of HSA6 between active and resting B-

lymphocytes. The human epidermal differentiation complex (1q21) was observed outside its chromosome territory in highly expressing cells and within the territory in cells when it is not expressed (Williams et al., 2002).

1.8 THESIS RESEARCH

Some progress has been made in elucidating the pattern of interphase organisation of chromosomes. Initial experiments observed chromosomes of a similar size, but very different gene densities, to be found at diametrically opposed locations in the interphase nucleus (see section 1.4.3; Croft et al., 1999). As an extension of these original data, work within our laboratory was undertaken to describe the position of every interphase chromosome territory in primary human fibroblasts and lymphoblastoid cells. I began my research with this study and my contribution to the published data (Boyle et al., 2001) is documented in Chapter 3. Taking these findings together, a model of interphase organisation was proposed where chromosomes are arranged in the cell according to their relative gene densities, rather than transcriptional status. To consolidate this proposal, I decided to investigate the nuclear locations of a number of chromosomes in several established human cell lines to identify any similarities and/or discrepancies (Chapter 3). Differences in spatial organisation between cell lines could suggest which chromosomal regions might be involved in the cellular programming of terminal differentiation.

Identification of a conserved pattern of interphase chromatin positioning gives weight to the hypothesis that there is an active underlying mechanism. This may be the control of gene expression, or indeed maintenance of genome integrity and shielding of important genomic regions from DNA damage. It is not trivial to identify the functional significance of a phenomenon such as spatial organisation of interphase chromatin location. Hence, experiments were devised where the proposed mechanisms responsible for nuclear arrangement might be tested. By identifying some of the factors involved in establishing spatial organisation one might gain information as to the underlying biological significance.

It can be speculated that histone modifications play a role in influencing the nuclear location of chromatin. Heterochromatin, at least in model organisms, appears to link the nuclear periphery and gene silencing. As gene-poor chromosomes are preferentially located towards the outer edges of the nucleus in human cells, it would be interesting to determine if this is

mediated by the molecular composition of peripheral chromatin. Using a cell-permeable chemical inhibitor of HDAC enzyme activity, I selectively increased the levels of histone acetylation in cultured human cells (Chapter 4). In order to detect any changes there may be to the spatial distribution of interphase chromatin, I determined the relative distributions of histone modifications, centromeric heterochromatin and chromosome territories following treatment.

Many believe that nuclear domains play a role in maintaining the interphase locations of chromosomes and genetic loci (see section 1.5). Although this has been categorically demonstrated in yeast with the identification of proteins responsible for tethering telomeres to the nuclear periphery (see section 1.6.1, Hediger et al., 2002), there is only suggested nuclear tethering in mammalian cells (Kosak et al., 2002; Chubb et al., 2002). I chose to directly test for the existence of a nuclear tethering mechanism in mammalian cells (Chapter 5). I investigated the role of nuclear periphery proteins in mediating nuclear organisation by selectively targeting the nuclear lamina. I determined the spatial organisation of chromosomes and centromeres in cells expressing dominant disease-associated mutations of lamin A protein. The three aspects of my project share the common goal of gathering more information on how the spatial organisation of the nucleus is determined.

CHAPTER 2

MATERIALS AND METHODS

All reagents were obtained from Sigma or Roche unless stated otherwise.

2.1 MOLECULAR BIOLOGY

2.1.1 Bacterial strains

Competent *Escherichia coli* XL1-blue or commercially produced DH5-α (subcloning or library efficient, Invitrogen) were used for all cloning procedures. Cultures were grown in Luria-Bertani (LB) medium with shaking or on L-agar plates at 37 °C.

2.1.2 Generating competent bacteria

1ml of an overnight culture of XL1-blue was added to a 100ml LB medium culture and grown, with shaking, to an absorbance at 600nm of 0.5-0.8. Cells were pelleted at 500g, resuspended in 50ml 0.1M Calcium chloride and incubated on ice for 25 minutes. After pelleting, cells were resuspended in 10ml freezing mix (15% glycerol, 50mM $CaCl_2$ in dH_2O). Aliquots were snap frozen on dry ice and stored at –80°C until required.

2.1.3 Bacterial transformation

Competent cells were incubated on ice with plasmid DNA or ligation product (Section 2.1.6.5) for at least 30 minutes. Transformations were then heat shocked at 42°C for 45 seconds. After addition of 500µl of LB medium, reactions were incubated for at least 45 minutes at 37°C before being plated on L-agar plates containing the appropriate antibiotic for selection (Ampicillin or Kanamycin both at 50µg/ml). Transformation plates were then grown overnight at 37 °C.

2.1.4 Isolation of plasmid DNA

Single bacterial colonies were picked and grown overnight in 5 or 100mls of LB medium with shaking at 37°C. Plasmid preparations were then harvested from these cultures using commercial mini- or maxiprep kits (Qiagen). Briefly, bacteria are lysed under alkaline conditions. The lysate is then neutralised and passed through a silica-gel membrane that

selectively absorbs DNA. The membrane is then washed before the plasmid DNA is eluted with dH_2O.

2.1.5 Purification of DNA

2.1.5.1 Phenol/Chloroform extraction

An equal volume of buffered phenol/chloroform (50% buffered phenol pH>7.8/48% chloroform v/v, 0.5% isoamylalcohol) was added to the DNA preparation and voretexed. This was centrifuged at ~12,000g for 15 minutes. The top (aqueous) layer was decanted into a fresh tube, avoiding any white precipitate that may be present at the boundary between the two layers and an equal volume of chloroform added. Vortexing and centrifugation was repeated. Again, the top layer was decanted. Ethanol precipitation was then performed to concentrate the DNA (section 2.1.5.2).

2.1.5.2 Ethanol precipitation

$1/10^{th}$ volume 5M sodium acetate and 2 volumes 100% ethanol were added to the DNA sample, the tube was vortexed and then centrifuged at ~12,000g for 10 minutes. The supernatant was discarded and the pellet washed in 70% ethanol (v/v with dH_2O). Centrifugation was repeated and the supernatant discarded. The pellet was dried at room temperature and resuspended in an appropriate volume of dH_2O.

2.1.6 DNA digestion and preparation

DNAs were digested with restriction enzymes (New England Biolabs) in reaction buffer in accordance with the manufacturers' instructions. Digestion products were then analysed and/or purified by gel electrophoresis or cleaned by ethanol precipitation and used for further cloning steps.

2.1.6.1 Gel electrophoresis

1-2% horizontal agarose ('HiPure' Low EEO agarose, BioGene UK) gels in 1x TAE (90mM Tris-HCl, 90mM glacial acetic acid, 2mM EDTA pH8.0) were used with 1x TAE electrophoresis buffer to resolve DNA samples, PCR products and plasmid digestion products. All samples had 1 volume of 6x loading buffer (15% Ficoll 400, 0.25% Bromophenol Blue, 0.25% xylene cyanol) added to 5 volumes of sample. Commercially

available DNA size markers (ϕX174 DNA *HaeIII* digest and λ DNA *HindIII* digest, Promega and Invitrogen respectively) were diluted to 50ng/μl with 500ng loaded per well to enable size determination and quantification of DNA fragments.

Ethidium bromide (EtBr; 2,7-diamino-10-ethyl-9-phenyl-phenathridium bromide), a DNA intercalating stain, was added to molten agarose to approximately 0.5μg/ml before pouring a gel. Stained DNA was then visualised and photographed using the EagleEye II system (Stratagene) and a thermal printer (Mitsubishi).

2.1.6.2 Gel purification of DNA fragments

For purification, agarose gel slices containing the appropriate DNA fragments were dissected from gels using clean razor blades. The DNA was extracted from the agarose using a commercial kit (Qiagen). Briefly, gel slices are melted in equilibration buffer. The solution is then passed over a silica-gel membrane that selectively binds DNA. Washing this membrane removes EtBr and residual agarose. The DNA is then eluted in the required volume of dH_2O.

2.1.6.3 Measuring quality and quantity of DNA

DNA concentration was measured by gel electrophoresis alongside DNA of known concentration (Section 2.1.6.3) and/or spectrophotometrically. For this, DNA was diluted 1:100 in TE (10mM Tris-HCl, 1mM EDTA, pH 7) and transferred to a quartz cuvette. The absorbance or optical density (OD) at 260nm (A_{260}) was measured for DNA using an Ultrospec 3000pro, Amersham Pharmacia Biotech. An OD of one corresponds to ~50μg/ml of DNA. To determine the purity of nucleic acid, the A_{280} can also be measured. Pure DNA has an A_{260} /A_{280} of 1.8 and values lower than these indicate contamination by proteins, RNA or phenol.

2.1.6.4 Dephosphorylation of DNA fragments

Linear plasmid DNA digested with the appropriate enzymes for a cloning step was treated with shrimp alkaline phosphotase in accordance with the manufacturers' instructions. This removes 5' phosphates from the ends of the DNA backbone preventing reformation of empty circular plasmid DNA. This subsequently increases the yield of positive ligation products, as successful ligation should only be achieved when phosphates are donated to the backbone ends by untreated DNA fragments with compatible digested ends.

2.1.6.5 Ligation of DNA fragments

50ng of digested vector was incubated with 3 times the molar ratio of cloning insert. 200 U (0.5µl) T4 DNA ligase enzyme (New England BioLabs) and the appropriate volume of 10x reaction buffer were used per ligation reaction, typically in a total volume of 20µl. The reactions were incubated at room temperature for one hour or overnight at 16°C. Subsequently, 10µl of a reaction were then used for bacterial transformation (section 2.1.3).

2.1.6.6 Sequencing of DNA fragments

All cloning products were sequenced to monitor the integrity of recombinant plasmids and inserts. In a protocol similar to Sanger di-deoxy sequencing, BigDye Terminator v2.0 (ABI Prism) chemistry was used as follows: 200ng of plasmid DNA, 0.8µM sequencing primer and BigDye were diluted in dH_2O in accordance with the manufacturers' instructions to a final volume of 10µl. Reactions were run on a DNA Engine Tetrad (MJ Research) for 25 cycles of 96°C 30 seconds 50°C 15 seconds and 60°C 4 minutes. Reactions were cleaned by addition of $1/10^{th}$ volume 5M sodium acetate pH4.6 and 2.5 x volume 100% ethanol, incubated 20 minutes on ice and then pelleted at ~12,000g for 15 minutes. Pellets were washed once in 70% ethanol and dried. Resuspended reactions were run through 50cm capillaries on POP6 polymer gels (3100 Genetic Analyser, Applied Biosystems) and data collection was performed using v3.7 of the supplied software.

2.2 MAMMALIAN CELL CULTURE

2.2.1 Cell Counting

Cells were counted using a haemocytometer (Weber Scientific International Ltd.) which has a chamber 0.1mm in height with an etched grid of $1mm^2$, subdivided into 400 squares. Therefore the total volume defined by the grid was $1x10^{-4}$ ml and cell concentrations per ml were obtained by multiplying the total number of cells over the grid by 10^4.

2.2.2 Thawing cells from storage in liquid nitrogen

Cells suspensions (6% DMSO in foetal calf serum (FCS)) were stored in liquid nitrogen. After thawing, aliquots were washed once with culture medium to remove DMSO and then seeded into 25cm^2 culture flasks.

2.2.3 Culture of transformed human cell lines

All cells were incubated at 37°C with 5% CO_2 and tissue culture medium contained penicillin (10000 units/ml) and streptomycin (650µg/ml).

2.2.3.1 Suspension cells:

K562 cells (female chronic myeloid leukaemia-derived, Witt et al., 2000) were grown as suspension cultures in Roswell Park Memorial Institute 1640 medium (RPMI, Invitrogen) supplemented with 10% FCS. Cells were split 1:3 – 1:5 in fresh medium every 2-3 days.

2.2.3.2 Monolayer cells:

HT1080 (male fibrosarcoma-derived; Chen et al., 1983), HeLa (female adenocarcinoma; Gey, 1952), 293 (female adenovirus transformed embryonic kidney; Graham et al., 1977), SW13 (female andrenal gland carcinoma-derived; Leibovitz et al., 1973) and RITVA (primary fibroblasts carrying an aniridia-associated translocation were transformed with hTERT by C. Griffiths) cell lines were grown in high glucose Dulbecco's Modified Eagle Medium (DMEM, Invitrogen) supplemented with 10% FCS. Cells were grown to near confluence before splitting into fresh culture flasks. To split cells the medium was poured off, flasks were rinsed once with PBS (phosphate buffered saline) and monolayers were then covered in a small volume of 10% trypsin-EDTA and incubated at 37°C for 5 minutes. Gentle agitation dislodged cells. Medium was added and cells were then pelleted at 400g for 5 minutes before being re-plated or fixed.

For immunofluorescence (section 2.5) cells were seeded directly onto sterile coverslips (processed through washes of 2M HCl, 100% ethanol, ddH2O, 100% ethanol and then flamed) in 6 well dishes or microscope slides (soaked for at least 1 hour in 100% ethanol with ~2 drops 8M HCl and flamed) in quadriperm slide chambers (VIVASCIENCE, Satorius).

2.2.4 Culture of primary human fibroblasts

Two male primary fibroblast cell lines (1HD and 2DD) with normal karyotypes derived from foreskin tissue were obtained from Dr J. Bridger, Brunel University. Primary female fibroblasts (HF19) derived from lung tissue were a gift from Dr P. Jeppesen, Roslin Institute. Cells were grown in high glucose DMEM supplemented with 10% FCS and passaged with 10% trypsin-EDTA as described above (section 2.2.3.2). Cells were seeded at concentrations of $1x10^5$ per slide or 75 cm^2 tissue culture flask. Primary cell lines can be maintained for a limited number of cell passages before they senesce.

2.2.5 Addition of drugs to cell cultures

Drugs were added to cell culture media at the specified concentrations for the appropriate number of minutes/days. Each day the media was decanted from flasks and fresh media and drug was added.

2.2.6 Transfection of human cell lines

$2x10^6$ cells were seeded into 6cm^2 dishes and grown to near confluence. For each transfection, 200µl of DMEM alone was incubated with 5µl of Lipofectamine2000 (Invitrogen) for 5 minutes. This was added to a further 200µl of DMEM with 50ng of plasmid DNA and incubated for 20 minutes. Cells were washed once with PBS before the addition of DMEM supplemented with 10% FCS (without antibiotics) and the transfection mix. Transfection plates were incubated overnight at 37° C and then fixed for immunofluorescence or passaged and re-plated.

Stable cell lines expressing recombinant proteins were also generated. Overnight transfections were trypsinised and removed from the 6cm^2 dishes. Transfected cells were then seeded at varying densities on 9cm and/or 14cm dishes. Permanent expression of the plasmid was selected for by DMEM + 10% FCS supplemented with drug (G418-sulphate at 400µg/ml, Hygromycin-B at 500µg/ml and Blasticydin at 500µg/ml). The selective medium was changed every 2 days. After 8-14 days growth under selection, cells were rinsed twice with PBS and then a thin layer of PBS was left coating the surface of the plate. Individual colonies (representing clonal expansion of one transfected cell) were taken up in 6.5µl of 10% trypsin-EDTA and transferred to a single well of a 24-well plate. Colonies were grown up in selective medium until splitting into a larger culture plate was required.

2.2.7 Analysis of cell cycle profile

Cells were harvested using 10% trypsin-EDTA as described above (section 2.2.3.2) and resuspended in PBS. $1x10^6$ cells were pelleted and fixed overnight at 4°C in 0.3ml 50%FCS/PBS (v/v), 0.9ml 70% ethanol/PBS (v/v). Samples were washed once with 5mM EDTA/PBS and resuspended in staining solution (50μg/ml Propidium iodide w/v pH 7.4, 100μg/ml RNase v/v, 0.1% Sodium azide in PBS w/v) for 1 hour at room temperature in the dark. Flow-assisted cell sorting (FACS) was performed on FACScan (Beckton Dickson) and cell cycle profiles were generated using Cellquest analysis software.

2.2.8 Cultures for live cell analysis

HT1080 cells and derived stable lines were seeded at 1-2x 10^5 in 2ml of medium onto DeltaT 0.17mm live cell chambers (Bioptechs Inc, Pennsylvania) with heat conductive glass bases. After overnight incubation, 100μl of HEPES pH7 was added to the medium to help regulate pH during analysis. For observation of transient transfections, cells were seeded onto chambers on the first day, transfected with the appropriate expression plasmid on the second day (section 2.2.6) and prepared for live cell analysis on the third day.

2.3 PREPARATIONS FROM MAMMALIAN CELLS

2.3.1 Harvesting and fixing cells in 3:1 methanol:acetic acid (MAA)

After harvesting, cells were suspended in a mildly hypotonic solution (0.033M KCl, 0.017M tri-Sodium Citrate). The hypotonic solution was added drop-wise with constant agitation to a final volume of 10ml (the concentration of cells in hypotonic should be $<2x10^7$/ml). The cell suspension was left at room temperature for 10 minutes before centrifuging at 400g for 5 minutes. Cells were then fixed with fresh 3:1 methanol:glacial acetic acid. 2ml of fix were added drop-wise to the cells while the tube was agitated. A further 8ml of fix were added and the tubes were placed on ice for a minimum of 15 minutes or stored at -20°C overnight. Cells were fixed twice more and stored indefinitely at -20°C.

2.3.2 Preparation of three-dimensionally preserved nuclei

1HD human fibroblasts were grown on Superfrost plus microscope slides (BDH). Slides had been previously been boiled in detergent for 10 minutes, washed 10 times each in tap water and distilled water, then stored in methanol. Each slide was flamed and placed in a

quadriperm slide chamber (Satorius). $1.5x10^5$ cells were seeded on each slide in 5ml medium. Seeding at this density results in approximately 70% confluency (the optimum density of cells for 3D FISH) after a further 16 hours in culture. Slides were rinsed twice in PBS and then fixed in 4% paraformaldehyde (pFa)/PBS for 10 mins at room temperature. After washing in 3x PBS slides were then quenched in 50mM NH_4Cl/PBS for 10 mins. Slides were directly added to 0.5% Saponin (w/v)/0.5% Triton-X100 (v/v) /PBS for permeabilisation for 10 mins followed by 3x PBS washes. In order to maintain 3D structure of cells, slides were transferred to 20% glycerol (v/v, high grade)/PBS for at least 30 mins. Slides incubated in glycerol were then snap frozen in liquid nitrogen and thawed at room temperature before being returned to the glycerol solution. Five rounds of freeze/thawing were performed to increase nuclear accessibility to probe without further compromising structural intensity with use of harsher detergent steps. After the fifth freeze/thaw step slides were either transferred to –80°C for storage or processed for 3-D FISH as described in section 2.6.

2.4 ANALYSIS OF CELLULAR PROTEINS

2.4.1 Harvesting cellular proteins

Cells grown in culture dishes were washed twice with PBS. Cell were then lysed in equal volumes of PBS and 2xSDS (Sodium dodecylsulphate) protein loading buffer (125mM Tris pH6.5, 4% SDS w/v, 10% β-mercaptoethanol v/v, 20% glycerol v/v, 0.1% bromophenol blue) and scraped from the surface of the dishes. Samples were boiled for 5 minutes and stored at –20°C until required.

2.4.2 Resolution of proteins on SDS PAGE denaturing gels

Cell protein extracts were harvested as described above (section 2.4.1) and resolved by sodium dodecylsulphide polyacrylamide gel electrophoresis (SDS-PAGE). Samples were thawed on ice and sonicated at 5μA for 10 seconds before loading. Denaturing polyacrylamide minigels (10-12% acrylamide v/v, 0.39M Tris-HCl pH8.8, 0.1% SDS w/v, 0.1% Ammonium persulphate w/v, 0.04% N,N,N',N'-tetramethylethylene diamine (TEMED) v/v) with stacking gels (5% acrylamide v/v, 0.13M Tris-HCl pH 6.8, 0.1% SDS w/v, 0.1% Ammonium persulphate w/v, 1% TEMED v/v) were poured using 30% acrylamide (29:1 acrylamide:bis-acrylamide v/v, Severn Biotech). Gels were resolved in

electrophoresis tanks (Mighty Small, Hoefer) in Tris-Glycine running buffer (25mM Tris, 250mM Glycine pH 8.3, 0.1% SDS w/v) at 110V for 2 hours. Pre-stained protein markers (BioRad) were loaded to aid with analysis.

Resolved protein gels had stacking gels removed and were rinsed twice in ddH_2O. Gels were then submerged in Coomassie Stain (0.25% Coomassie Brilliant Blue R-250 w/v, 45% methanol v/v, 45% dH_2O v/v, 10% glacial acetic acid v/v) for 1 hour with gentle agitation. The stain was discarded and gels were incubated overnight in destain (30% methanol v/v, 10% glacial acetic acid v/v) with gentle agitation.

2.4.3 Western Blotting

After SDS-PAGE (section 2.4.2) protein samples were transferred to polyvinylidene difluoride (PVDF) membrane for further analysis by semi-dry Western Blotting. Briefly, gels had the stacking gel removed and were washed twice with ddH_2O. PVDF membrane (Hybond-P, Amersham Pharmacia Biotech) was rinsed with methanol, dH_2O and then equilibrated in semi-dry transfer buffer (24mM Tris, 192mM Glycine, 20% methanol v/v). Transfer apparatus (W E B Company, Washington) was assembled in accordance with the manufacturers' instructions with the gel and membrane sandwiched on each side by 3 pieces of 3MM paper equilibrated in transfer buffer. The apparatus was run at 20mA for 1 hour. Successful transfer of protein was assessed by Ponceau S staining of the membrane – membranes were rinsed with methanol and then incubated with Ponceau S stain (0.1% w/v, 5% glacial acetic acid v/v) for 2 minutes. After two rinses with dH_2O membranes were visualised.

Membranes were blocked for 1 hour with agitation in 1x TS (150mM NaCl, 10mM Tris-HCl) with 5% milk protein (Marvel). Primary antibodies were diluted in 5% milk, 1xTS and incubated with membranes overnight at 4°C with shaking (antibody dilutions are shown in Table 2.1). Membranes were washed 3 times in 1xTST (1xTS, 0.05% Tween-20 v/v) and incubated with secondary antibodies (Table 2.2) for at least 1 hour. After a further 3 washes membranes were detected by enhanced chemiluminescence (ECL, Pierce) and signals were exposed on Kodak Biomax film.

Antibody	Species	Source	Dilution Factor
Anti-histone H3 C terminus (total)	Rabbit	A Verreault	1:5000
Anti-histone H4 acetylated lysine 9 (R41)	Rabbit	B Turner	1:5000
Anti-lamin A/C (Jol2)	Mouse	C Hutchison	1:10
Anti-GFP	Rabbit	Clontech, 8367-2	1:100

Table 2.1 Primary antibody dilutions for Western Blotting.

Antibody	Species	Source	Dilution Factor
Anti-mouse IgG (Fab) Horse radish peroxidase conjugate (HRP)	Goat	Sigma, A9917	1:5000
Anti-rabbit IgG (whole molecule) HRP	Goat	Sigma, A0545	1:5000

Table 2.2 Secondary antibody dilutions for Western Blotting.

Antibody	Species	Source	Dilution Factor
Anti-emerin	Goat	Santa Cruz, Sc-8084	1:250
Anti-lamin A	Goat	Santa Cruz, Sc-6214	1:250
Anti-lamin A /C (Jol2)	Mouse	C Hutchison	1:20
Anti-lamin A (Jol4)	Mouse	C Hutchison	1:20
Anti-lamin B	Goat	Santa Cruz, Sc-6216	1:250
Anti-nucleoporin (p62)	Goat	Santa Cruz, Sc-1915	1:250
CREST (Cummings)	Human	B. Sullivan	1:1000
Anti-Ki-67	Mouse	Sigma, P6834	1:100
Anti-histone H3 methylated at lysine 9 (linear)	Rabbit	Upstate, 07-212	1:500
Anti-histone H3 methylated lysine 9 (branched)	Rabbit	T Jenuwein	1:500
Anti-histone H3 acetylated lysine 9	Rabbit	Upstate, 06-942	1:250
Anti-histone H4 acetylated lysine 5 (R41)	Rabbit	B Turner	1:1000
Anti-Flag (M2, monoclonal)	Mouse	Sigma, F3165	1:200
Anti-Flag (polyclonal)	Rabbit	Sigma, F7425	1:200
Anti-fibrillarin	Rabbit	38F3, EnCor Biotechnology Inc	1:200
Anti-HP1α	Mouse	Chemicon International, MAB3446	1:250

Table 2.3 Primary antibody dilutions for immunofluorescence.

2.5 IMMUNOFLUORESCENCE

For immunofluorescence detection of proteins, mammalian cells were grown on slides as described (section 2.2.3.2). Slides were rinsed in PBS and fixed for 10 minutes in 4% paraformaldehyde (pFa) w/v/PBS, washed 3 times in PBS and permeabilised for 10 mins in 0.5% Triton-X100 v/v/PBS to allow antibody access. Slides were washed a further 3 times in PBS before being blocked for 5 minutes in 5% donkey serum/PBS v/v. Primary antibody dilutions in PBS were then applied to slides and incubated overnight in moistened chambers at room temperature. Slides were washed 3 times in PBS and secondary antibodies were applied and incubated for at least 1 hour in moist chambers at 37°C. All primary antibodies are listed in Table 2.3. All secondary antibodies were species-specific fluorescein or Texas

Antibody	Species	Source	Dilution Factor
Anti-rabbit FITC conjugate (IgG, heavy & light chain specific)	Donkey	Jackson Labs, 711-095-152	1:100
Anti-rabbit Texas Red conjugate (IgG, heavy & light chain)	Donkey	Jackson Labs, 711-075-152	1:100
Anti-mouse FITC conjugate (IgG, heavy & light chain)	Donkey	Jackson Labs, 715-095-150	1:100
Anti-mouse Texas Red conjugate (Fab'2, heavy & light)	Donkey	Jackson Labs, 715-075-150	1:100
Anti-human Texas Red conjugate (IgG, heavy & light)	Goat	Jackson Labs, 109-076-003	1:100
Anti-human Texas Red conjugate (IgG, heavy and light)	Donkey	Jackson Labs, 709-076-149	1:100
Anti-human FITC conjugate (IgG, heavy & light)	Goat	Jackson Labs, 109-095-088	1:100
Anti-goat FITC conjugate (IgG, heavy & light)	Donkey	Jackson Labs, 705-095-147	1:100

Table 2.4 Secondary antibody dilutions for immunofluorescence.

Red conjugates obtained from Jackson Labs (Table 2.4). The slides were washed again and all slides containing human cells were mounted with 1μg/ml 4,6-diamidino-2-phenylindole (DAPI), in Vectashield (Vector), 0.5μg/ml for mouse. Coverslips were sealed with rubber solution (Pang) and slides were stored in the dark at 4°C.

2.5.1 Triton-X100 extraction of nuclear proteins

Cells grown on microscope slides were subject to Triton-X100 extraction of nuclear proteins before immunofluorescence (section 2.5). Slides were washed twice with PBS supplemented with 0.5mM $MgCl_2$ and 0.5mM $CaCl_2$ and then with CSK buffer (10mM Pipes-KOH, pH7.0, 100mM NaCl, 300mM sucrose, 3mM $MgCl_2$). To extract nuclear proteins, slides were then incubated with 0.5%Triton-X100 v/v/0.5mM PMSF/CSK buffer for 5 mins at room temperature. Slides were washed 3x CSK buffer and then fixed for 10 mins in 4%pFa/PBS before being processed for immunofluorescence as described in section 2.5.

2.6 PREPARATION OF FLUORESCENCE *IN SITU* HYBRIDISATION (FISH) PROBES

DNA was labelled using biotin-16-dUTP or digoxigenin-11-dUTP. These analogues were incorporated into DNA by PCR or by nick translation. Following either method, unincorporated nucleotides were removed and efficiency of labelling was assessed.

2.6.1 Preparation of labelled human chromosome paints by PCR

Human micro-dissected chromosome arms (gifts of Michael Bittner; Guan et al., 1996) were amplified on a PTC-225 DNA Engine (MJ Research).

Biotin-16-dUTP or digoxigenin-11-dUTP (dig-dUTP) was incorporated directly by PCR into chromosome paints by adding these analogues to the PCR reaction mix. To directly label chromosome paints the reaction mix was as follows: 1 μl of PCR template (from a second round of amplification of original template stock), 0.2mM dATP; dCTP; dGTP, 0.3mM dTTP, 0.6mM biotin- or dig-dUTP, 400ng primer ($^{5'}$CCGACTCGAGNNNNNNATGTGG$^{3'}$)

3 U Taq polymerase (Roche), 2.5mM $MgCl_2$, 5µl Cetus PCR buffer II (10x) and the volume of the reaction made up to 50µl with distilled water. Amplification conditions were 3 minutes at 94 °C then 30 cycles of 94 °C for 30 seconds, 56 °C for 30 seconds and 72 °C initially for 2 minutes extending by 3 seconds per cycle.

Alternatively, when the PCR products were too large (bigger than about 500bp), cold, ethanol precipitated PCR products were biotin- or dig-labelled by nick translation (Section 2.6.2).

All chromosome PCR fragments were resolved on 2% agarose gels in TAE (Section 2.1.6.3).

2.6.2 Preparation of human alpha-satellite sequence probe

Alpha-satellite probe was amplified from total genomic DNA (Weier et al., 1991). The reaction mix was as follows: 200ng genomic DNA, 300ng forward primer ($^{5'}$A(A/T)(G/C)T(A/C)ACAGAGTT(G/T)AA$^{3'}$), 300ng back primer ($^{5'}$ATC(A/C)C(A/C)AAG(A/C/T)AGTTTC $^{3'}$), 0.2mM dNTP, 2.5mM $MgCl_2$ 1U Amplitaq and buffer (10x) diluted in accordance with the manufacturers' instructions. The amplification cycle had an initial denaturing step of 94°C for 180 secs followed by 30 cycles of 94°C for 120 secs then 45°C for 90 secs increasing by 7°C per minute to 72°C. There was a final extension period at 72°C for 120 secs. For the generation of probes, the PCR was performed with 0.2mM of dATP, dCTP and dGTP, 0.03mM dTTP and 0.6mM of dUTP conjugated to either biotin or dig. A PCR product of ~181bp (alpha-satellite repeat doublet) was resolved on 2% agarose/1xTAE gels.

2.6.3 Nick translation

1-1.5µg of DNA were added to 4µl 10x nick translation salts (0.5M Tris-HCl pH7.5, 0.1M $MgSO_4$, 1mM DTT, 500µg/ml Bovine serum albumin [BSA]), 4µl each of 2mM dATP, dGTP and dCTP, 2µl of 0.5mM dTTP and 4µl 1mM biotin-16-dUTP or digoxigenin-11-dUTP (Roche). DNase I (Invitrogen) was freshly diluted to a concentration of 20units/ml in dH_2O at 4°C and 2µl added to the reaction mixture to give a final concentration of 1unit/ml. After the addition of 1µl T4 DNA polymerase I (Invitrogen, 10units/µl), dH_2O was added to make the total volume of reaction mixture 40µl. The reaction was mixed thoroughly and allowed to proceed at 16°C for 90 minutes. The reaction was stopped by placing at –20°C or immediately processes for removal of unincorporated label (section 2.6.3).

2.6.4 Removal of unincorporated label

Quick spin columns (Roche) containing G50 Sephadex beads were used to remove any biotin-16-dUTP or dig-11-dUTP that remained free in solution as per the manufacturer's instructions. Cleaned probes were eluted in TE pH 7.5.

2.6.5 Quantifying label incorporation

Gridded nitrocellulose membranes were prepared by soaking briefly in dH_2O followed by 20x SSC (3M NaCl, 0.3M tri-sodium citrate, pH7.4) for 10 minutes then allowing to air dry. Labelled DNA probes were diluted to $1x10^{-3}$ and $1x10^{-4}$ in TE and 1µl of each was spotted twice onto a gridded membrane. After the spots had dried, a further 1µl was added to one of each dilution. On the same membrane 20, 10, 2 and 1pg of labelled lambda DNA standards (Roche) were spotted. DNA was cross-linked onto the membrane by exposure to 30mJ of UV irradiation.

The membrane was immersed in buffer 1 (0.1M Tris-HCl pH7.5, 0.15M NaCl) for 5 minutes at room temperature, then blocked in 5% Marvel in buffer 1 at 37°C for 30 minutes. 10µl streptavidin-alkaline phosphotase (Boehringer) and/or anti-digoxigenin-alkaline phosphotase (Boehringer) were added to 10ml of buffer 1 and placed in a sealed polythene bag with the membrane for 30 minutes at room temperature with continuous agitation. The membrane was washed twice in buffer 1 then equilibrated for 5 minutes in 0.1M Tris-HCl, pH9.5. The colour reaction was developed by incubation of the membrane, in a sealed polythene bag, with 5ml of 0.1M Tris-HCl, pH9.5 and 2 drops from bottles 1-3 from the alkaline phosphotase substrate kit IV (Vector). The substrates in this colour reaction are 5-bromo-4-chloro-3-indolyl phosphate and nitroblue tetrazolium, which produce a blue reaction product. A complete colour reaction was observed within a few hours and an estimate of the concentration of DNA labelled probe was made by comparison with the lambda standards.

2.7 FLUORESCENCE *IN SITU* HYBRIDISATION (FISH) ON MAA-FIXED NUCLEI

2.7.1 Slide preparation

Glass slides were prepared by soaking in detergent solution and washing with dH_2O before storage in a dilute solution of HCl in ethanol. Immediately prior to slide making, slides were polished with muslin.

Methanol:acetic acid fixed cells (Section 2.3.1) were removed from storage at -20°C, left to warm to room temperature for 30 minutes and centrifuged at 400g for 5 minutes. Fresh MAA fix was added until the cell suspension reached a 'milky' appearance. A single drop of cell suspension from a fine-tipped pastette was dropped onto a horizontal microscope slide from a height of about 30cm. The spread of cells on the slide was improved by coating the slides with a thin layer of moisture, usually by breathing. An air humidity of ~50% also aided spreading. Spreading was monitored by phase contrast microscopy. Slides were stored for 2-6 days prior to hybridisation.

2.7.2 Hybridisation

Slides were first treated with 100µg/ml RNase in 2x SSC for 1 hour at 37°C, washed briefly in 2x SSC and dehydrated through an ethanol series (2 minutes each in 70%, 90% and 100% ethanol). The slides were left to dry under vacuum for 10 minutes before being heated in a 70°C oven for 5 minutes and immediately denatured in 70% formamide, 2x SSC pH7.8 at 70°C for 1-2 min. After passing through 70% ethanol at 4°C and an ethanol series as above, slides were again vacuum dried.

Concurrent with slide preparation the probes were prepared. Labelled probes (Section 2.6) (~200ng) suspended in TE were precipitated with 5µg salmon sperm DNA and human C_0t 1 DNA (Invitrogen, 5 to 50µg depending on the potential repeat content of the probe). After the addition of two volumes of ethanol, probes were spun down under vacuum until they had precipitated, and re-suspended in 10µl hybridisation mix (50% deionised formamide, 10% dextran sulphate, and 1% Tween 20, in 2x SSC). Commercial probes were usually provided in or with hybridisation buffer and did not require addition of salmon sperm DNA or human C_0t 1 DNA. All chromosome paints were denatured at 70°C for 5 minutes and reannealed at

37°C for 15 minutes before spotting onto pre-cleaned coverslips. The denatured slides were carefully laid onto the appropriate coverslip and sealed with rubber solution (TipTop) before placing in a covered metal tray in a 37°C water bath overnight.

2.7.3 Washing and detection

After removal of the rubber cement, slides were immersed in 2x SSC at 45°C for 4x 3 minutes, with gentle agitation to facilitate detachment of the coverslips. Slides were then washed 4x 3 minutes in 0.1x SSC at 60°C before transferring to 4x SSC/ 0.1% Tween 20. Detection was carried out in a moist chamber pre-heated to 37°C. Biotin was detected with sequential layers of fluorochrome-conjugated avidin (Fluorescein isothiocyanate- (FITC) or Texas Red- (TR) avidin), biotinylated anti-avidin, and a further layer of fluorochrome-conjugated avidin. Detection reagents were diluted in SSCM (4x SSC, 5% Marvel dried skimmed milk) to the appropriate concentration (Table 2.3). After incubation with 40µl SSCM for 5 minutes at room temperature, 40µl of the appropriate detection layer was applied to each slide (Antibodies and dilution are listed in Table 2.3). Slides were incubated in the moist chamber at 37°C for 60 minutes, followed by 3 washes of 2 minutes in 4xSSC/0.1% Tween20 at 37°C.

All slides containing human cells were mounted with 1µg/ml DAPI in Vectashield (Vector), 0.5µg/ml for mouse. Coverslips were sealed with rubber solution (Pang) and slides were stored in the dark at 4°C.

Antibody or fluorochrome-conjugate	Species	Source	Stock concentration (mg/ml)	Dilution
FITC-avidin CS	Goat	Vector	2.0	1:500
TR-avidin CS	Gost	Vector	2.0	1:500
Biotinylated anti-avidin D	Goat	Vector	0.5	1:100

CS - cell sorting grade

Table 2.3 Antibodies and fluorochrome-conjugates used for FISH

2.8 FISH ON THREE-DIMENSIONALLY PRESERVED NUCLEI

This method was used to maintain the three-dimensional architecture of nuclei (Kurz et al., 1996; Croft et al., 1999) through the process of FISH.

Cells were grown and fixed on slides, as described in Section 2.2.3. Slides were placed in PBS for at least 2x 30 minutes then incubated in 2x SSC, 100µg/ml RNase for 1 hour at 37°C. Following this, slides were returned briefly to PBS and then placed in 0.1M HCl in dH_2O for 7 minutes before being returned to PBS again. Slides were then denatured in 70% formamide, 2xSSC (pH7.O) for 3 minutes then 50% formamide, 2xSSC (pH7.O) for 1 minute, both at 75 to 78°C. Probes were applied immediately after the second formamide incubation. Probes were prepared, hybridised and detected as described above. Chromosome domains were always detected using FITC-conjugated secondary antibodies (Table 2.3).

2.9 FISH ON PARAFFIN-EMBEDDED HUMAN TISSUE SECTIONS

Paraffin-embedded sections of human tissues (7-10µm thick) mounted on slides using Vectabond (Vector) were a gift from Prof. B Lane, University of Dundee. Sections were prepared for FISH using techniques developed by Shelagh Boyle, MRC Human Genetics Unit (Dundas et al., 2001; Newsome et al., 2003).

Slides were heated in an oven to 60°C for 20 minutes in order to melt the paraffin. This was followed by 4 washes for 10 minutes in Xylene to dissolve residual paraffin. Sections were then taken through an extended ethanol series similar to 2- and 3-D FISH protocols (sections 2.7 and 2.8) involving 4x 10 mins in 100% ethanol, 2x 5mins 95% ethanol and 2x 5mins 70% ethanol. Slides were rinsed briefly in ddH_2O before microwaving at full power (850W) in citrate buffer (0.01M citric acid monohydrate, pH 6) for 20-30mins. Slides were then left to cool in the citrate buffer, washed in ddH_2O and then subject to a modified FISH protocol. Slides were rinsed in 2xSSC at room temperature before being placed directly into 2xSCC at 75°C. Slides were denatured for 3 mins in 70%formamide/2xSSC at 75°C and plunged directly into ice cold 70% ethanol for 3 mins. This was followed by an ethanol series

through 3 minutes each in 90% and 100%. 300ng of probe per section was prepared as per the 2-D FISH protocol (section 2.7.2) and incubated on slides overnight at 37°C. The following day slides were washed and probe signal detected as with 2-D FISH (section 2.7.3).

2.10 FLUORESCENT IMAGING AND PROCESSING

After FISH or immunofluorescence, 2D slides were examined using a Zeiss Axioplan fluorescence microscope with a 100 Watt mercury bulb and equipped with a triple band-pass filter (Chroma #83000). Grey scale images for each fluorochrome were collected with a cooled CCD camera (Princeton Instruments Pentamax) using IPLAB software v3.6 (Scanlytics, USA).

Microscope slides were scanned in a methodical manner, beginning at the bottom left hand corner, scanning to the right, then moving upwards and scanning the next row of nuclei from right to left, etc. For chromosome position analysis, fifty bin 2 images (using 63x oil immersion objective, Zeiss) were collected of consecutive nuclei that fulfilled the inclusion criteria; intact nuclei containing two visible chromosome domains were imaged. For the purpose of running analysis scripts (section 3.2.1), the captured images were also required to be single nuclei which did not touch any other.

2.11 CAPTURE AND ANALYSIS OF 3D IMAGES

2.11.1 Fluorescence imaging and processing

3-D stacks of colour images (up to three colour – DAPI, FITC and Texas Red) were captured using an Axioplan microscope fitted with a 100 Watt mercury bulb, Ludl filter wheel Chroma filter set #81000 and motorised stage, and attached to a cooled CCD Kodak KAF 1401e sensor camera (Princeton Instruments). A script was devised (P. Perry) using IPLAB software (v3.6, Scanalytics) to capture bin 1 or bin 2 resolution level images: The DAPI excitation filter is selected and a "live" focus window displayed. The plane of best focus is interactively selected, as is a region of interest for capture. The number of optical slices to be collected, the z distance between each optical slice and the exposure times for each

fluorochrome signal (from an automatic test capture in the plane of best focus) are also determined. The microscope focus motor then moves the stage downward for half the total depth of the focus series to the starting point for capture. To compensate for backlash in the focus mechanism, the stage is moved downwards a further 200 microns, followed by an upward movement of the same distance. Image capture begins, collecting the specified DAPI, FITC or Texas Red images at each focal plane and placing each into a stacked file. The stage is then moved upwards the specified *z* distance before repeating the same capture sequence. After the final plane has been captured, the stage is returned to the original "best focus" focal plane. The stack files are then merged to provide a colour stack file that can be animated or projected. For each nucleus 25 to 30 bin 1/bin 2 image planes were captured at 0.5 μm intervals, so as to include the whole of the nucleus in the image stack.

2.11.2 Confocal imaging

3-D colour image stacks were taken using a Zeiss LSM510 confocal microscope equipped with two Helium Neon (HeNe) lasers (1mW 543nm and 5mW 633nm respectively) and an Argon (1.5mW 458, 488, 514nm) laser. As excitation of DAPI was not possible with this microscope configuration in order to visualise DNA, DNA was instead counterstained with TO-PR03 (Molecular Probes, working dilution 1:10,000 in Vectashield), a far-red emitting DNA stain, and immunofluorescence was visualised with FITC or TexasRed secondary antibodies.

Image files were captured according to the manufacturer's instruction, using the supplied LSM510 software. Briefly, before an imaging session the optimal settings were determined by setting the pinholes of each channel capturing data to >1 micron, in addition to this if the Argon 1.5mW laser was being used, laser output was adjusted to ~50% with a tube current of 6.1mA (optimal for imaging). The 'palette' software option was used to define the appropriate detector gain levels to produce an image in which the signal was neither too saturated nor too faint. Again, 25-30 optical sections through the *z*-plane were captured at 0.5 micron steps for each nucleus. Single 3-D stacks of a nucleus or several taken over a period of time were taken as required

2.12 LIVE CELL CONFOCAL IMAGING

Cells growing on DeltaT 0.17mm culture dishes (Bioptechs Inc) were mounted onto a heated stage (Bioptechs Inc) on a Zeiss LSM510 confocal microscope. An objective warmer system (Bioptechs Inc) was also used to help maintain a stable temperature of the medium inside the culture dish. For movie capture, the time series software option was used specifying the appropriate time delay between rounds of 3-D stack capture. To allow for accurate analysis (see section 2.10.3), each bleach-treated live cell was imaged in a large canvas along with additional cells which were imaged, but not bleached.

2.12.1 Fluorescence loss in photobleaching

In fluorescence loss in photobleaching (FLIP) experiments, a region of GFP-lamin A signal was selected and bleached repeatedly over a short period of time. A 3-D stack of the chosen cell was taken before treatment. A region of interest (ROI) of the lamina in the mid-focal plane was selected. This ROI was bleached with 10 laser iterations at 100% of 50% total laser output (~6.1mA). Following the bleach, 5 images were taken at 2sec intervals using 8% of laser output. The bleach procedure was then repeated, up to 16 rounds of bleaching.

2.12.2 Fluorescence recovery after photobleaching

In fluorescence recovery after photobleaching (FRAP) experiments, a region of GFP-lamin signal was selected, bleached once and then imaged over a recovery period. A 3-D stack of the cell was again taken before treatment (8% of 50% total laser power). A selected region of the lamina in the mid-focal plane was then bleached with 100 iterations at 100% of 50% total laser output (~6.1mA). Immediately following the bleach, 13 single images in the same plane were captured at 1sec intervals. 3-D *z*-plane stacks were then taken of the cell at 5min interval for a period of 70mins.

2.12.3 Calculating relative fluorescence intensity for data analysis

The sum of pixel counts within a selected ROI was calculated using the option in the software (IPLAB v3.6). It is accepted that repeated fluorescence imaging of samples will result in a small but significant loss of fluorescence over time. To correctly analyse FLIP and FRAP data one must calculate the loss of fluorescence intensity over time within a selected ROI. In order to make the data as accurate as possible, I used a normalisation

equation to calculate the relative intensity (I_{REL}) of fluorescence in each ROI of interest (Phair and Misteli, 2000), this is summarised below

$$I_{REL} = \frac{T_0 I_t}{T_t I_0}$$

where T_0 is the total cellular intensity of an untreated cell in the image at time zero (pre-bleach), T_t is the total cellular intensity of this same cell at the timepoint, I_0 is the intensity of the ROI at time zero and I_t is the intensity of the ROI at timepoint.

CHAPTER 3

THE 3-DIMENSIONAL ORGANISATION OF CHROMOSOMES IN HUMAN NUCLEI

3.1 INTRODUCTION

More than a hundred years ago the concept of chromosome territories was introduced. Microscope observations of Rabl and Boveri first proposed interphase chromosomes were discrete (not amphorphous or intertwined) entities showing polarity. The advent of fluorescence microscopy and nucleic acid probe technology has provided sophisticated tools to investigate the interphase arrangement of chromatin (van der Ploeg, 2000).

The first experimental evidence for discrete organisation of chromosomes within the nucleus documented the relative positions of two human chromosomes of a similar size in DNA base pairs but with very different gene densities in interphase. The gene-rich chromosome, HSA19, was in the centre of the nucleus while the gene-poor chromosome, HSA18, was at the nuclear edge in lymphocytes and lymphoblasts (Croft et al., 1999). This is corroborated by studies of translocation event frequencies in the human genome (Bickmore and Teague, 2002). This reports that the translocation frequency of chromosome regions is related to their nuclear location and hence gene density, for example HSA18/19 translocations are rare, while HSA19/21 translocations are common. This organisation is conserved (Tanabe et al., 2002b), however it is not clear to what extent it is present in different cell types of the same organism. To investigate the behaviour of whole territories in different cell types I chose to analyse territory position of chromosomes in a variety of cultured cell lines and also human tissue. Identifying a constant pattern of organisation would help to consolidate a functional model for preferential organisation of chromosome territories.

3.2 CHROMOSOME TERRITORIES ARE RADIALLY ARRANGED IN PRIMARY FIBROBLASTS

My initial research began as an extension of the report detailing preferential nuclear positions for chromosome territories (Croft et al., 1999). The rationale was that by identifying the interphase arrangement of the entire chromosome complement we could begin to address any biological significance. 2-D FISH with PCR amplified chromosome paint (Guan et al., 1996) was performed on 3:1 MAA fixed nuclei preparations of each cell type (section 2.6 and 2.7). Analysis of chromosome paint distribution was then performed as described below.

3.2.1 Analysis method

A programme had previously been developed that calculates the distribution of FISH chromosome paint signal in an interphase nucleus (Figure 3.1; Croft et al., 1999). Fifty fluorescent images from a single plane of focus were captured for each FISH experiment and processed in turn. Slides were scanned in a methodical manner, from one side to the other. Images were captured of isolated intact nuclei with two distinct chromosome territory signals. Briefly, the DAPI signal of the image is outlined and the total area of the nucleus (the DAPI signal) is calculated. This area is then divided into 5 concentric shells or annuli of equal area (Figure 3.1A), where shell 1 is the outer shell and shell 5 is the nuclear centre. The intensities of the DAPI signal (i.e. amount of DNA) and the fluorochrome (i.e. amount of chromosome paint; Figure 3.1A) are calculated within each shell. The intensity of chromosome paint signal is then calculated as a proportion of the total DNA signal. To generate a distribution curve the mean value of paint signal in each shell is calculated across a data set of 50 images. The output is represented as a histogram and examples are shown in Figure 3.1B. A distribution showing a straight line at 1 represents an even distribution of DNA/chromosome paint in each nuclear shell, suggesting random distribution. In this discussion, 'peripheral' chromosomes are those which have the highest degree of signal in the outer two nuclear shells (1 and 2), while 'internal' chromosomes are those with the highest proportion of signals in shells 4 and 5.

This analysis determines the relative distribution of chromosome territories in 2-D fluorescent images. While it has been shown to be broadly representative of the 3-D

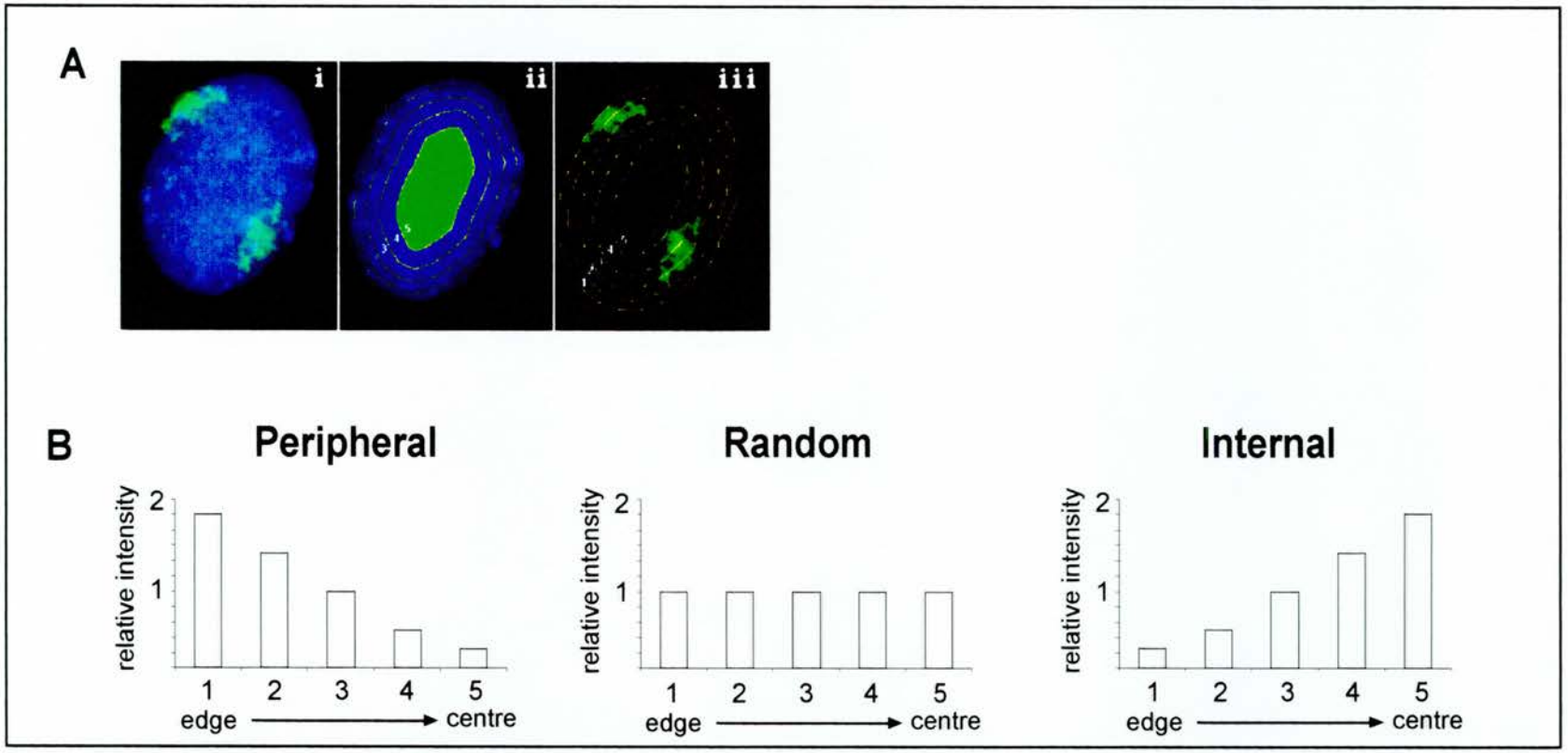

Figure 3.1 Erosion analysis of chromosome territory distribution in interphase nuclei.
2-D FISH images of 3:1 MAA fixed nuclei probed with whole chromosome territory paints are captured (**Ai**). The DNA signal (DAPI, blue) is segmented and divided into 5 concentric shells of equal area (**Aii**). The chromosome paint signal (FITC, green) is divided using the same 5 shells (**Aiii**). The relative intensity of chromosome paint signal within each shell is calculated as a ratio of the total DNA within the same shell (relative intensity = paint signal/DNA signal). The relative distribution of chromosome paint signal can be represented as a histogram (**B**). Peripheral chromosomes are enriched in the outer nuclear shells 1-2 (left), randomly distributed chromosomes show no enrichment in any shell (middle) and internal chromosomes are enriched in the central shell 4-5.

situation (Bridger et al., 2000; Mahy et al., 2002a) there are clear caveats. The collected fluorescent images are 2-D images of a 3-D object. A microscope focuses on the middle of the sample, but there will be some 'glare' from the remainder of the sample in the focal planes immediately above and below. This could be eliminated by focussing more accurately in the *z*-plane. However, any part of a chromosome territory at the top or bottom of the nucleus would be disregarded. For this reason alone, the 2-D image analysis appears to be a sufficient compromise.

Many researchers apply mathematical formulae and remodelling to address distribution in spherical and ellipsoidal shapes. 3-D analysis of the spatial distribution of chromosome territories is technically demanding and the statistics of this modelling are complex. Many analyses are based on physical measurements taken from fluorescent images, however, the optics of the microscopes can vary. Any conclusions drawn from such distribution analyses are only as valid as the microscope is accurate. It should also be remembered that many cells in culture and tissues have irregular nuclear shapes.

3.2.2 Chromosome territory distributions

The relative distributions of six chromosomes were determined in primary human dermal fibroblasts (male, passage 8) grown in 10% FCS and subsequently 3:1 MAA fixed. Previous analysis in female dermal fibroblasts indicated a peripheral distribution for the X chromosome (S. Boyle, personal communication). It was not known if this analysis was skewed due to the peripheral Xi Barr Body in female cells and hence, the distribution of the single active X chromosome in male cells was determined. The additional chromosomes (HSA12, 13, 16, 17 and 21) were analysed to complete a data set of territory distribution for the chromosome complement in this cell line.

Distribution histograms and representative images for each analysis are shown in Figure 3.2. It is clear that each chromosome does not follow the same pattern of interphase distribution in this analysis. HSA13 and the X chromosome are enriched in the outer nuclear shells while HSA21 is in the centre. HSA17 appears enriched in a 'mid-zone' of the nucleus, with a signal peak in shell 3. HSA12 has a distribution that is slightly skewed towards enrichment in the centre. Standard *t*-test analyses of the probability of chromosome territory signals being enriched in shell 1 vs. shell 5 reveal that the distributions of HSA13 and X signals are statistically significant ($P<0.0001$). Comparisons of shell 5 vs. shell 1 enrichment of HSA12, 16 and 21 chromosome paints have similar significance values ($P<0.0001$).

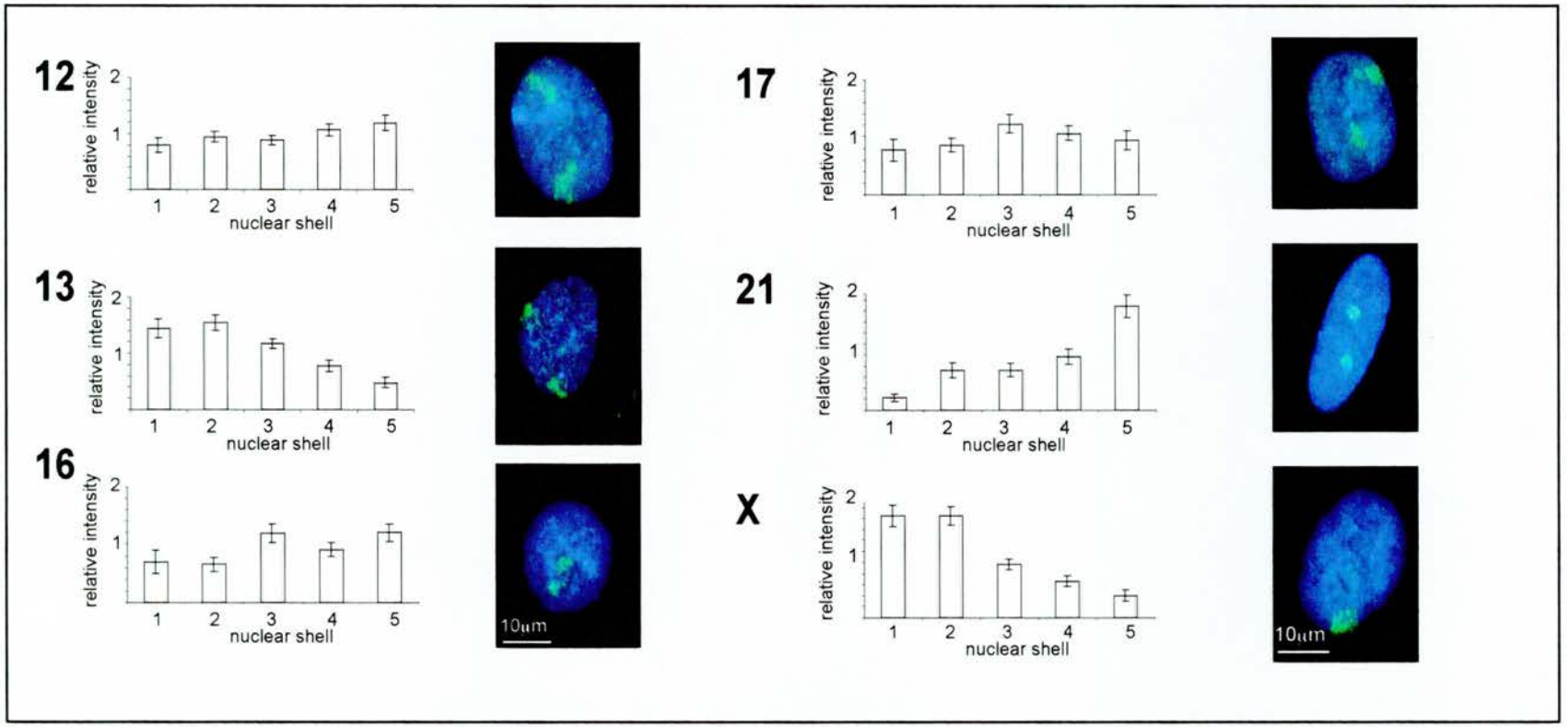

Figure 3.2 Relative distributions of chromosome territories in primary human skin fibroblasts. Chromosome territory distribution analysis was performed on 50 2-D FISH images of 3:1 MAA fixed primary fibroblast nuclei using whole chromosome paints. The mean distribution of relative chromosome paint signal (paint signal/DAPI signal) for each shell is represented as a histogram for HSA12, 13, 16, 17, 21 and the single X of male-derived cells (for discussion see text). Shell 1 represents the nuclear periphery and shell 5 is the nuclear centre. The error bars represent the standard error of the mean (S.E.M) for each data set. Blue = DAPI DNA, green = FITC chromosome paint.

The inactive X in female cells is found at the nuclear periphery (Belmont et al., 1986) and is evident as the Barr Body, a region of bright heterochromatic DAPI staining (see section 1.3.2; Lyon, 1961). Distribution analysis of X paint also shows a peripheral enrichment of this signal in female cells (S.Boyle, personal communication). It is therefore interesting that the single X chromosome in these male fibroblasts is peripheral (Figure 3.2). This would suggest that the X chromosome is located at, or near, the nuclear periphery when either active or inactive. Statistical comparison of the male vs. female X chromosome paint signals has a *P* value of 0.71 and hence this is not significant difference. I conclude that the peripheral location of the Xi is not sufficient to influence gene transcription.

All of these findings were reported along with the remaining data set for primary fibroblasts and the distribution of territories in lymphoblast cells (Boyle et al., 2001). It can be interpreted that the interphase chromosomes are broadly arranged with respect to their relative gene densities. Gene-poor chromosomes (e.g. HSA13, 18 and X; 2.9, 4.3 and 6.15 genes/Mb respectively, Ensembl Release 16.33.1, July 2003) are towards the outer edge of the nucleus while gene-rich chromosomes (e.g. HSA19; 22.5 genes/Mb) are towards the nuclear interior. The remaining chromosomes are not strictly arranged with respect to their gene densities; HSA12 and 17 (8.6 and 15.6 genes/Mb respectively) are randomly distributed while HSA16 and 21 (11.5 and 5.8 genes/Mb respectively) are towards the interior. This would suggest that factors other than gene density might influence the interphase location of a chromosome territory.

3.3 RADIAL ARRANGEMENT IS CONSERVED IN MANY CELL TYPES

To determine whether radial organisation is present in differentiated and transformed cells, analysis of chromosome territory location was repeated on a series of human cell types (section 2.2.3 and 2.2.4). Three primary fibroblast lines were compared - 1HD (male foreskin, passage 8), 2DD (male foreskin, passage 10) and HF19 (female lung, passage 14) -, in addition to HT1080 (fibrosarcoma), SW13 (andrenalcarcinoma), K562 (erythroid precursors) and 293 (embryonic kidney) cells. In general, the transformed cell lines (HT1080, SW13, K562 and 293 in Figures 3.3-3.5) all show strong conservation of a radial chromosome arrangement. In each of these cells lines, the chromosomes examined are located in relation to their relative gene densities; HSA13 and 18 are peripheral (Figures 3.3

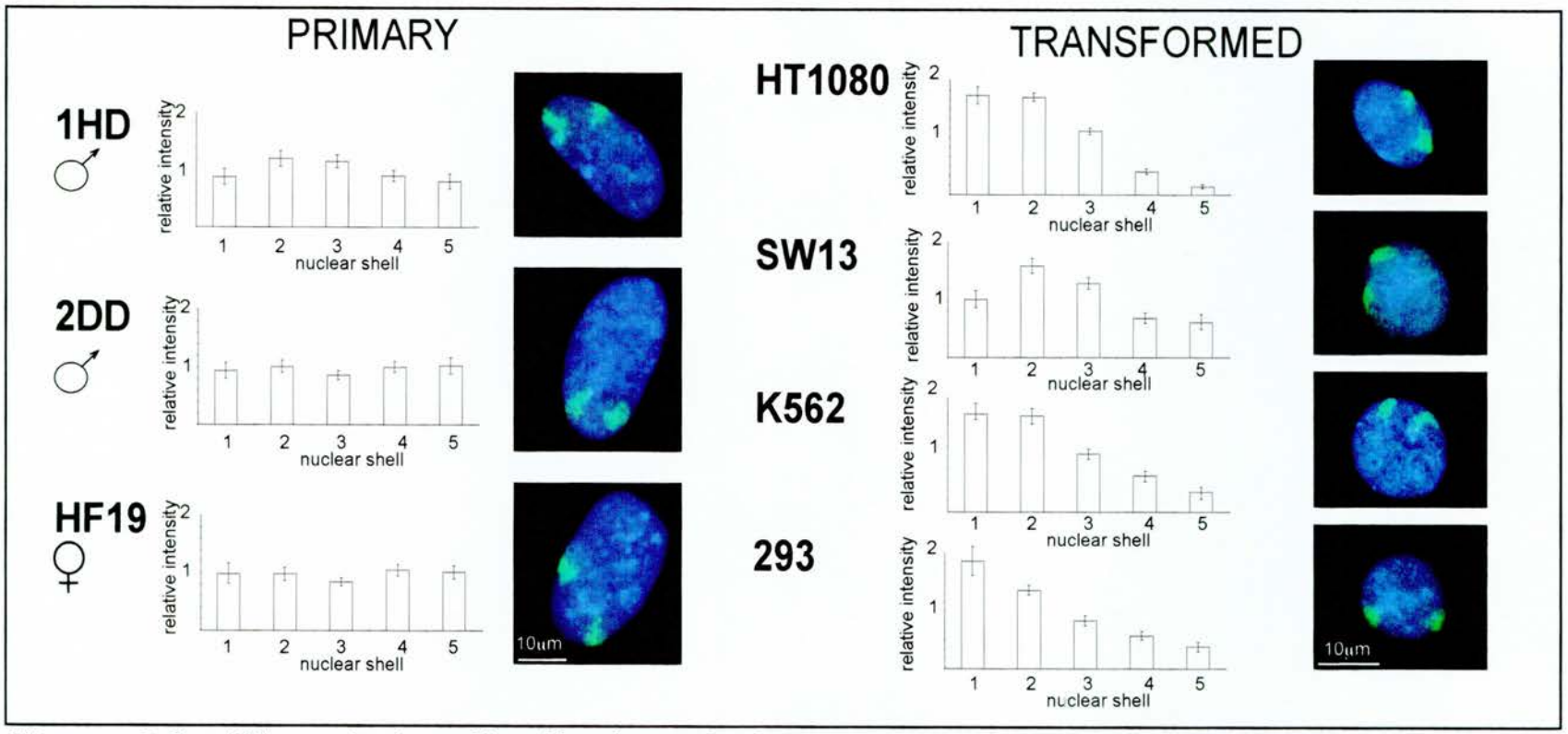

Figure 3.3 The relative distribution of chromosome 13 in different human cell lines. The distributions of chromosome 13 territories were analysed in 50 3:1 MAA fixed nuclei of primary (1HD, 2DD, HF19) and transformed (HT1080, SW13, K562, 293) cultured human cell lines (for discussion see text). The mean distribution of relative chromosome paint signal (paint signal/DAPI signal) for each shell is represented in a histogram. Shell 1 represents the nuclear periphery and shell 5 is the nuclear centre. The error bars represent the standard error of the mean (S.E.M) for each data set. blue = DAPI DNA, green = FITC chromosome paint.

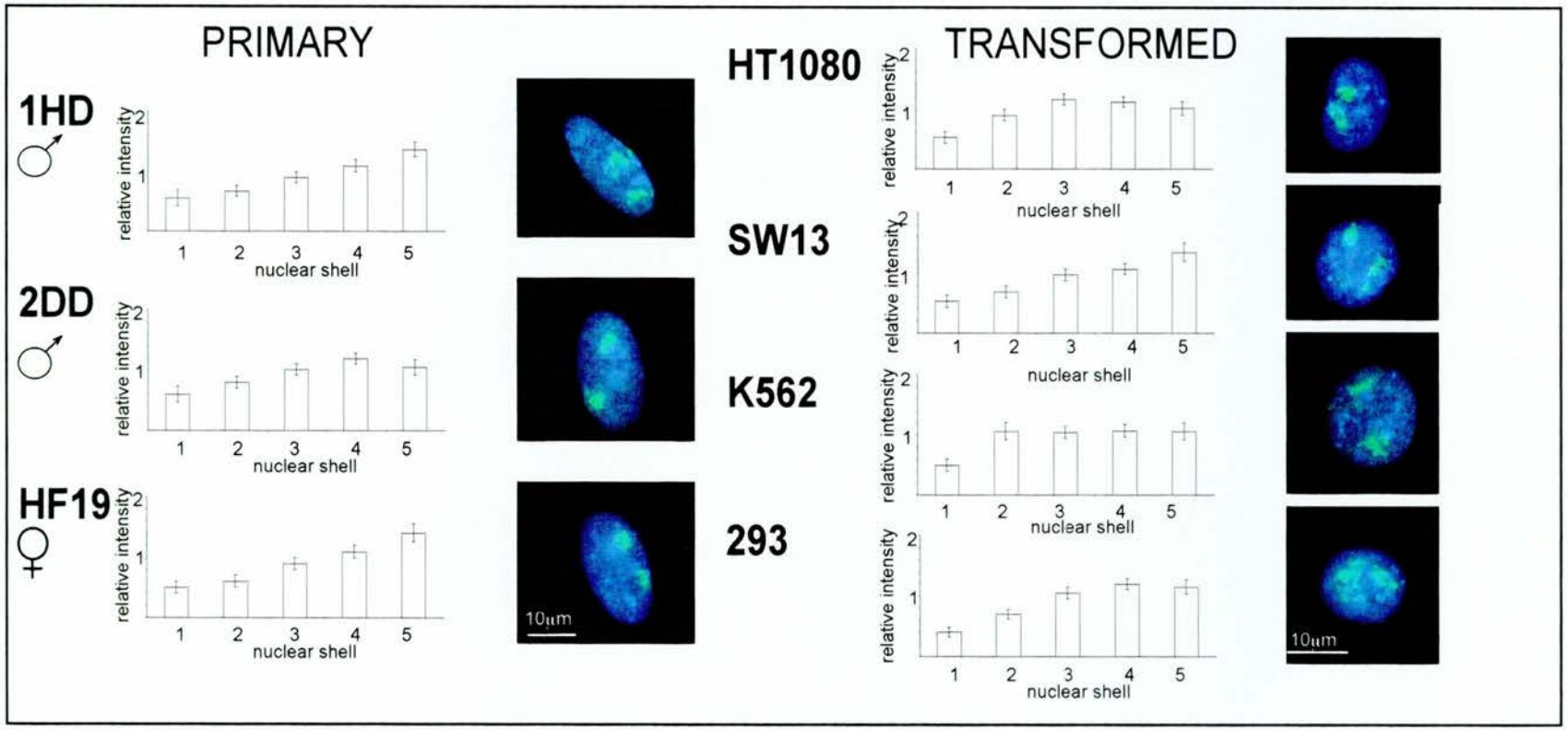

Figure 3.4 The relative distribution of chromosome 15 in different human cell lines.
The distributions of chromosome 15 territories were analysed in 50 3:1 MAA fixed nuclei of primary (1HD, 2DD, HF19) and transformed (HT1080, SW13, K562, 293) cultured human cell lines (for discussion see text). The mean distribution of relative chromosome paint signal (paint signal/DAPI signal) for each shell is represented in a histogram. Shell 1 represents the nuclear periphery and shell 5 is the nuclear centre. The error bars represent the standard error of the mean (S.E.M) for each data set. blue = DAPI DNA, green = FITC chromosome paint.

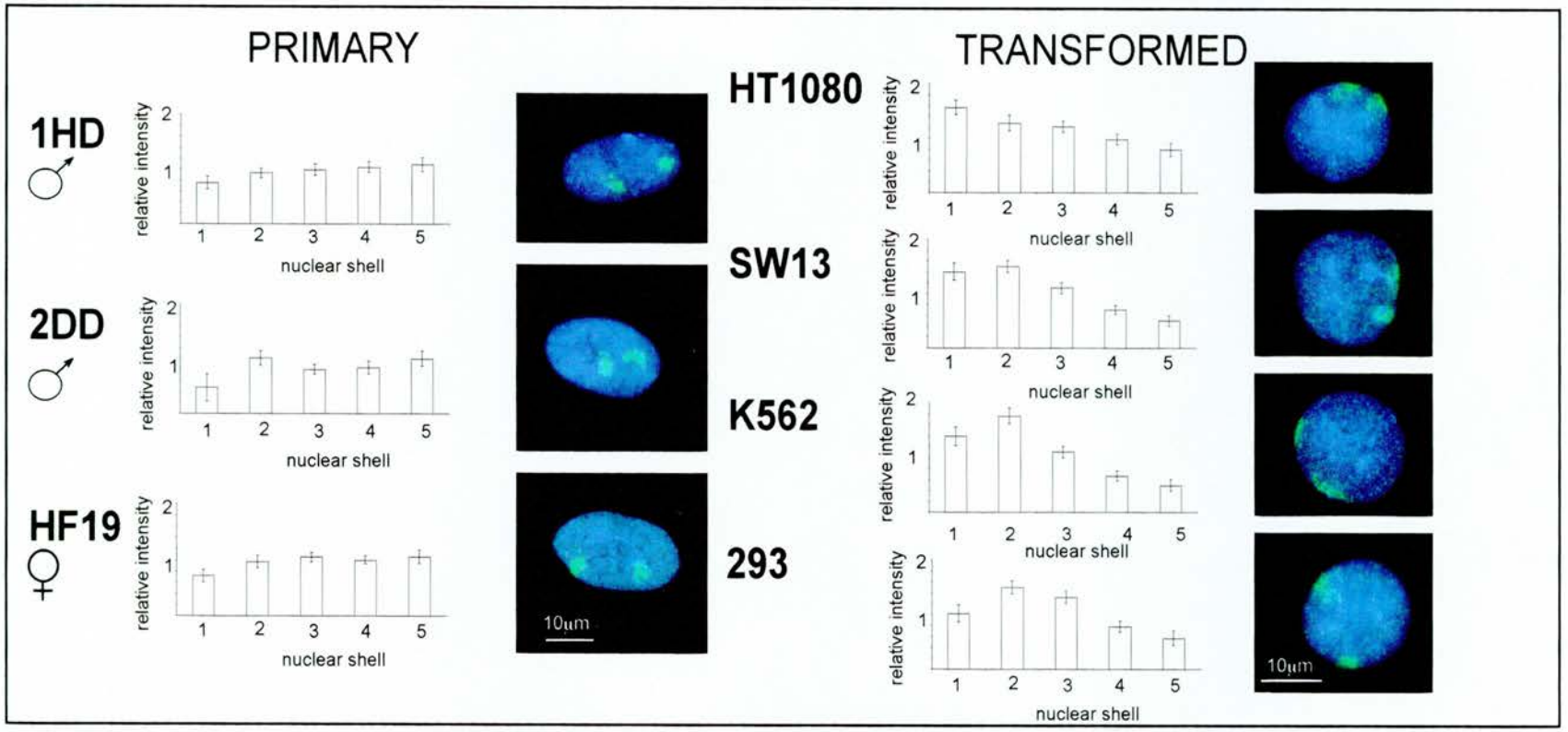

Figure 3.5 The relative distribution of chromosome 18 in different human cell lines.
The distributions of chromosome 18 territories were analysed in 50 3:1 MAA fixed nuclei of primary (1HD, 2DD, HF19) and transformed (HT1080, SW13, K562, 293) cultured human cell lines (for discussion see text). The mean distribution of relative chromosome paint signal (paint signal/DAPI signal) for each shell is represented in a histogram. Shell 1 represents the nuclear periphery and shell 5 is the nuclear centre. The error bars represent the standard error of the mean (S.E.M) for each data set. blue = DAPI DNA, green = FITC chromosome paint.

and 3.5) while 15 is internal (Figures 3.4). There is some heterogeneity to the results as, for example, in SW13 cells HSA13 does not show highest enrichment in shell 1 but shell 2. However, the smallest proportion of this chromosome signal is in the central shell (Figure 3.3). This pattern of distribution is also observed with HSA18 in 293 cells, where again the signal is most prominent in shell 2 (Figure 3.5). Analysis shows that these calculated distributions of chromosome territory positions are significant ($P<0.001$).

Data for the primary fibroblast lines is more difficult to interpret (Figures 3.3-3.5). In each primary cell line HSA15 appears to be enriched in the centre of the nucleus, in keeping with the radial arrangement model (Figures 3.4, $P<0.001$). However, the distributions of HSA13 and 18 appear to be somewhat even, with no obvious preference for the periphery or the centre (Figures 3.3 and 3.5). This suggests that the chromosome paint signals for these chromosomes are distributed randomly throughout the nucleoplasm. Statistical analysis of the significance of shell 1 signal intensity vs. shell 5 signal shows that HSA13 is not enriched at the periphery or the nuclear centre in 2DD or HF19 cells ($P=0.11$ and 0.88 respectively). However, in 1HD primary fibroblasts HSA13 is preferentially located at the nuclear edge (P=0.001). In addition to this, the statistical comparisons of the HSA18 data reveal that the signal intensities of this chromosome paint are preferentially enriched at the nuclear centre, in shell 5 (P=0.001).

This data for HSA18 location in primary fibroblasts directly contradict previous reports where HSA18 has been shown to be situated at the nuclear periphery in 1HD cells (Croft et al., 1999; Boyle et al., 2001). Cremer et al., (2001) reported that HSA18 is located in the centre of primary fibroblasts. However, the cells analysed in this particular experiment were confluent and by inference, quiescent through contact inhibition. It has been suggested that fibroblasts remodel their nuclear architecture in response to serum starvation (quiescence) and senescence (Bridger et al., 2000). Hence, the primary cells used in the Cremer et al., (2001) analysis may have senesced and repositioned HSA18 away from the nuclear edge. I have investigated the possibility that the cells used in my studies were quiescent or senescent by using a lamin A antibody (Jol 4) in IF experiments (see chapter 4). This antibody detects an epitope of lamin A that is only recognised in quiescent or senescent fibroblasts (Dyer et al., 1997). There is no antibody detection evident in the proliferating 1HD populations cultured and this argues against cell population senescence. I therefore conclude that the nuclear location of HSA18 territories is not comparable in primary and transformed human cell lines.

3.4 CHROMOSOME TERRITORIES IN HUMAN TISSUES

Tissue culture cell lines are routinely used as an *in vitro* system for modelling the *in vivo* situation. They are an invaluable resource as whole organism research is not always practical. The existing data for the spatial organisation of chromosome territories comes solely from studies on cultured cell lines. I was interested in observing chromosome territory organisation in human tissue to see if the *in vitro* radial arrangement is mirrored *in vivo*.

If chromosome territories could be readily visualised in tissue sections, there would also be an opportunity to follow chromosome position through differentiation. For this purpose I chose to examine chromosome territory position in skin because of availability of samples (Gift of Prof. B. Lane, Dundee) and because the differentiation process of this tissue is well laid out. Transverse sections through the epidermis reveal a clear differentiation profile (Figure 3.6). The basal layer (termed the stratum germinativum) consists of progenitor cells. From here, cells lose contact with the basement membrane and migrate upwards. A programme of terminal differentiation can be observed and the different layers of skin have particular characteristics and replication profiles. The keratinocytes proximal to the basement membrane of the epidermis (Stratum germinativum) are highly proliferative. The subsequent layers follow a terminal differentiation programme, the penultimate layer is quiescent and these cells shed their nuclei (Stratum lucidum). The outermost layer is dead enucleated cells (the 'squames' of the stratum corneum). A balance between proliferation of the basal layer and shedding of the top layer maintains tissue integrity (Byrne, 1997).

A protocol was developed by S. Boyle to perform FISH on paraffin-embedded human liver sections. This protocol was adapted to prepare 7μm paraffin-embedded sections of finger and thigh human epidermis (Gift from Prof. B. Lane, Dundee). Prior to a standard 2-D FISH procedure (see materials and methods), sections were treated with xylene (4 x 10 mins) to remove the paraffin. Samples were then microwaved in citrate buffer to breakdown the extracellular matrix within the tissue and the nuclear membranes of individual cells. It was noted that the extracellular matrix/membranes in finger epidermis is not broken down after 45 mins microwaving, as DAPI was not taken up into the nuclei of cells in these samples (data not shown). Hence, thigh epidermis sections, microwaved for 35 mins, were used in the experiments detailed below.

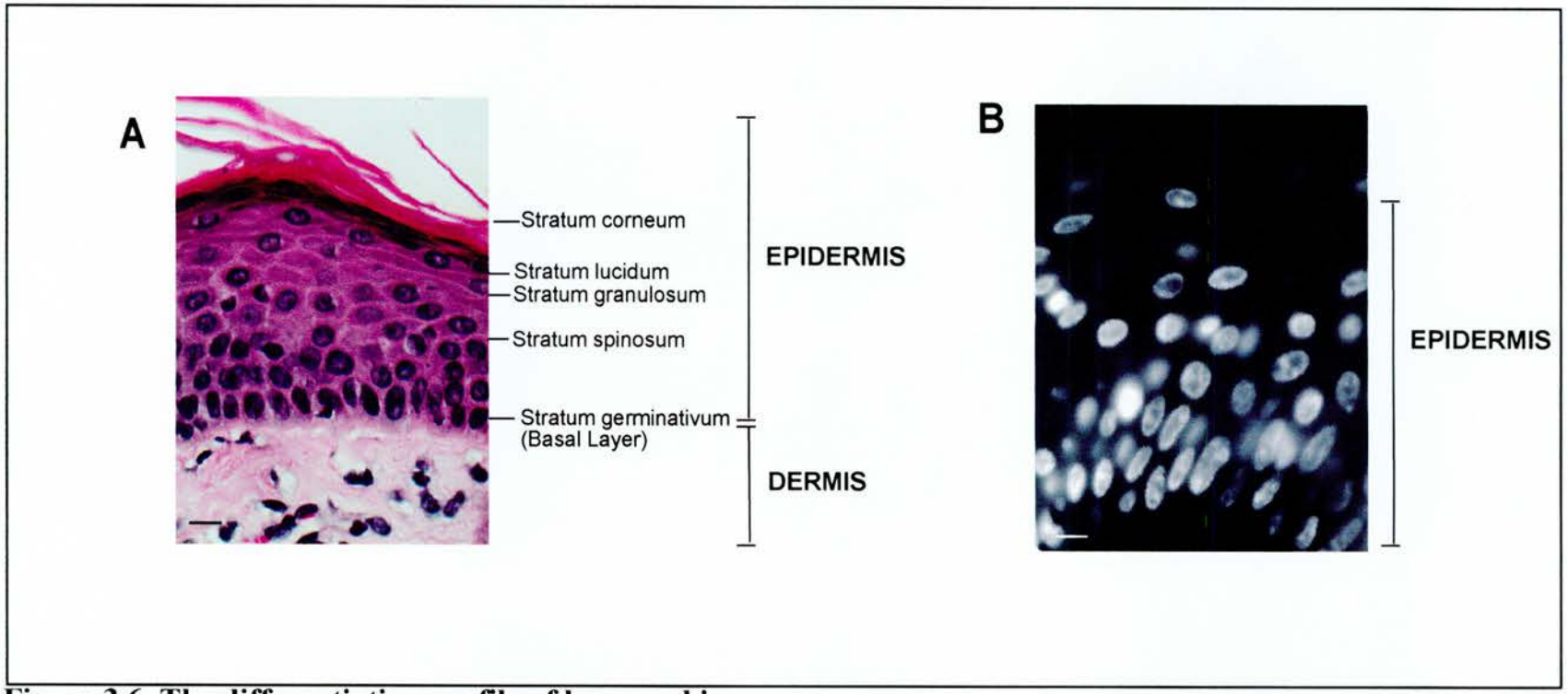

Figure 3.6 The differentiation profile of human skin.
Hematoxylin and eosin stained 7μm thick paraffin-embedded transverse section of human thigh skin (stained by D.Luny, University of Dundee. Gift from B.Lane) observed under the light microscope (**A**, x40 objective). Thigh sections were prepared for FISH (section 2.7) and probed with chromosome paints and IF antibodies. B shows a DAPI stained section of human thigh skin (x40 objective). Bars = 15μm.

In order to compare the interphase position of chromosome territories between human cells in culture (section 3.3) and *in vivo* I probed human epidermal sections with chromosome 13 and 15 paints (Figure 3.7). I found HSA13 peripheral in a variety of cultured cells and HSA15 central. In human skin sections, HSA13 is clearly visible at the periphery of three neighbouring cells (Figure 3.7A) while HSA15 is towards the centre of the nucleus (Figure 3.7B). This data suggests that these two chromosomes are radially arranged in the cells of human tissues, however, quantitative analysis should be done to confirm this. There are relatively high levels of background observed from the antibodies used to detect the biotin-labelled chromosome paints. This is due to the endogenous biotin of the cells reacting with the antibodies. This background is not saturating and the true chromosome paint signal can easily be distinguished. However, this can be overcome by using DIG-labelled paints rather than biotin.

The DAPI staining of the nuclei in prepared tissue sections (Figures 3.6 and 3.7) is not directly comparable to that of 3:1 MAA fixed nuclei (e.g. Figure 3.2) or 4% pFa fixed nuclei (e.g. Figure 4.3) of cultured human cells. In processed sections, nuclei appear to have rings of bright DAPI stain around the nuclear edge, with very little signal in the centre of the nucleus (Figure 3.7). I considered that the nucleolus in human tissues could be much larger than in cultured cells, and hence, prepared sections were probed using an anti-fibrillarin antibody (38F3, EnCor Biotechnology Inc; Figure 3.8A). In these sections, the fibrillarin of the nucleolus is located in the DAPI-sparse regions of these nuclei, but the fibrillarin signal does not account for all the DAPI negative region. I therefore conclude that this break in DAPI staining does not simply represent the nucleolus. This could be due to problems with dye access or represent different degrees of chromatin condensation within the nuclei of tissues. As HSA15 chromosome paint is evident in the centre of nuclei in DAPI-sparse regions, it is unlikely that they represent regions of no DNA (Figure 3.7B). This altered DAPI staining pattern could also be a consequence of DNA damage or degeneration as the age of these tissue sections is unknown. As the pattern of DNA staining is markedly different to that of culture cells processed for FISH it may be necessary to change the DNA stain and/or the distribution analysis method.

The epidermis provides an excellent model for observing cell differentiation and the basal layer of cells are actively dividing (Figure 3.6). It would therefore be interesting to follow the fate of chromosomes, and indeed specific genetic loci, known to relocate during

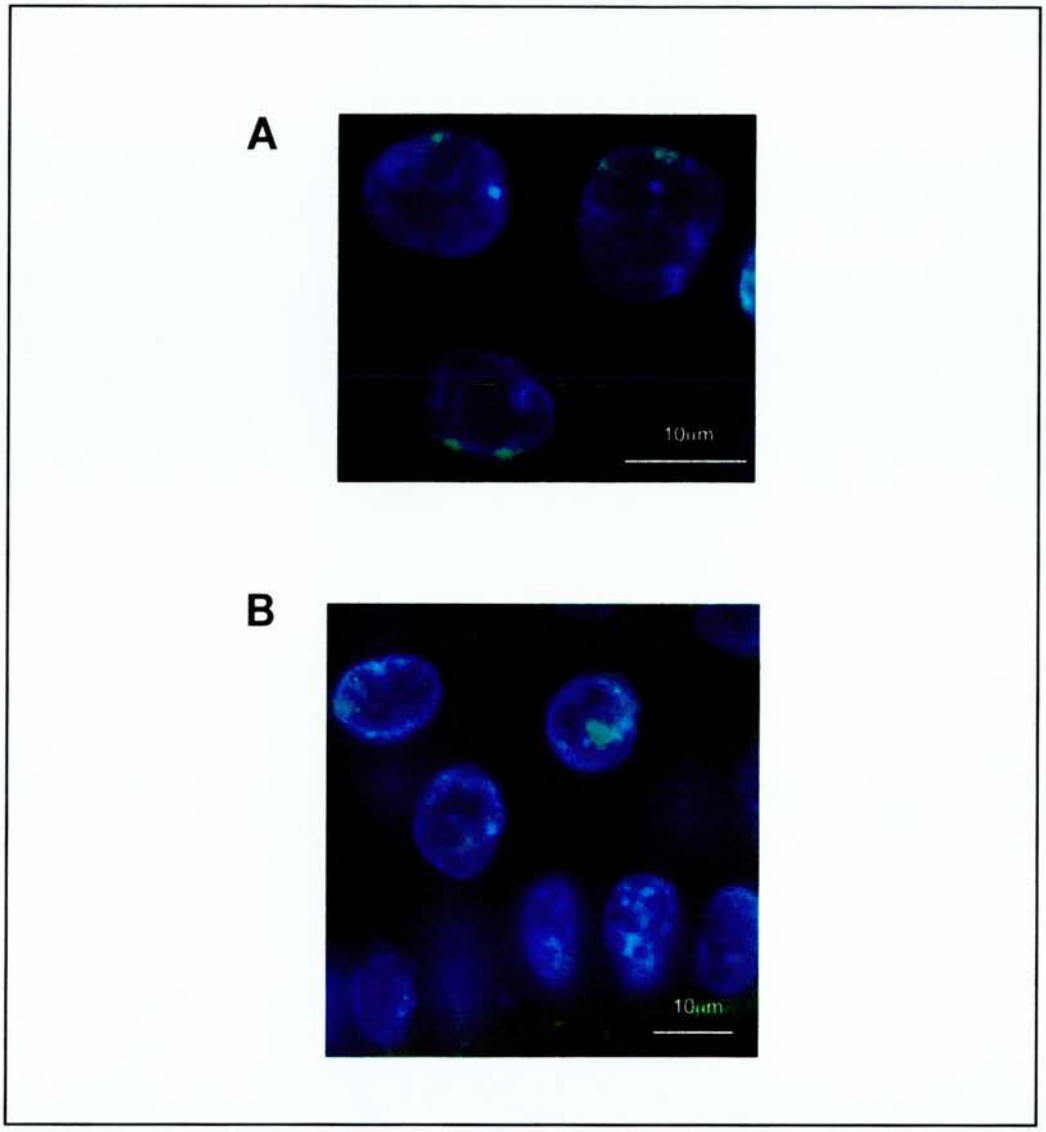

Figure 3.7 Chromosome territory FISH on human skin sections. FISH was performed on 7µm thick skin sections (gift from B. Lane) using whole chromosome paints. Fluorescence LM imaging using a x100 objective shows Chromosome 13 is located at the periphery of nuclei in neighbouring cells of the stratus spinosum (**A**). Chromosome 15 is located in the centre of cells in the stratus spinosum layer under x63 magnification. Blue = DAPI, green = FITC chromosome paint.

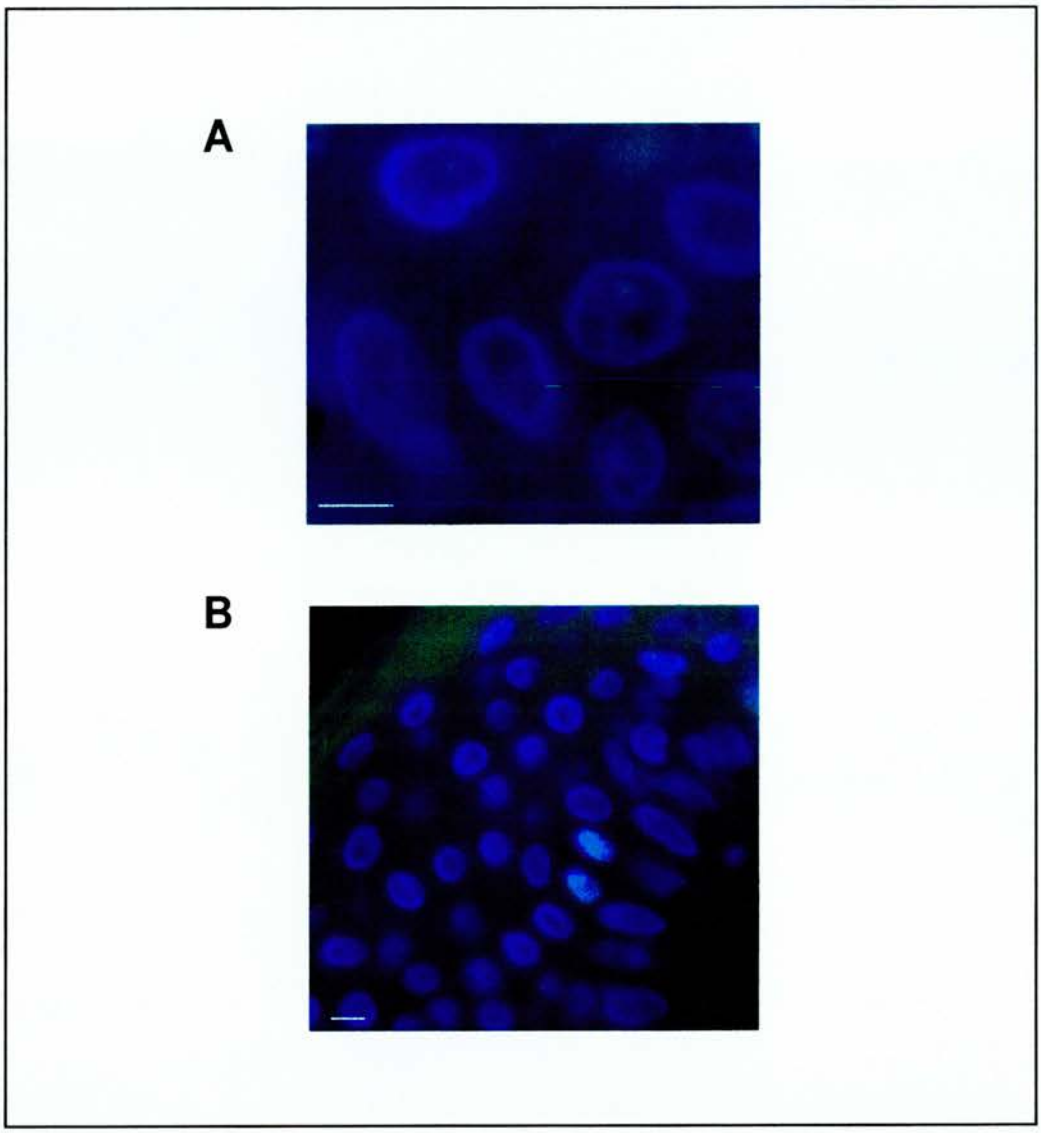

Figure 3.8 IF detection of the nucleolus in human tissue sections.
Wax-embedded 7μm thick transverse sections of human skin were microwaved in phosphate buffer (section 2.7) and probed with antibodies to detect the nucleous. Fibrillarin is detected in the nucleoli of neighbouring cells of the stratus spinosum layer of the epidermis (**A**). Ki-67, a proliferating cell antigen, is detected in a diffuse nuclear pattern (indicative of early G1 phase) in two neighbouring cells of the stratus spinosum and not in every cell of the stratum germinativum and stratus spinosum as expected (**B**). Bar = 15μm.

differentiation. To confirm the differentiation profile, I probed prepared tissue sections with anti-Ki-67 (Figure 3.8B). Ki-67 is a nucleolar antigen that is only detected in dividing cells (Gerdes et al., 1983). In this experiment, Ki-67 is only detected in a small subset of cells. However, this detection is not limited to the basal layer of cells and there is no obvious pattern to antibody signal.

FISH of chromosome territories has been performed on sections of human epidermis (section 3.7). In these visual observations, HSA13 is situated at the nuclear periphery (Figure 3.7A) and HSA15 is in the nuclear centre (Figure 3.7B). This pattern of localisation indicates that chromosomes are present in discrete territories in human tissues and that they are arranged with respect to their relative gene density. Territory distribution analyses (section 3.2.1) have been performed on compressed 3-D stacks of liver section FISH images (S.Boyle, personal communication). My intention was to use skin sections as an *in vivo* model for differentiation, however, anti-Ki-67 IF on epidermis sections shows only selected cells are replicating as shown by positive antigen detection (Figure 3.8A). This could mean that the differentiation profile in this tissue is more complex than suggested (Figure 3.6) or that there are antibody accessibility problems. It is likely that antibody access is not responsible for heterogeneic Ki-67 staining pattern as anti-fibrillarin antibodies show positive detection of this protein in every nucleus within a skin section (Figure 3.8A). For this reason, a systematic analysis of chromosome territories in the basal layer compared to the distal epidermal layers might not be a true comparison between dividing progenitor cells and quiescent differentiated cells. Using immuno-FISH techniques, where antibody detection of a differentiated cell protein is used in concert with chromosome paints (Dundas et al., 2001; Newsome et al., 2003), progenitor and differentiated cells can be identified. Basonuclin, Oct-1 and c-Myc are expressed exclusively in basal layer progenitor cells while Mad3 and Mad4 are expressed only in the upper layers of the epidermis (Byrne, 1997).

3.5 Discussion

Boyle et al., 2001 and Cremer et al., 2001 demonstrated that chromosomes (and their subcompartments; Sadoni et al., 1999; Skalnikova et al., 2000) are preferentially located in the nucleus with respect to gene density (a radial arrangement). The results in this chapter extend our observations of the radial arrangement of chromosome territories in different

human cell types (sections 3.2 and 3.3). Evidence has also been presented for the existence of radially arranged chromosome territories in human tissues (section 3.4).

I have shown that chromosome territory positions are not grossly altered in differentiation as several cell types have comparable chromosome locations. However, there are clear differences between the preferred position of HSA13 and 18 in different primary fibroblasts and the transformed cells investigated. It is not clear why this should be the case. Transformed cells, derived from several lineages, all have peripheral HSA18 and hence, it is considered that the process of transformation causes repositioning of these chromosomes to the nuclear edge. Transformed cells generally have a shorter generation time than primary cells and this could require a more stringent organisation of chromosome territories to facilitate efficient cell division. Analysis of additional territory positions in the cell lines studied here could reveal a similar repositioning of nuclear location for more chromosomes.

Since I began my PhD, the nuclear locations of HSA18 and 19 territories in the nuclei of several normal and tumour-derived cells have been determined (Cremer et al., 2003). The authors report that the opposing positions of HSA18 and 19 territories are maintained through the differentiation profile of hematopoesis and in also several tumour cells. However, their analyses also identified lines where radial organisation is relaxed or less structured (e.g. peripheral HSA19 material in a Hodgkin-derived cell line and internal HSA18 material in colon carcinoma metastasis). Both these cells lines harbour HSA18 or 19 translocations and altered nuclear location is only observed for the translocated 18 or 19 sequences. This is in agreement with the findings of (Croft et al., 1999) in which the HSA18 sequence of a derived t(18:19) chromosome is less peripheral than the intact chromosome.

Additional work revealed that the chicken genome is also arranged with respect to gene density. It was found that the gene-rich microchromosomes are in the centre of the chicken fibroblast nucleus (Tanabe et al., 2002a). Furthermore, the syntenic regions of HSA18 and 19 adopt peripheral and internal nuclear locations respectively in the lymphocytes of higher primates (Tanabe et al., 2002b). Taken together these data show that the radial arrangement of chromosome territories is conserved through evolution. Such conservation gives weight to the hypothesis that spatial organisation of the interphase nucleus has biological significance. Details of the functions associated with or influenced by the nuclear location of chromosome territories are lacking and we also do not know what mechanisms are involved. Is this spatial organisation a passive or active mechanism? A passive mechanism might arise

because territory localisation is merely a consequence of one or more cellular processes. In this situation, the formation of nuclear bodies would influence chromosome territory location, for example, maturation of the nucleolus. Immediately after cell division, the nuclear membranes of the daughter cells form and the metaphase chromatids decondense. The pre-nucleolar bodies are present on the rDNA repeats of acrocentric chromosomes after mitosis, and they then fuse to form the mature nucleolus (Hernandez-Verdun D. et al., 2002). Formation of the nucleolus could pull certain chromosomes to the nuclear centre. The occurrence of peripheral territories may simply be a result of exclusion from the nucleolus. However, close association of HSA17 and 19 with the nucleolus has also been described in fibroblasts (Bridger et al., 2000) and these chromosomes do not contain rDNA repeat sequences. Additionally, treating cells with 5,6-dichloro-β-D-ribofuranosylbenzimidazole (DRB) does not affect the relative position of HSA18 and 19 although it disperses the nucleoli (Croft et al., 1999).

Active formation of the radial arrangement of chromosomes could be driven by many cellular processes or have functional significance. As gene-rich chromatin appears to be enriched in the nuclear centre, transcription may drive radial arrangement of chromosome territories (Iborra and Cook, 2002). However, experiments using chemical inhibitors of transcription, actinomycin-D and DRB, do not disrupt chromosome territory position in treated cells (Croft et al., 1999). Alternatively, different positions for chromosome territories could arise if they contain different combinations of chromosome-associated proteins that in turn have different binding affinities for nuclear proteins. For example, it is known that gene-rich chromosomes are packaged into hyperacetylated histones (Jeppesen et al., 1992) and histone acetylation is enriched in the centre of the nucleus (Sadoni et al., 1999). Conversely, chromatin-associated proteins could contribute to tethering or anchoring specific sequences at the nuclear periphery which consists of the lamina and INM in mammalian cells. The role of histone acetylation in chromosome territory organisation is investigated in chapter 4 and the role of the nuclear lamina is addressed in chapter 5.

CHAPTER 4

ROLE OF HISTONE ACETYLATION IN NUCLEAR ORGANISATION

4.1 INTRODUCTION

Although it is widely accepted that the interphase nucleus is subject to a high degree of spatial organisation, the underlying mechanisms mediating this arrangement still prove elusive. A role for the physical composition of a chromosome or genetic region in influencing position is suggested as gene-rich and gene-poor sequences are located within different regions of the nucleus (Croft et al., 1999; Sadoni et al., 1999; Boyle et al., 2001). However, it has not been demonstrated whether it is the DNA sequence, or the chromatin composition of a chromosomal region that is more influential on 3-D nuclear location.

To investigate the mechanisms involved in spatial arrangement of the genome I chose to look at the role of chemical modification of histones, and hence chromatin composition (see section 1.1.3). A link between histone acetylation and transcription was originally proposed by Allfrey and colleagues in 1964 (Allfrey, 1964) and there are many now well-documented examples for the role of histone modifications in regulating gene expression. There are increased levels of acetylation on the single male X chromosome in *Drosophila* (Bone et al., 1994) and corresponding hypoacetylation levels on X chromosomes in female flies (Jeppesen and Turner, 1993). Microarray studies in yeast have revealed that HDAC activity is related to transcriptional control of a wide range of genes in this organism (Robyr et al., 2002). In mammalian cells, changes to histone acetylation profile in the promoter regions of genes have been associated with transcriptional activation of β-globin (Bulger et al., 2003), insulin (Chakrabarti et al., 2003) and the estrogen receptor genes (Macaluso et al., 2003). What is less well known is what role this might have with respect to 3-D positioning of chromatin during interphase. Early studies note that histone acetylation is not uniform along the length of metaphase chromosomes (Jeppesen et al., 1992) and it has also been reported to

be concentrated in the centre of the nucleus during interphase (Sadoni et al., 1999). This fits with the idea that increased histone acetylation can be associated with transcriptional 'readiness' of a genomic region and that gene-rich chromosomes, packaged in hyperacetylated chromatin, are located in the centre of the nucleus.

One study into the effect of disrupting the normal pattern of histone modifications has implied a role for histone acetylation in maintaining the 3-D position of centromeric chromatin. Taddei et al., 2001 treated cultured human and mouse cells with a chemical inhibitor of histone deacetylase enzyme (HDAC) activity, Trichostatin-A (TSA), which non-selectively increases the acetylation of histones. Centromeric heterochromatin is normally packaged into hypoacetylated histones (O'Neill and Turner, 1995). Treatment with TSA resulted in an increase of acetylation at centromeres and from visual observations of treated cells the authors suggested that the inhibition of HDACs results in a marked redistribution of centromeres during interphase. Untreated proliferating cells were observed to have centromeres distributed throughout the nuclear volume. In TSA-treated cells, centromeres were suggested to relocate to the periphery of the nucleus. I decided to investigate these findings further as they differ from previous work showing no obvious effect of TSA-treatment on the relative spatial organisation of chromosomes in interphase nuclei. In TSA-treated human cells gene-poor chromosome 18 is still located at the nuclear periphery and chromosome 19 is still in the centre of the nucleus (Croft et al., 1999).

4.2 TSA TREATMENT INCREASES LEVELS OF HISTONE ACETYLATION IN THE NUCLEUS

Two families (Class I and II) of HDAC enzymes have been identified (Leipe and Landsman, 1997). Several cell permeable reagents are available that are capable of inhibiting HDAC activity e.g. sodium butyrate, TSA, traponin, *Helminthosporium carbonum*-(HC) toxin and suberoylanilide hydroxamic acid (SAHA; Yoshida et al., 1995). In this study I have chosen to use TSA as it is a very specific and potent competitive inhibitor of deacetylases (Yoshida et al., 1990). TSA is also readily available from commercial sources and is the most widely used inhibitor of HDACs used experimental inhibitor of HDACs (Selker, 1998; Strait et al., 2002; Taddei et al., 2001). Crystallography studies have revealed the mechanism responsible for TSA inhibition of deacetylases. The *Aquifex aeolicus* deacetylase HDLP (homologue to human HDAC1 with 35% identity) has been shown to be inhibited by both

TSA and SAHA in a metal ion dependent manner (Finnin et al., 1999). Deacetylase family members have a conserved enzymatic domain which consists of a hydrophobic pocket (Leipe and Landsman, 1997). The long aliphatic chain of TSA can slot into this pocket and compete with endogenous substrates to block enzymatic activity (Finnin et al., 1999). An aromatic group, at the other end of the TSA molecule, further blocks substrate accessibility by capping or obstructing the opening of the hydrophobic pocket of the enzymatic domain.

Levels of histone acetylation in a cell are the result of a balance between the activities of HAT and HDAC enzymes. Therefore inhibiting the activity of HDACs should increase the overall acetylation levels in cells. To determine whether TSA was able to inhibit HDAC activity in human cell cultures and hence increase the levels of histone acetylation I performed western blot analyses of treated cells. Total protein extracts were prepared from HeLa cells treated with 100ng/ml TSA for up to 6 days. After SDS-PAGE resolution, the proteins were transferred to PVDF membrane and probed with an antibody specific for histone H4 acetylated at the residue lysine 5 (R41, Figure 4.1A; Turner and Fellows, 1989). Acetylation of H4 at lysine 5 is generally associated with hyperacetylation of chromatin (Zhang et al., 2002). Over the period of TSA-treatment there is a clear accumulation of acetylation at this residue by day 4. The same membrane was then probed with an antibody detecting histone H3 as a loading control. I conclude that TSA is inhibiting cellular HDAC activity and resulting in global hyperacetylation of histone H4 in treated cells.

4.3 TSA BLOCKS CELL CYCLE PROGRESSION

Chemical inhibition of cellular HDACs in tissue culture cells is known to block cell cycle progression and alter cellular morphology (Brinkmann et al., 2001). To identify the most appropriate concentration of TSA for my study I treated various human cell lines with increasing concentrations of TSA and analysed their cell cycle profiles by FACS analysis (section 2.2.7, Figure 4.1B and C). Primary fibroblasts were grown in the presence of 50-100ng/ml TSA over a period of days (1-5 days) and compared to an equivalent untreated cell population. Figure 4.1B shows that cultures grown in the presence of 50ng/ml (green plot) and 100ng/ml (red plot) TSA for 5 days show an increased proportion of cells in the G1 and G2 phases of the cell cycle, and a large decrease in the proportion of cells in S phase when compared to an equivalent untreated population (purple plot). As indicated by western blot analysis (Figure 4.1A) the drug effects increase histone acetylation levels with extended

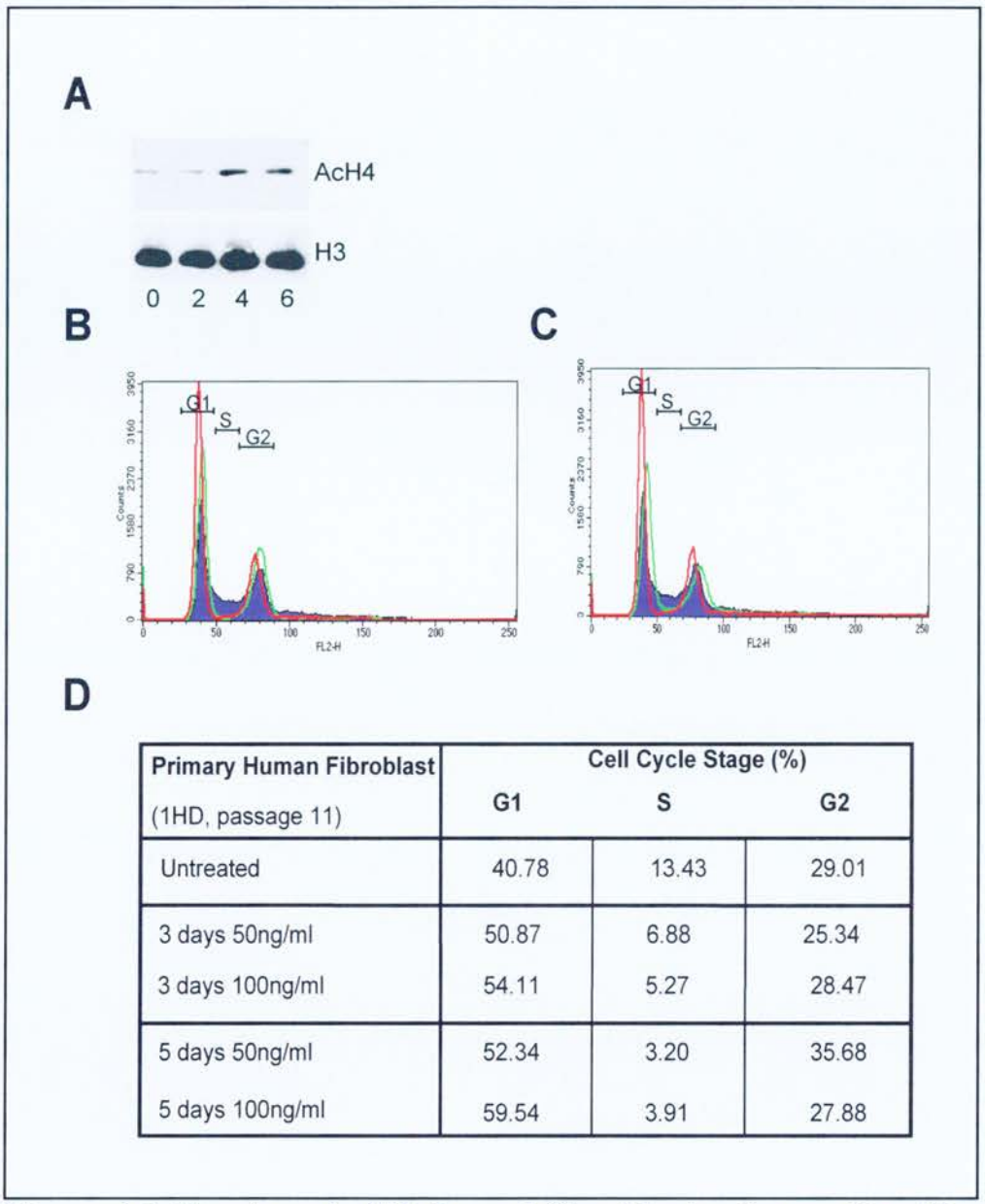

D

Primary Human Fibroblast (1HD, passage 11)	Cell Cycle Stage (%) G1	S	G2
Untreated	40.78	13.43	29.01
3 days 50ng/ml	50.87	6.88	25.34
3 days 100ng/ml	54.11	5.27	28.47
5 days 50ng/ml	52.34	3.20	35.68
5 days 100ng/ml	59.54	3.91	27.88

Figure 4.1 Treatment of HeLa and fibroblast culture cells with TSA.

Western blot analysis of total protein extracts (**A**). HeLa protein samples were harvested at 0, 2, 4 and 6 days of treatment with TSA at 100ng/ml. Acetylation of K5-H4 was detected using R41 antibody (Gift from B. Turner, see sections 2.2.7) and levels are seen to increase over a period of days. Detection of an antibody to total H3 was used as a loading control. FACS analysis of cell cycle profile in untreated and TSA-treated primary fibroblasts (1HD, **B-D**). Increasing concentrations of TSA blocks the cell cycle of human fibroblasts at G1 and G2 (**B**) as fibroblasts treated with 50 (green) and 100ng/ml (red) TSA for 5 days show a higher proportion of cells in G1 and G2 when compared to an equivalent untreated population (purple). Cell cycle disruption by TSA is established over a period of days (**C**) as fibroblasts treated with 100ng/ml TSA for 5 days (red) have more cells in G1 and G2 than 3 days treated samples (green) and untreated control cells (purple). Quantification of FACS analyses (**D**).

incubation periods.

Populations of cells treated with 100ng/ml TSA for 3 and 5 days were compared (Figure 4.1C). Cells treated with inhibitor for 3 days show enrichment in G1 and G2. Cells treated for a further 2 days show significantly higher numbers of G1 and G2 cells and a more marked decrease in the number of cells in S phase. Quantification of the FACS profiles is documented in Figure 4.1D. The number of cells within the G1, S and G2 phases of the cell cycle is represented as a percent of the total number of cells analysed in the experiment. These three values do not account for 100% of all cells in the experiment. There are some out-lying cells in every trace and these can be either apoptotic or aneuploid cells or indeed aggregates of more than one cell not sufficiently separated during sample preparation.

Human Fibrosarcoma (HT1080) and hTERT transformed fibroblast (RITVA) cells were also treated with TSA (Figure 4.2). The higher concentrations of TSA used for the fibroblast lines appear to be more cytotoxic for the HT1080 line (Figure 4.2C). When treated at 100ng/ml TSA these cells would only survive 2 days (data not shown), hence cells were treated at a reduced drug concentration which was sufficient to arrest cell cycle progression in treated cultures. Indeed, treating HT1080 cells with 75ng/ml of drug exerts substantial cytotoxic effect as a smaller number of cells are viable after 5 days of treatment than with 50ng/ml. However the surviving cells in the population are blocked in G1 and G2, and there are very small numbers of cells observed in S phase (Figure 4.2D). hTERT transformed fibroblasts can tolerate the same drug concentrations as the primary fibroblast line used and are also arrested in G1 and G2 (Figure 4.2A-B). These results show that cultured cells arrest at G1 and G2 stages of the cell cycle when treated with histone deacetylase inhibitor TSA.

4.4 TSA ALTERS THE NUCLEAR DISTRIBUTION OF HISTONE MODIFICATIONS

There is evidence for preferred nuclear distribution patterns of DNA sequences, histone modifications and chromatin-associated proteins. Protein interactions mediated by histone modifications may therefore determine the nuclear position of the chromatin fibre. For example, there might be specific interactions between hypoacetylated histones and components of the nuclear periphery. Western blot analysis of TSA-treated cells (Figure 4.1)

A

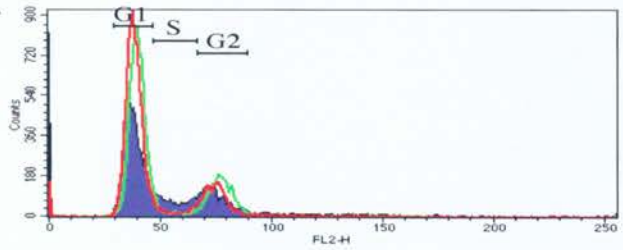

C

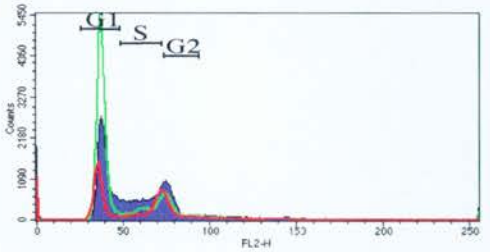

B

Transformed Fibroblasts (Telomerase+RITVA)	Cell Cycle Stage (%)		
	G1	S	G2
Untreated	50.50	12.78	17.43
3 days 75ng/ml	54.27	8.82	18.23
3 days 100ng/ml	65.81	6.65	17.91
5 days 75ng/ml	68.52	4.26	22.04
5 days 100ng/ml	73.29	4.69	17.31

D

Fibrosarcoma (HT1080)	Cell Cycle Stage (%)		
	G1	S	G2
Untreated	38.86	19.32	25.13
3 days 50ng/ml	52.63	13.58	17.02
3 days 75ng/ml	55.19	11.43	15.68
5 days 50ng/ml	63.82	8.71	16.19
5 days 75ng/ml	36.69	9.92	31.60

Figure 4.2 Treatment of transformed fibroblasts and fibrosarcoma cells with TSA. HTERT transformed fibroblasts (RITVA, **A** and **B**) and fibrosarcoma cells (HT1080, **C** and **D**) are also blocked in the cell cycle upon TSA treatment. In FACS analyses, untreated populations of cells (purple) were compared to cultures treated with two concentrations of TSA for 5 days. Transformed fibroblasts were treated with 75 (green) and 100ng/ml (red) of TSA (A), and HT1080 cells with 50 (green) and 75ng/ml (red, **C**). Quantification of FACS analyses (**B** and **D**).

showed an overall increase in the levels of acetylated K5-H4 in treated cells. This may be due to an increase in H4 acetylation at all genomic regions, or an enhanced acetylation at more specific sites. This was addressed here by determining the nuclear distribution of histone modifications in untreated and TSA-treated cells.

4.4.1 Histone acetylation

In order to understand the role, if any, that histone acetylation plays in nuclear organisation the distribution of H4 acetylation in human cultured cells was examined by immunofluorescence. Firstly, I used the R41 antibody, which detects histone H4 lysine 5 (K5-H4) acetylation (Figure 4.3). IF was performed on untreated and TSA-treated primary fibroblasts (1HD; 5 days, 100ng/ml: Figure 4.3 A and D respectively), hTERT transformed fibroblasts (5 days, 100ng/ml: Figure 4.3 B and E) and HT1080 cells (5 days, 75ng/ml: Figure 4.3 C and F).

Untreated fibroblasts show an uneven distribution of acetylation of H4 at K5 (acK5-H4) throughout most of the nuclear volume, (excluding nucleoli: Fig. 4.3A), but there are also regions at the nuclear periphery which show no K5-H4 acetylation (arrows). A similar pattern of antibody staining is also observed for this histone modification in the transformed fibroblasts and HT1080 cells (Figure 4.3B and C respectively). This pattern of localisation has been previously described for histone H4 lysine 8 acetylation (Sadoni et al., 1999). As expected, cells treated with TSA show an increased level of R41 staining, and hence histone K5-H4 acetylation, in the nucleus. Moreover, the distribution of acetylated K5-H4 in the nuclei of TSA-treated cells is markedly different from that of untreated cells. There is an apparent enrichment of this form of acetylation (represented by intense peripheral R41 signal) at the nuclear edge and there are fewer peripheral patches where K5-H4 acetylation staining is absent.

Quantification of the spatial distribution of histone H4 hyperacetylation in primary fibroblasts before and after treatment was performed by analysis of mid focal plane 3-D IF images (Figure 4.4). Firstly, the pixel intensities for DNA (DAPI) and acetylated K5-H4 (R41) staining were measured within a transverse section, 9 pixels wide, through a nucleus and were represented as line graphs. Examples of analysed images and line graphs for untreated (Figure 4.4A and B) and 5 day TSA-treated (Figure 4.4D and E) nuclei are shown in Figure 4.4. Comparing pixel profiles in the nuclei of untreated and treated cells indicates

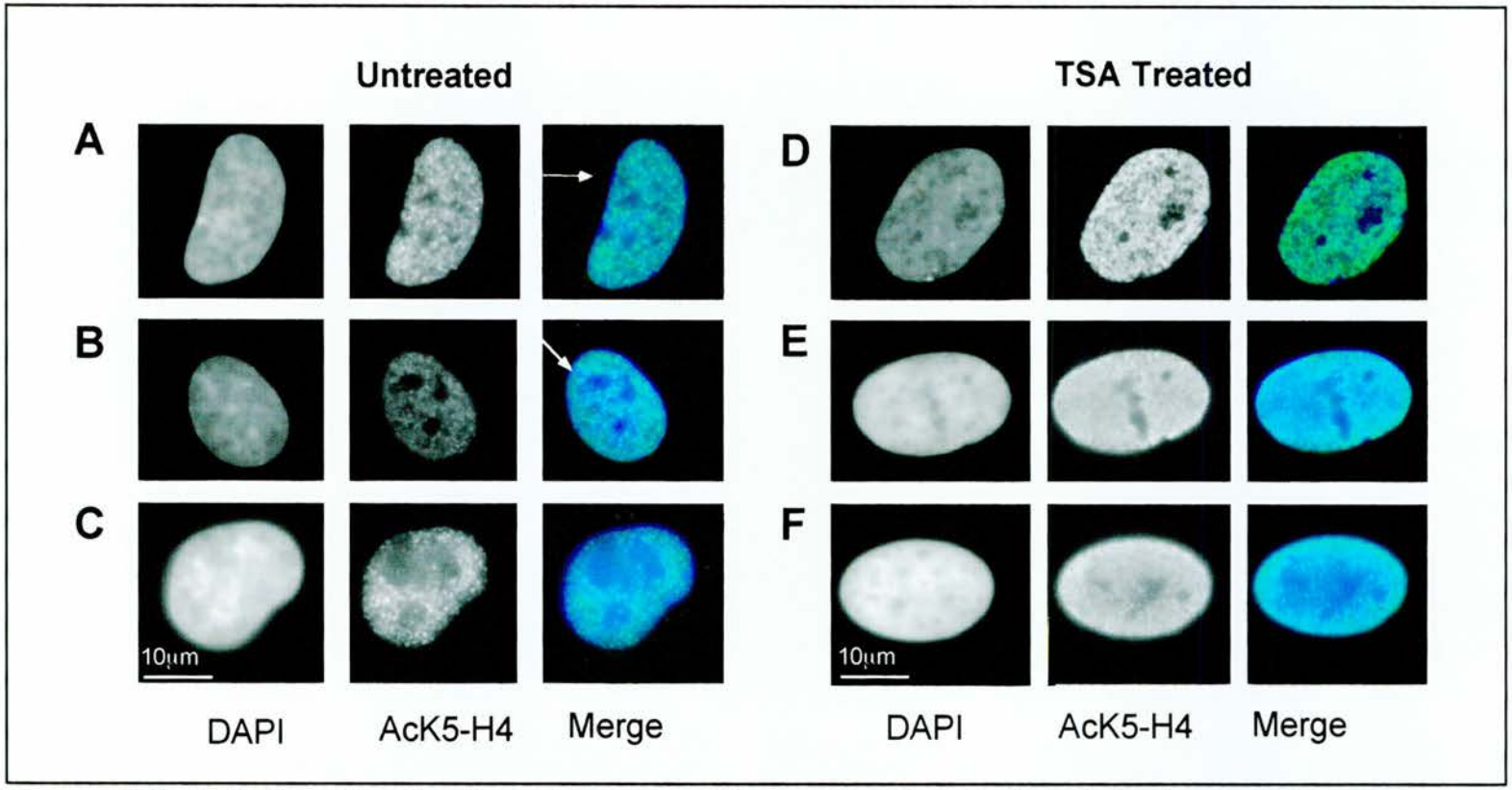

Figure 4.3 Cellular distribution of histone H4 acetylated at lysine 5 by immunofluorescence. Acetylation of K5-H4 in untreated and TSA-treated cells was visualised using antibody R41 in primary fibroblasts (1HD, **A** and **D**), hTERT transformed fibroblasts (RITVA, **B** and **E**) and fibrosarcoma cells (HT1080, **C** and **F**). In each cell line, a nuclear diffuse staining pattern is observed for this modification in untreated cells (**A-C**). Patches at the nuclear rim are evident where there is no antibody detection of this histone modification (arrows). Following 5 days of TSA treatment there is an obvious change to the IF pattern detected by this antibody (**D-F**). Blue = DAPI, green = acK5-H4.

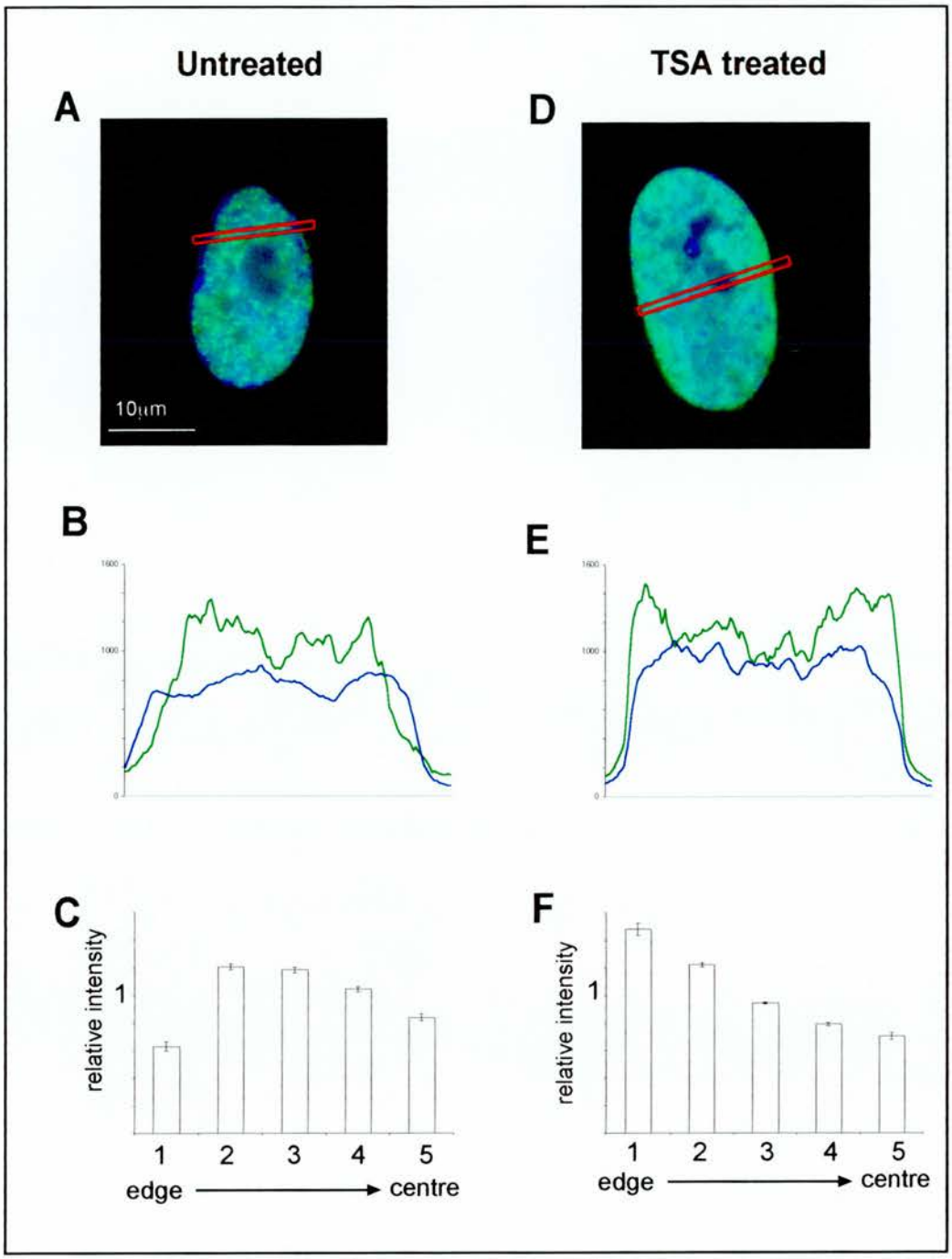

Figure 4.4 Quantification of cellular distribution of histone H4 acetylation at lysine 9.

Quantification of R41 IF signal was performed (for discussion see text) in untreated (**A-C**) and TSA treated (**D-F**) primary fibroblasts. Regions of interest 9 pixels wide are taken across a nuclear image (red, **A** and **D**). Total pixel intensities are represented as line traces along the length of each region (**B** and **E**). Erosion script analysis of (n=20) of untreated and treated nuclei is performed (Figure 3.1) to determine the average nuclear distribution of the fluorescent antibody signal (**C** and **F**). Relative intensity =R41 signal/DAPI signal, blue =DNA, green = acK9-H4 (R41).

that there is a nuclear redistribution of this histone modification after drug treatment. In untreated fibroblasts (Figure 4.4 B), R41 staining is depleted or absent from the nuclear edge as the DNA (DAPI) signal clearly begins at a point in the image well before the R41 signal intensity increases. Nuclei from TSA-treated fibroblasts (Figure 4.4E) show a significant change in the distribution of histone H4 hyperacetylation. Line trace analysis shows that R41 signal in these cells begins at the same point as DNA signal and indeed is at its most intense at the nuclear periphery (Figure 4.4E). There is no apparent redistribution of the DNA signal through the nucleus brought about by TSA-treatment and therefore movement of DNA/chromatin cannot account for the increased R41 signal at the nuclear edge.

In order to directly compare the global redistribution of R41 signal across a population of untreated and treated cells, up to 20 mid focal plane images were analysed using the nuclear erosion script described previously (section 3.2.1). The nuclear distribution of histone H4 hyperacetylation for untreated (Figure 4.4 C) and TSA-treated (Figure 4.4 F) fibroblasts was calculated by comparing the proportion of the total R41 stain and DAPI stain in 5 nuclear shells. In untreated cells, there is a low proportion of R41 signal in the peripheral shell (shell 1). After TSA-treatment a greater proportion of the IF signal is recorded in the outer nuclear shell and hence there is indeed a significant enrichment of histone H4 K5 acetylation in chromatin located at the nuclear periphery when TSA is used (P=0.003). A similar result was also found in both transformed fibroblasts and HT1080 cells before and after TSA treatment (Figure 4.10A).

Is this altered acetylation distribution specific for K5-H4? In order to address this, IF was used to detect histone H3 acetylation at lysine 9 (acK9-H3, Figure 4.5). Untreated fibroblasts (Figure 4.5A-C) appear to have a distribution of acK9-H3 that is broadly similar to that of acK5-H4 (Figure 4.3A-C). There is a lack of staining at regions of the nuclear edge and most of signal is in the nuclear centre. After treatment with TSA (Figure 4.5D-F) there is a redistribution of the staining and a clear enrichment of acK9-H3 at the nuclear edge, however this altered pattern was not as striking as that of K5-H4 IF. AcK9-H3 distribution was quantified in the same way as for acK5-H4 described in the previous section (Figure 4.6). The data for acK5-H4 and acK9-H3 distribution in HT1080 and RITVA cells is shown in Figure 4.10. These data show that there is an enrichment of acK9-H3 at the nuclear edge following TSA-treatment although statistical analysis suggests this is less significant that the redistribution of acK5-H4 observed (P=0.045). I conclude that there is a nuclear

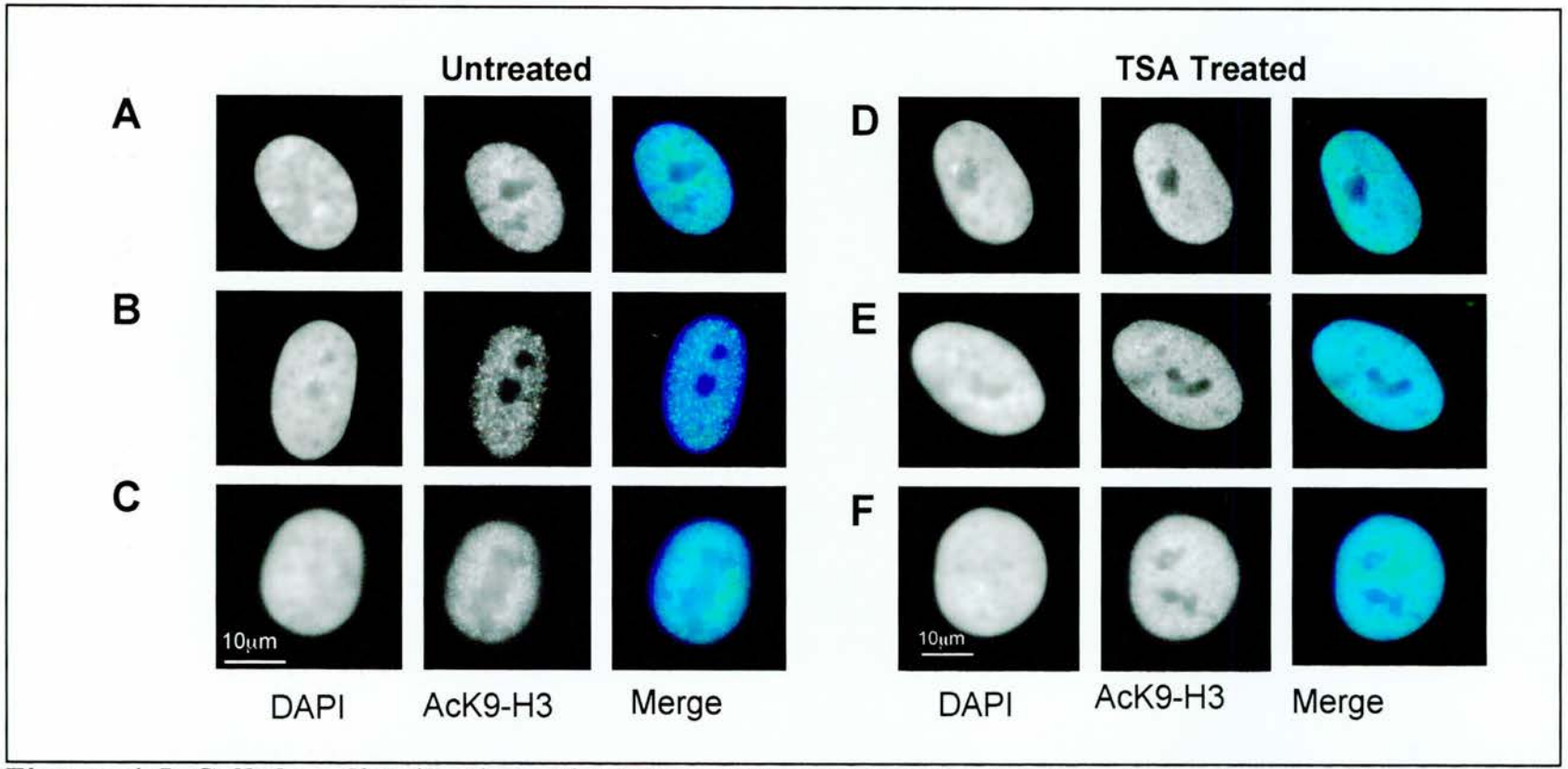

Figure 4.5 Cellular distribution of histone H3 acetylated at lysine 9 by immunofluorescence. Acetylation of K9-H3 in untreated and TSA-treated cells was visualised using antibody in primary fibroblasts (1HD, **A** and **D**), hTERT transformed fibroblasts (RITVA, **B** and **E**) and fibrosarcoma cells (HT1080, **C** and **F**). Again, a nuclear diffuse staining pattern is observed for this modification in untreated cells (**A-C**). Following 5 days of TSA treatment there is an obvious change to the IF pattern detected by this antibody (**D-F**). Staining is more even and there is an apparent rim of bright detection around the nuclear edge. Blue = DNA, green = acK9-H3.

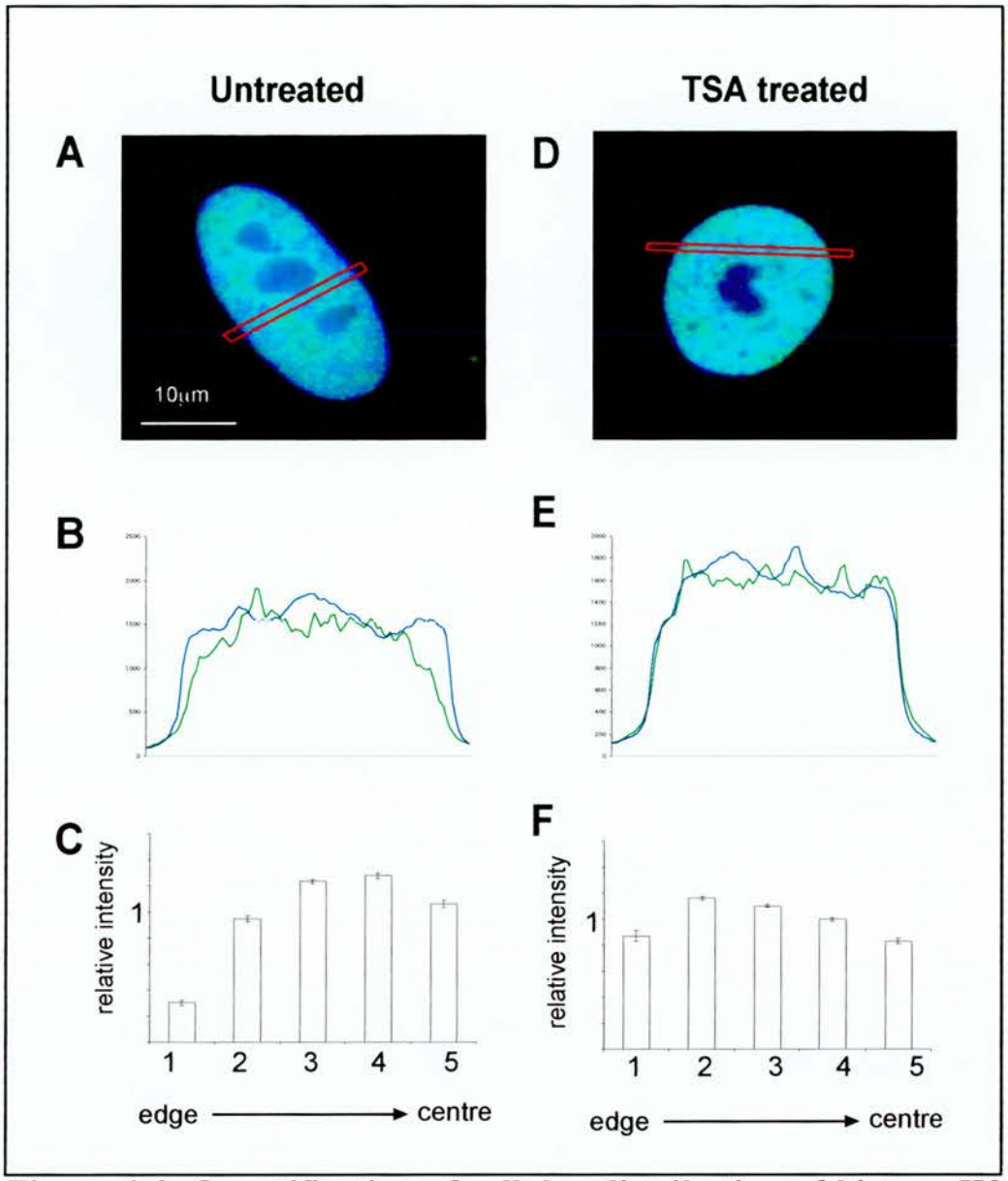

Figure 4.6 Quantification of cellular distribution of histone H3 acetylated at lysine 9.

Quantification of anti-acetylated K9-H3 signal was performed (for discussion see text) in untreated (**A-C**) and TSA treated (**D-F**) primary fibroblasts. Regions of interest 9 pixels wide are taken across a nuclear image (**A** and **D**). Total pixel intensities are represented as line traces along the length of each region (**B** and **E**). Erosion script analysis of 20 images of untreated and treated nuclei is performed to determine the average nuclear distribution of the fluorescent antibody signal (**C** and **F**). Relative intensity = acK9-H3 signal/DNA signal, blue = DNA, green = acK9-H3.

redistribution of histone acetylation and acK5-H4 is markedly increased at the nuclear edge, while acK9-H3 is less so, when cells are treated with TSA over a period of days.

4.4.2 Histone methylation

The previous section has shown that TSA-treatment alters the interphase distribution of acetylated histones. Histones can be modified with more than one chemical moiety and control of histone acetylation and methylation on the same, or neighbouring residues is thought to be very tightly linked (Zhang and Reinberg, 2001; Fischle et al., 2003b). Disrupting the balance of histone acetylation levels with TSA may also affect other modifications, such as histone methylation. As acetylation and methylation have not been found to exist on the same lysine residue of one H3 protein they are considered mutually exclusive modifications. In untreated cells, the chromatin at the nuclear periphery is hypoacetylated (Figures 4.3 and 4.4). These H3 molecules could be unmodified at K9 or methylated at this residue. In the latter case these methyl groups, or the histones that carry them, would need to be removed to allow for K9 acetylation in TSA-treated cells. If this is the case we should see a reciprocal change in the nuclear distribution of methylated K9-H3 (metK9-H3) in TSA-treated cells.

I also performed distribution analysis of histone K9-H3 methylation. IF was carried out using two antibodies to detect histone K9-H3 methylation. An antibody raised against a linear, di-methylated peptide (Figure 4.7, Upstate) was compared against the staining of an antibody raised against a linear, tri-methylated peptide (Figure 4.8, a gift from T. Jenuwein. Gilbert et al 2003). Untreated and treated cells show a relatively uniform pattern of dimethylated K9-H3 (met_2K9-H3, Figure 4.7). A slightly different staining pattern is observed with the tri-methylated K9-H3 (met_3K9-H3) antibody, signal is more uneven with brightly staining foci (Figure 4.8). In human cells, anti-met_3K9-H3 antibody detects centromeric heterochromatin and other sites while the anti-met_2K9-H3 does not (Gilbert et al., 2003). Quantification of the nuclear distribution of the two forms of K9-H3 methylation suggests that they do not share the same pattern of distribution (Figure 4.9, P=0.01). Example pixel traces are shown for met_2K9-H3 (Figure 4.9A, B, D and E). In untreated cells, there appears to be an even nuclear distribution of met_2K9-H3 and following TSA-treatment this histone modification has a comparable nuclear distribution (P=0.733). The nuclear distribution of met_3K9-H3 is not the same as that of met_3K9-H3 (P=0.01) in untreated cells (Figure 4.9C) as met_3K9-H3 is concentrated in the centre of the nucleus.

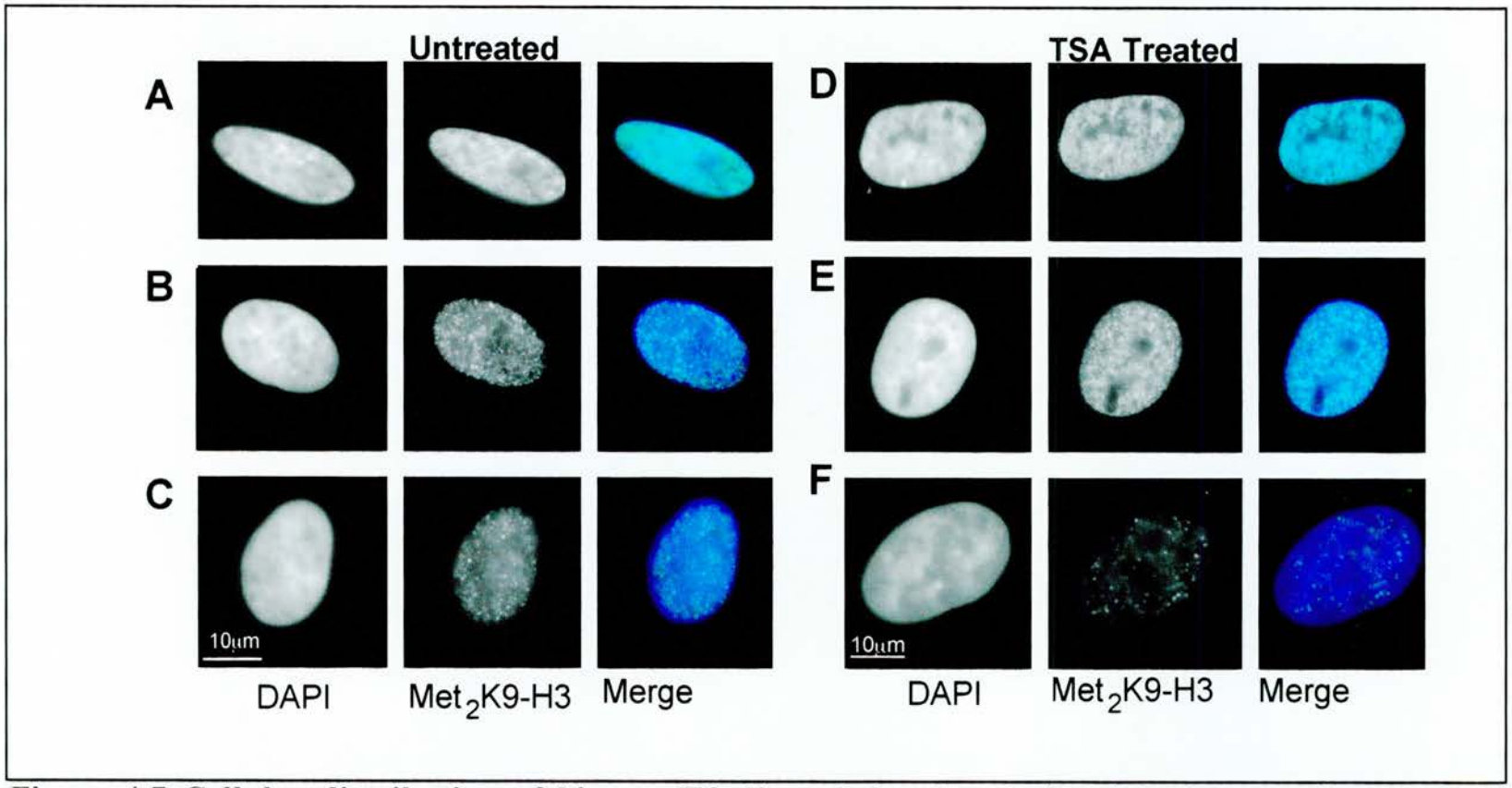

Figure 4.7 Cellular distribution of histone H3 di-methylated at lysine 9 by immunofluorescence. Di-methylation of K9-H3 in untreated and TSA-treated cells was visualised using anti-dimethylated MetK9-H3 antibody (Upstate) in primary fibroblasts (1HD, **A** and **D**), hTERT transformed fibroblasts (RITVA, **B** and **E**) and fibrosarcoma cells (HT1080, **C** and **F**). Again, a nuclear diffuse staining pattern is observed for this modification in untreated cells (**A-C**). Following 5 days of TSA treatment there is no apparent change to the IF pattern detected by this antibody (**D-F**). Blue = DNA, green = anti-dimethylated MetK9-H3 .

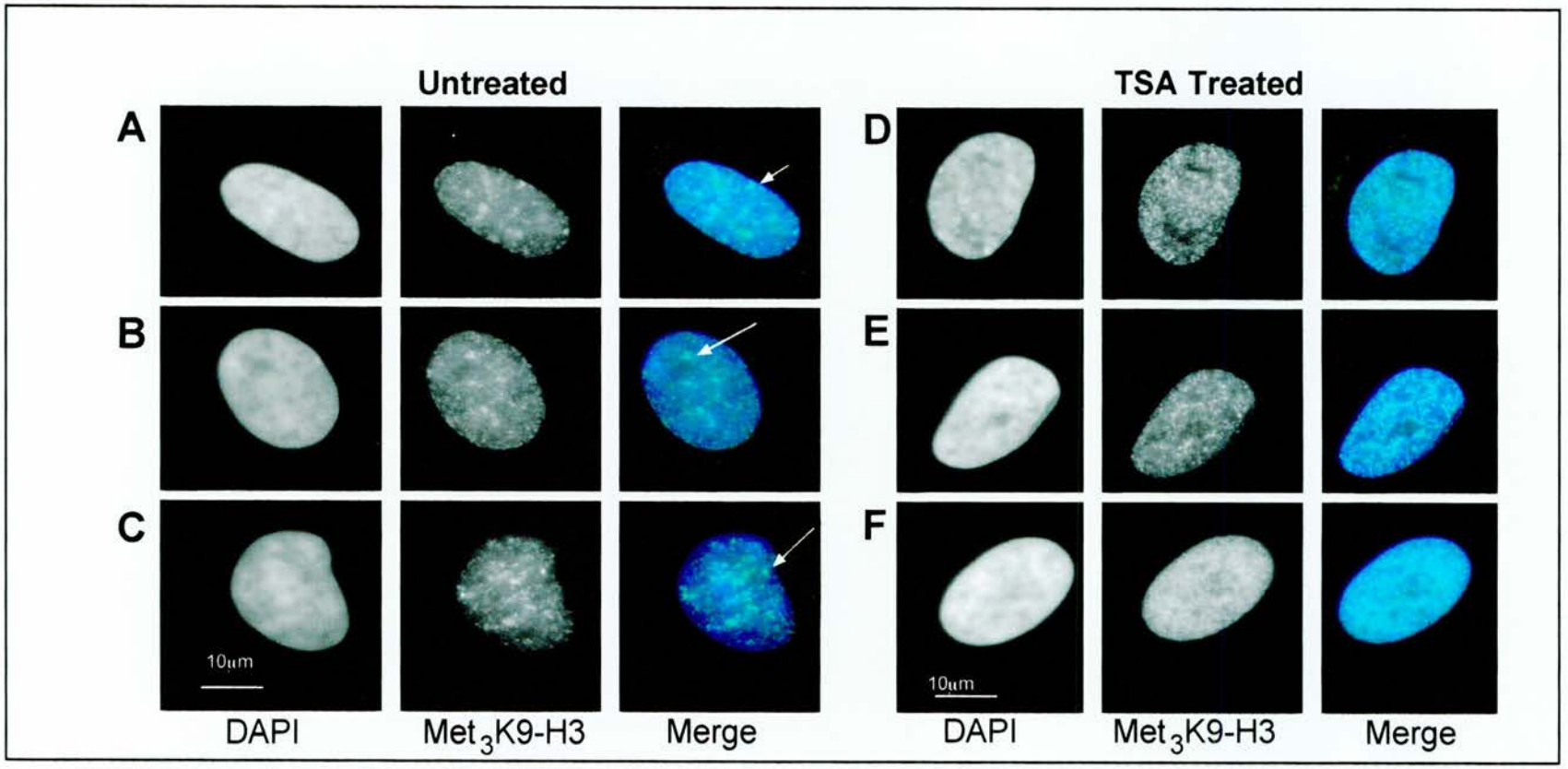

Figure 4.8 Cellular distribution of histone H3 tri-methylated at lysine 9 by immunofluorescence. Methylation of K9-H3 in untreated and TSA-treated cells visualised using anti-trimethylated MetK9-H3 antibody (gift from T.Jenuwein) in primary fibroblasts (1HD, **A** and **D**), hTERT transformed fibroblasts (RITVA, **B** and **E**) and fibrosarcoma cells (HT1080, **C** and **F**). Again, a nuclear diffuse staining pattern is observed for this modification in untreated cells (**A-C**), however bright stain foci are also evident (arrows). Following 5 days of TSA treatment there appears to be a more even staining pattern and the bright foci are less apparent (**D-F**). Blue = DNA, green = anti-trimethylated K9-H3.

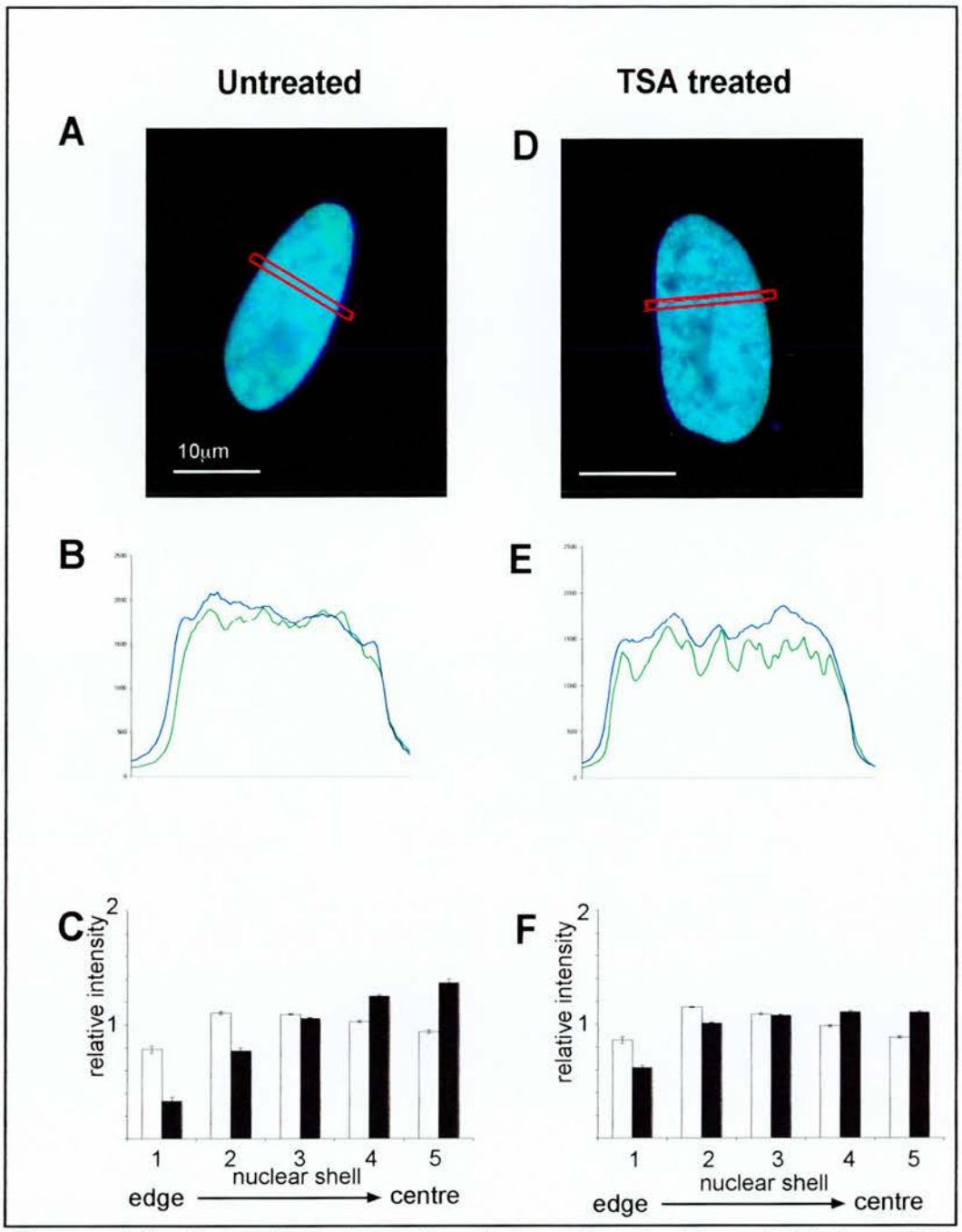

Figure 4.9 Quantification of cellular distribution of histone H3 methylation at lysine 9.

Quantification of methylated K9-H3 IF signal was performed (for discussion see text) in untreated (**A-C**) and TSA treated (**D-F**) primary fibroblasts. Regions of interest 9 pixels wide are taken across a nuclear image (red, **A** and **D**). Total pixel intensities are represented as line traces along the length of each region (**B** and **E**), Images and line traces represent IF of anti-dimethylated K9-H3. Erosion script analysis of (n=20) of untreated and treated nuclei is performed (Figure 3.1) to determine the average nuclear distribution of the fluorescent antibody signal (**C** and **F**), for dimethylated (open bars) and trimethylated (filled bars) K9-H3. Relative intensity = K9-H3 signal/DAPI signal, blue =DNA, green = antidimethylated K9-H3.

After treatment with TSA there is an increase of met_3K9-H3 at the nuclear edge (Figure 4.9F, P=0.04).

This analysis was then extended to describe the distribution of histone modifications in transformed fibroblasts and HT1080 cells (Figure 4.10). Acetylation of both K5-H4 and K9-H3 was found to increase at the nuclear edge upon TSA-treatment, in keeping with the findings for primary fibroblasts (Figures 4.4 and 4.6, P<0.04). The met_3K9-H3 distribution and its response to TSA-treatment is mirrored in these cells, this modification appears to be enriched at the nuclear edge. There are some changes to the distribution of histone distributions apparent from visual interpretations of the histograms, however, they are not statistically relevant in this analysis (P>0.06 in all comparisons).

It is commonly accepted that there is interplay between different modifications on the tails of histones, and this is proposed as the basis of the histone code hypothesis (Figure 1.3; Turner, 2002). Here it has been shown that in dividing cells, the nuclear periphery has patches where little or no acK9-H3 is seen. Following TSA-treatment, there is an enrichment of histone acetylation at the nuclear periphery (Figure 4.3). An increase in metK9-H3 is also evident at the nuclear periphery in TSA-treated cells, however, statistical comparisons of DNA signals in untreated and treated cells show no significant difference in DNA distribution. This excludes the possibility that enrichment of histone modifications is due to chromatin repositioning. My observations of methylation and acetylation repositioning in response to TSA-treatment suggest that these two histone modifications are not mutually exclusive, as enrichment of AcK9-H3 at the nuclear periphery of treated cells does not correspond with a decrease in metK9-H3 modifications at this nuclear site. Indeed these findings suggest that both histone H3 and H4 acetylation and met_3K9-H3 are enriched at the nuclear edge in response to inhibition of cellular HDAC activity.

Should histone modifications follow the histone code, a decrease in methyl H3 would be predicted under these experimental conditions. However, the significance of histone unmodified at this K9 residue must also be considered. Histone tails can be modified at several different sites, and an increase in K9-H3 acetylation may not require an equivalent decrease in methyl K9-H3. Histones are one of the most abundant cellular proteins and no doubt, there are thousands of H3 molecules within the nucleus primed to accept acetyl groups without requiring the removal of a methyl group at K9.

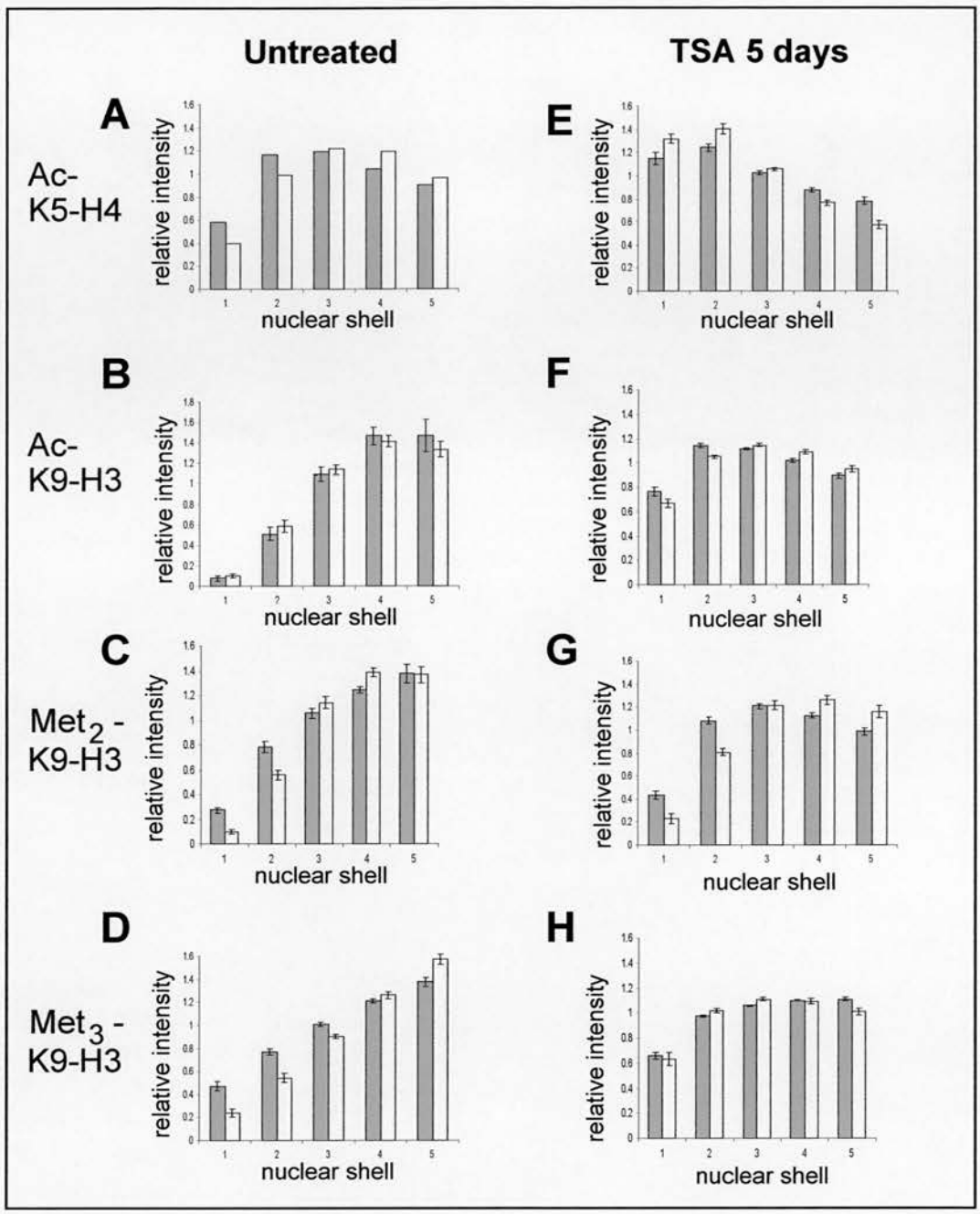

Figure 4.10 Quantification of cellular distribution of histone modifications in HT1080 and RITVA cells.

Quantification of IF signal was performed as before in untreated (**A-D**) and TSA treated (**E-H**) HT1080 (filled bars) and RITVA (open bars). Erosion script analysis of (n=20) of untreated and treated nuclei is performed (Figure 3.1) to determine the average nuclear distribution of the fluorescent antibody signal and represented as histograms. Shell 1 is the nuclear edge, shell 5 is the nuclear centre. Relative intensity =antibody signal/DAPI signal.

4.5 PROPERTIES OF HETEROCHROMATIN

Histone modifications are known to influence the binding of particular proteins such as HP1 to the nucleosomes and hence play a significant role in determining chromatin fibre composition and structure. HP1 proteins bind to chromatin via interaction of their chromodomains with methylated histone K9-H3 (Bannister et al., 2001; Lachner et al., 2001; Nakayama et al., 2001). HP1 binding is generally associated with formation of constitutive heterochromatin (section 1.2.2.1).

Taddei *et al.*, (2001) reported that following TSA-treatment the composition of heterochromatin was altered. In untreated cells, no histone acetylation was detectable at the centromeres of mouse chromosomes while after TSA-treatment there was a significant amount of acetylation at these genomic regions. Treatment of fission yeast with TSA leads to destabilisation of centromere function (Ekwall et al., 1997). Centromeres are specialised hypoacetylated (O'Neill and Turner, 1995) heterochromatic loci, composed of many specific centromeric proteins (Pidoux and Allshire, 2000).

To determine the acetylation state of centromeric heterochromatin, I performed co-immunofluorescence (Figure 4.11) with CREST antisera and R41 (an antibody that detects acK5-H4) in untreated and treated primary fibroblasts (Figure 4.11A and D), transformed fibroblasts (Figure 4.11B and E) and HT1080 cells (Figure 4.11C and F). In untreated cells, lack of acetylation at centromeres is apparent by the clear red signal of the CREST antisera in the merged images, any colocalisation would result in yellow signal. No yellow signal is seen in the merged images of TSA-treated cells. Centromeres at the nuclear periphery of treated cells, a region enriched in histone acetylation (see section 4.4.1), are in local areas of low K5-H4 acetylation and are still red (Figure 4.11, arrows). My observations reveal no histone K5-H4 acetylation at centromeres in any cell type before or after TSA-treatment.

In order to study the relationship between histone acetylation and heterochromatin proteins, I looked at the interaction between HP1α and regions of methylated and acetylated K9-H3. In this model, metK9-H3 would be replaced by acK9-H3 following TSA-treatment. In this case, the chromodomain of HP1 would no longer be able to bind centromeric chromatin.

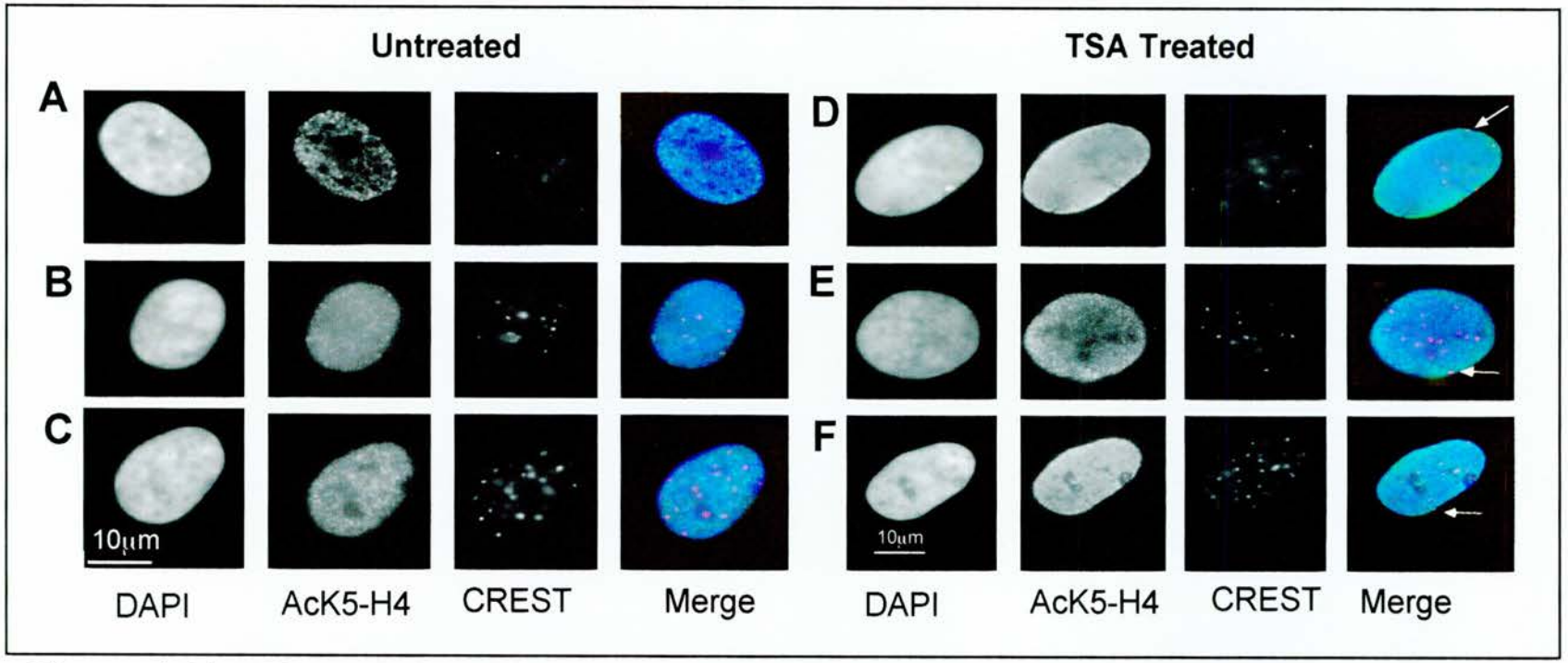

Figure 4.11 The relationship between acetylation and centromeres in TSA treated cells. Co-immunofluorescence with CREST antisera and R41 detects centromeres and acK5-H4 in primary fibroblasts (1HD, **A** and **D**), hTERT transformed fibroblasts (RITVA, **B** and **E**) and fibrosarcoma cells (HT1080, **C** and **F**). Before and after TSA treatment, there is little colocalisation of these two antibodies (see arrows). Blue = DNA, green = acK5-H4, red = centromeres.

Taddei *et al.*, (2001), also reported that the binding capabilities of HP1 isoforms are altered as a result of TSA-treatment. However, I have found a small but significant enrichment of histone K9-H3 methylation at the nuclear periphery following TSA-treatment and coincident with the increase in histone acetylation at the nuclear edge. Co-immunofluorescence was performed using CREST antisera and anti-HP1α antibody (Figure 4.12). Staining reveals that HP1α has an uneven distribution in untreated cells (Figure 4.12A) and this pattern is maintained following TSA-treatment (Figure 4.12C). Arrows in both merged images highlight regions where HP1α signal is adjacent to centromere signal.

I also considered that the binding properties of HP1α might be different following TSA-treatment. To address this, untreated and treated cells were incubated with detergent (0.5% TritonX-100, section 2.5.1) prior to pFa fixation for IF. This permeabilises cell membranes and allows any unbound proteins to be washed out before fixation. TritonX-100 pre-treatment does not remove all endogenous HP1α protein from untreated (Figure 4.12B) or TSA-treated cells (Figure 4.12D) and indeed adjacent centromere and HP1α signals are evident in both merged images. I conclude from these experiments that the basic composition of centromeric heterochromatin is not grossly perturbed by TSA-treatment, as centromeres do not show increased acK5-H4 levels or reduced HP1α binding.

4.6 HISTONE MODIFICATIONS AND NUCLEAR ORGANISATION

There are proteins that preferentially bind modified residues on histone tails (e.g. HP1 targeting metK9-H3, see above). As HP1 can bind to an INM protein, lamin B receptor (Ye et al., 1997b), it is inferred that methylation of K9-H3 may influence the ability of a locus to become tethered to the nuclear periphery. In order to test the hypothesis that histone modifications may act to determine the nuclear location of chromatin, I analysed the behaviour of chromosome territories, nuclear structures and centromeres in TSA-treated cells.

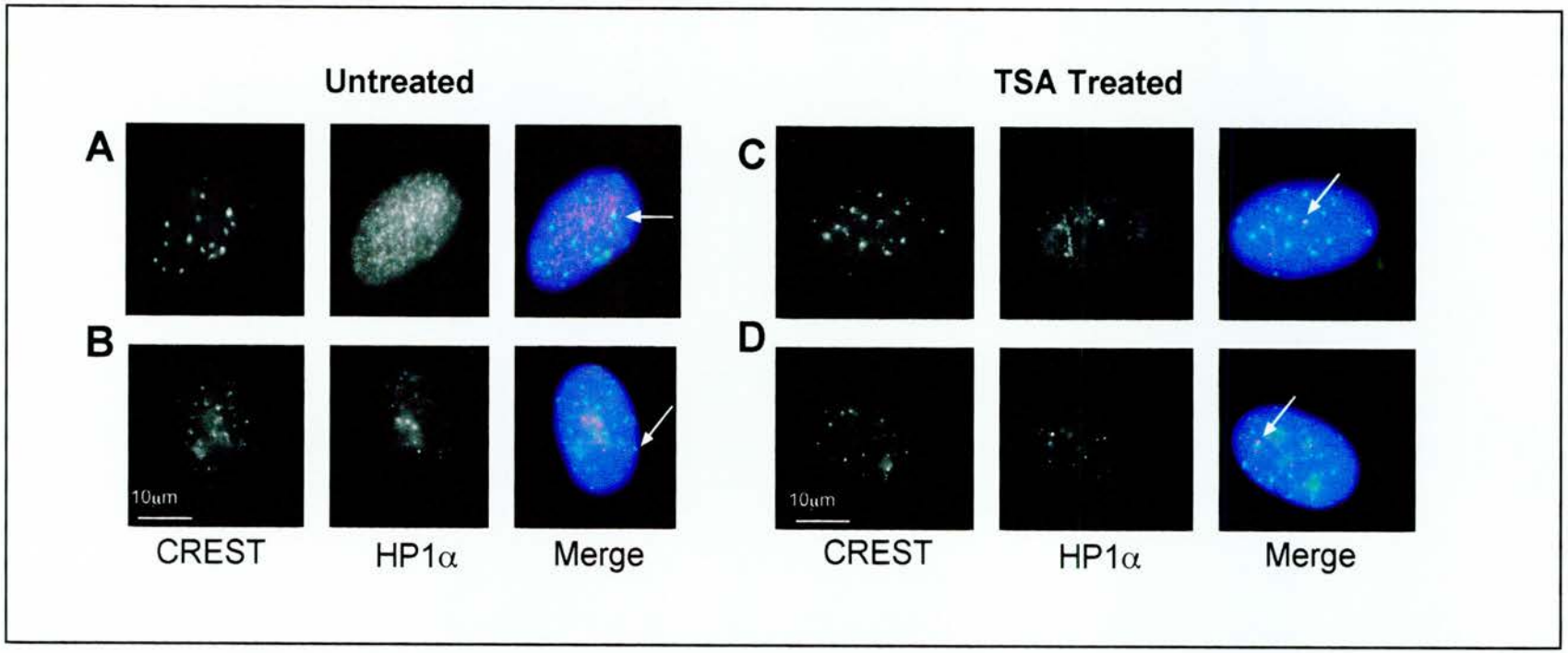

Figure 4.12 The composition of heterochromatin in TSA treated primary human fibroblasts. Co-immunofluorescence was performed with CREST antisera and anti-HP1α on untreated and treated primary human fibroblasts (**A** and **C**). Cells were also pre-incubated with 0.5% TritonX-100 before IF to allow wash out of unbound proteins (**B** and **D**). In each case, centromeres and HP1α signals are in close proximity when detected by co-IF (arrows) and this association is not distrupted by TSA treatment. Blue=DNA, red = HP1α, green = centromeres.

4.6.1 Chromosome territories

Data in this chapter demonstrate that disrupting endogenous HDAC activity leads to marked changes in the spatial distribution of acetylated histones. Increased acetylation at the nuclear periphery may be caused by a specific redistribution of acetylated chromatin in the nucleus. To address this, I determined the location of chromosome territories in cells treated with TSA and compared them to untreated cells. This experiment had previously been undertaken (Croft et al., 1999, TSA at 10ng/ml), however, the drug concentration used was not comparable to that of Taddei, *et al.*, 2001 (TSA at 100ng/ml) and therefore I chose to repeat this investigation. The data for chromosomes in primary fibroblasts are shown in Figure 4.13. Superficially, some chromosomes appear to relocate after TSA-treatment; however, this is due to variation in the experiment and is not statistically significant (P=0.63-0.92). However, the distributions before and after TSA-treatment are significantly different for HSA14 and the difference between chromosome territory signal in shell 5 vs. shell 1 is highly significant (P<0.001). This relocation was not due to altered DNA distribution in the nucleus (P>1) and hence I conclude that TSA-treatment results in repositioning of the bulk of HSA14 chromosome territory from the nuclear centre to the nuclear edge.

4.6.2 Nuclear structures

I have shown that there is a change to chromatin composition when cells are treated with TSA - are there associated changes to important nuclear structures? Targeted disruption of the normal regulation of histone modifications has been shown to disrupt the cell cycle (Figures 4.1 and 4.2). Several nuclear structures are known to alter composition in a cell cycle related manner and hence TSA-treatment may induce these changes. One nuclear structure considered a marker for cell cycle stage is the nucleolus (Gerdes et al., 1984). IF pictures shown in this chapter suggest that the gross morphology of the nucleolus is not greatly affected by TSA-treatment. In each image there are areas of weak DAPI signal and these typically represent the nucleolus. The composition of the nucleolus during TSA-treatment was followed using an antibody to Ki-67, a nucleolar protein (Figure 4.14 A). This antigen is only detectable in proliferating cells, and not quiescent cells (Gerdes et al., 1983). After treatment with HDAC inhibitor, a population of cells is arrested mainly in G1 but also in G2 of the cell cycle. Less than 5% of TSA-treated cells contain detectable Ki-67.

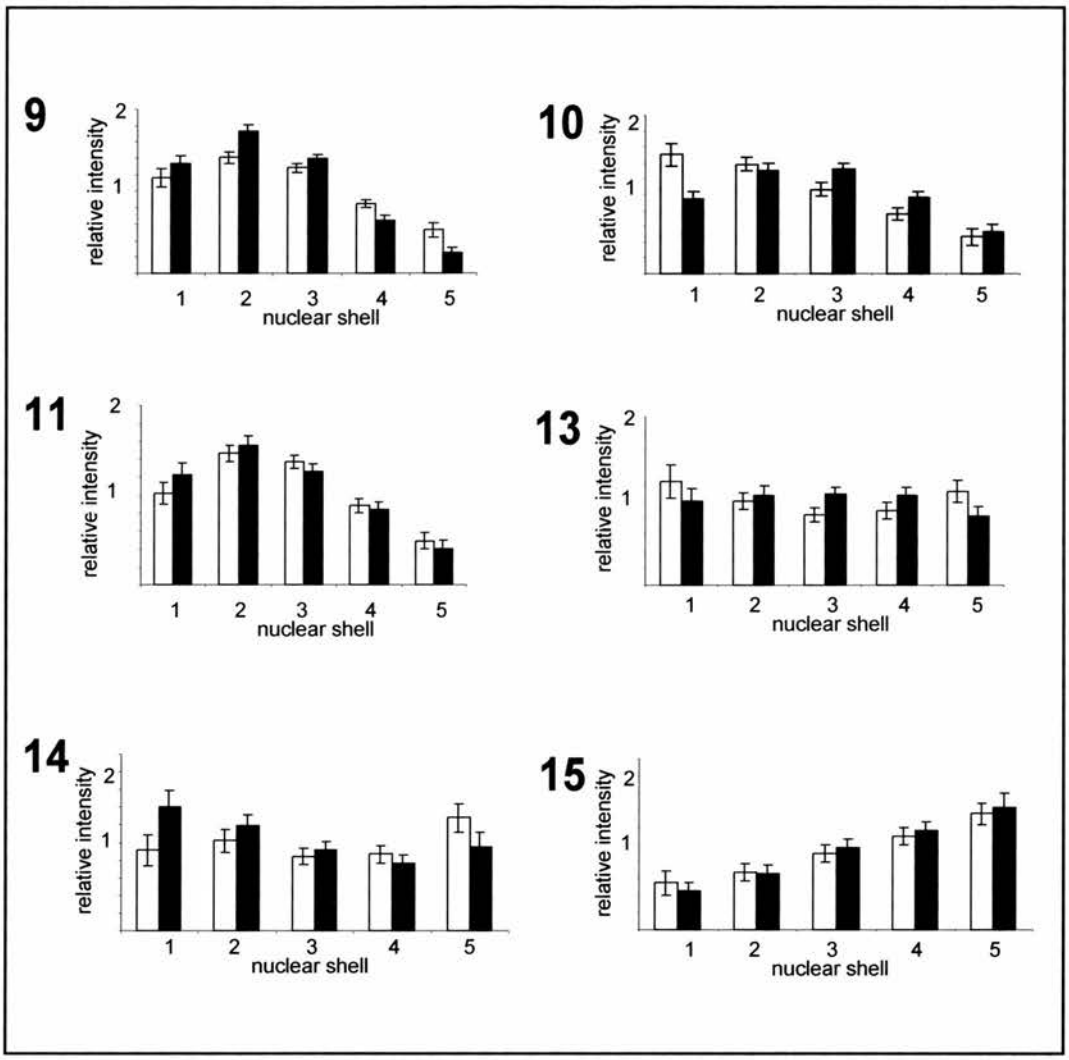

Figure 4.13 Chromosome territory distributions in TSA treated cells. The realtive distributions of chromosome territories were analysed (Figure 3.1) in primary human fibroblasts before (open bars) and after treatment with TSA (filled bars). The mean distribution of relative chromosome paints signal (paint signal/DAPI signal) for each shell is represented as a histogram for HSA9, 10, 11, 13, 14 and 15. Shell 1 represents the nuclear periphery and shell 5 is the nuclear centre. The error bars represent the standard error of the mean (S.E.M) for each data set.

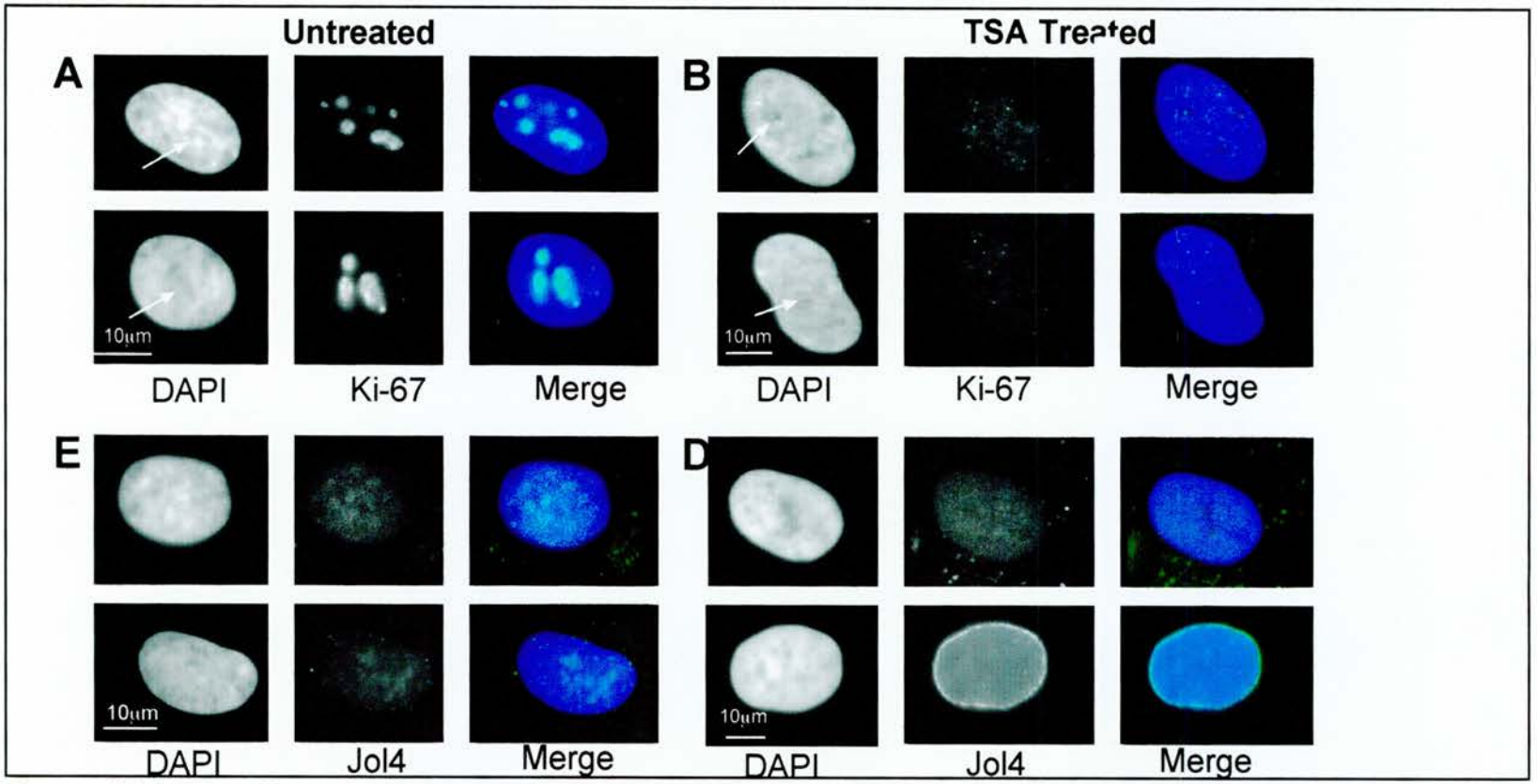

Figure 4.14 The effect of TSA treatment on the nucleolus and nuclear lamina of skin fibroblasts.
IF was performed on primary 1HD (upper panels) and transformed RITVA (lower panels) before (**A** and **E**) and after TSA treatment (**B** and **D**). Antibodies detecting a proliferating cell nucleolar antigen, Ki-67, show that following TSA treatment there is no detectable Ki-67 in these cells (**B**). Detection with Jol4 (that detects lamin A only in quiescent cells, gift from C. Hutchison) shows that following TSA treatment, the lamina is rearranged only in transformed RITVA cells (**D**). Blue = DNA, green = anti-Ki-67 (**A** and **B**) or anti-laminA (Jol4, **E** and **D**).

The composition of the nuclear periphery is also altered in cells that exit the cell cycle. To further characterise the cell cycle block induced by TSA-treatment, IF was performed using an antibody that will only detect lamin A in quiescent fibroblasts (Jol4, a gift from C. Hutchison; Dyer et al., 1997). Proliferating populations of primary fibroblasts show no nuclear stain when treated with this antibody, however cells starved of serum for a period of days (inducing quiescence) show a clear nuclear rim stain. This is attributed to reorganisation of the nuclear lamina when cells enter quiescence, revealing the target epitope (Dyer et al., 1997). Figure 4.14B shows the results of this staining on the cells lines studied. Interestingly, primary fibroblasts do not show Jol4 positive lamin A after TSA-treatment. In contrast, a clear rim of Jol4 detection is seen in treated RITVA cells. This suggests that TSA-treatment can induce quiescent reorganisation of the nuclear lamina in transformed fibroblasts but not primary fibroblasts.

4.6.3 Centromeres

TSA-treatment perturbs centromere function in yeast (Ekwall et al., 1997) and mammalian cells (Taddei et al., 2001). Taddei *et al.,* (2001) also reported redistribution of centromeres to the nuclear periphery with treatment of HDAC inhibitors. My initial observations of TSA-treated cells showed no obvious movement of centromeres, certainly nothing as striking as those reported. Centromeres appear to be arranged consistently in many varied cell types. In myoblasts (Chaly and Munro, 1996), neurons (Choh and De Boni, 1996) and heamatopoetic cells (Alcoa et al., 2000) centromeres are known to be associated with the nuclear periphery and the nucleolus.

Figure 4.11 shows that centromeres are distributed throughout the nucleoplasm in three cell line populations of untreated and treated cells. However, analyses of chromosome territories revealed some reorganisation of chromatin following treatment (section 4.6.1). I therefore chose to quantify the distribution of centromeres in order to detect any changes to this distribution after TSA-treatment.

Centromeres can be visualised as small discreet domains in the nucleus by IF with CREST anti-sera or as discrete chromatin regions using α-satellite repeat probes in FISH procedures (Weier et al., 1991). A common concern with quantitative analysis of IF or FISH images is that the techniques used (e.g. fixation and denaturation) create distortions and artefacts in the cell (Nath and Johnson, 2000; Levsky and Singer, 2003). Hence, microscope observations may not be a true representation of the living cell. I addressed this by observing cenp-A

GFP centromeres (Sullivan and Shelby, 1999) in living cells, cells fixed with 4% pFa (as per IF protocols, section 2.5) and then processed for FISH using an α-satellite repeat probe (section 2.6.2, Figure 4.15 A). Individual live cells were examined under coverslips with PBS (Figure 4.15 Ai), after fixation in 20% glycerol/PBS (a similar glycerol content to imaging mountants; Figure 4.15 Aii) and after 3-D FISH in Vectashield (Figure 4.15 Aiii). The same cells were relocated after each step using a microscope stage mounted with a vernier scale and low power magnification (x20) brightfield images for orientation. Comparing the centromere locations in these three samples reveals no distortion or gross redistribution of the normal arrangement of centromeres following fixation or 3-D FISH. Measurements of the distances (in pixels) between centromere pairs in cells treated under these experimental conditions reveals small differences following fixation and 3-D FISH (Table 4.1 below). Statistical analyses comparing centromere pair distances between live cells and fixed cells (P=0.38) or live cells and FISH samples (P=0.16) shows that centromere positions do not change significantly under these conditions. I am confident that analysing nuclear organisation by IF or FISH gives an accurate representation of the situation in the living cell at this resolution.

Pair	Live Cell	4% pFa Fixed	3-D FISH
1	25.8	27.8	30.8
2	10	8.6	10.6
3	16.8	15.2	19.9
4	20	16.6	15.8
5	17.7	18.6	18.4
6	22.8	21.1	25
7	12	10	10
8	20.2	20.2	21.5
9	13.6	15.6	15.6
10	20.9	21.2	20.6

Table 4.1 Pixel measurements between centromere signal pairs.

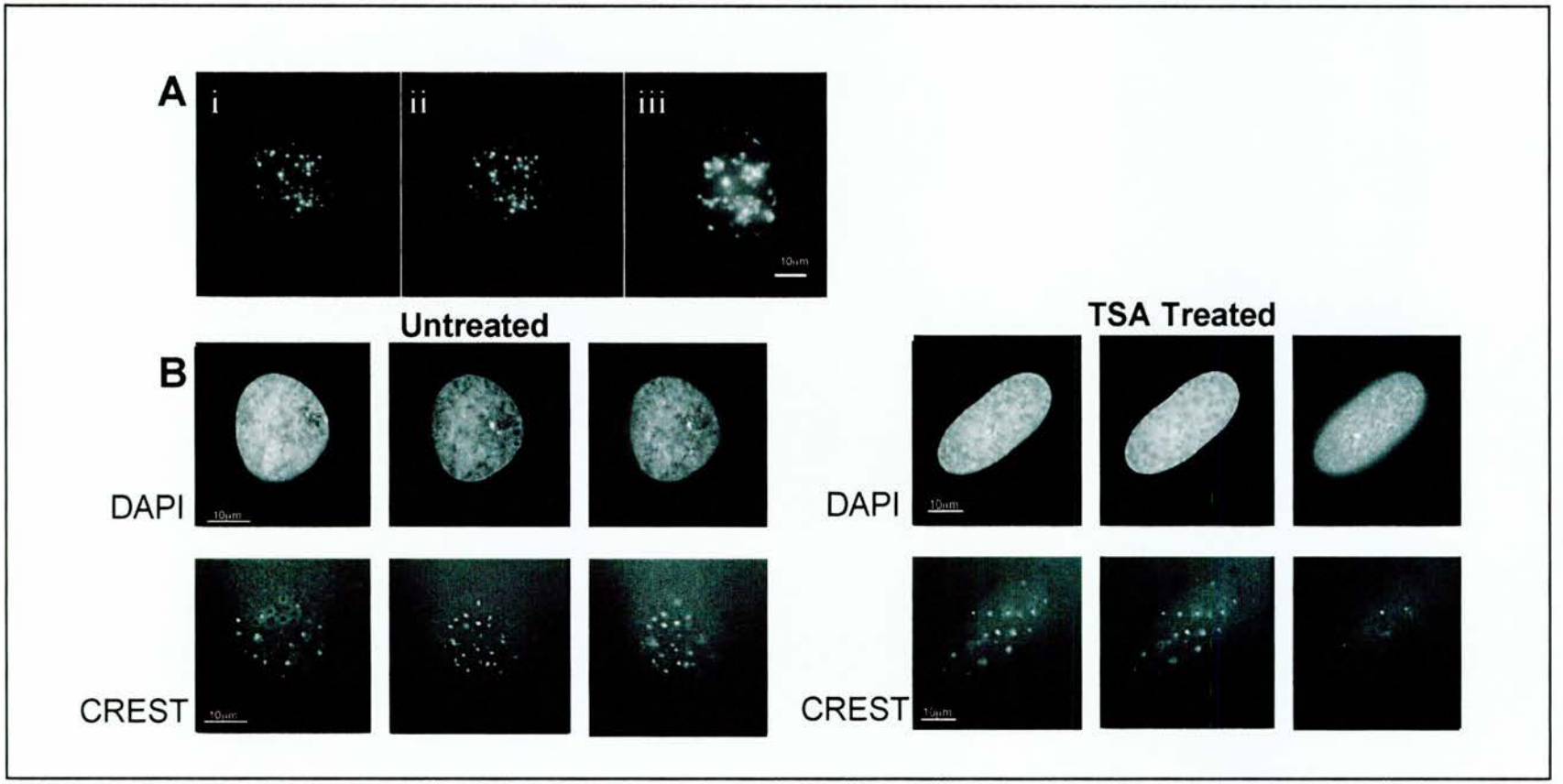

Figure 4.15 The distribution of centromeres in human cells when visualised by IF.
The affects of pFa fixation and FISH procedures were determined by analysis of an HT1080 cell line stably expressing GFP-cenpA. Cells were visualised line (**Ai**), following 4% pFa fixation (**Aii**) and following 3-D FISH using an α-satellite probe (**Aiii**). The gross pattern of centromere distribution is comparable between procedures. The centromeres of 1HD primary fibroblasts were detected by CREST antisera and visualised before and after TSA treatment (B). Images were deconvolved using Hazebuster (Scanalytics Inc), the separate DNA and centromere images are shown for one cell at 1micron distances in the z-plane.

The centromeres of untreated and TSA-treated primary fibroblasts were imaged to address their 3-D distribution rather than simply the distribution in the mid-focal plane of a cell (Figure 4.15B and C). 3-D stacks of IF images (centromeres detected by CREST antisera) were taken of cells and are shown as 1μm steps through the z-plane. In both untreated and treated cells, centromeres are at the nuclear edge but also in the nuclear centre. There is no obvious redistribution of centromeres to the nuclear periphery in treated cells compared with untreated cells.

To measure the position of objects (i.e. centromeres) relative to the nuclear periphery in 3-D space an analysis programme was developed (Box 4.1, Figure 4.16A-E). DNA staining by DAPI proved unsuitable for defining the top and bottom nuclear edges clearly due to signal glare and therefore IF of the nuclear lamina was chosen to define the edge of the nucleus. All images in this analysis were collected from IF samples probed with anti-emerin (Upstate) to delineate the nuclear periphery and CREST to visualise the centromeres (Figure 4.17A). Emerin antibodies were used routinely in this analysis as they only detect the nuclear lamina while lamin A, B or C antibodies will also detect internal lamin-containing nuclear structures, making the 3-D analysis more complex (section 1.5.2). To calculate the 3-D distribution of discrete nuclear entities (in this case centromeres) IPlab (v3.6, Scanalytics) analysis scripts were developed (Paul Perry). Stacks of confocal images were taken through the z plane of a nucleus and subjected to two rounds of image processing.

Briefly, the first round of processing involves converting the complex pixel data of the colour IF image into a simple black and white reconstructed 'nucleus' (Figure 4.17). This reconstruction is then analysed using a second script to calculate specific distances inside the 3-D volume (Box 4.2, Figure 4.16F). All measurements are initially calculated in pixels and later converted to microns. After processing, a computer reconstruction of the nucleus was generated (Figure 4.17B) and this is a numerical description of the distribution of centromere signal within a cell nucleus.

I was interested in comparing the distribution of centromeres between untreated and TSA-treated cells. In order to achieve this I required a method of directly comparing data sets between two populations of cells. This is difficult as fibroblast nuclei are generally flattened and ellipsoidal and nuclei within an unsynchronised population of fibroblasts are not of a uniform size. In addition to this centromere IF does not highlight a constant number of signals due to centromere clustering in the nucleoplasm. Determining the interphase

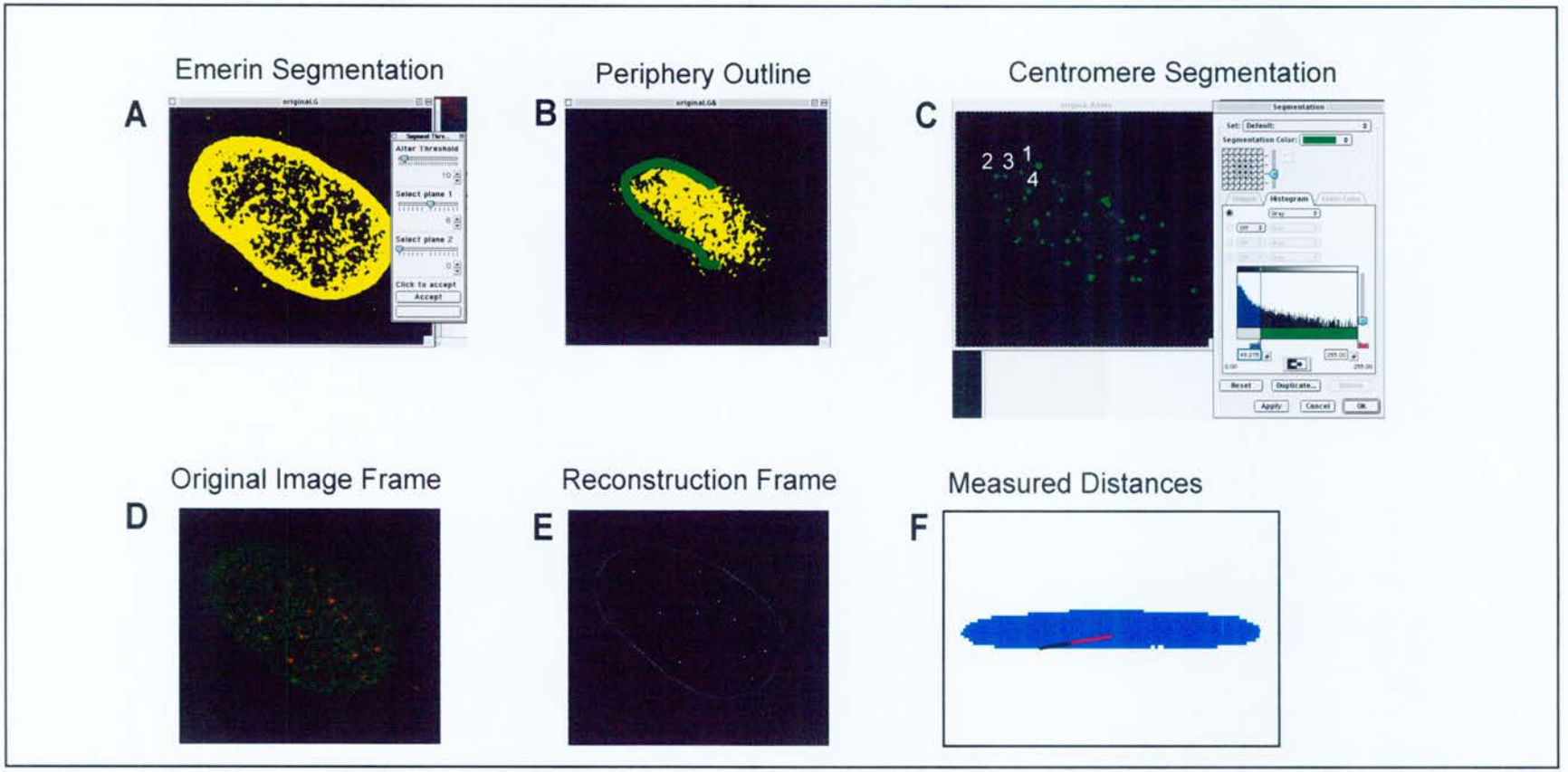

Figure 4.16 Quantitative algorithm to determine the nuclear distribution of centromeres.
The nuclear distribution of centromeres detected by CREST antisera was quantified using an algorithm composed using IPLAB (Scanalytics Inc). The nuclear edge is highlighted by segmentation of emerin antibody staining (**A**, yellow). The nuclear edge (green) is then manually drawn around the defined emerin signal (**B**). Centromeres defined by CREST are segmented and numbered (**C**). The information from an original confocal image (**D**, green = emerin, red = centromeres) is processed and reconstructed (**E**). Wire frame reconstructions of each image stack in the z-plane are used to generate a 3-D representation of the cell volume and distances from the centre to the nuclear edge can be measured within this (**F**).

Box 4.1

Generating simple 3-D reconstructions of colour IF images

TIFF colour images of cells stained for emerin and centromeres (CREST) were captured as described (section 2.11.2). The programme processes each image as follows:

1. The analysis script is provided with the appropriate scaling information for the captured image (pixel to micron conversion factor).
2. The emerin signal of the image stack is isolated and is subjected to interactive signal segmentation. The programme switches between 2 frames of the z-stack (normally the top and middle sections) and the user can increase or decrease the threshold of segmentation to help find the appropriate threshold for clearly showing the nuclear edge (for the entire stack of images, Figure 4.17A).
3. Beginning with the first frame of the z-stack, the user is shown the segmented emerin signal (the nuclear edge) which is used as a guide for interactive drawing of the nuclear periphery using a paintbrush tool (Figure 4.17B). Each frame is processed in turn.
4. The nuclear outline drawing from each frame is used to generate a white wire frame reconstruction of the nuclear outline in a new image stack (Figure 4.17E). The *x*-, *y*-, *z*-co-ordinates of the nuclear centroid are calculated. *x* and *y* are determined by the averaged *xy* centroid in all frames. The *z*-co-ordinate is simply the frame number of the stack that has the largest nuclear area.
5. The centromere (CREST) signal of the image stack is isolated and shown as a maximal projection of the stack (the signal in all frames is squashed onto one flat image, figure 4.17D). The segmentation of this signal can be increased or decreased interactively to ensure all regions of signal are included in the analysis.
6. One large region of signal can be separated into two smaller regions using the eraser option. This is useful as the programme cannot detect when two regions of signal close together may actually represent two discrete centromeres relatively near in *x*- and *y*-co-ordinates but distant in the *z* plane. Additionally, any signal detected corresponding to background signal outside the nucleus can be removed from the analysis at this stage.
7. Regions of centromere signal can be added using the paintbrush option. The analysis programme will only detect signal regions above a set threshold area (10 pixels). The user can ensure that the programme includes all appropriate signal regions by painting additional segments as appropriate.
8. Centromeres are numbered in ascending order beginning at the top left of the image and proceeding to the bottom right corner for reference.
9. The *x* and *y* co-ordinates of the centre of each centromere signal are defined and reported in a results table.
10. The mean signal intensity of each segmented centromere region is traced through the *z*-planes of the image. The *z*-plane number with the highest mean signal intensity defines the *z*-plane of the centromere. The *z*-plane number of each centromere is added to the results table.
11. The *x*-, *y*-, *z*-co-ordinate information generated in the results table is used to add the centroid and centromere locations to the 3-D reconstruction wire frame. White spots, representing the centromeres, are added to inside the nuclear edge wire frame and the nuclear centroid is shown as a green spot (Figure 4.17E).

Box 4.2

Using 3-D image reconstruction to calculate distances

The output generated by the above programme can be used to calculate distances in 3-D. This analysis requires both the wire frame reconstruction of the nuclear periphery and the numerical co-ordinate data of the centroid and centromeres.

1. Centromere number one is selected by the programme.
2. The angle formed between the nuclear centroid and a centromere when the stack is viewed from above is calculated. The 3-D image stack is rotated and a section is cut such that the centroid and centromere are in a straight line.
3. A line extends outwards from the centroid towards the centromere spot. This line continues through the centromere spot and stops when the line crosses the defined nuclear edge.
4. Two distances are calculated (in pixels) and added to the results table -
   (i) centroid to the centromere
   (ii) centroid to the nuclear edge
5. Each centromere is processed in turn until all calculations have been made.

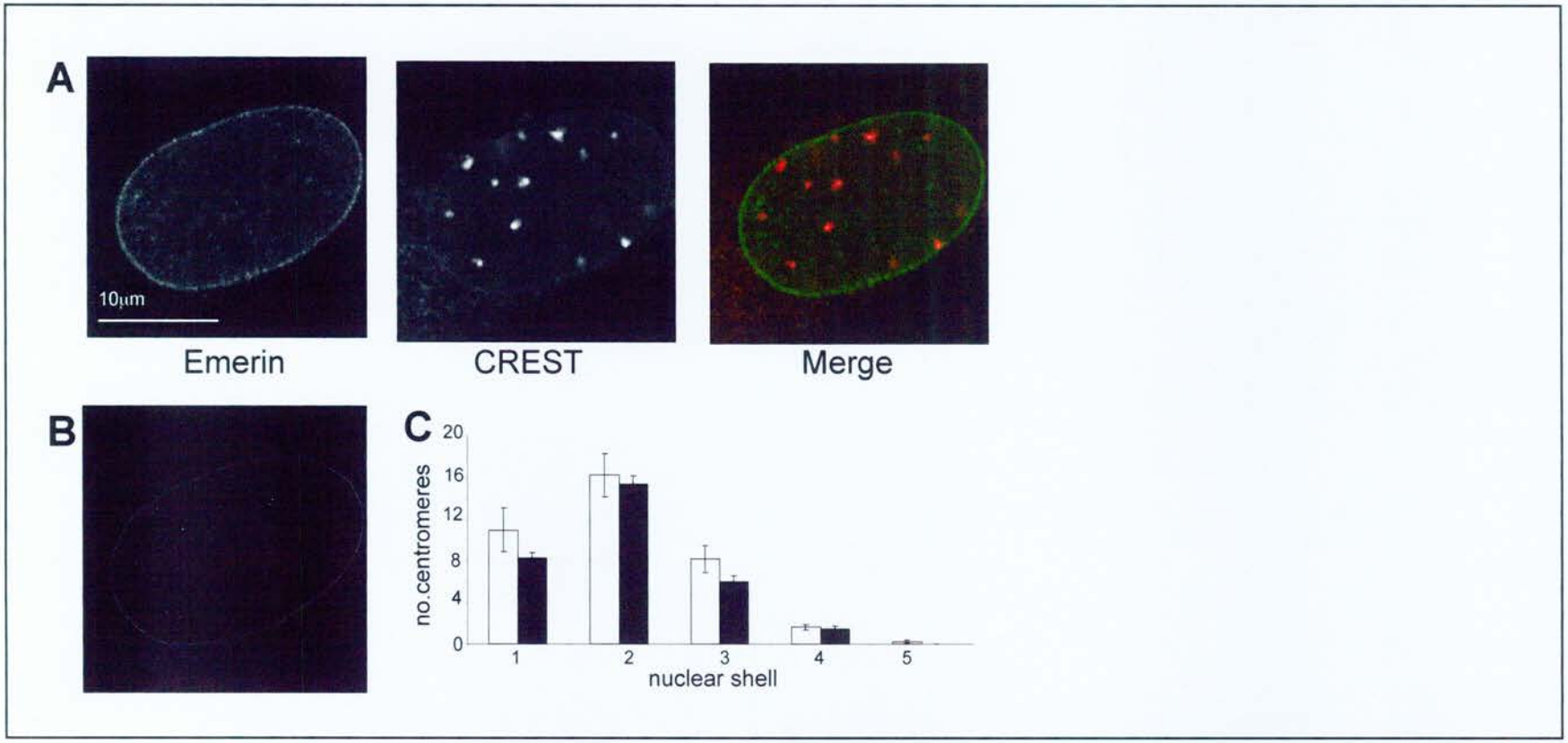

Figure 4.17 Comparing the nuclear distribution of centromeres in untreated and TSA treated primary fibroblasts. Confocal images of cells detected with CREST antisera and anti-emerin (Upstate) at 0.5μm intervals in the z-plane were collected (**A**). Each stack of images was processed using the algorithms described in boxes 4.1 and 4.2 to generate wire frames (**B**) and measurements were taken from the centroid of the nuclear volume, through each centromere, to the nuclear edge. Measurements were taken for untreated (open bars) and treated cells (filled bars) and these distributions of centromeres in the nuclear volume were compared (**C**, n=10). In untreated cells, mean no. of detected centromeres =37.3 and for TSA treated cells mean no. centromeres = 31.1. Shell 1 is the nuclear edge and shell 5 is the nuclear centre. Error bars show the standard error of the mean (S.E.M).

distribution of chromosome territories divides each nucleus into 5 concentric shells and calculates the percentage of chromosome paint signal in each shell (section 3.2.1; (Croft et al., 1999). I used this principle to divide the 3-D reconstructed nucleus into these same 5 concentric shells and illustrate the distribution of centromeres across these 5 regions. The distance from a centromere to the nuclear edge was calculated as a percentage of the total distance from the centroid, through the centromere, to the nuclear edge. The innermost shell (shell 5) of the nucleus was defined as that with 0-20% of the centroid-edge value. Shell four was 21-40%, shell three was 41-60%, shell two 61-80% and the outermost shell (shell 1) 81-100%. The number of centromere signals in these five nuclear shells was determined for 10 cells in untreated and TSA-treated populations. A histogram of centromere distribution was generated. Untreated fibroblasts have the highest proportion of their centromeres in the outer 61-80% of the nucleus (shell 2), and very few centromeres in the centre of the nucleus (shell 1, Figure 4.16C). Therefore fibroblast centromeres are concentrated at the nuclear periphery in agreement with what has been previously described (Chaly and Munro, 1996; Choh and De Boni, 1996; Alcobia et al., 2000). Cells treated with TSA also have the highest frequency of centromeres in the outer 61-80% of the nucleus (Figure 4.16C). I can identify no change to the distribution of centromeres in untreated and treated fibroblasts. Enrichment of centromeres in nuclear shell four is significant in both cell populations ($P<0.001$) and the distributions of centromeres in untreated and treated cells are not significantly different from each other ($P=0.78$). I conclude that centromeres concentrate toward the nuclear periphery in primary fibroblast nuclei and that this distribution is not altered when HDACs are inhibited by TSA.

Taddei, *et al.*, (2001), reported that TSA-treatment results in nuclear reorganisation specifically of centromeres while I found no evidence of this. What is the explanation for this? Firstly, the cells used are different. I have analysed primary human fibroblasts where they used HeLa cells. Primary fibroblasts were selected as, in contrast to HeLa cells, they are not transformed, their nuclear organisation has been extensively studied (Boyle et al., 2001) and they have a normal stable karyotype. I have demonstrated that the nuclear lamina responds differently to TSA-treatment in primary and transformed cells (Figure 4.14). This could suggest that primary and transformed cells respond differently, however, visual observations of RITVA cells suggest they do not relocate their centromeres following TSA-treatment (Figure 4.11). This should be quantified using the 3-D reconstruction and analysis scripts described in Boxes 4.1 and 4.2.

4.7 Discussion

The data in this chapter analyse the role of histone acetylation in spatial arrangement of the nucleus. By using a cell-permeable chemical inhibitor of HDAC activity, histone acetylation was increased in the nuclei of treated cells. To address the question of how this modification might be involved in nuclear organisation, I have described the distribution of the histone modifications themselves (section 4.4), chromosome territories (section 4.6.1), and centromeres (section 4.6.3) in treated cells. Further observations were made regarding the composition of defined chromatin compartments (section 4.5) and nuclear structures (section 4.6.2). Disruption of endogenous histone acetylation turnover will go some way to disrupt nuclear organisation at the level of chromosome territories and nuclear lamina. I found that TSA-treatment results in altered distribution of acetylated histones but not centromeric heterochromatin.

A specific distribution of histone modifications has been demonstrated for AcK9-H3, met_2- and met_3K9-H3 and AcK5-H4 here. I have described peripheral enrichment of histone acetylation following TSA-treatment (Figure 4.3 and 4.5). It is unlikely that TSA molecules can only target HDAC enzymes at the nuclear edge and cannot permeate all of the nucleoplasm as fluorescent molecules of varied sizes can diffuse rapidly (reviewed in Parada and Misteli, 2002). Further experiments are required to determine if HDACs are predominantly found at the nuclear edge. In this situation, histone modifications would be more rapidly turned over at the nuclear periphery and inhibition of HDAC activity would result in initial enrichment of acetylated histone levels at the nuclear edge. Endogenous HAT activity can now be targeted by synthesised chemical inhibitors which have recently been developed (Lau et al., 2000; Thompson et al., 2001; Costanzo et al., 2002; Balasubramanyam et al., 2003). It would be interesting to target the HAT transferase activity by chemical inhibition or RNAi knockdown and follow any redistribution of histone acetylation modifications in treated cells. Specific peripheral localisation of HDACs in cells would result in an enrichment of acetylated histones in the nuclear centre when HAT activity was disrupted.

Following TSA-treatment there is a small but significant increase to met_3K9-H3 levels at the nuclear periphery. Quantitative studies of histone methylation show that methylation begins during the S-G2 transition of the cell cycle, with all methylation being complete at the onset

of mitosis (Shepherd et al., 1971). Methylation turnover in the nucleus is also considered to be much less dynamic than histone acetylation (Byvoet, 1971) although there have been reports of constant methylation turnover in arrested cell populations (Annunziato and Hansen, 2000) and to date no histone demethylase activity has been reported in the cell (Zhang and Reinberg, 2001). TSA-treatment blocks the cell cycle before the onset of mitosis and treated cells are predominately blocked in G1. However, it should be noted that TSA takes several days to block the cell cycle (section 4.3) and methylation levels could be altered before this arrest.

TSA is a specific inhibitor of HDACs, however, it blocks cell cycle progression and may also contribute to misregulation of gene expression (section 4.3; Brinkmann et al., 2001; Mulholland et al., 2003). There is also some evidence from plants that chemical inhibition of HDACs by TSA-treatment can alter their DNA methylation status (Selker, 1998). Therefore any repositioning events could be due to secondary effects of TSA activity, rather than disrupted histone acetylation levels. This role for DNA methylation could be tested directly by Southern Blot analysis of genomic repeats in TSA-treated cells cells (Suzuki et al., 2002). Reciprocally, 5-aza-cytidine treatment of cells could be used to disrupt normal DNA methylation levels. In these experiments, the levels of histone modifications could be determined by western blot and immunofluorescence.

My data involve quantitative analysis of centromere distribution averaged across 10 randomly selected cells. There has previously been very little quantitative analysis of centromere position published until recently (Weierich et al., 2003). The data from Taddei, *et al.*, involves no such quantitative analysis and their conclusion appears to be based on one mid-plane section of a confocal microscope image. I conclude that, as in model organisms (Chaly and Munro, 1996; Choh and De Boni, 1996; Alcobia et al., 2000), centromeres are preferentially located at the nuclear periphery and that TSA-treatment does not alter this.

TSA, despite clearly altering patterns of histone acetylation in the nucleus, does not result in large scale changes in nuclear organisation of chromosomes or centromeres. Therefore I would suggest that histone acetylation is not important for maintaining chromosomal organisation. There is an intriguing paradox in the behaviour of HSAs 13/15 and 14. While each of these chromosomes are acrocentric, and hence interact with the nucleolus, they locate to different interphase locations; HSA13 is peripheral while HSA14 and 15 are internal. Previous work suggests that these chromosomes differ both at the sequence and

chromatin levels as the more internal chromosomes are predicted to be gene-rich, contain less heterochromatin and be acetylated (Boyle et al., 2001; Sadoni et al., 1999). Following TSA-treatment, only HSA14 relocates, becoming more peripheral. Hypothetically, hyperacetylation of HSA14 could create binding sites for peripheral tethering factors and result in recruitment of this chromosome to the periphery. To further investigate factors that may be important in the peripheral localisation of chromatin in the nucleus I have used genetic approaches to address this question (Chapter 5).

CHAPTER 5

ROLE OF THE NUCLEAR LAMINA IN NUCLEAR ORGANISATION

5.1 INTRODUCTION

One of the most conspicuous structures in the nucleus that might be involved in establishing and/or maintaining the organisation of chromatin is the nuclear periphery. In vertebrates this consists of the lamina and INM (Figure 1.9; see section 1.5.2 and 1.5.3). Chromatin mobility studies in both fission yeast and cultured human cells reveal that close proximity to the nuclear edge constrains the mobility of a genetic region (Hediger et al., 2002; Chubb et al., 2002). In fission yeast, the Ku and Sir proteins have been identified as the nuclear factors involved in anchoring telomeres to the nuclear envelope (Andrulis et al., 1998; Hediger et al., 2002). Yeast do not have a nuclear lamina and Ku/Sir proteins are not INM proteins. Therefore the protein Enhancer of silent chromatin (EscI) is proposed to be one of the factors which mediate anchoring of telomere/Ku/Sir complexes to the nuclear edge (Hediger et al., 2002). These, or equivalent, mechanisms might also be utilised in mammalian cells, however any direct interactions remain to be demonstrated.

As discussed in the introduction, the nuclear lamina is a filamentous network of lamin proteins. While many common properties have been found for each of the lamin proteins, here I have focussed on those of lamin A, as these functions are pertinent to the experiments contained within this chapter.

5.1.1 Lamin A protein functions

Lamin A protein has conserved central α-helical rod domains and non-conserved globular N- and C-terminal structural domains (Figure 5.1A; Fuchs and Weber, 1994). Crystallography of the C terminus reveals immunoglobulin-like folds (Figure 5.1B;

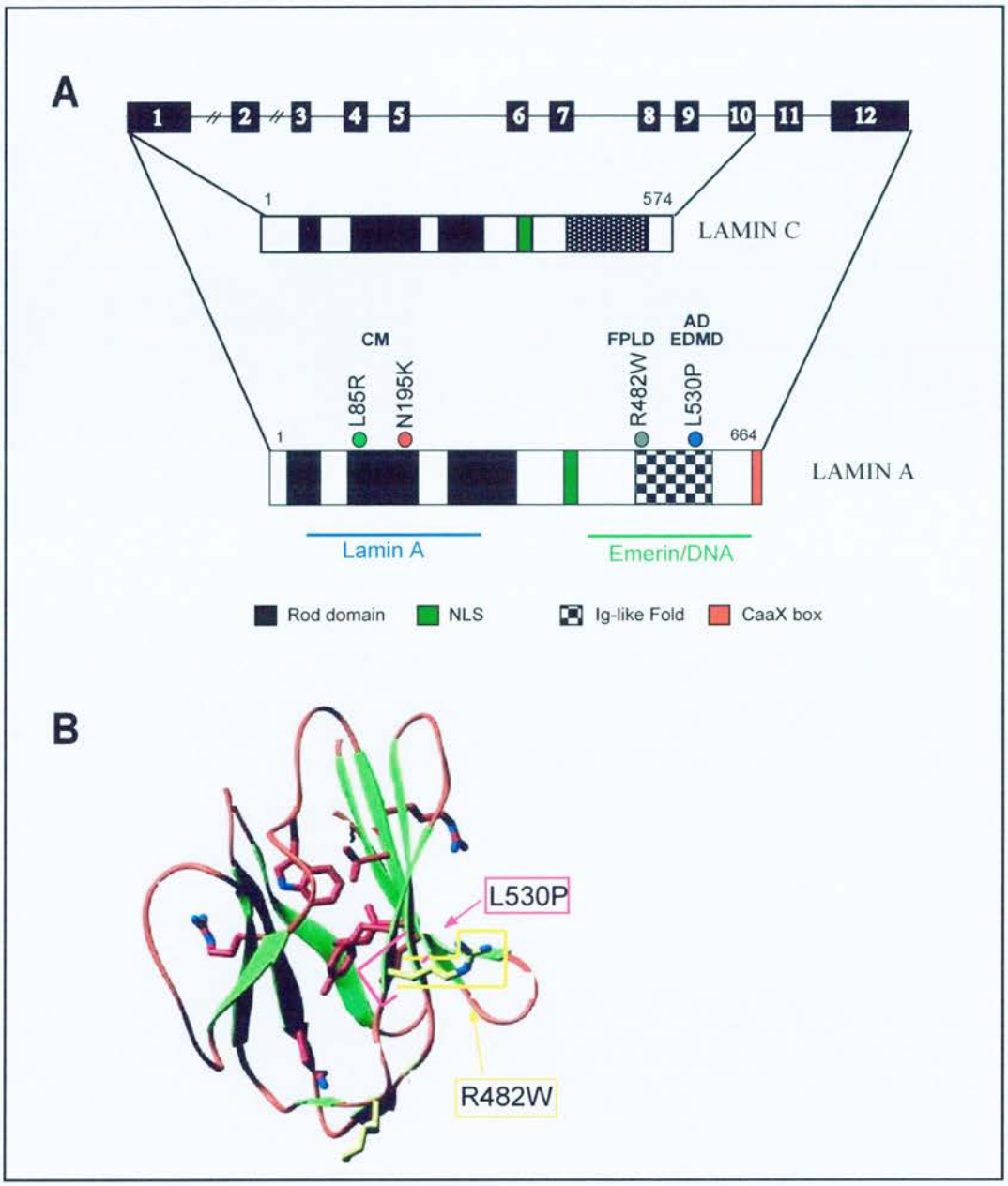

Figure 5.1 Lamin A gene and protein structure.
Schematic of the *LMNA* gene of HSA1 and the 574 and 664 amino acid lamin C and A proteins (**A**). Lamin C is a truncated splice variant of lamin A and lacks exons 11 and 12 which results in loss of the C-terminal CaaX motif (red). The central rod domain is indicated by 3 sub-domains (black). The NLS is shown by the green box (residues 417-422 of lamin A) and C-terminal CaaX sequence shown. The Ig-fold (residues 436-544 of lamin A) is shown (hatched). There are characterised functional regions of lamin A involved in lamin A dimerisation and emerin/DNA binding (blue and black lines respectively). The laminopathy mutations studied are highlighted (coloured circles). Crystal structure of the C-terminal Ig-fold (**B**). The positions of two laminopathy mutations are highlighted. R482W (yellow box) is a surface residue while L530P (pink box) is buried in the core of the domain.
Key – L85R (Cardiomyopathy, green), N195K (Cardiomyopathy, red), R482W(Lipodystrophy, grey), L530P(Autosomal-dominant EDMD, blue)

(Dhe-Paganon et al., 2002; Krimm et al., 2002). Many research groups have suggested that lamin A is important in building and maintaining the interphase nucleus. Lamin A can bind naked DNA and chromatin (Glass et al., 1993; Luderus et al., 1994; Stierle et al., 2003) or many nuclear envelope proteins *in vitro* (Section 1.5.3, summarised in Table 1.1).

These interactions facilitate targeting of nuclear membrane vesicles to chromosomes during mitosis (Burke and Gerace, 1986). Co-immunoprecipitation of lamin A and emerin/lamin C also showed that lamin A interaction is required to recruit these proteins to the INM (Vaughan et al., 2001). Lamins A and C were among the first cellular proteins to be silenced or 'knocked down' by RNA interference in human cell culture (Elbashir et al., 2001b; Harborth et al., 2001). In these experiments, absence of the lamin proteins results in mislocalisation of emerin as it accumulates in the ER of treated cells. Lamin A is also involved in assembling and correctly spacing nuclear pores (Goldberg et al., 1995; Zhang et al., 1996).

Lamin A protein can influence many complex nuclear biological processes, such as control of gene expression and DNA replication. A role for lamins in gene transcription was first proposed by (Nigg, 1989) as it was suggested they may sequester transcription factors. Lamin A protein can also interact with retinoblastoma protein (Ozaki et al., 1994), splicing factors (Jagatheesan et al., 1999; Kumaran et al., 2002) and TBP (Spann et al., 2002; Kumaran et al., 2002) and lamins are thought to influence cell differentiation (Rober et al., 1989; Lehner et al., 1987; Lourim and Lin, 1992). In addition, alteration to lamina composition has been reported with tumour progression (Dyer et al., 1997; Vaughan et al., 2001), although it should be noted that ectopic expression of lamin A does not alter the differentiation state of embryonic carcinoma cells (Peter and Nigg, 1991).

A role for lamins in DNA replication is suggested by the discovery that an N-terminal truncation of lamin A halts elongation of replication forks and disperses proliferating cell nuclear antigen protein (PCNA) in microinjection studies (Spann et al., 1997; Moir et al., 2000). Lamin A is also localised to sites of dNTP incorporation by immunofluorescence (Kennedy et al., 2000). Immunodepletion of the single embryonic protein (lamin B-type) in X*enopus* extracts also prevents DNA replication (Newport et al., 1990).

Model organism work has corroborated some of the lamin protein functions initially proposed by *in vitro* experiments. In *C. elegans*, RNA interference of the single lamin, *lmn-1*

(B-type), has an embryonic lethal phenotype. Microscopy of targeted embryos reveal changes in nuclear shape, missegregation of chromosomes and aberrant clustering of NPCs (Liu et al., 2000). A P-element insertion in the *Drosophila* lamin Dm_0 gene (B-type) results in retarded development, reduced viability and sterility in homozygotes. These flies also have impaired locomotion and clustering of NPCs (Lenz-Bohme et al., 1997). *LMNA* homozygous knockout mice show growth retardation, cardiac and skeletal muscle wasting (myopathy) and die at 4-8 weeks after birth (Sullivan et al., 1999). At the cellular level, there is patchy distribution of other lamina proteins e.g. LAP2β and lamin B, clustering of NPCs, and emerin mislocalises to the ER (Sullivan et al., 1999).

5.1.2 Human disease and the nuclear lamina

Recently, interest in the function of the nuclear lamina and associated proteins has increased. This has been largely due to the discovery of lamin A/C mutations in several human diseases, termed the laminopathies (Burke and Stewart, 2002). Perhaps more intriguing is the identification of mutations of lamin A/C (*LMNA)* or emerin genes in dominant (autosomal) and recessive (X-linked) forms of the same laminopathy, Emery-Derives Muscular Dystrophy (AD-EDMD and X-EDMD respectively; Bione et al., 1994; Bonne et al., 1999). Several laminopathies have now been described (Table 5.1). These progressive diseases have a range of symptoms, mainly skeletal and/or cardiac muscle wasting (myopathy), connective tissue contracture (i.e. tendons) and unusual or disrupted adipose tissue deposit. However, the more recently identified laminopathies - Hutchinson-Gilford Progeria Syndrome (HGPS; Eriksson et al., 2003; Sandre-Giovannoli et al., 2003), Mandibuloacral Dysplasia (MAD; Novelli et al., 2002) and atypical Werner's Syndrome (Chen et al., 2003) – appear not to affect the classic tissues and instead result in premature ageing, skull deformities and unusual skin pigmentation.

Laminopathies are essentially allelic variants. Disease is most commonly a result of various missense mutations along the length of the *LMNA* coding region, and at least 40 different mutations have been reported for AD-EDMD alone (reviewed in Ostlund and Worman, 2003). The genetics of laminopathy inheritance may not be classically Mendelian as pedigrees have been identified where more than one laminopathy is present (Bonne et al., 2000). This suggests that disease pathology could be influenced by modifying genes or environmental factors.

Syndrome	Gene Affected	Symptoms
X-linked Emery-Dreifus Muscular Dystrophy (X-EDMD, recessive)	*Emerin* OMIM 3103000	Contracture of elbows and Achilles' tendons Slow progressive muscle wasting Cardiomyopathy
Autosomal Dominant Emery-Dreifus Muscular Dystrophy (AD-EDMD, dominant)	*LMNA* OMIM 181350 OMIM 604929	Contracture of elbows and Achilles' tendons Slow progressive muscle wasting Cardiomyopathy
Dilated Cardiomyopathy (CM, dominant)	*LMNA* OMIM 115200	Ventricular dilation, impaired systole
Limb girdle muscular dystrophy with atrio-ventricular conduction disturbances (LGMP, dominant)	*LMNA* OMIM 159001	Skeletal myopathy and cardiac conduction defects
Dunnigan-type Familial Lipodystrophy (FPLD, dominant)	*LMNA* OMIM 151660	Complete or partial loss of adipose tissue following puberty.
Charcot-Marie-Tooth Disorder (CMTD, recessive)	*LMNA* OMIM 605588	Muscle weakness and wasting with loss of large myelinated fibres and axonal degeneration. Foot deformities.
Hutchison-Gilford Progeria Syndrome (HGPS, dominant)	*LMNA* OMIM 176670	Premature ageing. Failure to thrive. Delayed dentition, alopecia and sclerodermatous of the skin.
Mandibuloacral Dysplasia (MAD, recessive)	*LMNA* OMIM 248370	Postnatal growth retardation, craniofacial abnormalities and mottled cutaneous pigmentation.
Atypical Werner's Syndrome (AWS, recessive)	*LMNA*	Insulin resistance, type 2 diabetes and artherosclerosis. *Chen, et al., 2003 Lancet (362) p440*

Table 5.1 Symptoms of Human Laminopathies

OMIM= Online Mendelian Inheritance in Man

http://www.ncbi.nlm.nih.gov/entrez/query.fcgi?db=OMIM

With such a wide spectrum of symptoms arising from mutations of one gene, there is great speculation about the disease mechanisms of the laminopathies. There are currently four main hypotheses for laminopathy disease mechanisms - nuclear weakness, altered nuclear positioning in the cell, changes in gene expression or changes in ER composition (reviewed in Wilson, 2000; Hutchison et al., 2001; Burke and Stewart, 2002). Newport et al., (1990) suggest that lamin depleted nuclei are more fragile *in vitro* and such fragility has also been reported for hepatocytes of *LMNA* knockout mice (Sullivan et al., 1999). Nuclear weakness as a disease mechanism is favoured as it could explain why affected individuals are very rarely diagnosed at birth (Hutchison et al., 2001). Muscle tissue is syncitial (i.e. one large muscle cell has many nuclei), non-dividing and long-lived, hence, fibres may tolerate or absorb nuclear damage for a finite length of time. Myopathy would only present after a sustained period of damage over a number of years. However, this hypothesis may not be as valid for affected tissues that are not syncitial in nature, for example adipose or bone tissue. It has also been suggested that the position of the nucleus in the cell cytoplasm may influence disease progression (Burke and Stewart, 2002). Myopathy may result from altered nuclear location within the muscle fibre, where close proximity to the nerve synapse (at the neuromuscular junction), may be important to the interaction of lamin A with Syne-1 (=Myne1; Apel et al., 2000; Mislow et al., 2002b; Burke and Stewart, 2002). Finally, *LMNA* disease-associated mutations may result in changes to ER composition. As the ER membrane is contiguous with the INM, components failing to anchor, for example emerin, will drift back into the ER membrane (Ostlund et al., 2001). This may disrupt cholesterol and/or fatty acid metabolism and synthesis pathways that are important to muscle cells for calcium influx/signalling which control muscle contraction.

Preliminary patient microarray studies identified a possible 28 genes whose expression is altered in EDMD patients (Tsukahara et al., 2002). Comparison between mRNA transcript levels in wild type and EDMD fibroblasts reveal many mRNA levels are increased (including lamin C, fibroblast growth factor receptor, myosin light chain MLC-2 and estrogen-regulated breast cancer protein LIV-1) while others are decreased (including retinoic acid hydroxylase and neurogranin). A role for lamin proteins in gene expression was first proposed by (Nigg, 1989). Many studies have now revealed that lamins can interact with transcriptional machinery (see Section 5.1.1). EDMD model homozygous *LMNA* knockout mice show altered recruitment of pRB to heterochromatin (Sullivan et al., 1999). It has also been suggested that laminopathy mutations may result in reorganisation of interphase chromatin (Fidzianska et al., 1998; Ognibene et al., 1999; Wilson, 2000). *Ex-vivo*

fibroblast cultures and muscle biopsies from affected patients have shown misshapen nuclei and necrosis within the muscle fibres of patients with X-EDMD (Fidzianska et al., 1998; Ognibene et al., 1999) and mandibuloacral dysplasia (Novelli et al., 2002). EM analysis has also revealed regions of thicker nuclear lamina, associated with compacted regions of heterochromatin and localised regions where chromatin appears to have become detached from the nuclear periphery (Ognibene et al., 1999). However, studies in X-EDMD lymphoblasts (that express no emerin) revealed that chromosome territories are arranged as normal in these patient cells (Boyle et al., 2001). Therefore the authors conclude that emerin is not necessary for localisation of gene-poor chromosomes at the nuclear periphery.

5.1.3 How do disease-associated mutations in lamin A affect protein structure and function

Many of the identified disease-associated mutations of the *LMNA* gene occur within functional domains of the protein (Figure 5.1). How do these mutations affect the normal function of the protein and does the location of the mutation determine disease phenotype?

The lamin gene consists of 12 exons, and the mutations associated with pathological cardiac/skeletal muscle phenotypes are found within the first 11 exons (Figure 5.1). EDMD mutations have been found distributed throughout the *LMNA* sequence, and these are mainly missense mutations (Ostlund and Worman, 2003). LGMD and CM appear to be caused mainly by mutations in the N-terminal rod domains of the protein while FPLD and MAD mutations are clustered within the globular carboxyl-terminal domain (Mounkes et al., 2003a). The majority of FPLD mutations are clustered in exon 8. Missense mutations within the Ig-fold at the carboxy-terminus of the protein, at residue 482 (R482W and R482Q) show lower DNA binding affinities *in vitro;* Stierle et al., 2003). It has also been demonstrated that R482W (FPLD) and L530P (AD-EDMD) are at different locations within the Ig-fold domain. Crystal structure predictions place residue 482 on the external surface of the domain, while residue 530 is in the domain core (Figure 5.1B; Dhe-Paganon et al., 2002; Krimm et al., 2002). Hence, mutations at these residues may have different biological affects on the protein as R482W on the domain surface may disrupt/enhance the interaction of lamin A with other proteins or DNA while L530P may destabilise the structure of the domain. An interesting recent report shows that a dominant HGPS missense mutation at nucleotide 1824 (residue 608, exon 8) results in activation of a cryptic splicing site (Sandre-Giovannoli et al., 2003). This results in ~50 amino acids, and hence the CaaX box, being absent from the lamin A tail and patients have only 25% of normal protein levels.

5.2 Do disease-asscoiated mutations in lamin A affect nuclear organisation?

Given the biochemical evidence for lamin A binding to DNA/chromatin and INM proteins, I considered that lamin A may be the link bridge responsible for tethering peripheral chromosomes to the nuclear edge. If this is true, some laminopathy mutations may abolish (or enhance) the anchoring of chromatin to the nuclear edge. I therefore analysed many aspects of interphase nucleus organisation in cultured cells overexpressing the selected laminopathy mutation proteins. In order to investigate the biological effect of laminopathy mutations during interphase, I chose 4 missense mutations of lamin A protein for overexpression studies in human-derived cells. My rationale for this is that these mutations are responsible for autosomal dominant forms of disease and therefore can exert their phenotype in the presence of wild type protein. The locations of the selected mutations are illustrated in Figure 5.1A; L85R (Cardiomyopathy - CM), N195K (CM), R482W (Familial Partial Lipodystrophy - FPLD), L530P (Autosomal Dominant Emery-Dreifus Muscular Dystrophy – AD-EDMD). Although involved in the same disease, L85R and N195K were both selected as they have shown different behaviours when transiently expressed in mouse myoblasts (Ostlund et al., 2001). L85R mutant appears to behave as endogenous protein in these cells, while N195K forms large intra-nuclear protein aggregates, this suggests that the two mutations may affect lamin A's ability to polymerise into filaments. As mutations R482W and L530P are found at different positions within the Ig-fold, I also chose to investigate them.

5.2.1 Ectopic expression of lamin A mutants

N-terminal FLAG-tagged fusion constructs (SV40 promoter, pSVK expression vector backbone) of wild type and mutant pre-lamin A were obtained from Prof. H. Worman, Columbia University (Figure 5.2A ; Ostlund et al., 2001). Pre-lamin A is a precursor to mature lamin and is processed by the cell, removing 18 C-terminal amino acids, before incorporation into the nuclear lamina (Weber et al., 1989; Sinensky et al., 1994). In order to observe lamin A protein in living cells, I generated Green Fluorescent Protein (GFP)-fusions for each of the mutants. Wild type GFP-human lamin A (GFP-HLA) fusion (CMV promoter, pCDNA-3-EGFP expression vector backbone) was obtained from Dr Karnitz, The Mayo Clinic (Figure 5.2B; unpublished). A summary of the cloning strategy is shown in

Figure 5.2. Briefly, for each mutant in turn, FLAG-pre-lamin A coding sequence was excised from the pSVK backbone using EcoRI/SalI and the 2100bp insert fragment was purified. This was cloned into pUC21 digested with XhoI/EcoRI (Figure 5.2C; XhoI and SalI sites have compatible cohesive ends). From this cloning intermediate, a 1800bp AccI/SpeI fragment of the coding sequence (removing the FLAG tag and the first 175bp of lamin A) was purified. The AccI site is upstream of each mutant codon and the SpeI site is downstream of the stop codon. Due to the presence of more than one AccI enzyme site in the pCDNA backbone, generation of a GFP fusion of lamin A protein in this vector required a three-way ligation step. Following a complete AccI/EcoRI digest of GFP-lamin A pCDNA, fragments of 5.4kb (the vector backbone) and 894bp (GFP coding sequence plus 0-175bp of lamin A) were purified. The final ligation step of 894bp (GFP coding sequence plus 1-175bp of lamin A) to 1880bp (mutant pre-lamin A sequence) and 5.4kb vector backbone generated GFP-fusion expression constructs of each disease-associated mutant lamin A protein (Figure 5.2D).

Transient transfections (section 2.2.6) of both the original FLAG-tagged and my GFP-tagged constructs were performed to express the fusion proteins in HT1080 cells (Figure 5.3 Ai-iv and Bi-iv). Each protein was successfully expressed, processed and incorporated into the nuclear lamina in these cells, as evident by the bright nuclear ring visualised by anti-FLAG antibody or GFP signal. It was noted that transient expression of N195K in human cells showed no aggregation into intra-nuclear foci, in contrast to what has been reported in mouse myoblast cells (Figure 5.3; (Ostlund et al., 2001). There also appears to be a high level of nucleoplasmic protein in addition to protein at the nuclear periphery. Internal sites of FLAG-lamin A L530P and GFP-L85R are also seen in Figure 5.3. These are invaginations of the nuclear membrane and not intra-nuclear foci since they can be followed from the apical surface, through the z-plane to the middle or base of cells (data not shown). The presence of such invaginations has previously been reported for many types of culture cells (Bridger et al., 1993; Fricker et al., 1997; Broers et al., 1999).

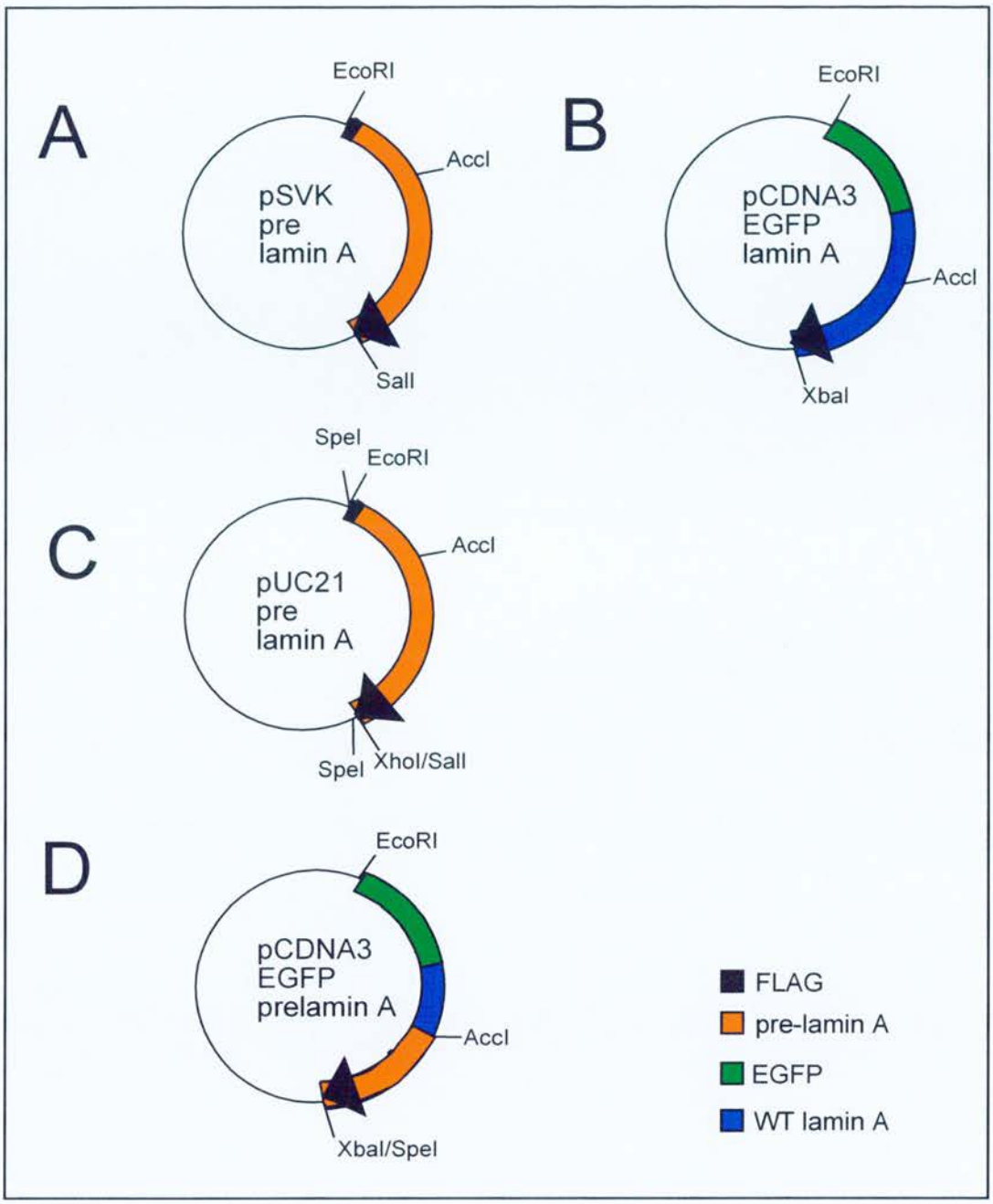

Figure 5.2 Experimental cloning strategy.
N-terminal FLAG-prelaminA constructs (wild type and mutant) were obtained from Prof. H. Worman, Columbia University (**A**). Using an existing N-terminal GFP-lamin A (wild-type) fusion construct (**B**; L. Karnitz, Mayo Clinic), via a pUC21 pre-lamin A mutant cloning intermediate (**C**), N-terminal GFP-prelamin A mutant constructs were generated (**D**). For details see text.

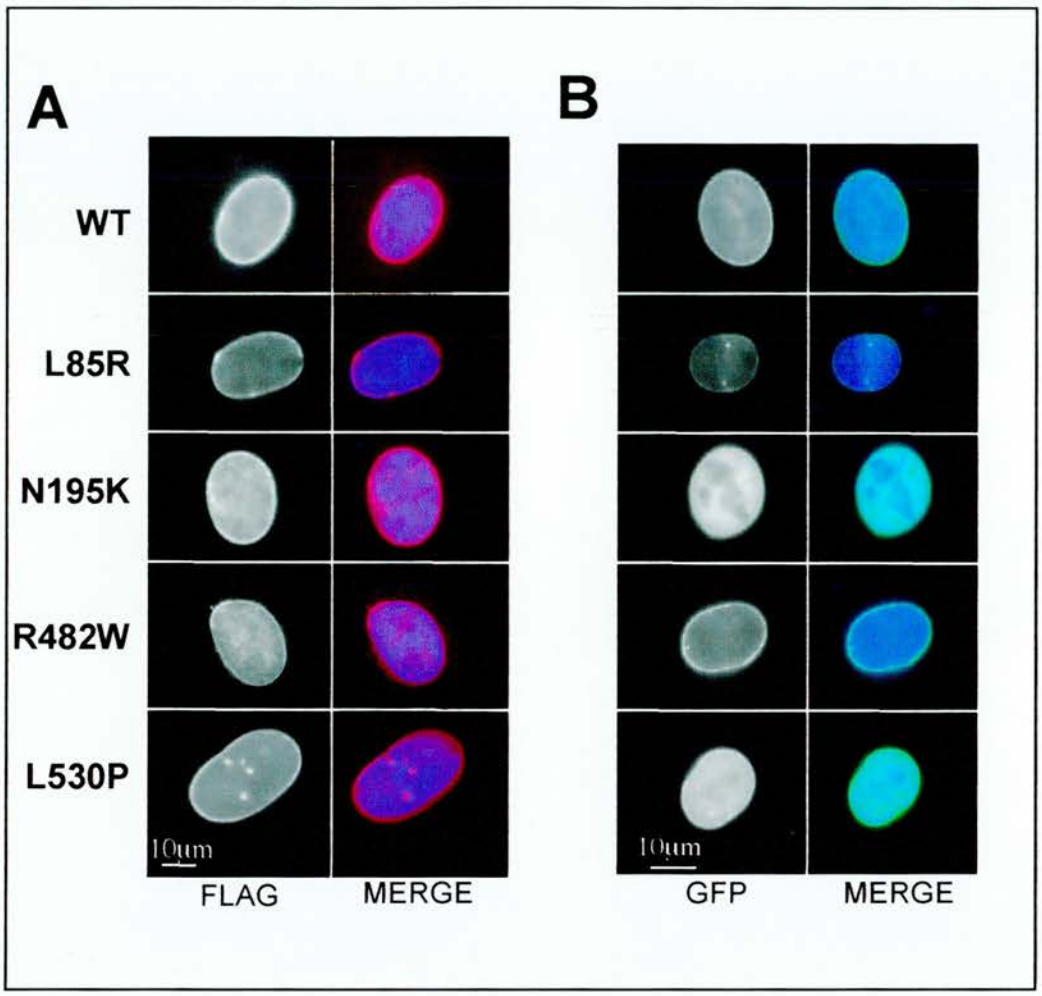

Figure 5.3 Transient expression of wild type and mutant pre-lamin A proteins.

Wild type and mutant (L85R, N195K, R482W and L530P) pre-lamin A were expressed in HT1080 cells from both FLAG-tagged and GFP-fusion lamin A constructs (Figure 5.2). FLAG-tagged protein was detected by IF (red, **A**), and GFP-fusion protein was directly visualised (green, **B**). Blue = DAPI, red = anti-flag antibody (M2), green = GFP.

5.3 INTERPHASE DYNAMICS OF DISEASE-ASSOCIATED LAMIN A PROTEINS

As discussed in Section 5.1.4, the selected lamin A mutations are at sites within different domains of the protein, that are implicated in different binding partnerships (Figure 5.1). I reasoned that as these mutations potentially disrupt the normal binding interaction with lamin A and other lamin A molecules or other nuclear compartments, they might also affect the mobility of lamin A protein in the nuclear lamina. To investigate this hypothesis I performed FLIP and FRAP in order to compare the dynamics of wild-type and mutant protein during interphase (see section 1.7 and Figure 1.12; Siggia et al., 2000; Lippincott-Schwartz et al., 2003). Using these approaches it has been determined that most nuclear proteins, e.g. transcription factors, are very dynamic (Phair and Misteli, 2000). However, some proteins, including histones and LBR (Ellenberg et al., 1997) are less mobile.

FLIP experiments are used to quantify the relative amounts of mobile fluorescently-tagged protein within a cell and, conversely, FRAP experiments allow the fraction of immobile proteins to be determined (Figure 1.12). In FLIP live cell experiments, a small region of fluorescent protein signal is bleached for many successive rounds (Lippincott-Schwartz et al., 2003). The bleach should not be intense enough to completely remove all fluorescence in the bleached region. Following each bleach cycle, the fluorescence intensity of a cellular region(s) outside the bleached area is measured. A decrease in fluorescence within non-bleached regions reflects outward movement or diffusion of fluorescent protein from this region to inside the bleach region. In FRAP experiments, a small region of fluorescent protein is bleached with sufficient intensity to greatly reduce or remove all fluorescence within this region of interest (ROI). Only one bleach is performed in FRAP and the fluorescence recovery within the bleached region is followed by image capture over a period of time. I chose to investigate the dynamics of GFP tagged lamin A mutant and wt proteins in both FLIP and FRAP analyses.

5.3.1 Fluorescence loss in photobleaching

I performed FLIP on regions of the fluorescent lamina of cells expressing wild type and N195K and L530P mutant GFP-lamin A protein (section 2.12.1, Figure 5.4). Following repetitive rounds of bleaching, the relative fluorescence of regions of an area of the lamina

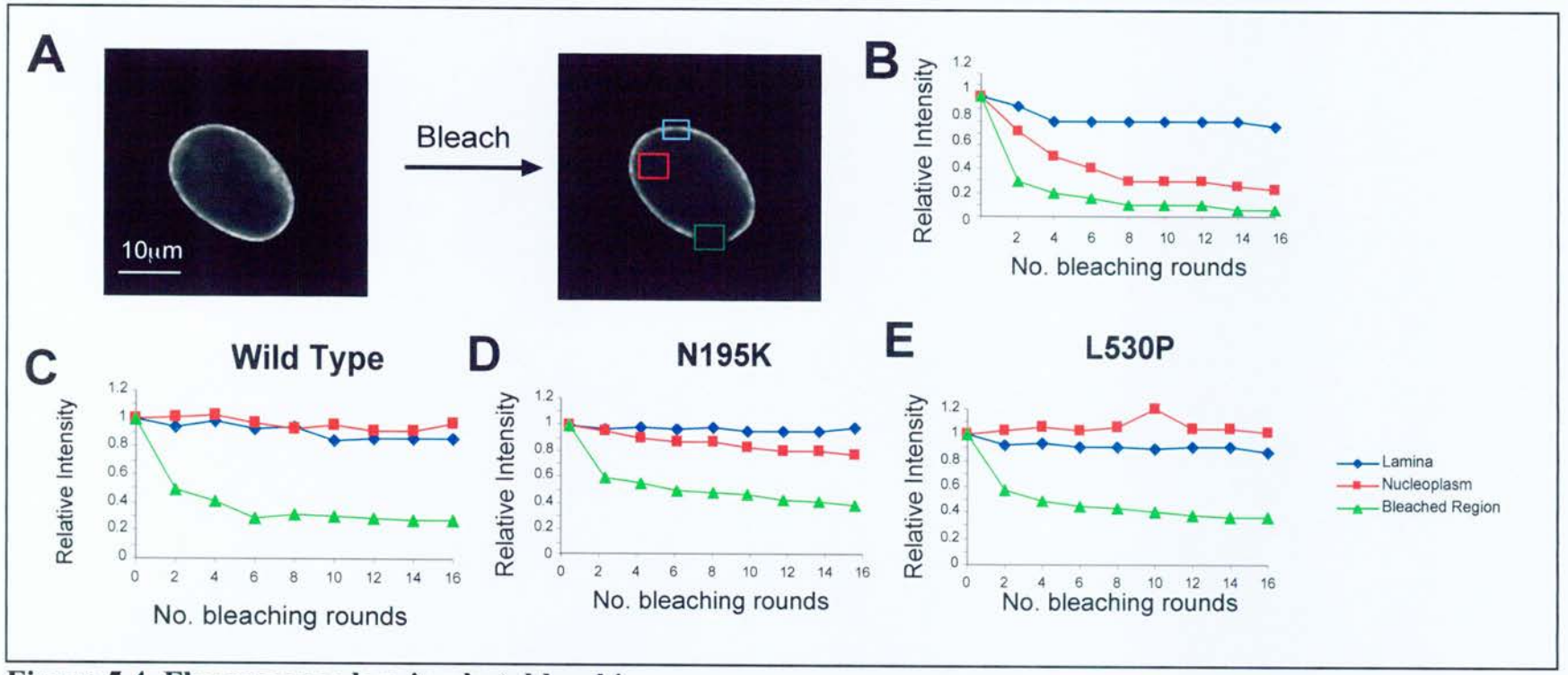

Figure 5.4 Fluorescence loss in photobleaching.
The dynamics of wild type, N195K and L530P GFP-prelamin A were followed in fluorescence loss in photobleaching experiments (FLIP). Cells with a GFP positive nuclear rim (**A**) were bleached at low laser power successively at a region of the nuclear lamina (green box). The fluorescence intensity of the bleached region, an untreated region of the lamina (blue box) and nucleoplasm (red box) is measured over a period of minutes. Summary of FLIP results for wt GFP-lamin C when expressed in CHO cells (n=7, Broers, *et al.*, 1999). The relative pixel intensity (post bleach intensity/pre-bleach intenity, normalised for fluorescence loss by the imaging proces, section 2.13) of wild type (**C**), N195K (**D**) and L530P (**E**) proteins in these experimental conditions are represented as line graphs (n=10). S.E.Ms for the data sets are as follows -
WT: bleached region = 0.04, unbleached lamina = 0.04, nucleoplasm = 0.05
N195K: bleached region = 0.03, unbleached lamina = 0.06, nucleoplasm = 0.02
L530P: bleached region = 0.06, unbleached lamina = 0.09, nucleoplasm = 0.06

(distant from the bleach) and the nucleoplasm were recorded every 2 seconds following the bleach (Figure 5.4A). The data for the fluorescence intensities for each of the proteins (wild type, N195K and L530P), averaged over 10 different cells from at least 3 separate experiments, are shown in Figure 5.4C. Levels for the bleached region (green), unbleached lamina region (blue) and nucleoplasm (red) are shown separately. These are normalised for the loss of fluorescence caused by the successive rounds of imaging (section 2.12.3). As expected, the intensity within the bleached region decreases for each of the proteins studied. The behaviour of wild-type and L530P lamin A appear similar. However, there are clear differences in the behaviours of the nucleoplasmic fraction of each protein. The wild type protein shows a small degree of fluorescence loss to the lamina-bound fraction (~14%) and this is also true for the L530P mutant (~13%). The nucleoplasmic fractions for both of these proteins loses negligible amounts of intensity (~3%). In contrast to this, the nucleoplasmic fraction of N195K mutant protein shows a clear decrease in fluorescence with successive rounds of bleaching, with a 23% loss of fluorescence after treatment.

FLIP has previously been performed on human GFP-lamin C protein (a truncated version of lamin A protein; see section 5.1.1) ectopically expressed in Chinese Hamster Ovary (CHO) cells (Broers et al., 1999). The authors report that under similar experimental conditions, the lamina loses an average of 28% fluorescence while the nucleoplasm loses 77% (represented in Figure 5.4B). Direct comparison of my data with these findings suggest that the lamina-bound fractions of lamin A and C have similar dynamics, while the nucleoplasmic form of lamin A may be less mobile than that of lamin C. This suggests that the N195K protein is more mobile in the nucleus that the wild type and L503P form. I conclude from these results that the two mutations may influence the mobility and turnover of lamin A in the interphase nucleus.

5.3.2 Fluorescence recovery after photobleaching

To further quantify the nuclear dynamics of the selected lamin A proteins for a longer period of time I performed FRAP experiments on live cells transiently expressing GFP fusion protein (section 2.12.2, Figure 5.5). A region of the fluorescent lamina of each cell was selected and bleached. The recovery of fluorescence within this bleached region (and 2 regions distant from the bleached area, as represented in Figure 5.4A) was then followed over a period of up to 70 minutes.

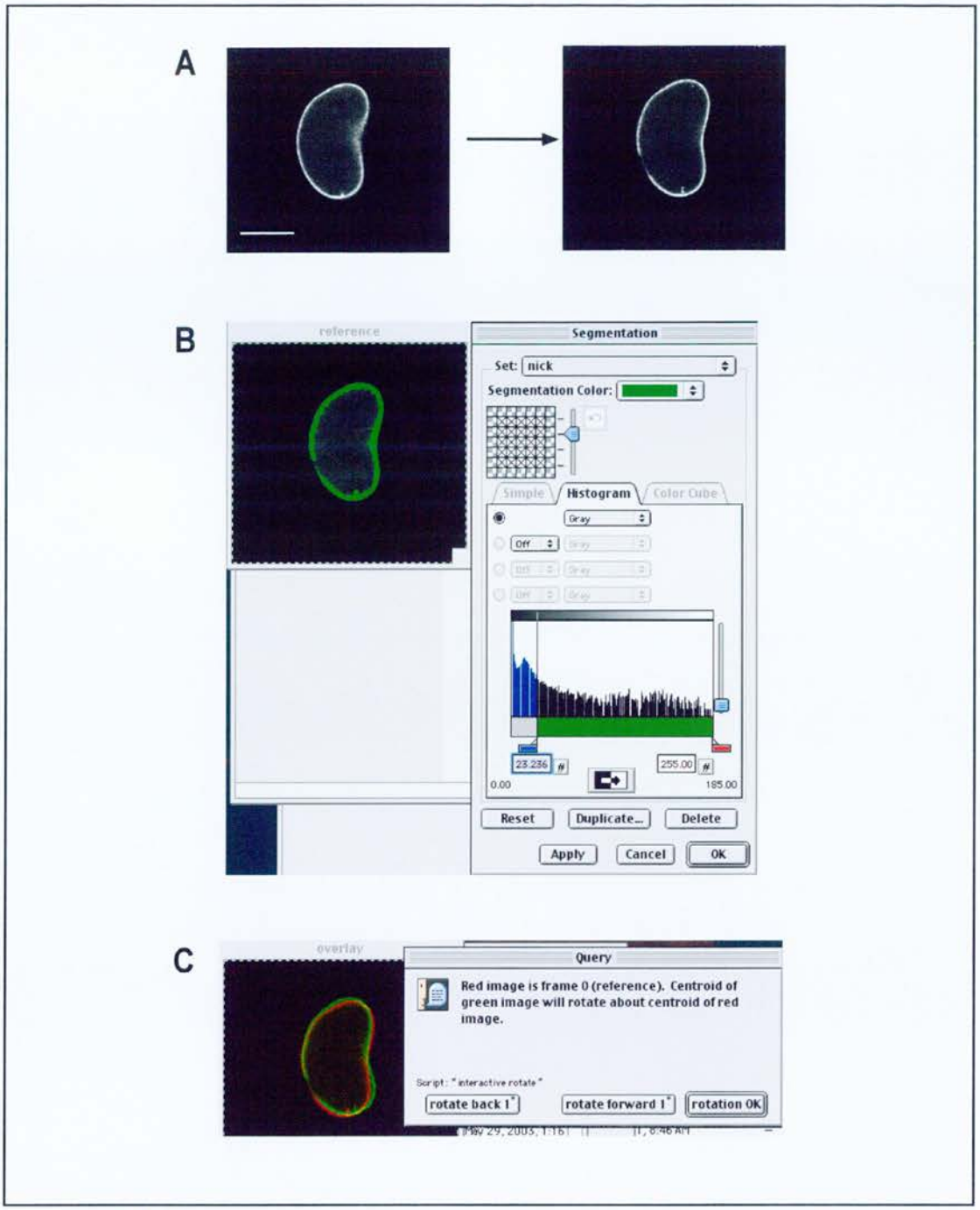

Figure 5.5 Interactive programme to for image alignment for analysis of FRAP data.

Image processing was required to quantitate the loss of fluorescence within the cell in FRAP experiments. HT1080 cells transiently expressing GFP-lamin A wt and mutant constructs were bleached at a region of interest of the fluorescent nuclear rim (**A**). A series of images taken at intervals following the bleach treatment were segmented (**B**). Each image in turn was interactively rotated about the centroid of the nucleus to align the bleached region of lamina rim signal (**C**), the pre-bleach image was used as an orientation reference (red). Bar = 10 μm.

Analysis of the region of interest presented a problem as experiments were performed on living cells rather than static, fixed samples and for this reason, the data sets collected cannot be directly analysed. FRAP analysis is concerned with measuring the fluorescence intensity within a particular region of interest (ROI) before and after a laser bleach treatment - this is inherently difficult if the sample moves. Over a long period, living cells are not static; they rotate and move across the culture dish. In addition to this, there is focus drift on the microscope. Hence, at the end of the analysis, the region of interest is invariably in a different position and plane of focus than it was at the beginning of the experiment. To address this, I collected 3-D stacks of treated cells at each time point after the bleach. These images stacks were then manually unstacked and the best-focus *z*-plane for the bleached region was selected. Each frame for each time point was then processed by an analysis script that enabled the images to be superimposed with the pre-bleach image and interactive processing scripts were composed (Box 5.1 and Figure 5.5, P. Perry, v3.6 IPlab, Scanalytics).

To understand the interphase dynamics of GFP-fusion lamin proteins, correctly aligned FRAP data sets were analysed. The fluorescence intensity of more than one ROI was calculated before and after laser bleaching using IPlab software options. Rectangular ROIs of 10 x 10 pixels were drawn at three different cellular locations; the bleach region, the nucleoplasm and an unbleached region of the lamina (Figure 5.4A). The sum of all pixels within this area was calculated by the programme for each image in the stack. This analysis was performed for 9 FRAP movies for each of the GFP-lamin A proteins (WT, L85R, N195K, R482W and L530P). To calculate the loss of fluorescence attributed to the imaging process alone, the sum of pixel intensity was also calculated for a control (unbleached) cell in each of the individual movies. Using a normalisation equation (section 2.12.3), the relative fluorescence intensity over time was calculated for each defined ROI. For direct comparison of GFP-lamin A dynamics in this experiment, the mean relative fluorescence intensity of each time point was calculated.

Figure 5.6A shows the relative recovery of fluorescence of the bleach region for wt and each mutant lamin A protein selected. The data represents the average recovery at each time point for at least 9 treated cells. Analysis of bleach region fluorescence for the wild-type protein (blue plot) reveals that after a period of 70 minutes approximately one eighth of the pre-bleach intensity has been recovered. This suggests that lamin A protein is relatively

Box 5.1

Alignment and analysis of fluorescence after photobleaching images

Considering the focus drift problem, before fluorescence intensities were calculated FRAP movies were fragmented and processed manually. The appropriate in-focus *z*-plane image was selected from each timepoint 3-D stack. Individual frames were grouped into one image stack, this produces a movie that shows one *z*-plane of the cell over the analysis period. Using the programme 'interactive rotate' each single *z*-plane movie was processed to correct for nuclear rotation and cell movement as follows (movies are black and white confocal data representing GFP signal only):

1. The first image of the stack (*z*-plane before bleach) is isolated and the signal is subjected to interactive segmentation. The user can increase or decrease the threshold of segmentation to determine the appropriate threshold for clearly defining the nuclear rim of GFP signal (Figure 5.5A).
2. The area and centroid co-ordinate of the defined image segment is calculated (i.e. the cell).
3. The next frame in the stack is shown (the first frame after bleach) with the segment outline defined (Figure 5.5A). As this will be incomplete (owing to the bleached region of lamina), the user is prompted to complete the segment outline with a paintbrush tool (Figure 5.5B).
4. The area and centroid co-ordinate of the defined image segment is calculated as before .
5. The programme then shows the first image in red and the second image in green, superimposed at the calculated centroid. Here, the second image can be rotated around the centroid to the left or right using the first image as a reference (Figure 5.5C).
6. Each remaining image in the stack is segmented and then manually rotated as described above. The first image of the stack (before bleach) is presented as the reference each time.

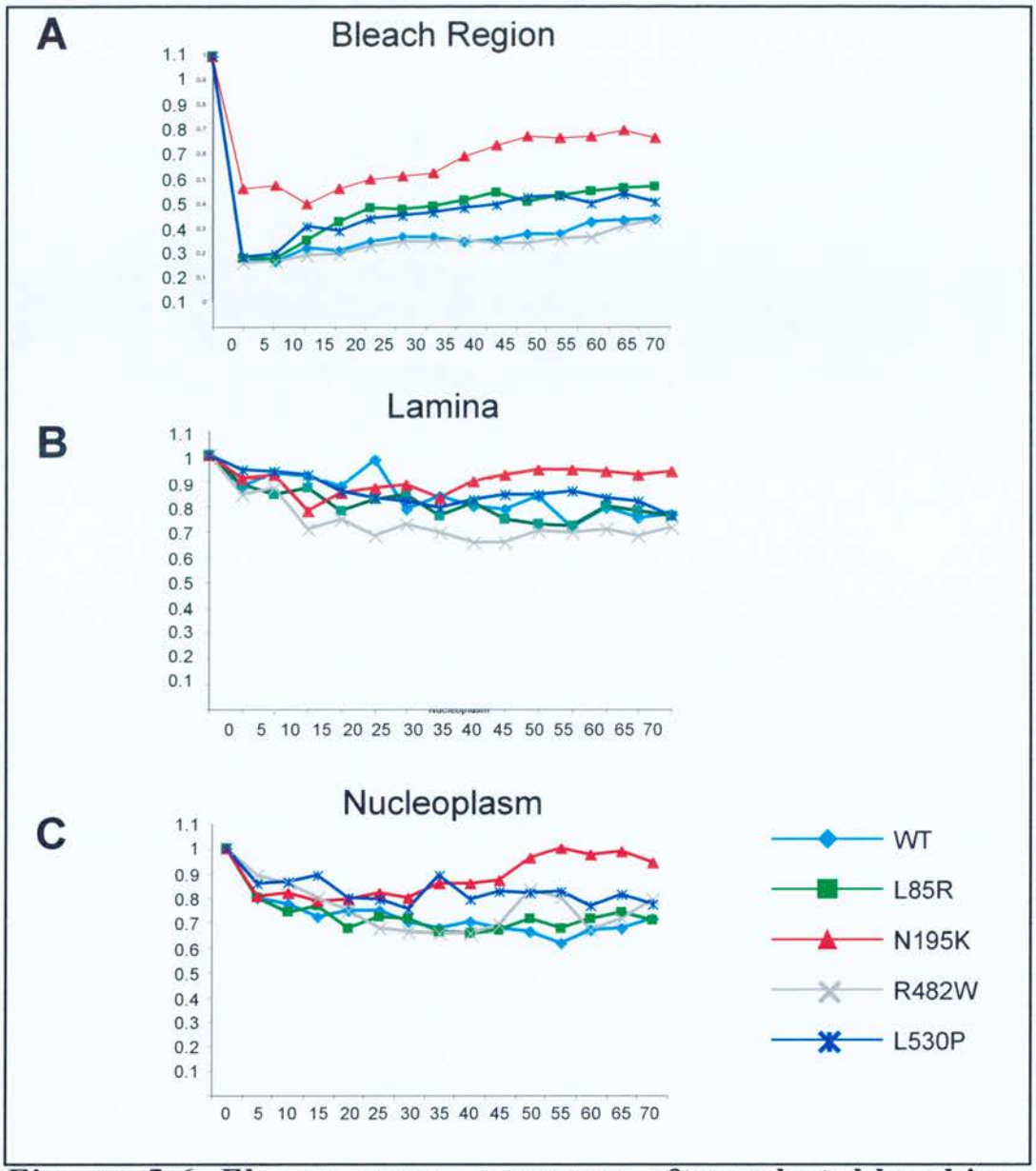

Figure 5.6 Fluorescence recovery after photobleaching. GFP-prelamin A fusion proteins were followed in fluorescence recovery after photobleaching (FRAP) experiments. The recovery of relative intensities of regions of interest within the bleached regions (A), at the unbleached lamina (B) and unbleached nucleoplasm (C) were followed after the bleach.

Standard errors –

WT: bleached region = <0.05, unbleached lamina = <0.09, nucleoplasm = <0.1
L85K: bleached region= <0..06, unbleached lamina = <0.09, nucleoplasm = <0.07
N195K: bleached region= <0.04, unbleached lamina = <0.2, nucleoplasm = <0.07
R482W: bleached region= <0.04, unbleached lamina = <0.07, nucleoplasm = <0.15
L530P: bleachedregion = <0.09, unbleached lamina = <0.09, nucleoplasm = <0.1

immobile during interphase and the extrapolated t½ for the protein in this ROI is 140 minutes. This finding is similar to FRAP experiments on other nuclear lamina components as >60% of LBR-GFP in the INM is immobile (Ellenberg et al., 1997). GFP-lamin C showed recovery of nucleoplasmic protein, but only negligible recovery of lamina-bound protein after periods of one hour following bleach (Broers et al., 1999) and data in (Moir et al., 2000) suggests less than 50% recovery for GFP-human lamin A protein in mouse cells after more than 3 hours following bleaching. To my knowledge, the experiments described here are the first FRAP analyses for human lamin protein in human cells.

The dynamics of R482W (grey plot) are almost identical to that of the wild-type protein and the extrapolated t½ = 145 mins. In contrast to wt protein L85R (green plot) and L530P (yellow) mutant lamin A proteins appear more mobile. For these mutations, extrapolated t½ are as follows: L85R = 75 mins, L530P = 80 mins. It is also clear that the behaviour of mutant N195K (red plot) is not similar to that of the other proteins (t½ = 30 mins) and it appears not to bleach to the same degree as the others. This can be attributed to the higher level of nucleoplasmic fluorescent protein in these cells (as discussed in section 5.2). Due to the nature of the region of interest drawing facility in the software used (IPlab, Scanalytics, USA), it is impossible to totally exclude all nucleoplasmic signal from the measurement area at the nuclear lamina. Evidently, the nucleoplasmic fraction of this mutant protein is highly mobile and can recover from the bleach rapidly. The fluorescence intensity was also followed over the course of the analysis at two additional nuclear sites (lamina; Figure 5.6B and nucleoplasm Figure 5.6C). In general, the fluorescence levels of the unbleached lamina and nucleoplasm decrease over time. This suggests fluorescent protein can relocate from the unbleached lamina and nucleoplasmic regions to be incorporated into the bleached lamina region resulting in slow recovery of fluorescence within the bleach region. Loss of fluorescence in the unbleached regions could be due to the successive imaging rounds, however the measurements have been normalised for this. Some decrease in fluorescence intensity could also be attributed to the processing and alignment used to superimpose post-bleach images, as some of the pixel values are lost when an image is rotated. However, the analysis and processing scripts used have been designed to minimise such pixel intensity losses.

By analysing protein behaviour in transient over-expression studies, some information can be obtained about the role of lamin A protein in cells. However, one cannot exclude the possibility that any observations are an artefact of the high levels of protein expression that

result from transient expression. For this reason, I decided to generate stable lines expressing the GFP-lamin A proteins.

5.4 EXPERIMENTAL DISRUPTION OF GENETIC LOCI POSITION

Cell lines were previously generated in our laboratory which have *E. coli* lac operator (LacO) sequence repeats integrated into random sites in the human genome (Chubb et al., 2002). By stably expressing GFP-lac inducer (LacI) protein in these cells, the integration sites can be visualised as GFP bright spots in live cells (Robinett et al., 1996; Chubb et al., 2002). I wished to analyse whether expression of mutant lamin A in these cells results in relocalisation of the LacO tagged loci.

However, I found that these cells were almost impossible to transfect with FLAG-tagged lamin A proteins as the majority of cells die after transfection (data not shown). I therefore used parental lines (harbouring only the LacO repeat integrations) and co-transfected them with GFP-LacI to visualise the LacO sites and FLAG-lamin A plasmid DNA. I selected a parental line with LacO integration at chromosome location 13q22. This is a peripheral genomic locus, and motion of this locus is constrained during interphase due to its proximity to the nuclear edge (Chubb et al., 2002). Cells harbouring this integration expressing wt and mutant lamin A proteins are shown in Figure 5.7. The 13q22 GFP bright spot is at, or near, the nuclear edge in all of the images. This suggests that the presence of mutant lamin A protein does not affect the nuclear location of this locus.

This was an interesting preliminary finding. However, I had technical difficulties with the procedure; I found that the frequency of cells expressing both GFP-LacI and FLAG-lamin A was very low (transfections of ~$2x10^6$ cells yielded approximately 5-10 double-positives). In addition to this, it was not always be possible to visualise the GFP bright spots in all of the 5-10 positive cells. As the practicalities of this experimental approach were not ideal, I decided to investigate the influence of lamin A mutants on nuclear organisation using other means.

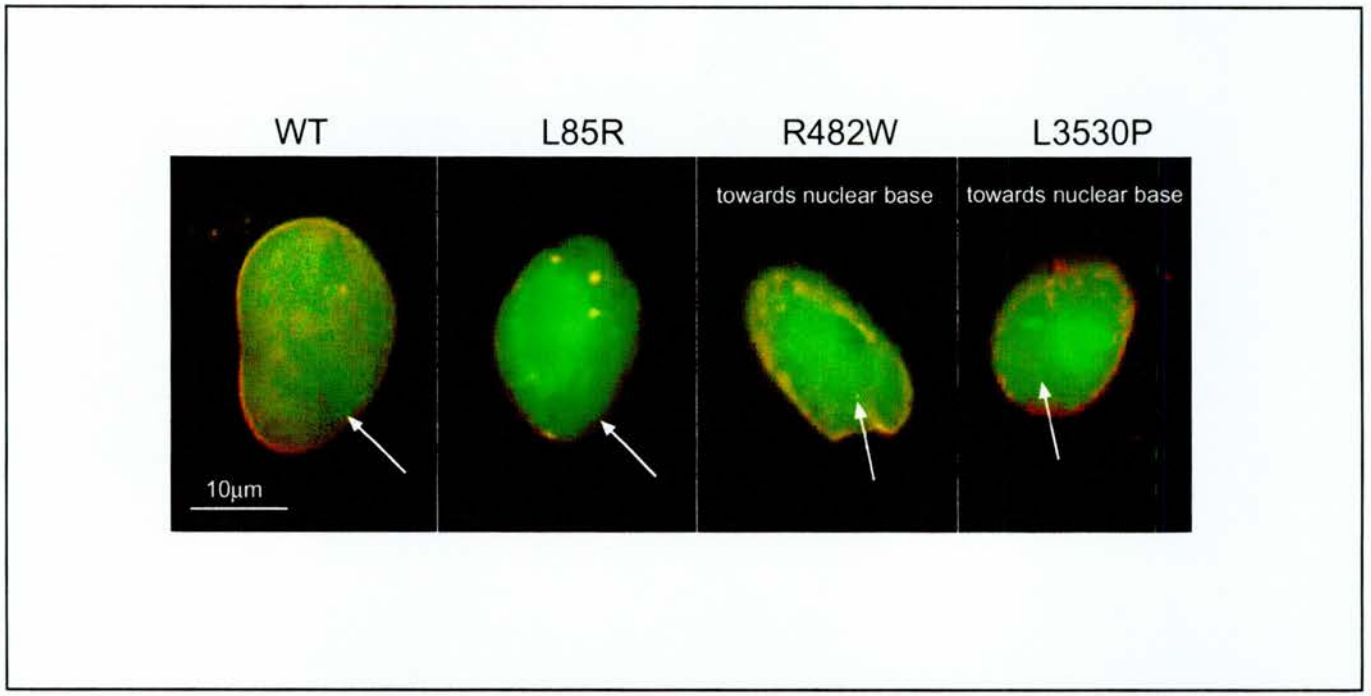

Figure 5.7 Expression of wild type and mutant pre-lamin A in cells with GFP-tagged genetic locus.

FLAG-prelamin A fusion proteins were expressed transiently in a stable line tagged at 13q22 with GFP (Chubb *et al.*, 2002). The genetic locus is evident as bright GFP spots (arrows). This locus is peripheral in the nuclei of all cells. Cells expressing R482W and L530P proteins have the GFP bright spot at the base of the nucleus. Green = GFP, red = anti-FLAG (M2).

5.5 STABLE EXPRESSION OF DISEASE-ASSOCIATED LAMIN A PROTEINS

To generate stable lines expressing each of the GFP fusion proteins, HT1080 cells were transfected with plasmid DNA (pCDNA3-prelaminA, Figure 5.2D). The following day, these cells were plated onto large culture dishes with the appropriate drug selection for the plasmid (G418-sulphate, 400μg/ml). After 10 days under selection, cell colonies were picked. The experimental numbers are detailed in Figure 5.8A. 11-37% of the colonies expressed GFP-lamin A and a broad range of expression levels was observed. For further analysis, one cell line was selected for each protein. Each of the selected clones had >95% of cells positively expressing GFP fusion protein. The selected cell lines also had a comparable level of GFP-lamin A expression to one another and this level was relatively low. Cells with higher expression levels did not have fusion protein localised evenly at the nuclear rim and aggregates of protein were observed around the nuclear edge and hence these lines were not selected for further analysis.

5.5.1 Characterisation of stable lines

In order to quantify the relative levels of protein expression in each clone, western blot analysis was performed using an antibody that detects both lamin A and lamin C (Jol2, Prof. C. Hutchison; Figure 5.8B). Endogenous lamin A and C are detected as bands of ~ 70 and 65 kDa respectively. Levels of endogenous protein appear unaffected by the expression of GFP-lamin A in all the stable lines as the levels are comparable to levels in the parent cell line, HT1080. An ~102kDa band is also detected by this antibody in each of the generated stable lines and this represents the expected size of GFP-lamin A fusion protein. The levels of recombinant protein expression are comparable between selected lines, and there are no detectable degradation products. From this western blot detection it is estimated that there is at least 2-3 times more GFP-lamin A than endogenous protein levels. Detection of the same PVDF membrane with an anti-GFP antibody (Clontech) detects one band for each stable line, at ~102kDa with no detection in the HT1080 sample lane (Figure 5.8B).

Fluorescent LM imaging of pFa fixed cells revealed that positively expressing cells show a clear GFP positive nuclear rim (Figure 5.9) and GFP and lamin A signals are coincident.

A

Expressed protein	No. Colonies	No. GFP positive
Wild Type	96	36
L85R	96	31
N195K	96	10
R482W	96	16
L530P	96	20

B

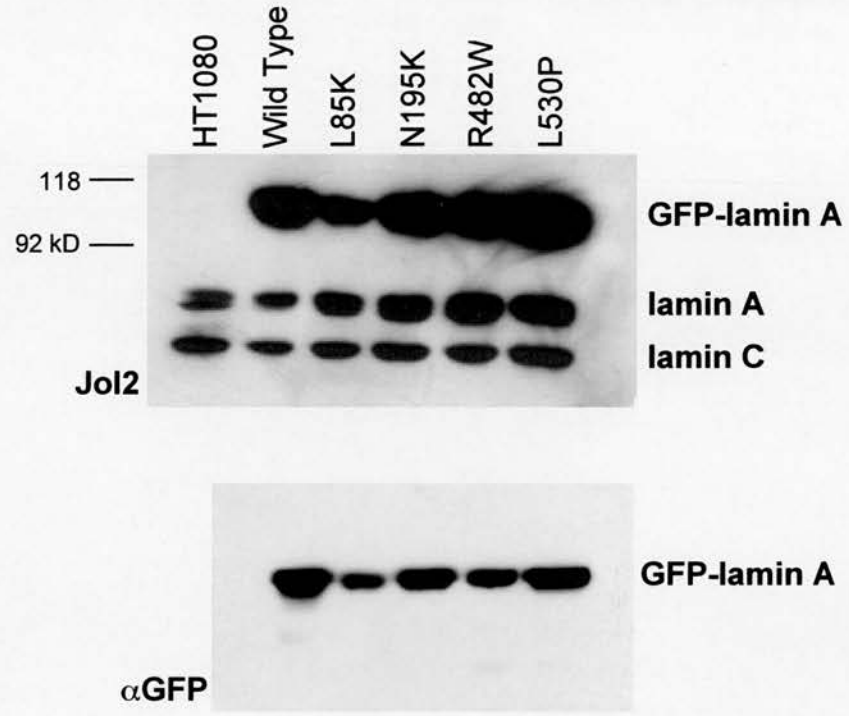

Figure 5.8 Stable expression of GFP-prelamin A fusion protein. HT1080 cells were transfected with GFP-lamin A expression plasmids to generate stable lines (see materials and methods). Cell transfections were performed using lipofectamine 2000 reagent and seeded sparsely onto culture dishes. Following 7 days of growth under G418 drug selection, individual colony clones were selected for growth expansion. 2 days later, the selected clones for each construct were screened for GFP expression using a fluorescent microscope. The GFP expression efficiency for each expression construct ranged from 10-37.5% (10-36 of 96 clones, **A**). Protein extracts from parental HT1080 cells and colonies of HT1080s transfected with wt and mutant lamin As were resolved by SDS-PAGE, transferred to membrane and incubated with antibody that detects both lamin A (70kDa) and lamin C (65kDa, Jol2, **B**). GFP -lamin A (102kDa) is detected in each transfectant.

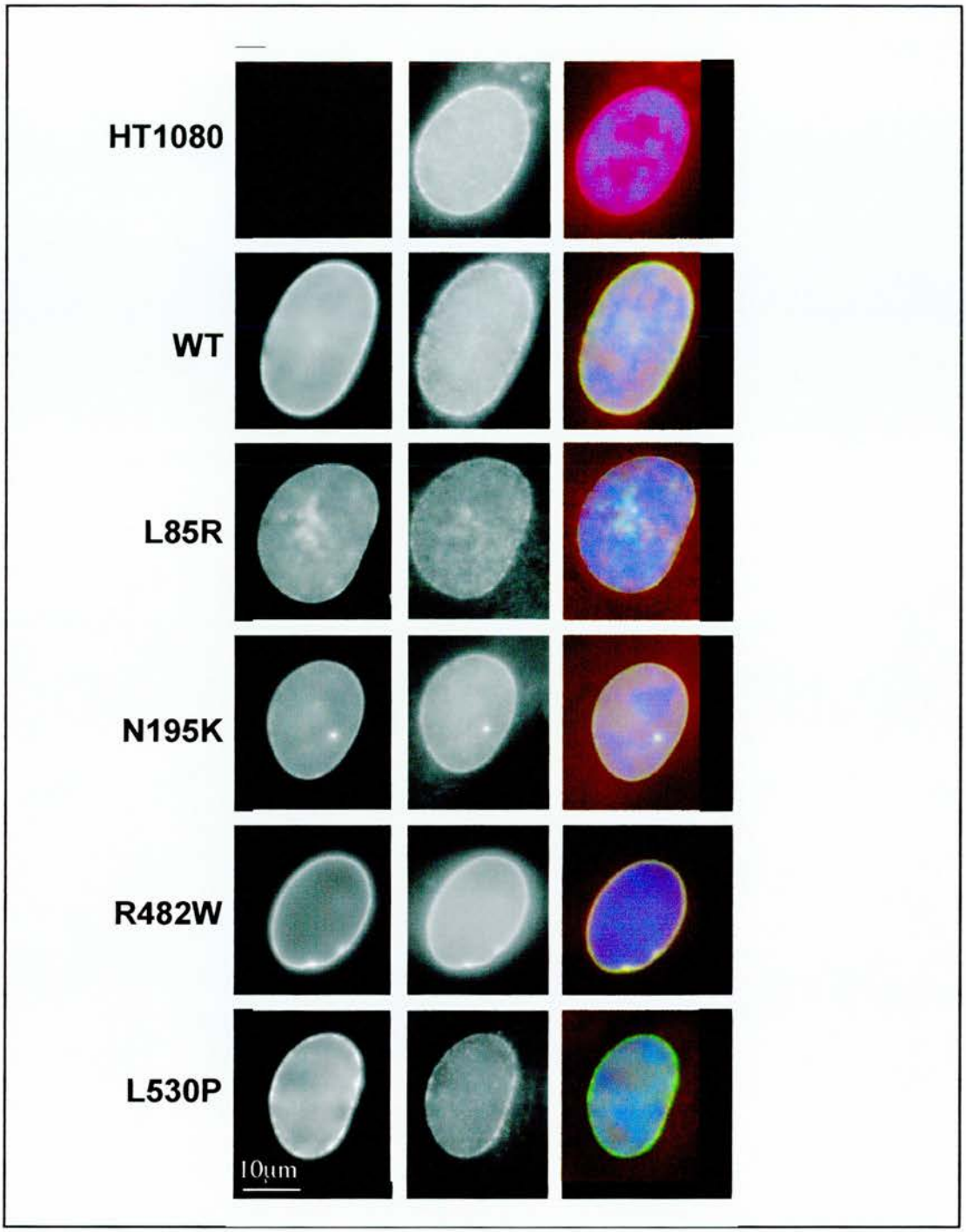

Figure 5.9 IF localisation of lamin A proteins expressed in cell lines.

Lamin A protein was visualised by immunofluorescence with an anti-lamin A antibody (Upstate) in HT1080 cells, and generated stable cell lines expressing GFP-prelamin A fusion constructs. HT1080 cells (top panel) have a clear nuclear rim of lamin A staining. GFP-lamin A stable lines (L85R, N195K, R482W and L530P) show a nuclear rim of GFP signal (left column) that colocalises with endogenous lamin A protein (middle column). Blue = DAPI, red = anti-lamin A, green = GFP.

5.5.2 Organisation of nuclear envelope and nuclear lamina proteins in lamin A transfectants

To examine whether the expression of GFP-lamin A fusion protein was affecting the incorporation of endogenous lamin A protein into the nuclear lamina, the cellular distribution of lamin A was followed using a lamin A antibody (Figure 5.9). By comparing the antibody signal between parental and stable lines, it was clear that both recombinant and endogenous proteins are incorporated into the lamina. As two of the mutants affect residues within the dimerisation domain of lamin A (L85R, N195K; Figure 5.1A), I considered that the lamina in cells expressing these proteins may be altered/compromised. This was addressed by using an antibody to lamin A (Jol4) that can detect a C-terminal protein epitope (beyond amino acid 572) when the lamina is rearranged during quiescence (Figure 5.10; Jol4, Prof. C. Hutchison, see section 4.6.2; Dyer et al., 1997; Agarwal et al., 2003). In HT1080 cells there are few spots of Jol4 signal within the nucleoplasm but no lamina rim is evident, as expected for proliferating cells. The same staining pattern is also seen in cells stably expressing wt and L85R GFP-lamin A. Some rim staining is evident in N195K and R482W stable lines but clear rim staining is seen in the L530P line

Previous studies have reported that cells from laminopathy patients have altered composition of the nuclear lamina (see section 5.1.3). I looked at the composition of the lamina in the GFP-lamin A stable lines using antibodies detecting lamin B (Figure 5.11), emerin (Figure 5.12) and nucleoporin (Figure 5.13). In the parental line, each of these antibodies detect an even nuclear rim, with emerin also detected in the ER. In transfectants, anti-lamin B antibody stains an even rim in all cell lines, with the exception of a more patchy signal in cells expressing R482W and L530P protein (Figure 5.11). These patches correspond to concentrations of GFP-lamin A. Anti-emerin antibody highlights an even nuclear rim, but also protein in the ER, for all cell lines (Figure 5.12). An antibody detecting nucleoporin p62 (Upstate), a component of nuclear pores (Buss and Stewart, 1995), also has a nuclear rim and ER staining pattern, however the nuclear rim has a more textured pattern (Figure 5.13). In the R482W stable line, patches of GFP-lamin A protein do not correspond to nucleoporin p62 stain and hence ectopic expression of lamin A does not disorganise nuclear pore complexes. I conclude there are negligible changes to lamina/INM composition in stable lamin A transfectants.

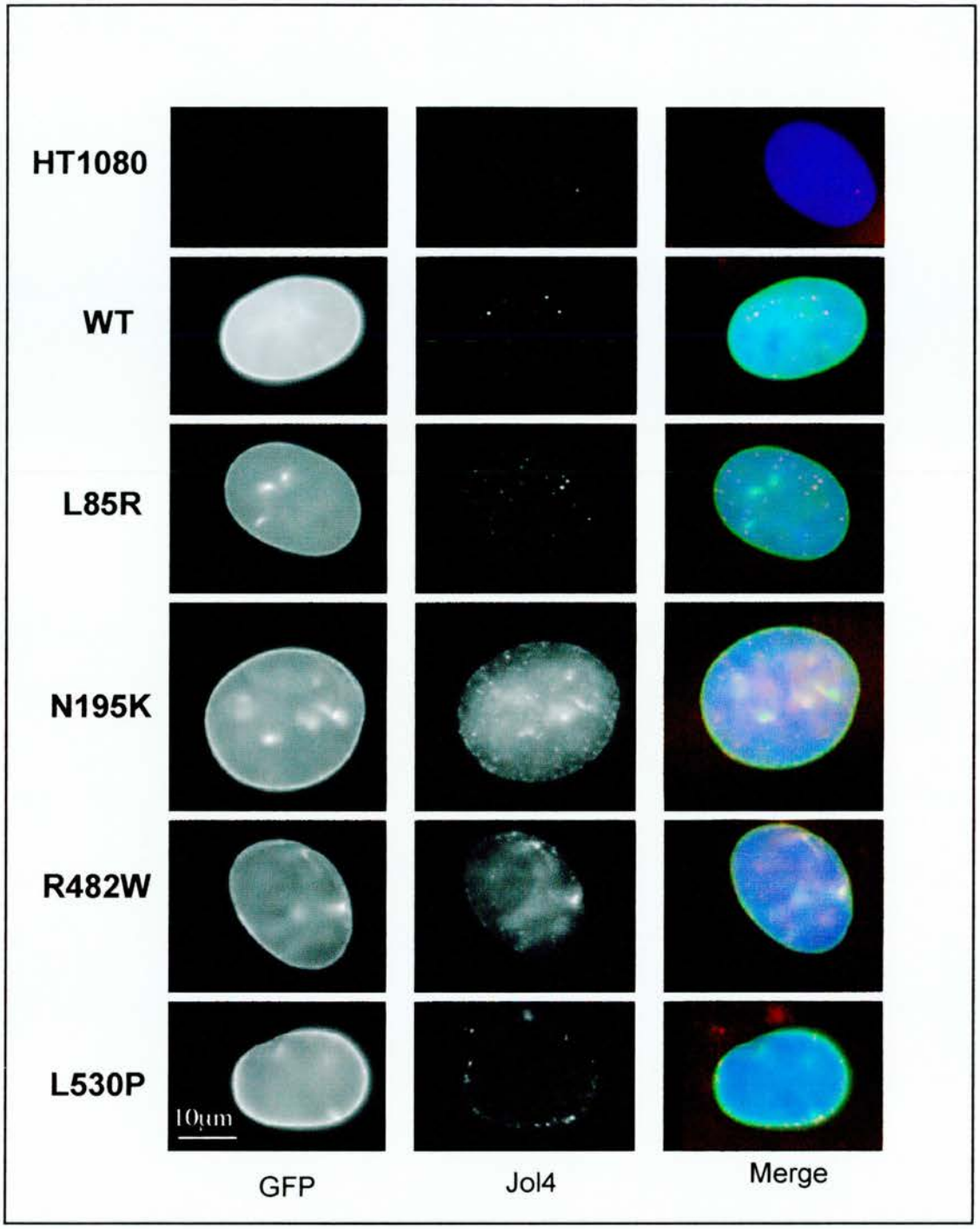

Figure 5.10 Localisation of lamin A epitopes in lamin A transfectants.
Lamin A protein was visualised in HT1080 cells and stable cell lines expressing GFP-prelamin A fusion constructs using Jol4 (Dyer *et al.*, 1997). This antibody detects an epitope of lamin A that is normally masked in proliferating cells. In HT1080 cells (top panel), Jol4 stains some spots in the nucleoplasm and cells expressing wild type and L85R protein also have this staining pattern. Mutants N195K, R482W and L530P show a higher level of Jol4 signal within the nucleoplasm and a nuclear rim is evident. Blue = DAPI, red = Jol4 anti-lamin A, green = GFP.

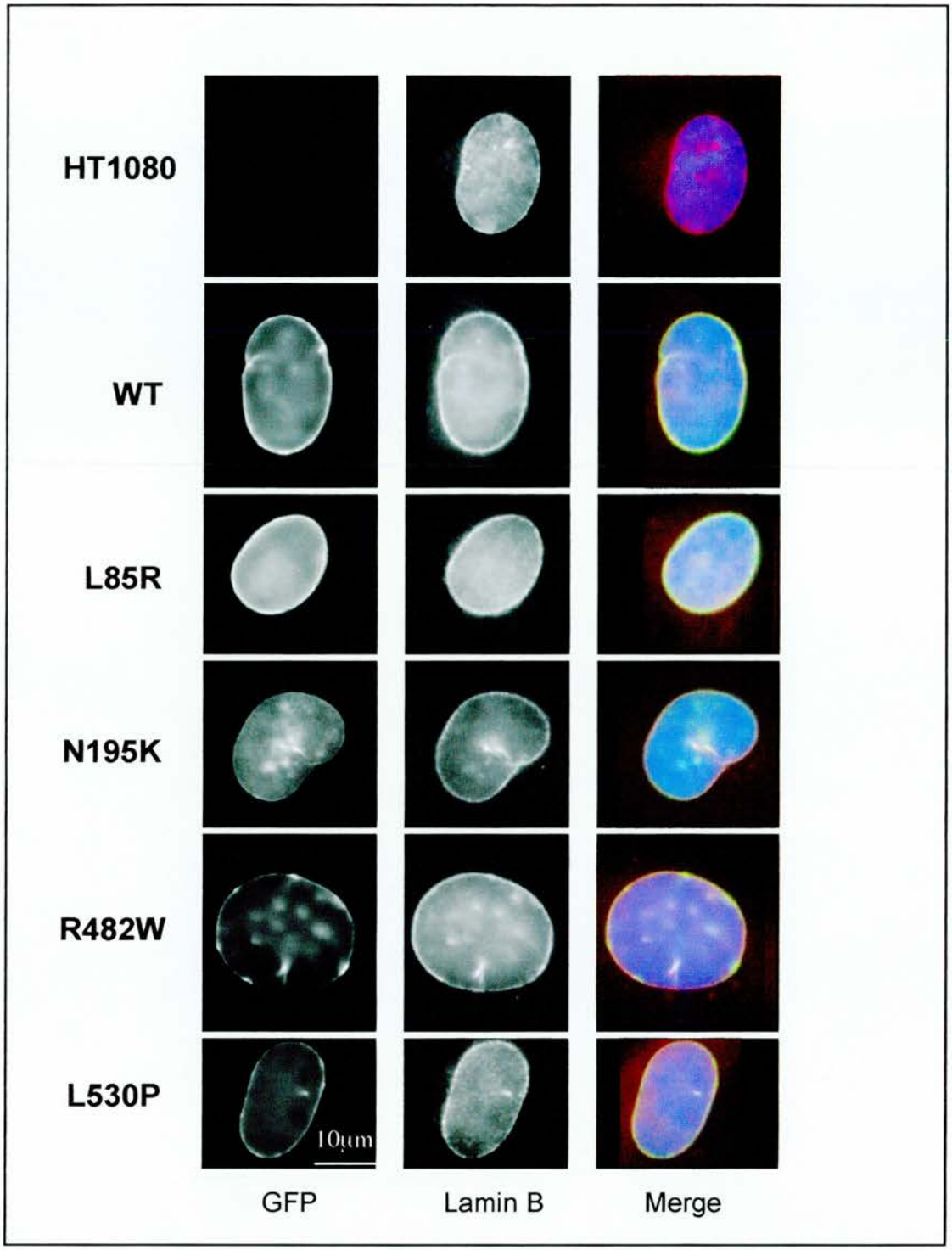

Figure 5.11 Localisation of lamin B proteins in lamin A transfectants.
Lamin B protein was visualised in HT1080 cells and stable tranfectants expressing GFP-prelamin A fusion constructs using an antibody (lamin B, Upstate). HT1080 cells (top panel) have a nuclear rim of lamin B staining and some nucleoplasmic staining. This localisation pattern is evident in each of the stable cells lines and the rim staining colocalises with GFP-lamin A (left column). Blue = DAPI, red = anti-lamin B, green = GFP.

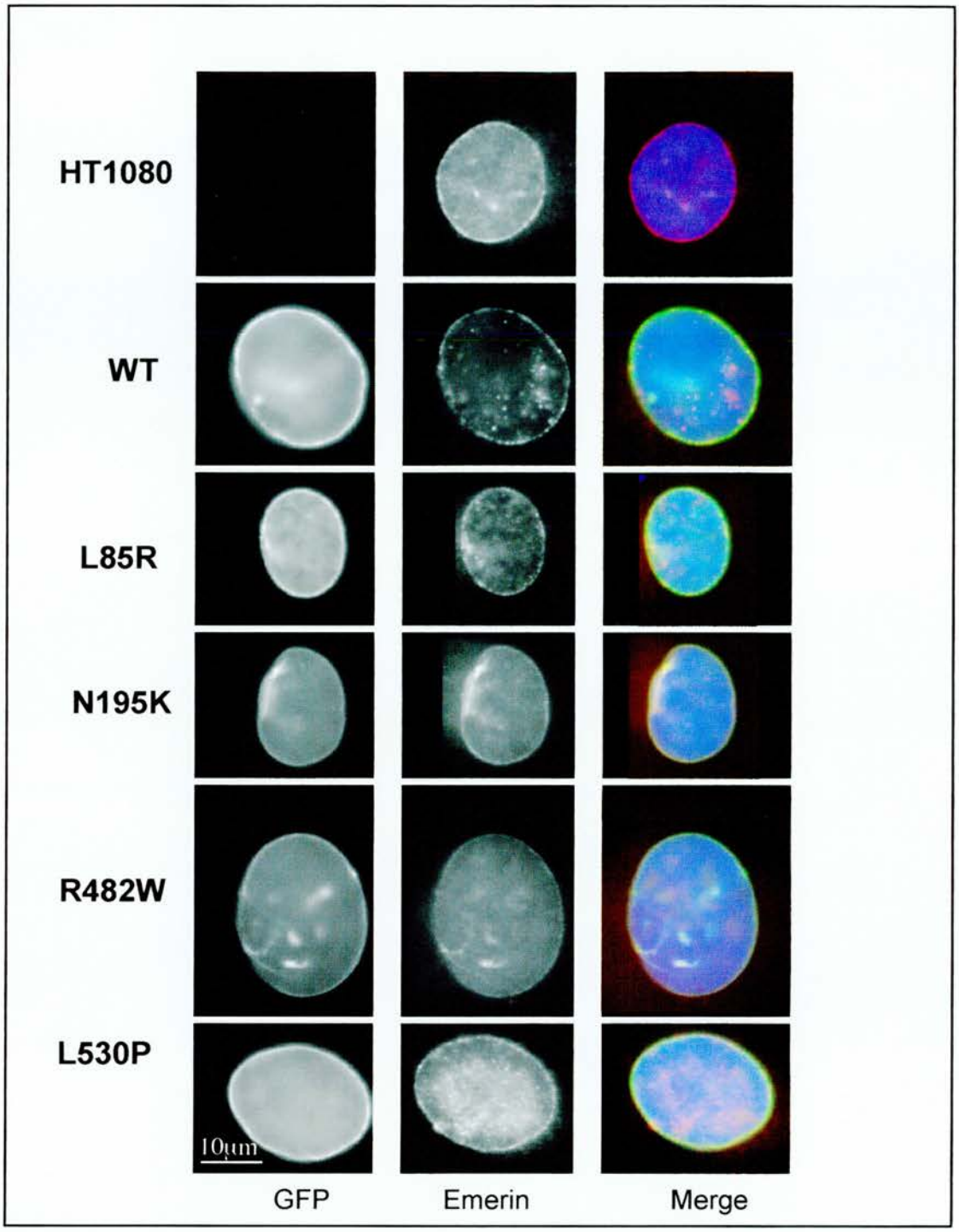

Figure 5.12 Localisation of emerin proteins in lamin A transfectants. Emerin protein was visualised in HT1080 cells and stable cell lines expressing GFP-prelamin A fusion constructs using an antibody that detects emerin (Upstate). HT1080 cells (top panel) have a nuclear rim of emerin staining. This staining pattern is evident in all stable lines and emerin colocalises with GFP lamin A protein (left column). In merge, blue = DAPI, red = anti-emerin, green = GFP.

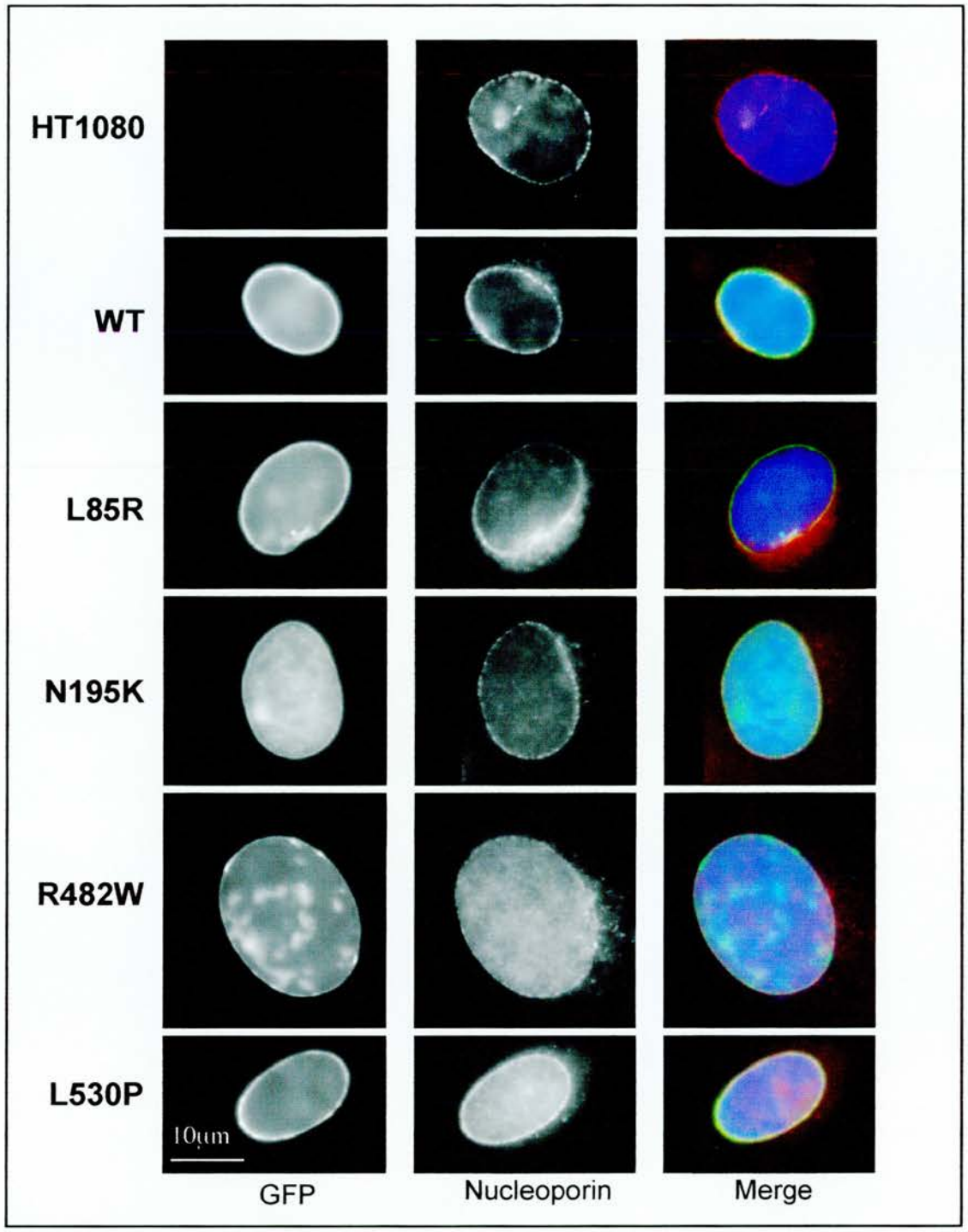

Figure 5.13 Localisation of nucleoporin proteins in lamin A transfectants.

Nucleoporin protein was visualised in HT1080 cells and generated stable cell lines expressing GFP-prelamin A fusion constructs using an antibody (nup p62, Upstate). HT1080 cells (top panel) have a dappled nuclear rim of nucleoporin staining. In cells expressing fusion proteins (wild type and mutants) there appears to be varied degrees of mislocalisation of nucleoporin, with increased staining outside of the nucleus, in what might be the ER.

In merge, blue = DAPI, red = anti-nucleoporin p62, green = GFP.

5.5.3 Spatial organisation of chromatin in lamin A transfectants

There is *in vitro* evidence to suggest that lamins have a role to play in spatial organisation of the genome (as discussed in section 5.1.2). In microinjection studies, anti-lamin A antibodies were reported to disrupt normal interphase organisation of chromatin (Benavente and Krohne, 1986). LM and EM reports have suggested that in *Drosophila* embryos and HeLa cells particular regions of chromatin are in close proximity to the lamina to allow direct interaction (Paddy et al., 1990). EM studies of muscle cell and fibroblast nuclei from EDMD patients have shown that condensed peripheral heterochromatin (Figure 1.4) is detached from the nuclear edge (Ognibene et al., 1999; Maraldi et al., 2002). In addition, two of the proteins selected for study are mutated within the predicted chromatin/DNA binding domain of lamin A (R482W and L530P; see Figure 5.1). Mutations at these residues are predicted to have different affects on lamin A protein (section 5.1.4). This hypothesis is corroborated by a recent report comparing the DNA binding affinities of wild-type and R482W mutant peptides (Stierle et al., 2003). The authors show that the R482W mutation has a decreased affinity for DNA. These findings further support the idea that lamins are actively involved in tethering chromatin to the nuclear edge in human cells.

In chapter 4, I showed that centromeres are preferentially localised close to the nuclear periphery and that disruption of histone acetylation does not affect this organisation. To determine whether the presence of epitope-tagged mutant lamin A has any affect on chromosome location I observed the IF pattern of centromere distribution using CREST antisera (Figure 5.14). In HT1080 cells, the centromeres are distributed throughout the nuclear volume and some are situated at the nuclear edge, while others are clustered in the centre of the cell, frequently around the nucleolus/nucleoli. The pattern of localisation is evident in each of the stable lines in this study. Confocal imaging of cells is required to perform quantitative analysis of centromere distribution however I experienced imaging problems. The GFP-protein levels in the selected stable lines were too high and the wavelength of GFP signal emmission (even at very low laser powers) excited the Texas Red secondary antibodies used to detect the CREST antisera. This overlap meant that the stable lines and IF samples prepared could not be used to quantify centromere distribution. To overcome this, a different secondary antibody is required that will not be excited by the wavelength of GFP emmitance. The fluorochrome Cy3 could be used for this analysis, however, there was not sufficient time to complete this analysis.

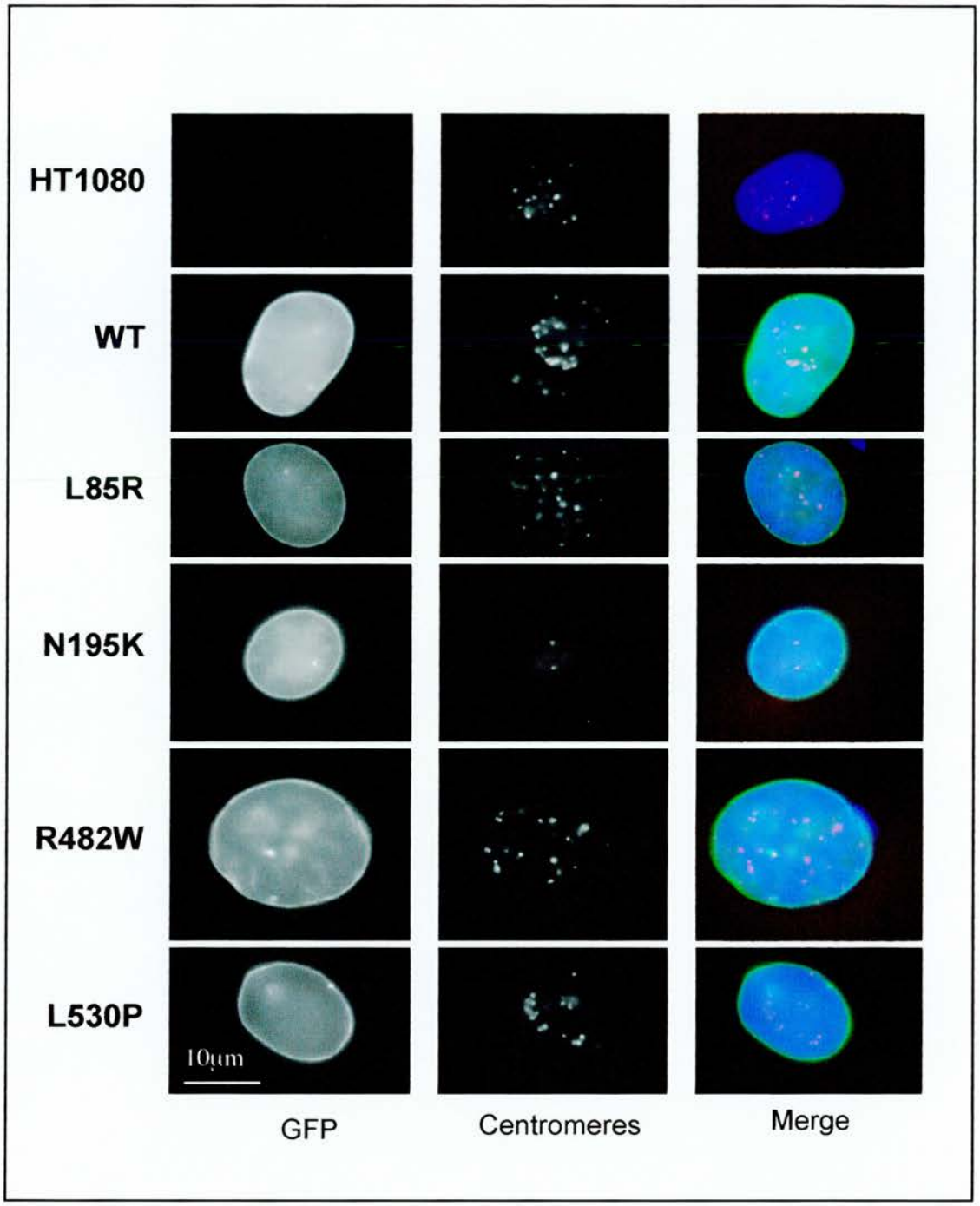

Figure 5.14 IF localisation of centromeres in cell lines. Centromeres were visualised in HT1080 cells and generated stable cell lines expressing GFP-prelamin A fusion constructs using CREST antisera (see material and methods). HT1080 cells (top panel) show distinct centromere spots distributed throughout the nucleoplasm. Some centromeres are adjacent to the nuclear periphery while others are in the centre of the nucleus. There is also a tendency for centromeres to cluster or arrange into groups. This localisation pattern in observed in each of the stable cell lines. Blue = DAPI, red = CREST, green = GFP.

To analyse whether an abnormal lamina perturbs the radial organisation of chromosomes in the nucleus, I used FISH to analyse the position of selected human chromosomes in the parental HT1080 line and lines stably expressing GFP-tagged wt and mutant lamin A. I used erosion analysis of chromosome paint hybridisation signals, as described in 3.2.1 and Figure 3.1. As discussed previously, a straight line at 1 represents a random distribution of chromosome signal in the 5 nuclear shells. The distribution pattern of chromosomes was directly compared between the parental line and lines expressing GFP proteins.

It was immediately evident that the pattern of localisation of chromosome 18 is visibly different from that of the parental HT1080 line in the GFP-tagged wt and mutant lamin A protein stable lines (Figure 5.15). For statistical analysis, the chromosome territory distribution in each stable line was directly compared to that of the parental HT1080 lines.

In the parental line, chromosome 18 is peripheral (Figure 3.5 and 5.15), yet in cells over-expressing GFP-lamin A (both wild-type and mutant) this chromosome is randomly distributed through the nuclear volume ($P<0.03$). This data suggests that chromosome 18 location is sensitive to levels of lamin A in the cell, as relocation is observed with both wild-type and mutant GFP-lamin A overexpression. The relocation of chromosome territory location is not influenced by an overall redistribution of DNA as the percentage of DAPI stain in the outer rim did not change significantly.

To follow up this finding, further peripheral chromosomes were located in the stable lines (Figure 5.16). No clear relocation of these chromosomes, as with that of chromosome 18, was observed. However, there may be more subtle differences in the location of these chromosomes in the form of a bi-modal response, particularly with HSA1 and -11. For HSA1, statistical analysis reveal that the territory distribution is significantly different between HT1080 cells and stable lines expressing wt ($P=0.0084$) and L530P ($P=0.01$) GFP-lamin A. However, there is no significant difference when HT1080 cells are compared with cells expressing L85R ($P=0.08$), N195K($P=0.08$) and R482W ($P=0.055$) GFP-lamin A proteins. HSA11 analysis does not reveal the same relationships between protein expression and territory distribution as HSA1. There are significant differences between HT1080 cells and cells expressing wt ($P=0.019$), L85R ($P=0.027$) and R482W ($P=0.04$) GFP-lamin A protein, but no difference between the parent line and cells expressing N195K ($P=0.07$) and L530P ($P=0.07$). In contrast, statistical comparisons of the HSA13 data show that there is no significant difference in territory location between the parental cell line and the selected

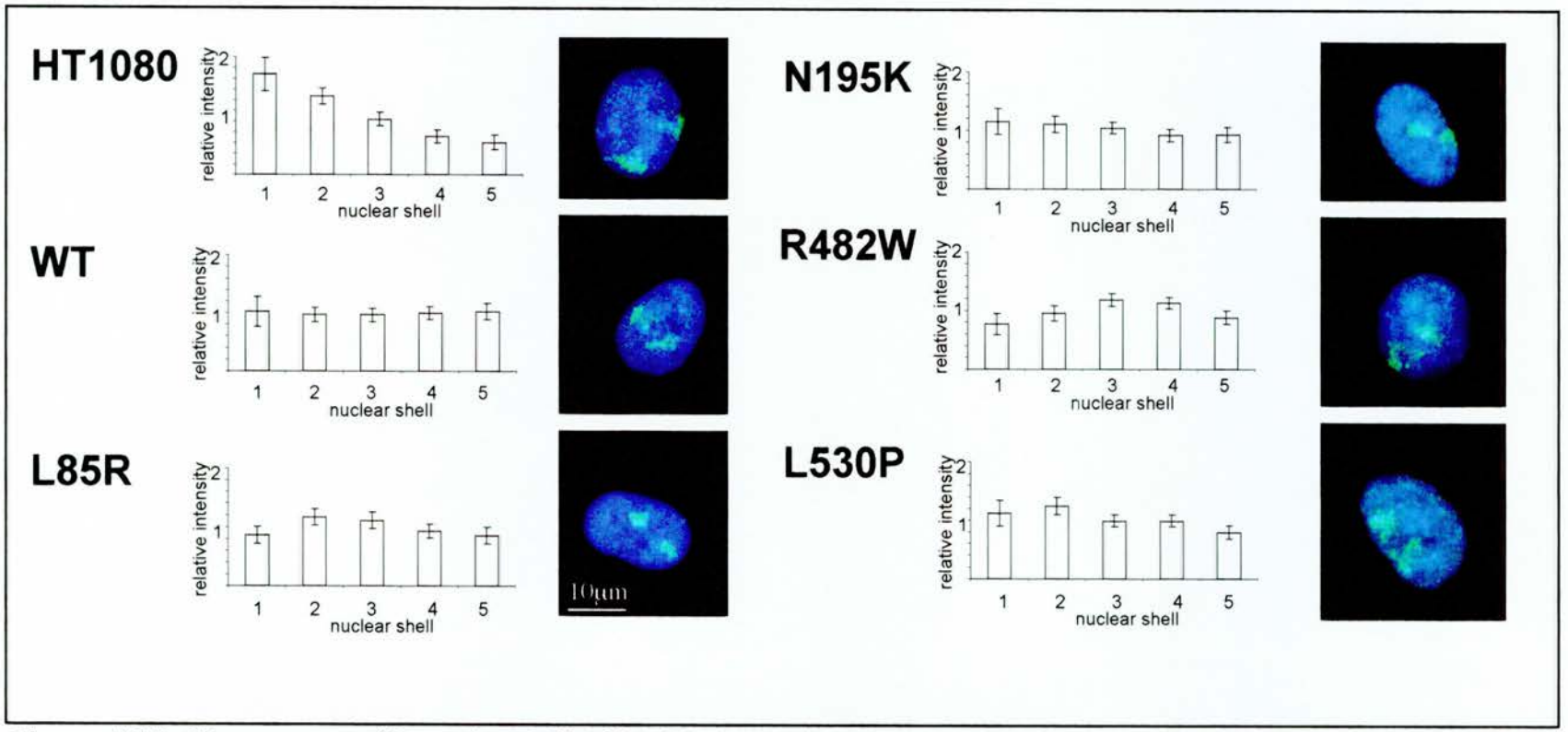

Figure 5.15 Chromosome 18 territory distribution in lamin A transfectants.
The distributions of chromosome 18 territories were analysed in 50 3:1 MAA fixed nuclei of HT1080 parental cell nuclei and the nuclei of cells stably expressing wt and mutant lamin A proteins. The mean distribution of relative chromosome paint signal (paint signal/DNA signal) for each shell is represented in a histogram. Shell 1 represents the nuclear periphery and shell 5 is the nuclear centre. The error bars represent the standard error of the mean (S.E.M) for each data set. Blue = DAPI DNA, green = FITC chromosome paint.

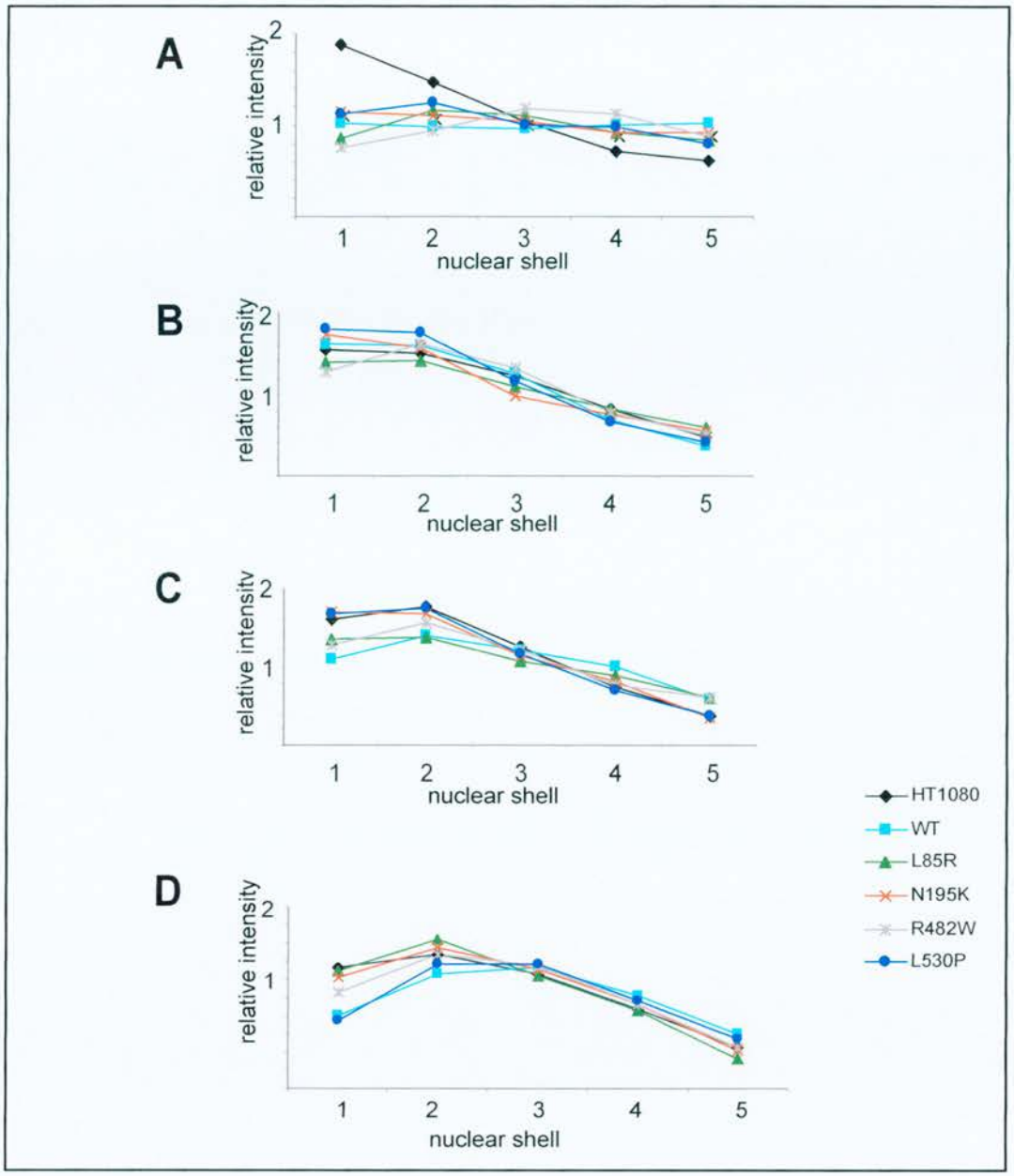

Figure 5.16 Comparing chromosome territory distributions in lamin A transfectants.

The distributions of chromosome territories were analysed in 50 3:1 MAA fixed HT1080 parental cell nuceli and the nuclei of cells stably expressing wt and mutant lamin A proteins. The mean distribution of relative chromosome paint signal (paint signal/DNA signal) for each shell is represented as a histogram. Shell 1 represents the nuclear periphery and shell 5 is the nuclear centre.

stable lines in this study (P=0.05-0.09). These data indicate that there may be a complex relationship between peripheral chromosomes and lamin A proteins. The overexpression of wt GFP-lamin A disrupts the localisation of some (HSA1, 11 and 18), but not all (HSA13), of the chromosomes observed in this analysis. I conclude from this that the chromosome territory relocations I have observed are not due to overexpression of epitope-tagged protein and are due to the properties of the protein or the nature of the chromatin/lamina interactions.

Lamin proteins have been implicated in mediating the size of the interphase nucleus *in vitro* (reviewed in Hutchison, 2002). I considered that altered levels of lamin A protein would therefore disrupt the average nuclear size of the stable cell lines in this study. The total area of DNA (DAPI stain in pixels) was calculated for each of the FISH images used in the chromosome territory analysis (250 images per line). The data is presented in Table 5.2 below. This shows that the mean nuclear areas within each of the stable line populations is significantly different to that of the parent cell line. Interestingly, overexpression of wt, L85R, N195K and L530P GFP-tagged protein results in a decrease to mean nuclear size while the presence of R482W protein increases the mean nuclear size. This suggests that the protein mutations influence lamin A function in different ways and that the Ig-fold domain interactions may influence this relationship.

	Cell Line					
	HT1080 parent	**WT**	**L85R**	**N195K**	**R482W**	**L530P**
Mean Nuclear Area (pixels)	9953.97	8119.35	7523.37	6692.66	10740.88	7081.52
Compare to HT1080 (P value)	-	0.0001	0.0001	0.0001	0.0006	0.0001

Table 5.2 Mean Nuclear Areas of lamin A transformants.

P values were calculated by comparing the data sets for each stable line compared to the HT1080 parent line in a standard *t*-test. 100 pixels = 21.4μm

5.6 Discussion

In this chapter, disease-associated lamin A fusion proteins have been used to help identify the role of the nuclear lamins in the spatial arrangement of chromatin. Selected mutants have missense mutations within four distinct regions of the lamin A protein, and these four mutations are associated with different disease pathologies (Figure 5.1). I have shown that different mutant proteins have different interphase dynamics when analysed in FRAP experiments (section 5.3.2). IF investigations of INM protein localisation reveal that stable lines expressing wt and mutant GFP tagged lamin A protein successfully recruit INM proteins to the nuclear periphery (section 5.5.2). Chromosome territory distribution analyses also show that the peripheral location of some chromosomes is disrupted in cells overexpressing mutant and wt GFP lamin A proteins (section 5.5.3).

5.6.1 Lamin A interphase dynamics

GFP-fusion constructs were expressed transiently for FLIP and FRAP experiments to determine the interphase dynamics of lamin A in human cells. My results support the findings of others (Broers et al., 1999; Moir et al., 2000) that GFP-tagged wild type lamin A is relatively immobile during interphase. However, I have determined that there is an increase in the mobility of protein at the nuclear periphery when lamin A protein contains the CM mutation, N195K. This mutation is within the rod domain of lamin A and therefore it is predicted that this mutation could affect the dimerisation of lamin A molecules. Hence, N195K mutant protein could be less efficiently incorporated into the lamina of cells. I have shown evidence that N195K protein is less efficiently incorporated into the lamina as there are high levels of nucleoplasmic signal in the stable lines used in my studies (see section 5.2, Figure 5.3).

The proteins of the lamina (lamins A, B and C) could have a degree of functional redundancy. This may result in compromised peripheral tethering, rather than complete loss of tethering, for N195K lamin A mutants. In this case, the INM and its associated proteins are very 'sticky' for lamin proteins (see section 1.5.4) and the nuclear periphery is a nuclear compartment where lamin A protein could interact with several proteins here (see section 1.5.3). Only some of these proteins will bind lamin A dimers or filaments, while others may be capable of binding monomers.

There is evidence for high mobility of INM proteins in the nucleus (e.g. emerin; Ostlund et al., 1999), however, the lamina is juxtaposed between the INM and chromatin. Peripheral chromatin in human cells has been shown to be less mobile than its nucleoplasmic counterpart (Chubb et al., 2002). As peripheral chromatin is restricted in its movement, lamin A protein could be equally constrained. The lamina is polymerised and depolymerised in response to cellular cues. When monomers disassociate from the lamina network, they may only be able to access or 'sample' a small area of the peripheral nucleoplasm before being reincorporated into the filament network at the INM.

As mutations in emerin and lamin A are causative for the same disease, it would be interesting to gain more information on their relationship within the cell. One way to begin to address this would be to follow the dynamics of emerin in cells expressing mutant lamins, or vice versa. Joint labelling experiments, using the GFP spectral variants CFP and YFP, could be used to gather information on any changes to dynamics. For example, YFP-emerin could be bleached and the recovery followed. Concurrently, the CFP-lamin A intensity and/or mobility in the same or distant cellular region could be measured. This method may provide more insight into the relationship between the two proteins as it can be more accurate than IF techniques and is performed in living cells. The dominant-negative mechanism of laminopathy mutations may also be addressed using joint labelling experiments. Perhaps wt protein mobility is affected by the presence of mutant protein in the lamina.

5.6.2 Recruitment of INM proteins

Using IF on all cell lines that stably express wt and mutant lamin As, I have found no obvious changes to the composition of the INM. These findings directly contradicts the previous work as it has been shown that *LMNA*$^{-/-}$ mice (Sullivan et al., 1999) and mammalian cells transiently expressing mutant proteins (Raharjo et al., 2001; Ostlund et al., 2001; Holt et al., 2003) mislocalise INM proteins. Differences between the results documented here and the findings of others could be due to the different cell lines used; HT1080 cells here, rather than mouse myoblasts or HeLa cells. HT1080 cells might have higher levels of endogenous wt lamin A protein which are sufficient to prevent mutant protein from exerting their predicted dominant-negative effects. However, I have shown by western blot (Figure 5.7) that the levels of tagged lamin A exceed those of endogenous lamin A. The relationship mirrors the protein levels in some laminopathy diseases as patients have 25% of expected levels of wt protein in HGPS (section 5.1.3). There is little information available on relative

protein levels for patients with other laminopathies. It is more likely that the results of transient experiments are due to very high levels of expression of mutant lamins.

I have addressed the recruitment of some, but not all, of the INM proteins in the stable lines expressing wt and mutant lamin A protein. There may be changes to the levels of the remaining INM proteins (e.g. LBR, the LAP isoforms and MAN-1) in these cells and this can be addressed using IF.

5.6.3 Lamin A and chromatin

While the results detailed in this chapter go some way to suggest that lamins could play a role in the organisation of chromatin, further investigations could consolidate these findings. It should be noted that SW13 cells (analysed in chapter 3) have peripheral HSA18 territories but express negligible amounts of lamin A protein and mislocalised emerin (Vaughan et al., 2001) and references therein). Studies of chromosome territory locations in EDMD patient cells lacking emerin also show that HSA18 is located at the nuclear periphery (Boyle et al., 2001). These reports suggest that neither lamin A nor emerin is necessary to localise HSA18 however, I have found that overexpression of tagged lamin A protein displaces HSA18 from the nuclear periphery.

Previous work has described that in biochemical extractions using high salt concentrations, gene-rich chromosome 19 is retained in the nucleus while gene-poor 18 is released to a DNA halo (Croft et al., 1999). One can address if the different lamin A mutations (and their inferred different effects on protein function) will change the attachments of chromosomes as the salt concentration required to remove HSA18 from the nucleus may change. Some chromatin-associated proteins are predicted to form the bridge between chromosomes and the nuclear periphery, for example, BAF (bound by LEM domains; Lee and Craigie, 1998; Lee et al., 2001; Segura-Totten et al., 2002) and HP1 (bound by LBR; Ye and Worman, 1996). Hence, it would also be interesting to look at the behaviour of chromatin associated proteins (by FRAP or IF) in these lines.

We could also gain further information on the role of lamin A protein in chromatin organisation by performing spatial analysis of the distribution of centromeres in stable lines. Any observed redistribution of centromeres could suggest that the centromeres, or chromosome regions proximal to centromeres, interact with nuclear lamins. This analysis

was not performed as the GFP levels in the cells provided confocal imaging problems when used in conjunction with the Texas Red antibodies in this study (the levels of GFP emmission excite the Texas red). However, there is no gross redistribution of centromeres in stable lines expressing mutant or wt GFP lamin A when observed by IF (Figure 5.12). HT1080 cells also show increased clustering of centromeres than primary fibroblasts (Figure 5.12 compared with Figure 4.11). HT1080 centromeres frequently associate in small 3-D spheres and it may prove difficult to resolve individual centromere signals with the initial version of the analysis program.

Previous work has shown that peripheral heterochromatin is detached from the periphery of laminopathy patient cells (Fidzianska et al., 1998; Ognibene et al., 1999). EM ultrastructural analysis of wt and mutant lines could be used to determine if the peripheral heterochromatin is mislocalised. It is interesting to consider that movement of chromatin away from the periphery could correlate with changes to gene expression. This would prove a direct link between nuclear position and transcriptional status in human cells. Microarray analyses comparing expression levels for HSA18 genes could identify if nuclear location and/or lamin A binding has a role in transcriptional control. This may go some way to identify proteins involved in the pathology of laminopathies. Microarray analysis of patient cells has identified that genes from diverse chromosomal locations were misregulated in EDMD fibroblasts (Tsukahara et al., 2002). Increased levels of mRNA from genes on chromosomes 1,8, 18 and 20 (lamin C, fibroblast growth factor receptor, estrogen regulated LIV-1 and myosin light chain-2 respectively) were described by these authors along with decreased transcript levels of genes from chromosomes 10 and 11 (retinoic acid hydroxylase and neurogranin respectively) however, *in vivo* protein levels were not investigated in this study.

5.6.4 Lamin A mutations and disease

In this study, disease-associated lamin A mutations have been shown to affect protein mobility and nuclear organisation of chromatin. However, the selected mutations are only representative of the diverse range of mutations described for this protein. It would be interesting to extend this original study and follow the behaviour of additional mutations. N-terminal truncated lamin A proteins, in particular the single CMTD (R298C) mutation and the HGPS truncation mutation (that deletes the CaaX box), have previously been shown to disrupt sites of RNA polymerase II (Spann et al., 2002) and mislocalise emerin (Ostlund et al., 2001) in studies, but what is the effect of C-terminal mutations? HGPS patients have been shown to have no detectable truncated protein in lymphocytes and only 25% of wt

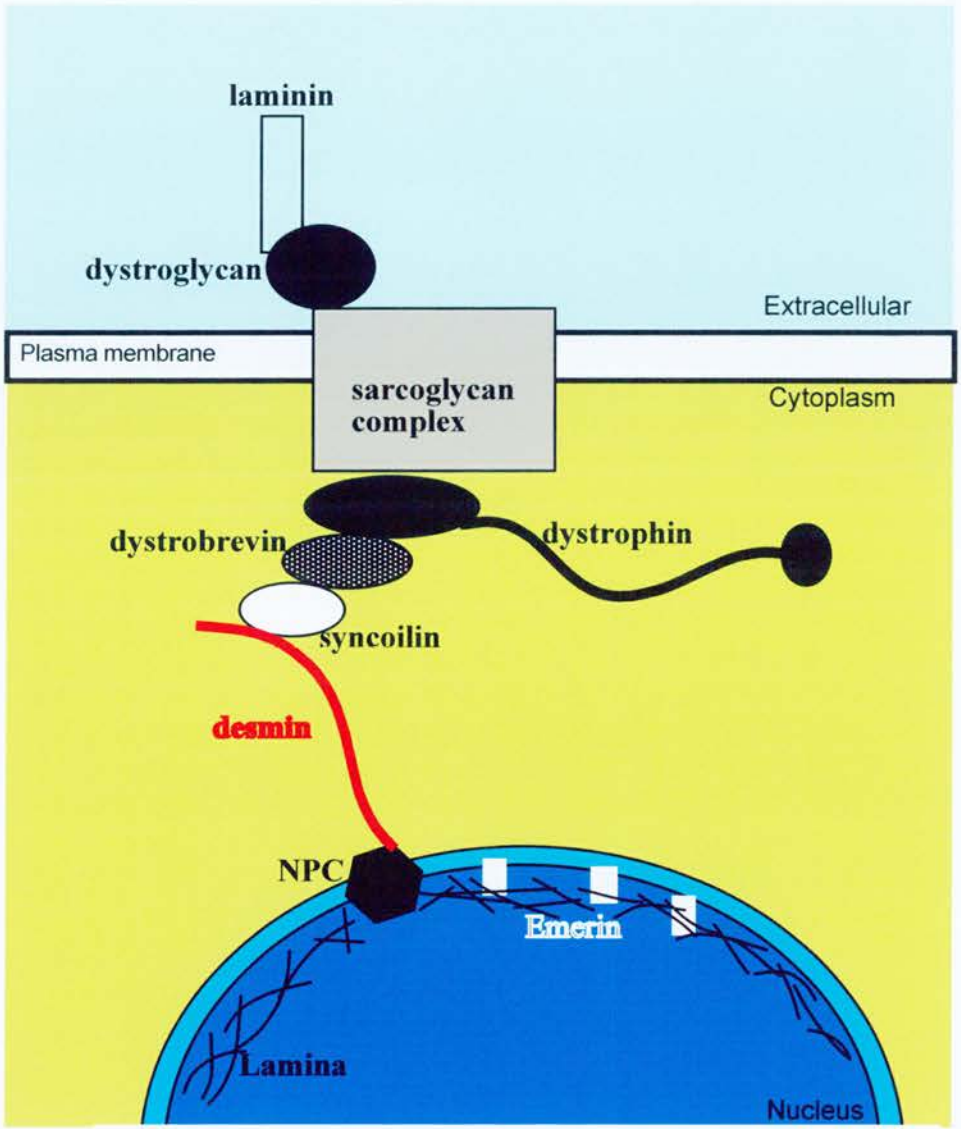

Figure 5.17 The karyocytoskeletal network model.
Schematic representing the proposed karyocytoskeletal network in muscle cells. It is proposed that a macromolecular skeleton is present in muscle cells that is involved in muscle fibre function. In this model, the extracellular matrix proteins and cell surface proteins are intrinsically linked to the nucleus via several protein interactions. Many of the proteins detailed in this interaction model are proteins known to be mutated in muscular dystrophy and dilated cardiomyopathy syndromes in patients.

levels of protein (Sandre-Giovannoli et al., 2003). Does the presence of the truncated transcript have a 'knock down' effect on endogenous proteins?

A new model is emerging that proposes lamin mutations may target muscle cells as the lamina is linked to a karyoskeletal network (Figure 5.17; Mounkes et al., 2003a; Ostlund and Worman, 2003). This suggests a cytoplasmic network connecting the extracellular matrix to the nuclear lamina, via the dystroglycan complex (including dystrophin and desmin) and the nuclear pores. The presence of this macromolecular structure has yet to be demonstrated *in vivo*. It would therefore be interesting to look at the distribution of chromosome territories in muscle cells, or indeed muscle biopsies from patients.

There have been some interesting recent developments in the study of laminopathies from transgenic mice studies. A transgenic line harbouring the AD-EDMD L530P mutation does not show any muscular dystrophy phenotype instead, these mice show clear symptoms of progeria (Mounkes et al., 2003b). The authors also suggest that this mutation may produce a message that is unstable due to aberrant splicing, although no data is presented to demonstrate this. Two additional mouse studies have linked deficient lamin A processing to a laminopathy disease mechanism as metalloproteinase mutations in the ZMPSTE24 cause laminopathy symptoms in homozygous-null mice (Pendas et al., 2002) and is the causative mutation of MAD in some patients (Agarwal et al., 2003).

CHAPTER 6

NUCLEAR ORGANISATION

In this thesis I have addressed whether the radial organisation of chromosomes is present in different cell types (Chapter 3) and whether nuclear organisation can be perturbed experimentally (Chapters 4 and 5). In Chapter 4, I used a biochemical approach (inhibition of HDACs with TSA) to investigate whether histone acetylation has a role in localising centromeres or chromosomes. In Chapter 5, I used genetic approaches (expression of mutant forms of lamin A) to investigate the role of the nuclear lamina in nuclear organisation.

6.1 RADIAL CHROMOSOME ORGANISATION IN NORMAL AND TRANSFORMED CELLS

The interphase locations of several chromosome territories were determined in many established human cell lines. In general, a radial organisation with respect to gene density is observed (Chapter 3). In both primary and transformed cell lines, the gene-rich chromosomes are towards the nuclear centre, while those with lower gene densities are towards the nuclear edge. These findings are in broad agreement with the work of Cremer et al., 2001 and their subsequent studies of both chicken and primate nuclei (Habermann et al., 2001; Tanabe et al., 2002b).

It is interesting that the spatial arrangement of chromosomes was generally comparable in primary and transformed cells, however, the locations of HSA18 territories is different between primary and transformed cells (internal vs. peripheral). Some differences in territory position for HSA6, 8 and 21 have been observed when primary fibroblasts and lymphoblastoid cells were compared (Boyle et al., 2001). It has yet to be determined if these differences in chromosome territory organisation are significant to the cell, perhaps influencing differentiation or cell lineage commitment. Observations of DNA replication

sites (Dimitrova and Berezney, 2002) and relative chromosome pairing (Parada et al., 2002) have shown no notable difference between the organisation in primary or transformed cells. A recent paper from the Cremer laboratory has also shown that location of HSA18 and 19 chromosomes is conserved in primary and transformed cells (Cremer et al., 2003). The authors go on to show that this location is conserved in human tissues. Together, these findings would suggest that spatial organisation of the nucleus is not grossly perturbed during cell transformation.

FISH paints do not highlight the entire linear sequence of each chromosome. Several reports have shown that genetic loci from chromosomes can loop out from the main body of the chromosome territory (Volpi et al., 2000; Williams et al., 2002; Mahy et al., 2002). The degree of looping out from the territory has also been shown to alter with differentiation (Williams et al., 2002, S. Chamberyon, personal communication). This implies that rather than whole chromosome territories relocating in response to differentiation or transformation, discrete chromatin regions may move relative to their chromosome territories. It would be interesting to disrupt the interphase location of a human gene, for example by recruiting it inappropriately to the nuclear periphery. This approach has already been used in yeast to show that forced association with the nuclear periphery causes transcriptional silencing of a gene (Andrulis et al., 1998).

6.2 HISTONE MODIFICATIONS

Most research on histone modifications has focussed on their role in controlling gene expression at a local level (Bulger et al., 2003; Chakrabarti et al., 2003; Macaluso et al., 2003). Little work has addressed what role histone modifications may have in global nuclear architecture. Hence, there was considerable interest when Taddei *et al.*,2001 reported that TSA-treatment of human and mouse cells resulted in relocalisation of chromatin in the nucleus. Specifically, movement of the centromeres to the nuclear periphery was described following TSA-treatment, however, their analysis lacked quantification. In chapter 4, I have shown that although TSA-treatment increases levels of acK5-H4 (Figure 4.1) and alters the nuclear distribution of acK5-H4 and acK9-H3 (Figures 4.4 and 4.6) the localisation of centromeres is not altered. Together with P. Perry, I developed an algorithm to allow quantification of IF signals in the 3-D nuclear space with respect to the nuclear periphery. This shows that centromeres are in close proximity to the nuclear periphery in human cells and this is consistent with previous reports (Chaly and Munro, 1996; Choh and De Boni,

1996; Alcobia et al., 2000) and that this distribution is not significantly altered in TSA-treated cells (Figure 4.16). I can only conclude that Taddei *et al.* 2001 selected unrepresentative images of untreated and treated cells in their report.

As some disruption of nuclear organisation is observed when histone acetylation levels are increased it would also be interesting to look at what effect decreased acetylation levels may have. It would be predicted that decreased histone acetylation would also have little effect on nuclear organisation however this remains to be tested. Selected inhibitors of acetyltransferase activity have been developed and could be used to address this (Lau et al., 2000; Balasubramanyam et al., 2003).

I have also described changes to methylated histone distribution following TSA-treatment. Currently there are no chemical inhibitors of histone methyltransferases available. I am sure that molecules will be developed that can inhibit the SET domain of methyltransferases and these can then be used in the same way as TSA to investigate the role of histone methylation in nuclear organisation. Chemical inhibition of enzyme activity can have varying degrees of specificity and hence the experimental results may not be representative of what role histone modifications play in nuclear organisation. Specific targeting of particular HDAC/HAT/HMT activities may be done through RNAi 'knock-down'. This genetic approach could be used to address the role of particular histone modifications in nuclear organisation.

Growing evidence suggests that histone modifications are involved in complex patterning or programming of particular events where different combinations can translate to very different outputs. Increasing total nuclear histone acetylation in these experiments is a crude way of implying a role in spatial organisation. As histone modifications appear to be linked to DNA methylation, it would be interesting to look at chromosome territories in cells treated with 5-aza-cytidine, a chemical that blocks DNA methylation. Many studies have reported synergism between the action of Trichostatin-A and 5-aza-cytidine, suggesting that histone modifications and DNA methylation mechanisms are linked (Selker, 1998; Takebayashi et al., 2001). Any altered positioning could be addressed genetically as DNA methylation is disrupted in ICF syndrome patients (OMIM 242860).

6.3 THE NUCLEAR PERIPHERY

I investigated the role a nuclear lamina component, lamin A, in peripheral tethering of chromatin (Chapter 5). In these experiments, I observed that HSA18 detaches from the nuclear periphery in cells overexpressing GFP-tagged wild type and mutant lamin A. However, the additional chromosomes analysed did not show a comparable degree of repositioning. It could be that lamin A protein is only involved in the peripheral tethering of a subset of chromosomes, including HSA18. An interpretation of these results is that detachment of peripheral territories is due to excess lamin molecules saturating the binding sites of INM molecules (e.g. emerin) and hence failure to correctly tether chromosomes. Alternatively, presence of the GFP moiety could interfere with lamina polymerisation and function, lamin A function was not directly tested in this study. Altered polymerisation of epitope-tagged lamin A could also affect the protein dynamics measured by FRAP experiments. It would therefore be interesting to compare purified recombinant FLAG-tagged and GFP-lamin A protein in biochemical studies to address whether the properties (e.g. polymerisation and emerin binding) of wt and mutant fusion proteins are similar. The ultrastructure of the nuclear lamina in stable lines expressing wt and mutant tagged-lamin A could also be investigated by EM and compared to that of the parental HT1080 cell line. This would go some way to demonstrate whether the integrity of the lamina network is compromised by the presence of ectopically expressed fusion proteins or the laminopathy protein mutations.

Limited progress in elucidating the role of proteins in nuclear organisation can be made if the proteins are mutated in human disease, for example the laminopathy mutations studied here. However, even with characterised genetic mutations of lamin A we known little of the molecular pathogenesis of the associated diseases. Currently, we do not have sufficient molecular tools to address the interdependence of many proteins in cultured cells as is possible with genetic mutants studies in model organisms. It is interesting that chromosomes are radially arranged in SW13 cells, as they contain greatly reduced levels of lamin A (Vaughan et al., 2001). This could suggest functional redundancy between lamins and INM proteins. In these cells, low levels of lamin A might not affect the overall location of chromosome territories as other binding events can compensate for this loss. Functional redundancy of lamin proteins tethering chromatin could be directly tested by using lamin B/C RNAi in SW13 cells. Lamin proteins can be efficiently targeted by RNAi as they were the first mammalian proteins to be knocked down by this technique (Elbashir et al., 2001).

The INM protein LBR has been recently implicated in the organisation of chromatin and/or the maintenance of nuclear shape. LBR mutations have been ascribed to the autosomal recessive human disease Pelger-Huet Anomaly (OMIM 169400) where patient neutrophils have abnormal nuclei (Hoffmann et al., 2002). It would be interesting to look at the nuclear organisation of lymphoblast and fibroblast cells from these patients as organisation may also be perturbed in these cell types.

6.4 A PREDICTED ROLE FOR NUCLEAR ORGANISATION

We are becoming increasingly aware of the spatial organisation of the nucleus. The radial pattern of chromosome organisation is generally conserved (Boyle et al., 2001; Habermann et al., 2001; Tanabe et al., 2002b) and this suggest that there may be biological significance for this pattern of nuclear organisation.

It has been proposed that the genome has a radial arrangement in the nucleus in order to maintain genome integrity (Tanabe et al., 2002a). Statistical analyses of the frequency of chromosome translocation events show that the incidence of translocations can be influenced by the nuclear location of chromosome territories, for example, translocation events involving internal HSA17, 19 and 22 occur at a higher expected frequency (Bickmore and Teague, 2002; Cornforth et al., 2002). The distribution of chromosome territories during interphase may serve to lower the incidence of detrimental translocation events between important chromosome sequences. An extension of this is 'body guard hypothesis' where gene-poor sequences are organised around the periphery of the nucleus and serve to protect the more gene-rich regions from damage by UV radiation or oxidising free radicals (Tanabe et al., 2002a) and references therein). Higher incidence of DNA damage events within gene-poor regions would minimise the amount of mutations occurring within protein coding sequence. The 'body guard' hypothesis could be tested by insulting cells with UV radiation or treating with chemicals such as hydrogen peroxide, which increases the levels of reactive oxygen species in the cell, and following the relative distribution of DNA damage. UV radiation induces single strand DNA breaks and creates specific base photoproducts including thymine dimers, while free radicals create several modified bases including 8-oxo-2'deoxyguanosine (Cooke et al., 2003). The nuclear distribution of damaged DNA bases detected by specific antibodies could analysed by IF (Chapter 4). Alternatively, cell lines expressing GFP labelled nucleotide excision repair enzymes (UV-damage repair mechanism,

(Houtsmuller et al., 1999) or base excision repair enzymes (oxidative damage repair mechanism (Bernstein et al., 2002) could be exposed to UV radiation or oxidising agents under live cell imaging conditions. This would allow the active process of DNA repair to be followed over time.

Radial arrangement of chromosome territories may also play a role in efficient DNA replication or cell division. In this case, chromosomes would be arranged in discrete territories to avoid chromatin strand intertwining during DNA synthesis and the prophase-anaphase transition. In cells with a high proliferative index (e.g. transformed or cancerous cells) one might expect a strict radial arrangement of chromosomes compared to a more relaxed organisation in slower dividing cells. My comparisons between chromosome territories in primary and transformed cells suggest that territories are more clearly maintained in transformed cells. In order to address this hypothesis directly, slowly dividing cells could be transformed and the chromosome territory locations (and mean territory areas) in primary and transformed cells from the same genetic background could be compared. Alternatively, the chromosome locations and areas in highly proliferative epidermal basal cells could be compared with chromosome locations in differentiated keratinocytes in the same tissue section (chapter 3).

The association of particular genes or chromosome loci with various nuclear protein domains may be related to control of nuclear processes including transcription and DNA replication. A situation is imagined where the chromatin loops radiating out from the body of its chromosome territory are the driving force for maintaining specific nuclear organisation. In this hypothesis, combinations of loops from different chromosomes could contribute to specific nuclear locations creating specialised neighbourhoods or chromatin hubs for permissive for particular processes (Visser and Aten, 1999; Jackson, 2003; de Laat and Grosveld, 2003).

If chromatin looping is the most influential factor for driving nuclear processes then it is predicted repositioning of whole chromosome territories would not be required during differentiation of through the cell cycle (Tanabe et al., 2002a). It could be argued that alterations in chromosome looping would not be sufficient to maintain large-scale changes in gene expression. Chromosomes do not share identical nuclear locations in every cell type (Boyle et al., 2001; Cremer et al., 2001; Cremer et al., 2003) and there is evidence for large scale nuclear reorganisation following quiescence (Bridger et al., 2000). Clearly, more

detailed studies of nuclear organisation are required to address the question of how nuclear location influences or controls gene expression during differentiation.

6.5 FUTURE CONSIDERATIONS

The current molecular tools and imaging capabilities limit the questions that can be addressed about the mechanisms and significance of nuclear organisation. We currently lack genetic approaches in human cells that can be used to directly investigate the *in vivo* relationships of proteins and nuclear organisation. The conclusions drawn from experiments where recombinant proteins, which may not be fully functional, are expressed at non-physiological levels in cultured cell lines may misrepresent the real situation. In addition to this, current LM investigation of spatial relationships cannot accurately resolve very small distances. New imaging technologies have been developed that can resolve distances as small as 20nm in living cells (O'Brien et al., 2003) although, as with any imaging process, sample preparation is critical as it limits the possibility of artefacts.

Understanding the mechanisms and functional implications of chromatin composition and spatial location of a gene or chromosomes may help us to create efficient therapies for a wide range of genetic diseases. Many genetic diseases are caused by misregulated gene expression, although the molecular details for individual diseases may not be clear. Therapeutic research for many genetic diseases aims to correct causative mutations in the patient's DNA. This can only be successfully achieved if we fully appreciate the biological mechanisms of gene expression. It is becoming clear that chromatin context and spatial locations of genes are as significant to control of gene expression as the primary DNA coding sequences alone.

REFERENCES

Aagaard, L., G.Laible, P.Selenko, M.Schmid, R.Dorn, G.Schotta, S.Kuhfittig, A.Wolf, A.Lebersorger, P.B.Singh, G.Reuter, and T.Jenuwein. 1999. Functional mammalian homologues of the Drosophila PEV-modifier Su(var)3-9 encode centromere-associated proteins which complex with the heterochromatin component M31. *EMBO J.* 18:1923-1938.

Abney, J.R., B.Cutler, M.L.Fillbach, D.Axelrod, and B.A.Scalettar. 1997. Chromatin dynamics in interphase nuclei and its implications for nuclear structure. *J. Cell Biol.* 137:1459-1468.

Aebi,U., J.Cohn, L.Buhle, and L.Gerace.1986. The nuclear lamina is a meshwork of intermediate-type filaments Nature 323, 560-564.

Agalioti, T., G.Chen, and D.Thanos. 2002. Deciphering the transcriptional histone acetylation code for a human gene. *Cell* 111:381-392.

Agarwal, A.K., J.P.Fryns, R.J.Auchus, and A.Garg. 2003. Zinc metalloproteinase, ZMPSTE24, is mutated in mandibuloacral dysplasia. *Hum. Mol. Genet.* 12:1995-2001.

Akasaka, T., M.van Lohuizen, L.N.van der, Y.Mizutani-Koseki, M.Kanno, M.Taniguchi, M.Vidal, M.Alkema, A.Berns, and H.Koseki. 2001. Mice doubly deficient for the Polycomb Group genes Mel18 and Bmi1 reveal synergy and requirement for maintenance but not initiation of Hox gene expression. *Development* 128:1587-1597.

Alcobia, I., R.Dilao, and L.Parreira. 2000. Spatial associations of centromeres in the nuclei of hematopoietic cells: evidence for cell-type-specific organizational patterns. *Blood* 95:1608-1615.

Alland, L., R.Muhle, H.Hou, Jr., J.Potes, L.Chin, N.Schreiber-Agus, and R.A.DePinho. 1997. Role for N-CoR and histone deacetylase in Sin3-mediated transcriptional repression. *Nature* 387:49-55.

Allfrey,V.G. Faulkner, R. and Mirsky, A. E. 1964. Acetylation and Methylation of histones and their possible role in the regulation of RNA synthesis. Proc.Natl.Acad.Sci U.S.A 51, 786-794.

Allison, D.C. and A.L.Nestor. 1999. Evidence for a relatively random array of human chromosomes on the mitotic ring. *J. Cell Biol.* 145:1-14.

Andrulis, E.D., A.M.Neiman, D.C.Zappulla, and R.Sternglanz. 1998. Perinuclear localization of chromatin facilitates transcriptional silencing [published erratum appears in Nature 1998 Oct 1;395(6701):525]. *Nature* 394:592-595.

Andrulis, E.D., D.C.Zappulla, A.Ansari, S.Perrod, C.V.Laiosa, M.R.Gartenberg, and R.Sternglanz. 2002. Esc1, a nuclear periphery protein required for Sir4-based plasmid anchoring and partitioning. *Mol. Cell Biol.* 22:8292-8301.

Annunziato, A.T. and J.C.Hansen. 2000. Role of histone acetylation in the assembly and modulation of chromatin structures. *Gene Expr.* 9:37-61.

Antequera, F., J.Boyes, and A.Bird. 1990. High levels of de novo methylation and altered chromatin structure at CpG islands in cell lines. *Cell* 62:503-514.

Antequera, F., D.Macleod, and A.P.Bird. 1989. Specific protection of methylated CpGs in mammalian nuclei. *Cell* 58:509-517.

Apel, E.D., R.M.Lewis, R.M.Grady, and J.R.Sanes. 2000. Syne-1, a dystrophin- and Klarsicht-related protein associated with synaptic nuclei at the neuromuscular junction. *J. Biol. Chem.* 275:31986-31995.

Arents, G., R.W.Burlingame, B.C.Wang, W.E.Love, and E.N.Moudrianakis. 1991. The nucleosomal core histone octamer at 3.1 A resolution: a tripartite protein assembly and a left-handed superhelix. *Proc. Natl. Acad. Sci. U. S. A* 88:10148-10152.

Ashery-Padan, R., N.Ulitzur, A.Arbel, M.Goldberg, A.M.Weiss, N.Maus, P.A.Fisher, and Y.Gruenbaum. 1997. Localization and posttranslational modifications of otefin, a protein required for vesicle attachment to chromatin, during Drosophila melanogaster development. *Mol Cell Biol* 17: 4114-23.

Balasubramanyam, K., V.Swaminathan, A.Ranganathan, and T.K.Kundu. 2003. Small molecule modulators of histone acetyltransferase p300. *J. Biol. Chem.*278: 19134-40.

Bannister, A.J., P.Zegerman, J.F.Partridge, E.A.Miska, J.O.Thomas, R.C.Allshire, and T.Kouzarides. 2001. Selective recognition of methylated lysine 9 on histone H3 by the HP1 chromo domain. *Nature* 410:120-124.

Bazett-Jones, D.P., K.Kimura, and T.Hirano. 2002. Efficient supercoiling of DNA by a single condensin complex as revealed by electron spectroscopic imaging. *Mol. Cell* 9:1183-1190.

Beisel C, Imhof A, Greene J, Kremmer E, and Sauer F. 2002. Histone methylation by the Drosophila epigenetic transcriptional regulator Ash1. *Nature* 419, 857-862.

Beletskii, A., Y.K.Hong, J.Pehrson, M.Egholm, and W.M.Strauss. 2001. PNA interference mapping demonstrates functional domains in the noncoding RNA Xist. *Proc. Natl. Acad. Sci U. S. A* 98:9215-9220.

Bell, A.C. and G.Felsenfeld. 2000. Methylation of a CTCF-dependent boundary controls imprinted expression of the Igf2 gene. *Nature* 405:482-485.

Bell, A.C., A.G.West, and G.Felsenfeld. 1999. The protein CTCF is required for the enhancer blocking activity of vertebrate insulators. *Cell* 98:387-396.

Belmont, A. 2003. Dynamics of chromatin, proteins, and bodies within the cell nucleus. *Curr. Opin. Cell Biol.* 15:304-310.

Belmont, A.S., F.Bignone, and P.O.Ts'o. 1986. The relative intranuclear positions of Barr bodies in XXX non- transformed human fibroblasts. *Exp Cell Res.* 165:165-179.

Belmont, A.S. and K.Bruce. 1994. Visualization of G1 chromosomes: a folded, twisted, supercoiled chromonema model of interphase chromatid structure. *J. Cell Biol.* 127:287-302.

Belmont, A.S., S.Dietzel, A.C.Nye, Y.G.Strukov, and T.Tumbar. 1999. Large-scale chromatin structure and function. *Curr. Opin. Cell Biol.* 11:307-311.

Belyaev, N.D., A.M.Keohane, and B.M.Turner. 1996. Histone H4 acetylation and replication timing in Chinese hamster chromosomes. *Exp. Cell Res.* 225:277-285.

Benavente, R. and G.Krohne. 1986. Involvement of nuclear lamins in postmitotic reorganization of chromatin as demonstrated by microinjection of lamin antibodies. *J. Cell Biol.* 103:1847-1854.

Berezney, R., M.Mortillaro, H.Ma, C.Meng, J.Samarabandu, X.Wei, S.Somanathan, W.S.Liou, S.J.Pan, and P.C.Cheng. 1996. Connecting nuclear architecture and genomic function. *J. Cell Biochem.* 62:223-226.

Bernstein, C., H.Bernstein, C.M.Payne, and H.Garewal. 2002. DNA repair/pro-apoptotic dual-role proteins in five major DNA repair pathways: fail-safe protection against carcinogenesis. *Mutat. Res.* 511:145-178.

Bestor, T.H. 2000. The DNA methyltransferases of mammals. *Hum. Mol. Genet.* 9:2395-2402.

Bickmore, W.A. and K.Oghene. 1996. Visualizing the spatial relationships between defined DNA sequences and the axial region of extracted metaphase chromosomes. *Cell* 84:95-104.

Bickmore, W.A. and A.T.Sumner. 1989. Mammalian chromosome banding--an expression of genome organization. *Trends Genet.* 5:144-148.

Bickmore, W.A. and P.Teague. 2002. Influences of chromosome size, gene density and nuclear position on the frequency of constitutional translocations in the human population. *Chromosome. Res.* 10:707-715.

Bione, S., E.Maestrini, S.Rivella, M.Mancini, S.Regis, G.Romeo, and D.Toniolo. 1994. Identification of a novel X-linked gene responsible for Emery-Dreifuss muscular dystrophy. *Nat. Genet.* 8:323-327.

Bird, A.P. and A.P.Wolffe. 1999. Methylation-induced repression--belts, braces, and chromatin. *Cell* 99:451-454.

Bjorkroth,B., C.Ericsson, M.M.Lamb, and B.Daneholt. 1988. Structure of the chromosome axis during transcription. Chromosoma 96, 333-340.

Bobrow, M. and J.Heritage. 1980. Nonrandom segregation of nucleolar organizing chromosomes at mitosis? *Nature* 288:79-81.

Boggs, B.A., P.Cheung, E.Heard, D.L.Spector, A.C.Chinault, and C.D.Allis. 2002. Differentially methylated forms of histone H3 show unique association patterns with inactive human X chromosomes. *Nat. Genet.* 30:73-76.

Bone, J.R., J.Lavender, R.Richman, M.J.Palmer, B.M.Turner, and M.I.Kuroda. 1994. Acetylated histone H4 on the male X chromosome is associated with dosage compensation in Drosophila. *Genes Dev.* 8:96-104.

Bonne, G., M.R.Di Barletta, S.Varnous, H.M.Becane, E.H.Hammouda, L.Merlini, F.Muntoni, C.R.Greenberg, F.Gary, J.A.Urtizberea, D.Duboc, M.Fardeau, D.Toniolo, and K.Schwartz. 1999. Mutations in the gene encoding lamin A/C cause autosomal dominant Emery-Dreifuss muscular dystrophy. *Nat. Genet.* 21:285-288.

Bonne, G., E.Mercuri, A.Muchir, A.Urtizberea, H.M.Becane, D.Recan, L.Merlini, M.Wehnert, R.Boor, U.Reuner, M.Vorgerd, E.M.Wicklein, B.Eymard, D.Duboc, I.Penisson-Besnier, J.M.Cuisset, X.Ferrer, I.Desguerre, D.Lacombe, K.Bushby, C.Pollitt, D.Toniolo, M.Fardeau, K.Schwartz, and F.Muntoni. 2000. Clinical and molecular genetic spectrum of autosomal dominant Emery- Dreifuss muscular dystrophy due to mutations of the lamin A/C gene. *Ann. Neurol.* 48:170-180.

Bornfleth, H., P.Edelmann, D.Zink, T.Cremer, and C.Cremer. 1999. Quantitative motion analysis of subchromosomal foci in living cells using four-dimensional microscopy [In Process Citation]. *Biophys. J.* 77:2871-2886.

Boveri T. 1909. Die Blastomerenkerne von *Ascaris megalocephala* und die Theorie der Chromosomenindividualitat. Arch Zellforschung 3, 181-286.

Boyle, S., S.Gilchrist, J.M.Bridger, N.L.Mahy, J.A.Ellis, and W.A.Bickmore. 2001. The spatial organization of human chromosomes within the nuclei of normal and emerin-mutant cells. *Hum. Mol. Genet.* 10:211-219.

Bramlage, B., U.Kosciessa, and D.Doenecke. 1997. Differential expression of the murine histone genes H3.3A and H3.3B. *Differentiation* 62:13-20.

Bridger, J.M., S.Boyle, I.R.Kill, and W.A.Bickmore. 2000. Re-modelling of nuclear architecture in quiescent and senescent human fibroblasts [In Process Citation]. *Curr. Biol.* 10:149-152.

Bridger, J.M., I.R.Kill, and P.Lichter. 1998. Association of pKi-67 with satellite DNA of the human genome in early G1 cells. *Chromosome. Res.* 6:13-24.

Bridger, J.M., I.R.Kill, M.O'Farrell, and C.J.Hutchison. 1993. Internal lamin structures within G1 nuclei of human dermal fibroblasts. *J. Cell Sci.* 104 (Pt 2):297-306.

Brinkmann, H., A.L.Dahler, C.Popa, M.M.Serewko, P.G.Parsons, B.G.Gabrielli, A.J.Burgess, and N.A.Saunders. 2001. Histone hyperacetylation induced by histone deacetylase inhibitors is not sufficient to cause growth inhibition in human dermal fibroblasts. *J. Biol. Chem.* 276:22491-22499.

Broers, J.L., B.M.Machiels, G.J.van Eys, H.J.Kuijpers, E.M.Manders, R.van Driel, and F.C.Ramaekers. 1999. Dynamics of the nuclear lamina as monitored by GFP-tagged A-type lamins. *J. Cell Sci.* 112 (Pt 20):3463-3475.

Brown, K.E., J.Baxter, D.Graf, M.Merkenschlager, and A.G.Fisher. 1999. Dynamic repositioning of genes in the nucleus of lymphocytes preparing for cell division. *Mol. Cell* 3:207-217.

Brown, K.E., S.S.Guest, S.T.Smale, K.Hahm, M.Merkenschlager, and A.G.Fisher. 1997. Association of transcriptionally silent genes with Ikaros complexes at centromeric heterochromatin. *Cell* 91:845-854.

Brownell, J.E., J.Zhou, T.Ranalli, R.Kobayashi, D.G.Edmondson, S.Y.Roth, and C.D.Allis. 1996. Tetrahymena histone acetyltransferase A: a homolog to yeast Gcn5p linking histone acetylation to gene activation. *Cell* 84:843-851.

Bruno, S., F.Ghiotto, F.Fais, M.Fagioli, L.Luzi, P.G.Pelicci, C.E.Grossi, and E.Ciccone. 2003. The PML gene is not involved in the regulation of MHC class I expression in human cell lines. *Blood* 101:3514-3519.

Bulger, M., D.Schubeler, M.A.Bender, J.Hamilton, C.M.Farrell, R.C.Hardison, and M.Groudine. 2003. A complex chromatin landscape revealed by patterns of nuclease sensitivity and histone modification within the mouse beta-globin locus. *Mol. Cell Biol.* 23:5234-5244.

Bultman, S., T.Gebuhr, D.Yee, C.La Mantia, J.Nicholson, A.Gilliam, F.Randazzo, D.Metzger, P.Chambon, G.Crabtree, and T.Magnuson. 2000. A Brg1 null mutation in the mouse reveals functional differences among mammalian SWI/SNF complexes. *Mol. Cell* 6:1287-1295.

Burgess-Beusse, B., C.Farrell, M.Gaszner, M.Litt, V.Mutskov, F.Recillas-Targa, M.Simpson, A.West, and G.Felsenfeld. 2002. The insulation of genes from external

enhancers and silencing chromatin. *Proc. Natl. Acad. Sci. U. S. A* 99 Suppl 4:16433-16437.

Burke, B. and L.Gerace. 1986. A cell free system to study reassembly of the nuclear envelope at the end of mitosis. *Cell* 44:639-652.

Burke, B. and C.L.Stewart. 2002. Life at the edge: the nuclear envelope and human disease. *Nat. Rev. Mol. Cell Biol.* 3:575-585.

Buss, F. and M.Stewart. 1995. Macromolecular interactions in the nucleoporin p62 complex of rat nuclear pores: binding of nucleoporin p54 to the rod domain of p62. *J. Cell Biol.* 128:251-261.

Byrne, C. 1997. Regulation of gene expression in developing epidermal epithelia. *Bioessays* 19:691-698.

Byvoet, P. 1971. Uptake of label into methylated amino acids from rat tissue histones after in vivo administration of (Me- 14 C)methionine. *Biochim. Biophys. Acta* 238:375a-376b.

Callan, H.G. 1986. Lampbrush chromosomes. *Mol. Biol. Biochem. Biophys.* 36:1-252.

Callan, H.G., J.G.Gall, and C.A.Berg. 1987. The lampbrush chromosomes of Xenopus laevis: preparation, identification, and distribution of 5S DNA sequences. *Chromosoma* 95:236-250.

Cao, R., L.Wang, H.Wang, L.Xia, H.Erdjument-Bromage, P.Tempst, R.S.Jones, and Y.Zhang. 2002. Role of histone H3 lysine 27 methylation in Polycomb-group silencing. *Science* 298:1039-1043.

Caron, H., B.van Schaik, M.M.van der, F.Baas, G.Riggins, P.van Sluis, M.C.Hermus, R.van Asperen, K.Boon, P.A.Voute, S.Heisterkamp, A.van Kampen, and R.Versteeg. 2001. The human transcriptome map: clustering of highly expressed genes in chromosomal domains. *Science* 291:1289-1292.

Carr, A.M., S.M.Dorrington, J.Hindley, G.A.Phear, S.J.Aves, and P.Nurse. 1994. Analysis of a histone H2A variant from fission yeast: evidence for a role in chromosome stability. *Mol. Gen. Genet.* 245:628-635.

Carruthers, L.M., J.Bednar, C.L.Woodcock, and J.C.Hansen. 1998. Linker histones stabilize the intrinsic salt-dependent folding of nucleosomal arrays: mechanistic ramifications for higher-order chromatin folding. *Biochemistry* 37:14776-14787.

Carter, D., L.Chakalova, C.S.Osborne, Y.F.Dai, and P.Fraser. 2002. Long-range chromatin regulatory interactions in vivo. *Nat. Genet.*32: 623-6.

Caspersson, T., S.Farber, G.E.Foley, J.Kudynowski, E.J.Modest, E.Simonsson, U.Wagh, and L.Zech. 1968. Chemical differentiation along metaphase chromosomes. *Exp. Cell Res.* 49:219-222.

Cavalli, G. and R.Paro. 1999. Epigenetic inheritance of active chromatin after removal of the main transactivator. *Science* 286:955-958.

Chakrabarti, S.K., J.Francis, S.M.Ziesmann, J.C.Garmey, and R.G.Mirmira. 2003. Covalent histone modifications underlie the developmental regulation of insulin gene transcription in pancreatic beta cells. *J. Biol. Chem.* 278:23617-23623.

Chaly, N. and S.B.Munro. 1996. Centromeres reposition to the nuclear periphery during L6E9 myogenesis in vitro. *Exp. Cell Res.* 223:274-278.

Chen, D., H.Ma, H.Hong, S.S.Koh, S.M.Huang, B.T.Schurter, D.W.Aswad, and M.R.Stallcup. 1999. Regulation of transcription by a protein methyltransferase. *Science* 284:2174-2177.

Chen, L., L.Lee, B.A.Kudlow, H.G.Dos Santos, O.Sletvold, Y.Shafeghati, E.G.Botha, A.Garg, N.B.Hanson, G.M.Martin, I.S.Mian, B.K.Kennedy, and J.Oshima. 2003. LMNA mutations in atypical Werner's syndrome. *Lancet* 362:440-445.

Chen, T.R., R.J.Hay, and M.L.Macy. 1983. Intercellular karyotypic similarity in near-diploid cell lines of human tumor origins. *Cancer Genet. Cytogenet.* 10:351-362.

Cheung, P., C.D.Allis, and P.Sassone-Corsi. 2000. Signaling to chromatin through histone modifications. *Cell* 103:263-271.

Cheutin, T., A.J.McNairn, T.Jenuwein, D.M.Gilbert, P.B.Singh, and T.Misteli. 2003. Maintenance of stable heterochromatin domains by dynamic HP1 binding. *Science* 299:721-725.

Choh, V. and U.De Boni. 1996. Spatial repositioning of centromeric domains during regrowth of axons in nuclei of murine dorsal root ganglion neurons in vitro. *J. Neurobiol.* 31:325-332.

Christensen, M.O., H.U.Barthelmes, F.Boege, and C.Mielke. 2002. The N-terminal domain anchors human topoisomerase I at fibrillar centers of nucleoli and nucleolar organizer regions of mitotic chromosomes. *J. Biol. Chem.* 277:35932-35938.

Chubb, J.R., S.Boyle, P.Perry, and W.A.Bickmore. 2002. Chromatin motion is constrained by association with nuclear compartments in human cells. *Curr. Biol.* 12:439-445.

Clemson, C.M., J.A.McNeil, H.F.Willard, and J.B.Lawrence. 1996. XIST RNA paints the inactive X chromosome at interphase: evidence for a novel RNA involved in nuclear/chromosome structure. *J. Cell Biol.* 132:259-275.

Cooke, M.S., M.D.Evans, M.Dizdaroglu, and J.Lunec. 2003. Oxidative DNA damage: mechanisms, mutation, and disease. *FASEB J.* 17:1195-1214.

Cornforth, M.N., K.M.Greulich-Bode, B.D.Loucas, J.Arsuaga, M.Vazquez, R.K.Sachs, M.Bruckner, M.Molls, P.Hahnfeldt, L.Hlatky, and D.J.Brenner. 2002. Chromosomes are predominantly located randomly with respect to each other in interphase human cells. *J. Cell Biol.* 159:237-244.

Costanzi, C. and J.R.Pehrson. 1998. Histone macroH2A1 is concentrated in the inactive X chromosome of female mammals. *Nature* 393:599-601.

Costanzo, A., P.Merlo, N.Pediconi, M.Fulco, V.Sartorelli, P.A.Cole, G.Fontemaggi, M.Fanciulli, L.Schiltz, G.Blandino, C.Balsano, and M.Levrero. 2002. DNA damage-dependent acetylation of p73 dictates the selective activation of apoptotic target genes. *Mol. Cell* 9:175-186.

Craig, J.M. and W.A.Bickmore. 1993. Chromosome bands--flavours to savour. *Bioessays* 15:349-354.

Craig, J.M. and W.A.Bickmore. 1994. The distribution of CpG islands in mammalian chromosomes. *Nat. Genet.* 7:376-382.

Craig, J.M., S.Boyle, P.Perry, and W.A.Bickmore. 1997. Scaffold attachments within the human genome. *J. Cell Sci* 110 (Pt 21):2673-2682.

Cremer, M., K.Kupper, B.Wagler, L.Wizelman, J.J.Hase, Y.Weiland, L.Kreja, J.Diebold, M.R.Speicher, and T.Cremer. 2003. Inheritance of gene density-related higher order chromatin arrangements in normal and tumor cell nuclei. *J. Cell Biol.* 162:809-820.

Cremer, M., J.von Hase, T.Volm, A.Brero, G.Kreth, J.Walter, C.Fischer, I.Solovei, C.Cremer, and T.Cremer. 2001. Non-random radial higher-order chromatin arrangements in nuclei of diploid human cells. *Chromosome. Res.* 9:541-567.

Cremer, T. and C.Cremer. 2001. Chromosome territories, nuclear architecture and gene regulation in mammalian cells. *Nat. Rev. Genet.* 2:292-301.

Cremer, T., C.Cremer, H.Baumann, E.K.Luedtke, K.Sperling, V.Teuber, and C.Zorn. 1982a. Rabl's model of the interphase chromosome arrangement tested in Chinese hamster cells by premature chromosome condensation and laser-UV- microbeam experiments. *Hum. Genet.* 60:46-56.

Cremer, T., C.Cremer, T.Schneider, H.Baumann, L.Hens, and M.Kirsch-Volders. 1982b. Analysis of chromosome positions in the interphase nucleus of Chinese hamster cells by laser-UV-microirradiation experiments. *Hum. Genet.* 62:201-209.

Cremer, T., G.Kreth, H.Koester, R.H.Fink, R.Heintzmann, M.Cremer, I.Solovei, D.Zink, and C.Cremer. 2000. Chromosome territories, interchromatin domain compartment, and

nuclear matrix: an integrated view of the functional nuclear architecture. *Crit Rev. Eukaryot. Gene Expr.* 10:179-212.

Croft, J.A., J.M.Bridger, S.Boyle, P.Perry, P.Teague, and W.A.Bickmore. 1999. Differences in the localization and morphology of chromosomes in the human nucleus. *J. Cell Biol.* 145:1119-1131.

Csankovszki, G., A.Nagy, and R.Jaenisch. 2001. Synergism of Xist RNA, DNA methylation, and histone hypoacetylation in maintaining X chromosome inactivation. *J. Cell Biol.* 153:773-784.

Csink, A.K. and S.Henikoff. 1996. Genetic modification of heterochromatic association and nuclear organization in Drosophila. *Nature* 381:529-531.

Czermin, B., R.Melfi, D.McCabe, V.Seitz, A.Imhof, and V.Pirrotta. 2002. Drosophila enhancer of Zeste/ESC complexes have a histone H3 methyltransferase activity that marks chromosomal Polycomb sites. *Cell* 111:185-196.

Dasso, M., S.Dimitrov, and A.P.Wolffe. 1994. Nuclear assembly is independent of linker histones. *Proc. Natl. Acad. Sci. U. S. A* 91:12477-12481.

de Laat, W. and F.Grosveld. 2003. Spatial organization of gene expression: the active chromatin hub. *Chromosome. Res.* 11:447-459.

De Souza, C.P., A.H.Osmani, L.P.Wu, J.L.Spotts, and S.A.Osmani. 2000. Mitotic histone H3 phosphorylation by the NIMA kinase in Aspergillus nidulans. *Cell* 102:293-302.

DeCamillis, M., N.S.Cheng, D.Pierre, and H.W.Brock. 1992. The polyhomeotic gene of Drosophila encodes a chromatin protein that shares polytene chromosome-binding sites with Polycomb. *Genes Dev.* 6:223-232.

Dechat, T., S.Vlcek, and R.Foisner. 2000. Review: lamina-associated polypeptide 2 isoforms and related proteins in cell cycle-dependent nuclear structure dynamics. *J. Struct. Biol.* 129:335-345.

Dernburg, A.F., K.W.Broman, J.C.Fung, W.F.Marshall, J.Philips, D.A.Agard, and J.W.Sedat. 1996. Perturbation of nuclear architecture by long-distance chromosome interactions. *Cell* 85:745-759.

Dhalluin, C., J.E.Carlson, L.Zeng, C.He, A.K.Aggarwal, and M.M.Zhou. 1999. Structure and ligand of a histone acetyltransferase bromodomain. *Nature* 399:491-496.

Dhe-Paganon, S., E.D.Werner, Y.I.Chi, and S.E.Shoelson. 2002. Structure of the globular tail of nuclear lamin. *J. Biol. Chem.* 277:17381-17384.

Dietzel, S., K.Schiebel, G.Little, P.Edelmann, G.A.Rappold, R.Eils, C.Cremer, and T.Cremer. 1999. The 3D positioning of ANT2 and ANT3 genes within female X chromosome territories correlates with gene activity. *Exp Cell Res.* 252:363-375.

Dillon, N. and R.Festenstein. 2002. Unravelling heterochromatin: competition between positive and negative factors regulates accessibility. *Trends Genet.* 18:252-258.

Dimitrova, D.S. and R.Berezney. 2002. The spatio-temporal organization of DNA replication sites is identical in primary, immortalized and transformed mammalian cells. *J. Cell Sci.* 115:4037-4051.

Dimitrova, D.S. and D.M.Gilbert. 1999. The spatial position and replication timing of chromosomal domains are both established in early G1 phase [In Process Citation]. *Mol. Cell* 4:983-993.

Doring, V. and R.Stick. 1990. Gene structure of nuclear lamin LIII of Xenopus laevis; a model for the evolution of IF proteins from a lamin-like ancestor. *EMBO J.* 9:4073-4081.

Dundas, S.R., S.Boyle, C.O.Bellamy, W.Hawkins, O.J.Garden, J.A.Ross, and W.Bickmore. 2001. Dual Y-chromosome painting and immunofluorescence staining of archival human liver transplant biopsies. *J. Histochem. Cytochem.* 49:1321-1322.

Dundr, M. and T.Misteli. 2001. Functional architecture in the cell nucleus. *Biochem. J.* 356:297-310.

Dwyer, N. and G.Blobel. 1976. A modified procedure for the isolation of a pore complex-lamina fraction from rat liver nuclei. *J. Cell Biol.* 70:581-591.

Dyer, J.A., I.R.Kill, G.Pugh, R.A.Quinlan, E.B.Lane, and C.J.Hutchison. 1997. Cell cycle changes in A-type lamin associations detected in human dermal fibroblasts using monoclonal antibodies. *Chromosome. Res.* 5:383-394.

Earnshaw, W.C., B.Halligan, C.A.Cooke, M.M.Heck, and L.F.Liu. 1985. Topoisomerase II is a structural component of mitotic chromosome scaffolds. *J. Cell Biol.* 100:1706-1715.

Earnshaw, W.C. and M.M.Heck. 1985. Localization of topoisomerase II in mitotic chromosomes. *J. Cell Biol.* 100:1716-1725.

Ebbert, R., A.Birkmann, and H.J.Schuller. 1999. The product of the SNF2/SWI2 paralogue INO80 of Saccharomyces cerevisiae required for efficient expression of various yeast structural genes is part of a high-molecular-weight protein complex. *Mol. Microbiol.* 32:741-751.

Ekwall, K., T.Olsson, B.M.Turner, G.Cranston, and R.C.Allshire. 1997. Transient inhibition of histone deacetylation alters the structural and functional imprint at fission yeast centromeres. *Cell* 91:1021-1032.

Elbashir, S.M., J.Harborth, W.Lendeckel, A.Yalcin, K.Weber, and T.Tuschl. 2001a. Duplexes of 21-nucleotide RNAs mediate RNA interference in cultured mammalian cells. *Nature* 411:494-498.

Elbashir, S.M., W.Lendeckel, and T.Tuschl. 2001b. RNA interference is mediated by 21- and 22-nucleotide RNAs. *Genes Dev.* 15:188-200.

Ellenberg, J., E.D.Siggia, J.E.Moreira, C.L.Smith, J.F.Presley, H.J.Worman, and J.Lippincott-Schwartz. 1997. Nuclear membrane dynamics and reassembly in living cells: targeting of an inner nuclear membrane protein in interphase and mitosis. *J. Cell Biol.* 138:1193-1206.

Ellis, D.J., H.Jenkins, W.G.Whitfield, and C.J.Hutchison. 1997. GST-lamin fusion proteins act as dominant negative mutants in Xenopus egg extract and reveal the function of the lamina in DNA replication. *J. Cell Sci.* 110 (Pt 20):2507-2518.

Ericsson, C., H.Mehlin, B.Bjorkroth, M.M.Lamb, and B.Daneholt. 1989. The ultrastructure of upstream and downstream regions of an active Balbiani ring gene. *Cell* 56:631-639.

Eriksson, M., W.T.Brown, L.B.Gordon, M.W.Glynn, J.Singer, L.Scott, M.R.Erdos, C.M.Robbins, T.Y.Moses, P.Berglund, A.Dutra, E.Pak, S.Durkin, A.B.Csoka, M.Boehnke, T.W.Glover, and F.S.Collins. 2003. Recurrent de novo point mutations in lamin A cause Hutchinson-Gilford progeria syndrome. *Nature*.

Ferreira, J., G.Paolella, C.Ramos, and A.I.Lamond. 1997. Spatial organization of large-scale chromatin domains in the nucleus: a magnified view of single chromosome territories. *J. Cell Biol.* 139:1597-1610.

Festenstein, R., S.N.Pagakis, K.Hiragami, D.Lyon, A.Verreault, B.Sekkali, and D.Kioussis. 2003. Modulation of heterochromatin protein 1 dynamics in primary Mammalian cells. *Science* 299:719-721.

Fidzianska, A., D.Toniolo, and I.Hausmanowa-Petrusewicz. 1998. Ultrastructural abnormality of sarcolemmal nuclei in Emery-Dreifuss muscular dystrophy (EDMD). *J. Neurol. Sci.* 159:88-93.

Finnin, M.S., J.R.Donigian, A.Cohen, V.M.Richon, R.A.Rifkind, P.A.Marks, R.Breslow, and N.P.Pavletich. 1999. Structures of a histone deacetylase homologue bound to the TSA and SAHA inhibitors. *Nature* 401:188-193.

Fischle, W., S.Emiliani, M.J.Hendzel, T.Nagase, N.Nomura, W.Voelter, and E.Verdin. 1999. A new family of human histone deacetylases related to Saccharomyces cerevisiae HDA1p. *J. Biol. Chem.* 274:11713-11720.

Fischle, W., Y.Wang, and C.D.Allis. 2003a. Binary switches and modification cassettes in histone biology and beyond. *Nature* 425:475-479.

Fischle, W., Y.Wang, and C.D.Allis. 2003b. Histone and chromatin cross-talk. *Curr. Opin. Cell Biol.* 15:172-183.

Fisher, D.Z., N.Chaudhary, and G.Blobel. 1986. cDNA sequencing of nuclear lamins A and C reveals primary and secondary structural homology to intermediate filament proteins. *Proc. Natl. Acad. Sci. U. S. A* 83:6450-6454.

Flaus, A. and T.Owen-Hughes. 2001. Mechanisms for ATP-dependent chromatin remodelling. *Curr. Opin. Genet. Dev.* 11:148-154.

Foisner, R. and L.Gerace. 1993. Integral membrane proteins of the nuclear envelope interact with lamins and chromosomes, and binding is modulated by mitotic phosphorylation. *Cell* 73:1267-1279.

Forsberg, E.C., K.M.Downs, H.M.Christensen, H.Im, P.A.Nuzzi, and E.H.Bresnick. 2000. Developmentally dynamic histone acetylation pattern of a tissue-specific chromatin domain. *Proc. Natl. Acad. Sci U. S. A* 97:14494-14499.

Francis, N.J., A.J.Saurin, Z.Shao, and R.E.Kingston. 2001. Reconstitution of a functional core polycomb repressive complex. *Mol. Cell* 8:545-556.

Frey, M.R., A.D.Bailey, A.M.Weiner, and A.G.Matera. 1999. Association of snRNA genes with coiled bodies is mediated by nascent snRNA transcripts. *Curr. Biol.* 9:126-135.

Fricker, M., M.Hollinshead, N.White, and D.Vaux. 1997. Interphase nuclei of many mammalian cell types contain deep, dynamic, tubular membrane-bound invaginations of the nuclear envelope. *J. Cell Biol.* 136:531-544.

Fuchs,E. and K.Weber. Annu.Rev.Biochem. 1994. Intermediate Filaments: Structure dynamics function and disease. 63, 345-382.

Fuks, F., P.J.Hurd, R.Deplus, and T.Kouzarides. 2003. The DNA methyltransferases associate with HP1 and the SUV39H1 histone methyltransferase. *Nucleic Acids Res.* 31:2305-2312.

Funabiki, H., I.Hagan, S.Uzawa, and M.Yanagida. 1993. Cell cycle-dependent specific positioning and clustering of centromeres and telomeres in fission yeast. *J. Cell Biol.* 121:961-976.

Furukawa, K., C.E.Fritze, and L.Gerace. 1998. The major nuclear envelope targeting domain of LAP2 coincides with its lamin binding region but is distinct from its chromatin interaction domain. *J. Biol. Chem.* 273:4213-4219.

Furukawa, K. and Y.Hotta. 1993. cDNA cloning of a germ cell specific lamin B3 from mouse spermatocytes and analysis of its function by ectopic expression in somatic cells. *EMBO J.* 12:97-106.

Galy, V., J.C.Olivo-Marin, H.Scherthan, V.Doye, N.Rascalou, and U.Nehrbass. 2000. Nuclear pore complexes in the organization of silent telomeric chromatin. *Nature* 403:108-112.

Ganesan, S., D.P.Silver, R.A.Greenberg, D.Avni, R.Drapkin, A.Miron, S.C.Mok, V.Randrianarison, S.Brodie, J.Salstrom, T.P.Rasmussen, A.Klimke, C.Marrese, Y.Marahrens, C.X.Deng, J.Feunteun, and D.M.Livingston. 2002. BRCA1 Supports XIST RNA Concentration on the Inactive X Chromosome. *Cell* 111:393-405.

Gartenberg, M.R. 2000. The Sir proteins of Saccharomyces cerevisiae: mediators of transcriptional silencing and much more. *Curr. Opin. Microbiol.* 3:132-137.

Garvey, S.M., C.Rajan, A.P.Lerner, W.N.Frankel, and G.A.Cox. 2002. The muscular dystrophy with myositis (mdm) mouse mutation disrupts a skeletal muscle-specific domain of titin. *Genomics* 79:146-149.

Gasser, S.M., T.Laroche, J.Falquet, d.l.T.Boy, and U.K.Laemmli. 1986. Metaphase chromosome structure. Involvement of topoisomerase II. *J. Mol. Biol.* 188:613-629.

Gerasimova, T.I. and V.G.Corces. 1998. Polycomb and trithorax group proteins mediate the function of a chromatin insulator. *Cell* 92:511-521.

Gerdes, J., H.Lemke, H.Baisch, H.H.Wacker, U.Schwab, and H.Stein. 1984. Cell cycle analysis of a cell proliferation-associated human nuclear antigen defined by the monoclonal antibody Ki-67. *J. Immunol.* 133:1710-1715.

Gerdes, J., U.Schwab, H.Lemke, and H.Stein. 1983. Production of a mouse monoclonal antibody reactive with a human nuclear antigen associated with cell proliferation. *Int. J. Cancer* 31:13-20.

Gerlich, D., J.Beaudouin, B.Kalbfuss, N.Daigle, R.Eils, and J.Ellenberg. 2003. Global Chromosome Positions Are Transmitted through Mitosis in Mammalian Cells. *Cell* 112:751-764.

Gerull, B., M.Gramlich, J.Atherton, M.McNabb, K.Trombitas, S.Sasse-Klaassen, J.G.Seidman, C.Seidman, H.Granzier, S.Labeit, M.Frenneaux, and L.Thierfelder. 2002. Mutations of TTN, encoding the giant muscle filament titin, cause familial dilated cardiomyopathy. *Nat. Genet.* 30:201-204.

Gey,G. 1952. Tissue culture studies of the proliferative capacity of cervical carcinoma and normal epithelium. *Cancer Res.* 264-265.

Gilbert, N., S.Boyle, H.Sutherland, H.J.De Las, J.Allan, T.Jenuwein, and W.A.Bickmore. 2003. Formation of facultative heterochromatin in the absence of HP1. *EMBO J.* 22:5540-5550.

Glass, C.A., J.R.Glass, H.Taniura, K.W.Hasel, J.M.Blevitt, and L.Gerace. 1993. The alpha-helical rod domain of human lamins A and C contains a chromatin binding site. *EMBO J.* 12:4413-4424.

Goldberg, M., H.Jenkins, T.Allen, W.G.Whitfield, and C.J.Hutchison. 1995. Xenopus lamin B3 has a direct role in the assembly of a replication competent nucleus: evidence from cell-free egg extracts. *J. Cell Sci.* 108 (Pt 11):3451-3461.

Goldberg, M., H.Lu, N.Stuurman, R.Ashery-Padan, A.M.Weiss, J.Yu, D.Bhattacharyya, P.A.Fisher, Y.Gruenbaum, and M.F.Wolfner. 1998. Interactions among Drosophila nuclear envelope proteins lamin, otefin, and YA. *Mol. Cell Biol.* 18:4315-4323.

Goldman, A.E., R.D.Moir, M.Montag-Lowy, M.Stewart, and R.D.Goldman. 1992. Pathway of incorporation of microinjected lamin A into the nuclear envelope. *J. Cell Biol.* 119:725-735.

Goldman, R.D., Y.Gruenbaum, R.D.Moir, D.K.Shumaker, and T.P.Spann. 2002. Nuclear lamins: building blocks of nuclear architecture. *Genes Dev.* 16:533-547.

Goldmark, J.P., T.G.Fazzio, P.W.Estep, G.M.Church, and T.Tsukiyama. 2000. The Isw2 chromatin remodeling complex represses early meiotic genes upon recruitment by Ume6p. *Cell* 103:423-433.

Graham, F.L., J.Smiley, W.C.Russell, and R.Nairn. 1977. Characteristics of a human cell line transformed by DNA from human adenovirus type 5. *J. Gen. Virol.* 36:59-74.

Grant, P.A., L.Duggan, J.Cote, S.M.Roberts, J.E.Brownell, R.Candau, R.Ohba, T.Owen-Hughes, C.D.Allis, F.Winston, S.L.Berger, and J.L.Workman. 1997. Yeast Gcn5 functions in two multisubunit complexes to acetylate nucleosomal histones: characterization of an Ada complex and the SAGA (Spt/Ada) complex. *Genes Dev.* 11:1640-1650.

Grigoryev, S.A., J.Bednar, and C.L.Woodcock. 1999. MENT, a heterochromatin protein that mediates higher order chromatin folding, is a new serpin family member. *J. Biol. Chem.* 274:5626-5636.

Grosveld, F., G.B.van Assendelft, D.R.Greaves, and G.Kollias. 1987. Position-independent, high-level expression of the human beta-globin gene in transgenic mice. *Cell* 51:975-985.

Grozinger, C.M., C.A.Hassig, and S.L.Schreiber. 1999. Three proteins define a class of human histone deacetylases related to yeast Hda1p. *Proc. Natl. Acad. Sci. U. S. A* 96:4868-4873.

Guan, X.Y., H.Zhang, M.Bittner, Y.Jiang, P.Meltzer, and J.Trent. 1996. Chromosome arm painting probes. *Nat. Genet.* 12:10-11.

Haberma, F.A., M.Cremer, J.Walter, G.Kreth, J.von Hase, K.Bauer, J.Wienberg, C.Cremer, T.Cremer, and I.Solovei. 2001. Arrangements of macro- and microchromosomes in chicken cells. *Chromosome. Res.* 9:569-584.

Habermann,F.A., M.Cremer, J.Walter, G.Kreth, J.von Hase, K.Bauer, J.Wienberg, C.Cremer, T.Cremer, and I.Solovei. Chromosome.Res. 9, 569-584. 2001.

Hackman, P., A.Vihola, H.Haravuori, S.Marchand, J.Sarparanta, J.De Seze, S.Labeit, C.Witt, L.Peltonen, I.Richard, and B.Udd. 2002. Tibial muscular dystrophy is a titinopathy caused by mutations in TTN, the gene encoding the giant skeletal-muscle protein titin. *Am. J. Hum. Genet.* 71:492-500.

Hall, I.M., G.D.Shankaranarayana, K.Noma, N.Ayoub, A.Cohen, and S.I.Grewal. 2002. Establishment and maintenance of a heterochromatin domain. *Science* 297:2232-2237.

Harborth, J., S.M.Elbashir, K.Bechert, T.Tuschl, and K.Weber. 2001. Identification of essential genes in cultured mammalian cells using small interfering RNAs. *J. Cell Sci.* 114:4557-4565.

Hark, A.T., C.J.Schoenherr, D.J.Katz, R.S.Ingram, J.M.Levorse, and S.M.Tilghman. 2000. CTCF mediates methylation-sensitive enhancer-blocking activity at the H19/Igf2 locus. *Nature* 405:486-489.

Hart, C.M. and U.K.Laemmli. 1998. Facilitation of chromatin dynamics by SARs. *Curr. Opin. Genet. Dev.* 8:519-525.

Heard, E., C.Rougeulle, D.Arnaud, P.Avner, C.D.Allis, and D.L.Spector. 2001. Methylation of histone H3 at Lys-9 is an early mark on the X chromosome during X inactivation. *Cell* 107:727-738.

Hebbes, T.R., A.L.Clayton, A.W.Thorne, and C.Crane-Robinson. 1994. Core histone hyperacetylation co-maps with generalized DNase I sensitivity in the chicken beta-globin chromosomal domain. *EMBO J.* 13:1823-1830.

Hediger, F., F.R.Neumann, G.Van Houwe, K.Dubrana, and S.M.Gasser. 2002. Live Imaging of Telomeres. yKu and Sir Proteins Define Redundant Telomere-Anchoring Pathways in Yeast. *Curr. Biol.* 12:2076-2089.

Heinzel, T., R.M.Lavinsky, T.M.Mullen, M.Soderstrom, C.D.Laherty, J.Torchia, W.M.Yang, G.Brard, S.D.Ngo, J.R.Davie, E.Seto, R.N.Eisenman, D.W.Rose, C.K.Glass, and M.G.Rosenfeld. 1997. A complex containing N-CoR, mSin3 and histone deacetylase mediates transcriptional repression. *Nature* 387:43-48.

Hendrich,B. and W.A.Bickmore. 2001. Human diseases with underlying defects in chromatin structure and modification. Hum.Mol.Genet. 10, 1-10.

Hendrich, B. and A.Bird. 1998. Identification and characterization of a family of mammalian methyl-CpG binding proteins. *Mol. Cell Biol.* 18:6538-6547.

Hernandez-Verdun D., R.P., and G.-Y.J.2002. Emerging concepts of nucleolar assembly J.Cell Sci. 115, 2265-2270.

Heun, P., T.Laroche, K.Shimada, P.Furrer, and S.M.Gasser. 2001. Chromosome dynamics in the yeast interphase nucleus. *Science* 294:2181-2186.

Hirano, T. and T.J.Mitchison. 1994. A heterodimeric coiled-coil protein required for mitotic chromosome condensation in vitro. *Cell* 79:449-458.

Hirschhorn, J.N., S.A.Brown, C.D.Clark, and F.Winston. 1992. Evidence that SNF2/SWI2 and SNF5 activate transcription in yeast by altering chromatin structure. *Genes Dev.* 6:2288-2298.

Hochstrasser, M., D.Mathog, Y.Gruenbaum, H.Saumweber, and J.W.Sedat. 1986. Spatial organization of chromosomes in the salivary gland nuclei of Drosophila melanogaster. *J. Cell Biol.* 102:112-123.

Hoffmann, K., C.K.Dreger, A.L.Olins, D.E.Olins, L.D.Shultz, B.Lucke, H.Karl, R.Kaps, D.Muller, A.Vaya, J.Aznar, R.E.Ware, N.S.Cruz, T.H.Lindner, H.Herrmann, A.Reis, and K.Sperling. 2002. Mutations in the gene encoding the lamin B receptor produce an altered nuclear morphology in granulocytes (Pelger Huet anomaly). *Nat. Genet.* 31:410-414.

Holt, I., C.Ostlund, C.L.Stewart, N.N.Man, H.J.Worman, and G.E.Morris. 2003. Effect of pathogenic mis-sense mutations in lamin A on its interaction with emerin in vivo. *J. Cell Sci.* 116:3027-3035.

Houtsmuller, A.B., S.Rademakers, A.L.Nigg, D.Hoogstraten, J.H.Hoeijmakers, and W.Vermeulen. 1999. Action of DNA repair endonuclease ERCC1/XPF in living cells. *Science* 284:958-961.

Hsu, J.Y., Z.W.Sun, X.Li, M.Reuben, K.Tatchell, D.K.Bishop, J.M.Grushcow, C.J.Brame, J.A.Caldwell, D.F.Hunt, R.Lin, M.M.Smith, and C.D.Allis. 2000. Mitotic phosphorylation of histone H3 is governed by Ipl1/aurora kinase and Glc7/PP1 phosphatase in budding yeast and nematodes. *Cell* 102:279-291.

Hudson, D.F., P.Vagnarelli, R.Gassmann, and W.C.Earnshaw. 2003. Condensin is required for nonhistone protein assembly and structural integrity of vertebrate mitotic chromosomes. *Dev. Cell* 5:323-336.

Hutchison, C.J. 2002. Lamins: building blocks or regulators of gene expression? *Nat. Rev. Mol. Cell Biol.* 3:848-858.

Hutchison, C.J., M.Alvarez-Reyes, and O.A.Vaughan. 2001. Lamins in disease: why do ubiquitously expressed nuclear envelope proteins give rise to tissue-specific disease phenotypes? *J. Cell Sci.* 114:9-19.

Iborra, F.J. and P.R.Cook. 2002. The interdependence of nuclear structure and function. *Curr. Opin. Cell Biol.* 14:780-785.

Imai, S., C.M.Armstrong, M.Kaeberlein, and L.Guarente. 2000. Transcriptional silencing and longevity protein Sir2 is an NAD- dependent histone deacetylase. *Nature* 403:795-800.

Ishii, K. and U.K.Laemmli. 2003. Structural and dynamic functions establish chromatin domains. *Mol. Cell* 11:237-248.

Isogai, Y. and R.Tjian. 2003. Targeting genes and transcription factors to segregated nuclear compartments. *Curr. Opin. Cell Biol.* 15:296-303.

Jackson, D.A. 2003. The anatomy of transcription sites. *Curr. Opin. Cell Biol.* 15:311-317.

Jackson, J.P., A.M.Lindroth, X.Cao, and S.E.Jacobsen. 2002. Control of CpNpG DNA methylation by the KRYPTONITE histone H3 methyltransferase. *Nature* 416:556-560.

Jackson, V., A.Shires, N.Tanphaichitr, and R.Chalkley. 1976. Modifications to histones immediately after synthesis. *J. Mol. Biol.* 104:471-483.

Jacobson, R.H., A.G.Ladurner, D.S.King, and R.Tjian. 2000. Structure and function of a human TAFII250 double bromodomain module. *Science* 288:1422-1425.

Jaehning, J.A. and R.G.Roeder. 1977. Transcription of specific adenovirus genes in isolated nuclei by exogenous RNA polymerases. *J. Biol. Chem.* 252:8753-8761.

Jagatheesan, G., S.Thanumalayan, B.Muralikrishna, N.Rangaraj, A.A.Karande, and V.K.Parnaik. 1999. Colocalization of intranuclear lamin foci with RNA splicing factors. *J. Cell Sci.* 112 (Pt 24):4651-4661.

James, T.C. and S.C.Elgin. 1986. Identification of a nonhistone chromosomal protein associated with heterochromatin in Drosophila melanogaster and its gene. *Mol. Cell Biol.* 6:3862-3872.

Jeppesen, P., A.Mitchell, B.Turner, and P.Perry. 1992. Antibodies to defined histone epitopes reveal variations in chromatin conformation and underacetylation of centric heterochromatin in human metaphase chromosomes. *Chromosoma* 101:322-332.

Jeppesen, P. and B.M.Turner. 1993. The inactive X chromosome in female mammals is distinguished by a lack of histone H4 acetylation, a cytogenetic marker for gene expression. *Cell* 74:281-289.

Jin, Q.W., J.Fuchs, and J.Loidl. 2000. Centromere clustering is a major determinant of yeast interphase nuclear organization. *J. Cell Sci.* 113 (Pt 11):1903-1912.

Jones, P.L., G.J.Veenstra, P.A.Wade, D.Vermaak, S.U.Kass, N.Landsberger, J.Strouboulis, and A.P.Wolffe. 1998. Methylated DNA and MeCP2 recruit histone deacetylase to repress transcription. *Nat. Genet.* 19:187-191.

Kellum, R. and P.Schedl. 1991. A position-effect assay for boundaries of higher order chromosomal domains. *Cell* 64:941-950.

Kennedy, B.K., D.A.Barbie, M.Classon, N.Dyson, and E.Harlow. 2000. Nuclear organization of DNA replication in primary mammalian cells. *Genes Dev.* 14:2855-2868.

Kill, I.R., J.M.Bridger, K.H.Campbell, G.Maldonado-Codina, and C.J.Hutchison. 1991. The timing of the formation and usage of replicase clusters in S-phase nuclei of human diploid fibroblasts. *J. Cell Sci.* 100 (Pt 4):869-876.

Kim, J., S.Sif, B.Jones, A.Jackson, J.Koipally, E.Heller, S.Winandy, A.Viel, A.Sawyer, T.Ikeda, R.Kingston, and K.Georgopoulos. 1999. Ikaros DNA-binding proteins direct formation of chromatin remodeling complexes in lymphocytes. *Immunity.* 10:345-355.

Kimura, K. and T.Hirano. 1997. ATP-dependent positive supercoiling of DNA by 13S condensin: a biochemical implication for chromosome condensation. *Cell* 90:625-634.

Kimura, K., V.V.Rybenkov, N.J.Crisona, T.Hirano, and N.R.Cozzarelli. 1999. 13S condensin actively reconfigures DNA by introducing global positive writhe: implications for chromosome condensation. *Cell* 98:239-248.

Kleinjan, D.J. and H.van, V. 1998. Position effect in human genetic disease. *Hum. Mol. Genet.* 7:1611-1618.

Kornberg, R.D. and Y.Lorch. 1999. Twenty-five years of the nucleosome, fundamental particle of the eukaryote chromosome. *Cell* 98:285-294.

Kosak, S.T., J.A.Skok, K.L.Medina, R.Riblet, M.M.Le Beau, A.G.Fisher, and H.Singh. 2002. Subnuclear compartmentalization of immunoglobulin loci during lymphocyte development. *Science* 296:158-162.

Krebs, J.E., M.H.Kuo, C.D.Allis, and C.L.Peterson. 1999. Cell cycle-regulated histone acetylation required for expression of the yeast HO gene. *Genes Dev.* 13:1412-1421.

Krimm, I., C.Ostlund, B.Gilquin, J.Couprie, P.Hossenlopp, J.P.Mornon, G.Bonne, J.C.Courvalin, H.J.Worman, and S.Zinn-Justin. 2002. The Ig-like structure of the C-terminal domain of lamin A/C, mutated in muscular dystrophies, cardiomyopathy, and partial lipodystrophy. *Structure. (Camb.)* 10:811-823.

Kumaran, R.I., B.Muralikrishna, and V.K.Parnaik. 2002. Lamin A/C speckles mediate spatial organization of splicing factor compartments and RNA polymerase II transcription. *J. Cell Biol.* 159:783-793.

Kuo, M.H. and C.D.Allis. 1998. Roles of histone acetyltransferases and deacetylases in gene regulation. *Bioessays* 20:615-626.

Kurz, A., S.Lampel, J.E.Nickolenko, J.Bradl, A.Benner, R.M.Zirbel, T.Cremer, and P.Lichter. 1996. Active and inactive genes localize preferentially in the periphery of chromosome territories. *J. Cell Biol.* 135:1195-1205.

Lachner, M., D.O'Carroll, S.Rea, K.Mechtler, and T.Jenuwein. 2001. Methylation of histone H3 lysine 9 creates a binding site for HP1 proteins. *Nature* 410:116-120.

Lamond, A.I. and W.C.Earnshaw. 1998. Structure and function in the nucleus. *Science* 280:547-553.

Langmore, J.P. and J.R.Paulson. 1983. Low angle x-ray diffraction studies of chromatin structure in vivo and in isolated nuclei and metaphase chromosomes. *J. Cell Biol.* 96:1120-1131.

Lau, O.D., T.K.Kundu, R.E.Soccio, S.Ait-Si-Ali, E.M.Khalil, A.Vassilev, A.P.Wolffe, Y.Nakatani, R.G.Roeder, and P.A.Cole. 2000. HATs off: selective synthetic inhibitors of the histone acetyltransferases p300 and PCAF. *Mol. Cell* 5:589-595.

Leach, T.J., M.Mazzeo, H.L.Chotkowski, J.P.Madigan, M.G.Wotring, and R.L.Glaser. 2000. Histone H2A.Z is widely but nonrandomly distributed in chromosomes of Drosophila melanogaster. *J. Biol. Chem.* 275:23267-23272.

Lee, K.K., T.Haraguchi, R.S.Lee, T.Koujin, Y.Hiraoka, and K.L.Wilson. 2001. Distinct functional domains in emerin bind lamin A and DNA-bridging protein BAF. *J. Cell Sci.* 114:4567-4573.

Lee, M.S. and R.Craigie. 1998. A previously unidentified host protein protects retroviral DNA from autointegration. *Proc. Natl. Acad. Sci. U. S. A* 95:1528-1533.

Lehner, C.F., R.Stick, H.M.Eppenberger, and E.A.Nigg. 1987. Differential expression of nuclear lamin proteins during chicken development. *J. Cell Biol.* 105:577-587.

Leibovitz, A., W.M.McCombs, III, D.Johnston, C.E.McCoy, and J.C.Stinson. 1973. New human cancer cell culture lines. I. SW-13, small-cell carcinoma of the adrenal cortex. *J. Natl. Cancer Inst.* 51:691-697.

Leipe, D.D. and D.Landsman. 1997. Histone deacetylases, acetoin utilization proteins and acetylpolyamine amidohydrolases are members of an ancient protein superfamily. *Nucleic Acids Res.* 25:3693-3697.

Leitch, A.R. 2000. Higher levels of organization in the interphase nucleus of cycling and differentiated cells. *Microbiol. Mol. Biol. Rev.* 64:138-152.

Lenz-Bohme, B., J.Wismar, S.Fuchs, R.Reifegerste, E.Buchner, H.Betz, and B.Schmitt. 1997. Insertional mutation of the Drosophila nuclear lamin Dm0 gene results in defective nuclear envelopes, clustering of nuclear pore complexes, and accumulation of annulate lamellae. *J. Cell Biol.* 137:1001-1016.

Levsky, J.M. and R.H.Singer. 2003. Fluorescence in situ hybridization: past, present and future. *J. Cell Sci.* 116:2833-2838.

Lewis, J.D., R.R.Meehan, W.J.Henzel, I.Maurer-Fogy, P.Jeppesen, F.Klein, and A.Bird. 1992. Purification, sequence, and cellular localization of a novel chromosomal protein that binds to methylated DNA. *Cell* 69:905-914.

Li, G., G.Sudlow, and A.S.Belmont. 1998. Interphase cell cycle dynamics of a late-replicating, heterochromatic homogeneously staining region: precise choreography of condensation/decondensation and nuclear positioning. *J. Cell Biol.* 140:975-989.

Li, Q., K.R.Peterson, X.Fang, and G.Stamatoyannopoulos. 2002. Locus control regions. *Blood* 100:3077-3086.

Lippincott-Schwartz, J., N.Altan-Bonnet, and G.H.Patterson. 2003. Photobleaching and photoactivation: following protein dynamics in living cells. *Nat. Cell Biol.* Suppl:S7-14.

Litt, M.D., M.Simpson, F.Recillas-Targa, M.N.Prioleau, and G.Felsenfeld. 2001. Transitions in histone acetylation reveal boundaries of three separately regulated neighboring loci. *EMBO J.* 20:2224-2235.

Liu, J., T.R.Ben Shahar, D.Riemer, M.Treinin, P.Spann, K.Weber, A.Fire, and Y.Gruenbaum. 2000. Essential roles for Caenorhabditis elegans lamin gene in nuclear organization, cell cycle progression, and spatial organization of nuclear pore complexes. *Mol. Biol. Cell* 11:3937-3947.

Lourim, D. and J.J.Lin. 1992. Expression of wild-type and nuclear localization-deficient human lamin A in chick myogenic cells. *J. Cell Sci.* 103 (Pt 3):863-874.

Luderus,M.E., J.L.den Blaauwen, O.J.B.de Smit, D.A.Compton, and R.van Driel. 1994. Binding of Matrix Attachment Regions to Lamin Polymers Involves Single-Stranded Regions and the Minor Groove. Mol.Cell Biol. 14, 6297-6305.

Luger, K., A.W.Mader, R.K.Richmond, D.F.Sargent, and T.J.Richmond. 1997. Crystal structure of the nucleosome core particle at 2.8 A resolution. *Nature* 389:251-260.

Lyko, F. and R.Paro. 1999. Chromosomal elements conferring epigenetic inheritance. *Bioessays* 21:824-832.

Lyon, M.F. 1961. Gene action in the X-chromosome of the mouse (Mus musculus L.). *Naturwissenschaften* 190:372-373.

Macaluso, M., C.Cinti, G.Russo, A.Russo, and A.Giordano. 2003. pRb2/p130-E2F4/5-HDAC1-SUV39H1-p300 and pRb2/p130-E2F4/5-HDAC1-SUV39H1-DNMT1 multimolecular complexes mediate the transcription of estrogen receptor-alpha in breast cancer. *Oncogene* 22:3511-3517.

Machado, C. and D.J.Andrew. 2000. D-Titin: a giant protein with dual roles in chromosomes and muscles. *J. Cell Biol.* 151:639-652.

Machado, C., C.E.Sunkel, and D.J.Andrew. 1998. Human autoantibodies reveal titin as a chromosomal protein. *J. Cell Biol.* 141:321-333.

Mahy, N.L., P.E.Perry, and W.A.Bickmore. 2002a. Gene density and transcription influence the localization of chromatin outside of chromosome territories detectable by FISH. *J. Cell Biol.* 159:753-763.

Mahy, N.L., P.E.Perry, S.Gilchrist, R.A.Baldock, and W.A.Bickmore. 2002b. Spatial organization of active and inactive genes and noncoding DNA within chromosome territories. *J. Cell Biol.* 157:579-589.

Maison, C., D.Bailly, A.H.Peters, J.P.Quivy, D.Roche, A.Taddei, M.Lachner, T.Jenuwein, and G.Almouzni. 2002. Higher-order structure in pericentric heterochromatin involves a distinct pattern of histone modification and an RNA component. *Nat. Genet.* 30:329-334.

Manders, E.M., H.Kimura, and P.R.Cook. 1999. Direct imaging of DNA in living cells reveals the dynamics of chromosome formation. *J. Cell Biol.* 144:813-821.

Manuelidis, L. 1985. Individual interphase chromosome domains revealed by in situ hybridization. *Hum. Genet.* 71:288-293.

Manuelidis, L. and T.L.Chen. 1990. A unified model of eukaryotic chromosomes. *Cytometry* 11:8-25.

Maraldi, N.M., G.Lattanzi, P.Sabatelli, A.Ognibene, and S.Squarzoni. 2002. Functional domains of the nucleus: implications for Emery-Dreifuss muscular dystrophy. *Neuromuscul. Disord.* 12:815-823.

Marmorstein, R. 2001. Protein modules that manipulate histone tails for chromatin regulation. *Nat. Rev. Mol. Cell Biol.* 2:422-432.

Marshall, W.F., A.F.Dernburg, B.Harmon, D.A.Agard, and J.W.Sedat. 1996. Specific interactions of chromatin with the nuclear envelope: positional determination within the nucleus in Drosophila melanogaster. *Mol. Biol. Cell* 7:825-842.

Marshall, W.F., A.Straight, J.F.Marko, J.Swedlow, A.Dernburg, A.Belmont, A.W.Murray, D.A.Agard, and J.W.Sedat. 1997. Interphase chromosomes undergo constrained diffusional motion in living cells. *Curr. Biol.* 7:930-939.

Martins, S., S.Eikvar, K.Furukawa, and P.Collas. 2003. HA95 and LAP2 beta mediate a novel chromatin-nuclear envelope interaction implicated in initiation of DNA replication. *J. Cell Biol.* 160:177-188.

Mattson, B.A. and D.F.Albertini. 1990. Oogenesis: chromatin and microtubule dynamics during meiotic prophase. *Mol. Reprod. Dev.* 25:374-383.

McGhee, J.D., J.M.Nickol, G.Felsenfeld, and D.C.Rau. 1983. Histone hyperacetylation has little effect on the higher order folding of chromatin. *Nucleic Acids Res.* 11:4065-4075.

McKeon, F.D., M.W.Kirschner, and D.Caput. 1986. Homologies in both primary and secondary structure between nuclear envelope and intermediate filament proteins. *Nature* 319:463-468.

Meehan, R., J.Lewis, S.Cross, X.Nan, P.Jeppesen, and A.Bird. 1992. Transcriptional repression by methylation of CpG. *J. Cell Sci. Suppl* 16:9-14.

Meehan, R.R., J.D.Lewis, S.McKay, E.L.Kleiner, and A.P.Bird. 1989. Identification of a mammalian protein that binds specifically to DNA containing methylated CpGs. *Cell* 58:499-507.

Meier, J., K.H.Campbell, C.C.Ford, R.Stick, and C.J.Hutchison. 1991. The role of lamin LIII in nuclear assembly and DNA replication, in cell- free extracts of Xenopus eggs. *J. Cell Sci.* 98 (Pt 3):271-279.

Minc, E., J.C.Courvalin, and B.Buendia. 2000. HP1gamma associates with euchromatin and heterochromatin in mammalian nuclei and chromosomes. *Cytogenet. Cell Genet.* 90:279-284.

Mislow, J., J.Holaska, M.Kim, K.Lee, M.Segura-Totten, K.Wilson, and E.McNally. 2002a. Nesprin-1alpha self-associates and binds directly to emerin and lamin A in vitro. *FEBS Lett.* 525:135.

Mislow, J.M., M.S.Kim, D.B.Davis, and E.M.McNally. 2002b. Myne-1, a spectrin repeat transmembrane protein of the myocyte inner nuclear membrane, interacts with lamin A/C. *J. Cell Sci.* 115:61-70.

Mohr, E., L.Trieschmann, and U.Grossbach. 1989. Histone H1 in two subspecies of Chironomus thummi with different genome sizes: homologous chromosome sites differ largely in their content of a specific H1 variant. *Proc. Natl. Acad. Sci U. S. A* 86:9308-9312.

Moir, R.D., M.Montag-Lowy, and R.D.Goldman. 1994. Dynamic properties of nuclear lamins: lamin B is associated with sites of DNA replication. *J. Cell Biol.* 125:1201-1212.

Moir,R.D., T.P.Spann, and R.D.Goldman. 1995. The Dynamic Properties and Possible Functions of Nuclear Lamins. Int.Rev.Cytol. 162B, 141-182.

Moir, R.D., M.Yoon, S.Khuon, and R.D.Goldman. 2000. Nuclear lamins A and B1: different pathways of assembly during nuclear envelope formation in living cells. *J. Cell Biol.* 151:1155-1168.

Mounkes, L., S.Kozlov, B.Burke, and C.L.Stewart. 2003a. The laminopathies: nuclear structure meets disease. *Curr. Opin. Genet. Dev.* 13:223-230.

Mounkes, L.C., S.Kozlov, L.Hernandez, T.Sullivan, and C.L.Stewart. 2003b. A progeroid syndrome in mice is caused by defects in A-type lamins. *Nature* 423:298-301.

Mulholland, N.M., E.Soeth, and C.L.Smith. 2003. Inhibition of MMTV transcription by HDAC inhibitors occurs independent of changes in chromatin remodeling and increased histone acetylation. *Oncogene* 22:4807-4818.

Muller, J., C.M.Hart, N.J.Francis, M.L.Vargas, A.Sengupta, B.Wild, E.L.Miller, M.B.O'Connor, R.E.Kingston, and J.A.Simon. 2002. Histone methyltransferase activity of a Drosophila Polycomb group repressor complex. *Cell* 111:197-208.

Munkel, C., R.Eils, S.Dietzel, D.Zink, C.Mehring, G.Wedemann, T.Cremer, and J.Langowski. 1999. Compartmentalization of interphase chromosomes observed in simulation and experiment. *J. Mol. Biol.* 285:1053-1065.

Nagele, R., T.Freeman, L.McMorrow, and H.Y.Lee. 1995. Precise spatial positioning of chromosomes during prometaphase: evidence for chromosomal order. *Science* 270:1831-1835.

Nagele, R.G., T.Freeman, L.McMorrow, Z.Thomson, K.Kitson-Wind, and H.Lee. 1999. Chromosomes exhibit preferential positioning in nuclei of quiescent human cells. *J. Cell Sci.* 112 (Pt 4):525-535.

Nakayama, J., J.C.Rice, B.D.Strahl, C.D.Allis, and S.I.Grewal. 2001. Role of histone H3 lysine 9 methylation in epigenetic control of heterochromatin assembly. *Science* 292:110-113.

Nakayasu, H. and R.Berezney. 1989. Mapping replicational sites in the eucaryotic cell nucleus. *J. Cell Biol.* 108:1-11.

Nan, X., H.H.Ng, C.A.Johnson, C.D.Laherty, B.M.Turner, R.N.Eisenman, and A.Bird. 1998. Transcriptional repression by the methyl-CpG-binding protein MeCP2 involves a histone deacetylase complex. *Nature* 393:386-389.

Nath, J. and K.L.Johnson. 2000. A review of fluorescence in situ hybridization (FISH): current status and future prospects. *Biotech. Histochem.* 75:54-78.

Neigeborn, L. and M.Carlson. 1984. Genes affecting the regulation of SUC2 gene expression by glucose repression in Saccharomyces cerevisiae. *Genetics* 108:845-858.

Newport, J.W., K.L.Wilson, and W.G.Dunphy. 1990. A lamin-independent pathway for nuclear envelope assembly. *J. Cell Biol.* 111:2247-2259.

Newsome, P.N., I.Johannessen, S.Boyle, E.Dalakas, K.A.McAulay, K.Samuel, F.Rae, L.Forrester, M.L.Turner, P.C.Hayes, D.J.Harrison, W.A.Bickmore, and J.N.Plevris. 2003. Human cord blood-derived cells can differentiate into hepatocytes in the mouse liver with no evidence of cellular fusion. *Gastroenterology* 124:1891-1900.

Ng, H.H. and A.Bird. 1999. DNA methylation and chromatin modification. *Curr. Opin. Genet. Dev.* 9:158-163.

Nielsen, A.L., M.Oulad-Abdelghani, J.A.Ortiz, E.Remboutsika, P.Chambon, and R.Losson. 2001a. Heterochromatin formation in mammalian cells: interaction between histones and HP1 proteins. *Mol. Cell* 7:729-739.

Nielsen, S.J., R.Schneider, U.M.Bauer, A.J.Bannister, A.Morrison, D.O'Carroll, R.Firestein, M.Cleary, T.Jenuwein, R.E.Herrera, and T.Kouzarides. 2001b. Rb targets histone H3 methylation and HP1 to promoters. *Nature* 412:561-565.

Nigg, E.A. 1989. The nuclear envelope. *Curr. Opin. Cell Biol.* 1:435-440.

Nili, E., G.S.Cojocaru, Y.Kalma, D.Ginsberg, N.G.Copeland, D.J.Gilbert, N.A.Jenkins, R.Berger, S.Shaklai, N.Amariglio, F.Brok-Simoni, A.J.Simon, and G.Rechavi. 2001. Nuclear membrane protein LAP2beta mediates transcriptional repression alone and together with its binding partner GCL (germ-cell-less). *J. Cell Sci.* 114:3297-3307.

Nishioka, K., S.Chuikov, K.Sarma, H.Erdjument-Bromage, C.D.Allis, P.Tempst, and D.Reinberg. 2002. Set9, a novel histone H3 methyltransferase that facilitates transcription by precluding histone tail modifications required for heterochromatin formation. *Genes Dev.* 16:479-489.

Nogami, M., A.Kohda, H.Taguchi, M.Nakao, T.Ikemura, and K.Okumura. 2000. Relative locations of the centromere and imprinted SNRPN gene within chromosome 15 territories during the cell cycle in HL60 cells. *J. Cell Sci* 113 (Pt 12):2157-2165.

Novelli, G., A.Muchir, F.Sangiuolo, A.Helbling-Leclerc, M.R.D'Apice, C.Massart, F.Capon, P.Sbraccia, M.Federici, R.Lauro, C.Tudisco, R.Pallotta, G.Scarano, B.Dallapiccola, L.Merlini, and G.Bonne. 2002. Mandibuloacral dysplasia is caused by a mutation in LMNA-encoding lamin A/C. *Am. J. Hum. Genet.* 71:426-431.

O'Brien, T.P., C.J.Bult, C.Cremer, M.Grunze, B.B.Knowles, J.Langowski, J.McNally, T.Pederson, J.C.Politz, A.Pombo, G.Schmahl, J.P.Spatz, and R.van Driel. 2003. Genome function and nuclear architecture: from gene expression to nanoscience. *Genome Res.* 13:1029-1041.

O'Neill, D.W., S.S.Schoetz, R.A.Lopez, M.Castle, L.Rabinowitz, E.Shor, D.Krawchuk, M.G.Goll, M.Renz, H.P.Seelig, S.Han, R.H.Seong, S.D.Park, T.Agalioti, N.Munshi, D.Thanos, H.Erdjument-Bromage, P.Tempst, and A.Bank. 2000. An ikaros-containing chromatin-remodeling complex in adult-type erythroid cells. *Mol. Cell Biol.* 20:7572-7582.

O'Neill, L.P. and B.M.Turner. 1995. Histone H4 acetylation distinguishes coding regions of the human genome from heterochromatin in a differentiation-dependent but transcription-independent manner. *EMBO J.* 14:3946-3957.

Ognibene, A., P.Sabatelli, S.Petrini, S.Squarzoni, M.Riccio, S.Santi, M.Villanova, S.Palmeri, L.Merlini, and N.M.Maraldi. 1999. Nuclear changes in a case of X-linked Emery-Dreifuss muscular dystrophy. *Muscle Nerve* 22:864-869.

Ohsumi, K., C.Katagiri, and T.Kishimoto. 1993. Chromosome condensation in Xenopus mitotic extracts without histone H1. *Science* 262:2033-2035.

Okano, M., D.W.Bell, D.A.Haber, and E.Li. 1999. DNA methyltransferases Dnmt3a and Dnmt3b are essential for de novo methylation and mammalian development. *Cell* 99:247-257.

Okano, M., S.Xie, and E.Li. 1998. Cloning and characterization of a family of novel mammalian DNA (cytosine-5) methyltransferases. *Nat. Genet.* 19:219-220.

Orlando, V. 2003. Polycomb, epigenomes, and control of cell identity. *Cell* 112:599-606.

Ostlund, C., G.Bonne, K.Schwartz, and H.J.Worman. 2001. Properties of lamin A mutants found in Emery-Dreifuss muscular dystrophy, cardiomyopathy and Dunnigan-type partial lipodystrophy. *J. Cell Sci.* 114:4435-4445.

Ostlund, C., J.Ellenberg, E.Hallberg, J.Lippincott-Schwartz, and H.J.Worman. 1999. Intracellular trafficking of emerin, the Emery-Dreifuss muscular dystrophy protein. *J. Cell Sci.* 112 (Pt 11):1709-1719.

Ostlund, C. and H.J.Worman. 2003. Nuclear envelope proteins and neuromuscular diseases. *Muscle Nerve* 27:393-406.

Owen, D.J., P.Ornaghi, J.C.Yang, N.Lowe, P.R.Evans, P.Ballario, D.Neuhaus, P.Filetici, and A.A.Travers. 2000. The structural basis for the recognition of acetylated histone H4 by the bromodomain of histone acetyltransferase gcn5p. *EMBO J.* 19:6141-6149.

Ozaki, T., M.Saijo, K.Murakami, H.Enomoto, Y.Taya, and S.Sakiyama. 1994. Complex formation between lamin A and the retinoblastoma gene product: identification of the domain on lamin A required for its interaction. *Oncogene* 9:2649-2653.

Paddy, M.R., A.S.Belmont, H.Saumweber, D.A.Agard, and J.W.Sedat. 1990. Interphase nuclear envelope lamins form a discontinuous network that interacts with only a fraction of the chromatin in the nuclear periphery. *Cell* 62:89-106.

Pal-Bhadra, M., U.Bhadra, and J.A.Birchler. 2002. RNAi related mechanisms affect both transcriptional and posttranscriptional transgene silencing in Drosophila. *Mol. Cell* 9:315-327.

Parada, L., P.McQueen, P.Munson, and T.Misteli. 2002. Conservation of relative chromosome positioning in normal and cancer cells. *Curr. Biol.* 12:1692.

Parada, L. and T.Misteli. 2002. Chromosome positioning in the interphase nucleus. *Trends Cell Biol.* 12:425.

Parker, C.S. and R.G.Roeder. 1977. Selective and accurate transcription of the Xenopus laevis 5S RNA genes in isolated chromatin by purified RNA polymerase III. *Proc. Natl. Acad. Sci U. S. A* 74:44-48.

Paull, T.T., E.P.Rogakou, V.Yamazaki, C.U.Kirchgessner, M.Gellert, and W.M.Bonner. 2000. A critical role for histone H2AX in recruitment of repair factors to nuclear foci after DNA damage. *Curr. Biol.* 10:886-895.

Paulson, J.R. and U.K.Laemmli. 1977. The structure of histone-depleted metaphase chromosomes. *Cell* 12:817-828.

Paulson, J.R. and J.P.Langmore. 1983. Low angle x-ray diffraction studies of HeLa metaphase chromosomes: effects of histone phosphorylation and chromosome isolation procedure. *J. Cell Biol.* 96:1132-1137.

Pehrson, J.R. and V.A.Fried. 1992. MacroH2A, a core histone containing a large nonhistone region. *Science* 257:1398-1400.

Pendas, A.M., Z.Zhou, J.Cadinanos, J.M.Freije, J.Wang, K.Hultenby, A.Astudillo, A.Wernerson, F.Rodriguez, K.Tryggvason, and C.Lopez-Otin. 2002. Defective prelamin A processing and muscular and adipocyte alterations in Zmpste24 metalloproteinase-deficient mice. *Nat. Genet.* 31:94-99.

Peter, M. and E.A.Nigg. 1991. Ectopic expression of an A-type lamin does not interfere with differentiation of lamin A-negative embryonal carcinoma cells. *J. Cell Sci.* 100 (Pt 3):589-598.

Peters, A.H., J.E.Mermoud, D.O'Carroll, M.Pagani, D.Schweizer, N.Brockdorff, and T.Jenuwein. 2002. Histone H3 lysine 9 methylation is an epigenetic imprint of facultative heterochromatin. *Nat. Genet.* 30:77-80.

Petruk, S., Y.Sedkov, S.Smith, S.Tillib, V.Kraevski, T.Nakamura, E.Canaani, C.M.Croce, and A.Mazo. 2001. Trithorax and dCBP acting in a complex to maintain expression of a homeotic gene. *Science* 294:1331-1334.

Phair, R.D. and T.Misteli. 2000. High mobility of proteins in the mammalian cell nucleus. *Nature* 404:604-609.

Picketts, D.J., D.R.Higgs, S.Bachoo, D.J.Blake, O.W.Quarrell, and R.J.Gibbons. 1996. ATRX encodes a novel member of the SNF2 family of proteins: mutations point to a common mechanism underlying the ATR-X syndrome. *Hum. Mol. Genet.* 5:1899-1907.

Pidoux, A.L. and R.C.Allshire. 2000. Centromeres: getting a grip of chromosomes. *Curr. Opin. Cell Biol.* 12:308-319.

Plath, K., S.Mlynarczyk-Evans, D.A.Nusinow, and B.Panning. 2002. Xist RNA and the mechanism of X chromosome inactivation. *Annu. Rev. Genet.* 36:233-278.

Prigent, C. and S.Dimitrov. 2003. Phosphorylation of serine 10 in histone H3, what for? *J. Cell Sci.* 116:3677-3685.

Rabl,C. Morphologisches Jahrbuch 10: 214-330. 1885.

Raharjo, W.H., P.Enarson, T.Sullivan, C.L.Stewart, and B.Burke. 2001. Nuclear envelope defects associated with LMNA mutations cause dilated cardiomyopathy and Emery-Dreifuss muscular dystrophy. *J. Cell Sci.* 114:4447-4457.

Rattner, J.B. and C.C.Lin. 1985. Radial loops and helical coils coexist in metaphase chromosomes. *Cell* 42:291-296.

Rea, S., F.Eisenhaber, D.O'Carroll, B.D.Strahl, Z.W.Sun, M.Schmid, S.Opravil, K.Mechtler, C.P.Ponting, C.D.Allis, and T.Jenuwein. 2000. Regulation of chromatin structure by site-specific histone H3 methyltransferases. *Nature* 406:593-599.

Redon, C., D.Pilch, E.Rogakou, O.Sedelnikova, K.Newrock, and W.Bonner. 2002. Histone H2A variants H2AX and H2AZ. *Curr. Opin. Genet. Dev.* 12:162-169.

Reyes, J.C., J.Barra, C.Muchardt, A.Camus, C.Babinet, and M.Yaniv. 1998. Altered control of cellular proliferation in the absence of mammalian brahma (SNF2alpha). *EMBO J.* 17:6979-6991.

Rice, J.C. and C.D.Allis. 2001. Histone methylation versus histone acetylation: new insights into epigenetic regulation. *Curr. Opin. Cell Biol.* 13:263-273.

Richards, E.J. and S.C.Elgin. 2002. Epigenetic codes for heterochromatin formation and silencing: rounding up the usual suspects. *Cell* 108:489-500.

Rober, R.A., K.Weber, and M.Osborn. 1989. Differential timing of nuclear lamin A/C expression in the various organs of the mouse embryo and the young animal: a developmental study. *Development* 105:365-378.

Robinett, C.C., A.Straight, G.Li, C.Willhelm, G.Sudlow, A.Murray, and A.S.Belmont. 1996. In vivo localization of DNA sequences and visualization of large-scale chromatin organization using lac operator/repressor recognition. *J. Cell Biol.* 135:1685-1700.

Robyr, D., Y.Suka, I.Xenarios, S.K.Kurdistani, A.Wang, N.Suka, and M.Grunstein. 2002. Microarray deacetylation maps determine genome-wide functions for yeast histone deacetylases. *Cell* 109:437-446.

Rogakou, E.P., C.Boon, C.Redon, and W.M.Bonner. 1999. Megabase chromatin domains involved in DNA double-strand breaks in vivo. *J. Cell Biol.* 146:905-916.

Romano, G. 1992. Histone variants during sea urchin development. *Cell Biol. Int. Rep.* 16:197-206.

Roth, M.B. and J.G.Gall. 1987. Monoclonal antibodies that recognize transcription unit proteins on newt lampbrush chromosomes. *J. Cell Biol.* 105:1047-1054.

Ruiz-Carrillo, A., L.J.Wangh, and V.G.Allfrey. 1975. Processing of newly synthesized histone molecules. *Science* 190:117-128.

Sabbattini, P., M.Lundgren, A.Georgiou, C.Chow, G.Warnes, and N.Dillon. 2001. Binding of Ikaros to the lambda5 promoter silences transcription through a mechanism that does not require heterochromatin formation. *EMBO J.* 20:2812-2822.

Sachs, R.K., E.G.van den, B.Trask, H.Yokota, and J.E.Hearst. 1995. A random-walk/giant-loop model for interphase chromosomes. *Proc. Natl. Acad. Sci. U. S. A* 92:2710-2714.

Sadoni, N., S.Langer, C.Fauth, G.Bernardi, T.Cremer, B.M.Turner, and D.Zink. 1999. Nuclear organization of mammalian genomes. Polar chromosome territories build up functionally distinct higher order compartments. *J. Cell Biol.* 146:1211-1226.

Saitoh, N., I.G.Goldberg, E.R.Wood, and W.C.Earnshaw. 1994. ScII: an abundant chromosome scaffold protein is a member of a family of putative ATPases with an unusual predicted tertiary structure. *J. Cell Biol.* 127:303-318.

Saitoh, Y. and U.K.Laemmli. 1994. Metaphase chromosome structure: bands arise from a differential folding path of the highly AT-rich scaffold. *Cell* 76:609-622.

Sandre-Giovannoli, A., R.Bernard, P.Cau, C.Navarro, J.Amiel, I.Boccaccio, S.Lyonnet, C.L.Stewart, A.Munnich, M.Le Merrer, and N.Levy. 2003. Lamin a truncation in Hutchinson-Gilford progeria. *Science* 300:2055.

Santisteban, M.S., T.Kalashnikova, and M.M.Smith. 2000. Histone H2A.Z regulats transcription and is partially redundant with nucleosome remodeling complexes. *Cell* 103:411-422.

Santos-Rosa, H., R.Schneider, A.J.Bannister, J.Sherriff, B.E.Bernstein, N.C.Emre, S.L.Schreiber, J.Mellor, and T.Kouzarides. 2002. Active genes are tri-methylated at K4 of histone H3. *Nature* 419:407-411.

Santoso, B., B.D.Ortiz, and A.Winoto. 2000. Control of organ-specific demethylation by an element of the T-cell receptor-alpha locus control region. *J. Biol. Chem.* 275:1952-1958.

Sasseville, A.M. and Y.Raymond. 1995. Lamin A precursor is localized to intranuclear foci. *J. Cell Sci.* 108 (Pt 1):273-285.

Saunders, W.S., C.Chue, M.Goebl, C.Craig, R.F.Clark, J.A.Powers, J.C.Eissenberg, S.C.Elgin, N.F.Rothfield, and W.C.Earnshaw. 1993. Molecular cloning of a human homologue of Drosophila heterochromatin protein HP1 using anti-centromere autoantibodies with anti-chromo specificity. *J. Cell Sci* 104 (Pt 2):573-582.

Schaufele, F., J.F.Enwright, III, X.Wang, C.Teoh, R.Srihari, R.Erickson, O.A.MacDougald, and R.N.Day. 2001. CCAAT/enhancer binding protein alpha assembles essential cooperating factors in common subnuclear domains. *Mol. Endocrinol.* 15:1665-1676.

Schramke, V. and R.Allshire. 2003. Hairpin RNAs and retrotransposon LTRs effect RNAi and chromatin-based gene silencing. *Science* 301:1069-1074.

Sedat, J. and L.Manuelidis. 1978. A direct approach to the structure of eukaryotic chromosomes. *Cold Spring Harb. Symp. Quant. Biol.* 42 Pt 1:331-350.

Segura-Totten, M., A.K.Kowalski, R.Craigie, and K.L.Wilson. 2002. Barrier-to-autointegration factor: major roles in chromatin decondensation and nuclear assembly. *J. Cell Biol.* 158:475-485.

Selker, E.U. 1998. Trichostatin A causes selective loss of DNA methylation in Neurospora. *Proc. Natl. Acad. Sci. U. S. A* 95:9430-9435.

Shao, Z., F.Raible, R.Mollaaghababa, J.R.Guyon, C.T.Wu, W.Bender, and R.E.Kingston. 1999. Stabilization of chromatin structure by PRC1, a Polycomb complex. *Cell* 98:37-46.

Shelby, R.D., K.M.Hahn, and K.F.Sullivan. 1996. Dynamic elastic behavior of alpha-satellite DNA domains visualized in situ in living human cells. *J. Cell Biol.* 135:545-557.

Shepherd, G.R., J.M.Hardin, and B.J.Noland. 1971. Methylation of lysine residues of histone fractions in synchronized mammalian cells. *Arch. Biochem. Biophys.* 143:1-5.

Shiels, C., S.A.Islam, R.Vatcheva, P.Sasieni, M.J.Sternberg, P.S.Freemont, and D.Sheer. 2001. PML bodies associate specifically with the MHC gene cluster in interphase nuclei. *J. Cell Sci* 114:3705-3716.

Shopland, L.S., C.V.Johnson, M.Byron, J.McNeil, and J.B.Lawrence. 2003. Clustering of multiple specific genes and gene-rich R-bands around SC-35 domains: evidence for local euchromatic neighborhoods. *J. Cell Biol.* 162:981-990.

Siggia, E.D., J.Lippincott-Schwartz, and S.Bekiranov. 2000. Diffusion in inhomogeneous media: theory and simulations applied to whole cell photobleach recovery. *Biophys. J.* 79:1761-1770.

Silva, J., W.Mak, I.Zvetkova, R.Appanah, T.B.Nesterova, Z.Webster, A.H.Peters, T.Jenuwein, A.P.Otte, and N.Brockdorff. 2003. Establishment of histone h3 methylation on the inactive x chromosome requires transient recruitment of eed-enx1 polycomb group complexes. *Dev. Cell* 4:481-495.

Simon, J.A. and J.W.Tamkun. 2002. Programming off and on states in chromatin: mechanisms of Polycomb and trithorax group complexes. *Curr. Opin. Genet. Dev.* 12:210-218.

Sinensky, M., K.Fantle, M.Trujillo, T.McLain, A.Kupfer, and M.Dalton. 1994. The processing pathway of prelamin A. *J. Cell Sci.* 107 (Pt 1):61-67.

Singh, P.B., J.R.Miller, J.Pearce, R.Kothary, R.D.Burton, R.Paro, T.C.James, and S.J.Gaunt. 1991. A sequence motif found in a Drosophila heterochromatin protein is conserved in animals and plants. *Nucleic Acids Res.* 19:789-794.

Skalnikova, M., S.Kozubek, E.Lukasova, E.Bartova, P.Jirsova, A.Cafourkova, I.Koutna, and M.Kozubek. 2000. Spatial arrangement of genes, centromeres and chromosomes in human blood cell nuclei and its changes during the cell cycle, differentiation and after irradiation. *Chromosome. Res.* 8:487-499.

Sleutels, F., G.Tjon, T.Ludwig, and D.P.Barlow. 2003. Imprinted silencing of Slc22a2 and Slc22a3 does not need transcriptional overlap between Igf2r and Air. *EMBO J.* 22:3696-3704.

Sleutels, F., R.Zwart, and D.P.Barlow. 2002. The non-coding Air RNA is required for silencing autosomal imprinted genes. *Nature* 415:810-813.

Smith, K.P., P.T.Moen, K.L.Wydner, J.R.Coleman, and J.B.Lawrence. 1999. Processing of endogenous pre-mRNAs in association with SC-35 domains is gene specific. *J. Cell Biol.* 144:617-629.

Smith, M.M. 2002. Centromeres and variant histones: what, where, when and why? *Curr. Opin. Cell Biol.* 14:279-285.

Spann, T.P., A.E.Goldman, C.Wang, S.Huang, and R.D.Goldman. 2002. Alteration of nuclear lamin organization inhibits RNA polymerase II- dependent transcription. *J. Cell Biol.* 156:603-608.

Spann, T.P., R.D.Moir, A.E.Goldman, R.Stick, and R.D.Goldman. 1997. Disruption of nuclear lamin organization alters the distribution of replication factors and inhibits DNA synthesis. *J. Cell Biol.* 136:1201-1212.

Spector, D.L. 2003. The dynamics of chromosome organization and gene regulation. *Annu. Rev. Biochem.* 72:573-608.

Steffensen, S., P.A.Coelho, N.Cobbe, S.Vass, M.Costa, B.Hassan, S.N.Prokopenko, H.Bellen, M.M.Heck, and C.E.Sunkel. 2001. A role for Drosophila SMC4 in the resolution of sister chromatids in mitosis. *Curr. Biol.* 11:295-307.

Stern, M., R.Jensen, and I.Herskowitz. 1984. Five SWI genes are required for expression of the HO gene in yeast. *J. Mol. Biol.* 178:853-868.

Stick, R. and P.Hausen. 1985. Changes in the nuclear lamina composition during early development of Xenopus laevis. *Cell* 41:191-200.

Stierle, V., J.Couprie, C.Ostlund, I.Krimm, S.Zinn-Justin, P.Hossenlopp, H.J.Worman, J.C.Courvalin, and I.Duband-Goulet. 2003. The carboxyl-terminal region common to lamins A and C contains a DNA binding domain. *Biochemistry* 42:4819-4828.

Strahl, B.D. and C.D.Allis. 2000. The language of covalent histone modifications. *Nature* 403:41-45.

Strahl, B.D., R.Ohba, R.G.Cook, and C.D.Allis. 1999. Methylation of histone H3 at lysine 4 is highly conserved and correlates with transcriptionally active nuclei in Tetrahymena. *Proc. Natl. Acad. Sci. U. S. A* 96:14967-14972.

Strait, K.A., B.Dabbas, E.H.Hammond, C.T.Warnick, S.J.Iistrup, and C.D.Ford. 2002. Cell cycle blockade and differentiation of ovarian cancer cells by the histone deacetylase inhibitor trichostatin A are associated with changes in p21, Rb, and Id proteins. *Mol. Cancer Ther.* 1:1181-1190.

Strambio-de-Castillia, C., G.Blobel, and M.P.Rout. 1999. Proteins connecting the nuclear pore complex with the nuclear interior. *J. Cell Biol.* 144:839-855.

Strukov, Y.G., Y.Wang, and A.S.Belmont. 2003. Engineered chromosome regions with altered sequence composition demonstrate hierarchical large-scale folding within metaphase chromosomes. *J. Cell Biol.* 162:23-35.

Stuurman, N., S.Heins, and U.Aebi. 1998. Nuclear lamins: their structure, assembly, and interactions. *J. Struct. Biol.* 122:42-66.

Sullivan, G.J., J.M.Bridger, A.P.Cuthbert, R.F.Newbold, W.A.Bickmore, and B.McStay. 2001. Human acrocentric chromosomes with transcriptionally silent nucleolar organizer regions associate with nucleoli. *EMBO J.* 20:2867-2877.

Sullivan, K.F., M.Hechenberger, and K.Masri. 1994. Human CENP-A contains a histone H3 related histone fold domain that is required for targeting to the centromere. *J. Cell Biol.* 127:581-592.

Sullivan, K.F. and R.D.Shelby. 1999. Using time-lapse confocal microscopy for analysis of centromere dynamics in human cells. *Methods Cell Biol.* 58:183-202.

Sullivan, T., D.Escalante-Alcalde, H.Bhatt, M.Anver, N.Bhat, K.Nagashima, C.L.Stewart, and B.Burke. 1999. Loss of A-type lamin expression compromises nuclear envelope integrity leading to muscular dystrophy. *J. Cell Biol.* 147:913-920.

Sumner, A.T., H.J.Evans, and R.A.Buckland. 1971. New technique for distinguishing between human chromosomes. *Nat. New Biol.* 232:31-32.

Sumner, A.T., M.H.Taggart, R.Mezzanotte, and L.Ferrucci. 1990. Patterns of digestion of human chromosomes by restriction endonucleases demonstrated by in situ nick translation. *Histochem. J.* 22:639-652.

Sun, H.B., J.Shen, and H.Yokota. 2000. Size-dependent positioning of human chromosomes in interphase nuclei. *Biophys. J.* 79:184-190.

Suntharalingam, M. and S.R.Wente. 2003. Peering through the pore: nuclear pore complex structure, assembly, and function. *Dev. Cell* 4:775-789.

Suzuki, T., M.Fujii, and D.Ayusawa. 2002. Demethylation of classical satellite 2 and 3 DNA with chromosomal instability in senescent human fibroblasts. *Exp. Gerontol.* 37:1005-1014.

Swedlow, J.R. and T.Hirano. 2003. The making of the mitotic chromosome: modern insights into classical questions. *Mol. Cell* 11:557-569.

Taddei, A., C.Maison, D.Roche, and G.Almouzni. 2001. Reversible disruption of pericentric heterochromatin and centromere function by inhibiting deacetylases. *Nat. Cell Biol.* 3:114-120.

Tagawa, Y., A.Nanashima, T.Yasutake, K.Hatano, J.E.Nishizawa-Takano, and H.Ayabe. 1997. Differences in spatial localization and chromatin pattern during different phases of cell cycle between normal and cancer cells. *Cytometry* 27:327-335.

Tajbakhsh, J., H.Luz, H.Bornfleth, S.Lampel, C.Cremer, and P.Lichter. 2000. Spatial distribution of GC- and AT-rich DNA sequences within human chromosome territories. *Exp Cell Res.* 255:229-237.

Takagi, N. 1974. Differentiation of X chromosomes in early female mouse embryos. *Exp. Cell Res.* 86:127-135.

Takebayashi, S., M.Nakao, N.Fujita, T.Sado, M.Tanaka, H.Taguchi, and K.Okumura. 2001. 5-Aza-2'-deoxycytidine induces histone hyperacetylation of mouse centromeric heterochromatin by a mechanism independent of DNA demethylation. *Biochem. Biophys. Res. Commun.* 288:921-926.

Tamaru, H. and E.U.Selker. 2001. A histone H3 methyltransferase controls DNA methylation in Neurospora crassa. *Nature* 414:277-283.

Tanabe, H., F.A.Habermann, I.Solovei, M.Cremer, and T.Cremer. 2002a. Non-random radial arrangements of interphase chromosome territories: evolutionary considerations and functional implications. *Mutat. Res.* 504:37-45.

Tanabe, H., S.Muller, M.Neusser, J.von Hase, E.Calcagno, M.Cremer, I.Solovei, C.Cremer, and T.Cremer. 2002b. Evolutionary conservation of chromosome territory arrangements in cell nuclei from higher primates. *Proc. Natl. Acad. Sci. U. S. A* 99:4424-4429.

Taverna, S.D., R.S.Coyne, and C.D.Allis. 2002. Methylation of histone h3 at lysine 9 targets programmed DNA elimination in tetrahymena. *Cell* 110:701-711.

Thomas, J.O. 1999. Histone H1: location and role. *Curr. Opin. Cell Biol.* 11:312-317.

Thompson, P.R., H.Kurooka, Y.Nakatani, and P.A.Cole. 2001. Transcriptional coactivator protein p300. Kinetic characterization of its histone acetyltransferase activity. *J. Biol. Chem.* 276:33721-33729.

Tolhuis, B., R.J.Palstra, E.Splinter, F.Grosveld, and W.de Laat. 2002. Looping and interaction between hypersensitive sites in the active beta-globin locus. *Mol. Cell* 10:1453-1465.

Tsukahara, T., S.Tsujino, and K.Arahata. 2002. CDNA microarray analysis of gene expression in fibroblasts of patients with X-linked Emery-Dreifuss muscular dystrophy. *Muscle Nerve* 25:898-901.

Tsukiyama, T. 2002. The in vivo functions of atp-dependent chromatin-remodelling factors. *Nat. Rev. Mol. Cell Biol.* 3:422-429.

Tumbar, T., G.Sudlow, and A.S.Belmont. 1999. Large-scale chromatin unfolding and remodeling induced by VP16 acidic activation domain. *J. Cell Biol.* 145:1341-1354.

Turner, B.M. 1998. Histone acetylation as an epigenetic determinant of long-term transcriptional competence. *Cell Mol. Life Sci.* 54:21-31.

Turner, B.M. 2002. Cellular memory and the histone code. *Cell* 111:285-291.

Turner, B.M., A.J.Birley, and J.Lavender. 1992. Histone H4 isoforms acetylated at specific lysine residues define individual chromosomes and chromatin domains in Drosophila polytene nuclei. *Cell* 69:375-384.

Turner, B.M. and G.Fellows. 1989. Specific antibodies reveal ordered and cell-cycle-related use of histone-H4 acetylation sites in mammalian cells. *Eur. J. Biochem.* 179:131-139.

Turner, B.M., L.Franchi, and H.Wallace. 1990. Islands of acetylated histone H4 in polytene chromosomes and their relationship to chromatin packaging and transcriptional activity. *J. Cell Sci.* 96 (Pt 2):335-346.

Umesono, K., T.Toda, S.Hayashi, and M.Yanagida. 1983. Cell division cycle genes nda2 and nda3 of the fission yeast Schizosaccharomyces pombe control microtubular organization and sensitivity to anti-mitotic benzimidazole compounds. *J. Mol. Biol.* 168:271-284.

van der Ploeg, M. 2000. Cytochemical nucleic acid research during the twentieth century. *Eur. J. Histochem.* 44:7-42.

van Holde, K. and J.Zlatanova. 1996. What determines the folding of the chromatin fiber? *Proc. Natl. Acad. Sci U. S. A* 93:10548-10555.

van Leeuwen, F., P.R.Gafken, and D.E.Gottschling. 2002. Dot1p modulates silencing in yeast by methylation of the nucleosome core. *Cell* 109:745-756.

Varga-Weisz, P.D. and P.B.Becker. 1998. Chromatin-remodeling factors: machines that regulate? *Curr. Opin. Cell Biol.* 10:346-353.

Vaughan, A., M.Alvarez-Reyes, J.M.Bridger, J.L.Broers, F.C.Ramaekers, M.Wehnert, G.E.Morris, W.G.F.Whitfield, and C.J.Hutchison. 2001. Both emerin and lamin C depend on lamin A for localization at the nuclear envelope. *J. Cell Sci.* 114:2577-2590.

Vaute, O., E.Nicolas, L.Vandel, and D.Trouche. 2002. Functional and physical interaction between the histone methyl transferase Suv39H1 and histone deacetylases. *Nucleic Acids Res.* 30:475-481.

Vazquez, J., A.S.Belmont, and J.W.Sedat. 2001. Multiple regimes of constrained chromosome motion are regulated in the interphase Drosophila nucleus. *Curr. Biol.* 11:1227-1239.

Verschure, P.J., D.K.van, I, E.M.Manders, and R.van Driel. 1999. Spatial relationship between transcription sites and chromosome territories. *J. Cell Biol.* 147:13-24.

Versteeg, R., B.D.van Schaik, M.F.van Batenburg, M.Roos, R.Monajemi, H.Caron, H.J.Bussemaker, and A.H.van Kampen. 2003. The human transcriptome map reveals extremes in gene density, intron length, GC content, and repeat pattern for domains of highly and weakly expressed genes. *Genome Res.* 13:1998-2004.

Visintin, R. and A.Amon. 2000. The nucleolus: the magician's hat for cell cycle tricks. *Curr. Opin. Cell Biol.* 12:752.

Visser, A.E. and J.A.Aten. 1999. Chromosomes as well as chromosomal subdomains constitute distinct units in interphase nuclei. *J. Cell Sci.* 112 (Pt 19):3353-3360.

Visser, A.E., R.Eils, A.Jauch, G.Little, P.J.Bakker, T.Cremer, and J.A.Aten. 1998. Spatial distributions of early and late replicating chromatin in interphase chromosome territories. *Exp. Cell Res.* 243:398-407.

Visser, A.E., F.Jaunin, S.Fakan, and J.A.Aten. 2000. High resolution analysis of interphase chromosome domains. *J. Cell Sci.* 113 (Pt 14):2585-2593.

Vogelstein, B., D.M.Pardoll, and D.S.Coffey. 1980. Supercoiled loops and eucaryotic DNA replicaton. *Cell* 22:79-85.

Volpe, T.A., C.Kidner, I.M.Hall, G.Teng, S.I.Grewal, and R.A.Martienssen. 2002. Regulation of heterochromatic silencing and histone H3 lysine-9 methylation by RNAi. *Science* 297:1833-1837.

Volpi, E.V., E.Chevret, T.Jones, R.Vatcheva, J.Williamson, S.Beck, R.D.Campbell, M.Goldsworthy, S.H.Powis, J.Ragoussis, J.Trowsdale, and D.Sheer. 2000. Large-scale chromatin organization of the major histocompatibility complex and other regions of human chromosome 6 and its response to interferon in interphase nuclei. *J. Cell Sci.* 113:1565-1576.

Vorburger, K., G.T.Kitten, and E.A.Nigg. 1989. Modification of nuclear lamin proteins by a mevalonic acid derivative occurs in reticulocyte lysates and requires the cysteine residue of the C-terminal CXXM motif. *EMBO J.* 8:4007-4013.

Wade, P.A., A.Gegonne, P.L.Jones, E.Ballestar, F.Aubry, and A.P.Wolffe. 1999. Mi-2 complex couples DNA methylation to chromatin remodelling and histone deacetylation. *Nat. Genet.* 23:62-66.

Walter, J., L.Schermelleh, M.Cremer, S.Tashiro, and T.Cremer. 2003. Chromosome order in HeLa cells changes during mitosis and early G1, but is stably maintained during subsequent interphase stages. *J. Cell Biol.* 160:685-697.

Wang, H., R.Cao, L.Xia, H.Erdjument-Bromage, C.Borchers, P.Tempst, and Y.Zhang. 2001. Purification and functional characterization of a histone H3-lysine 4-specific methyltransferase. *Mol. Cell* 8:1207-1217.

Wang, J.C. 2002. Cellular roles of DNA topoisomerases: a molecular perspective. *Nat. Rev. Mol. Cell Biol.* 3:430-440.

Wareham, K.A., M.F.Lyon, P.H.Glenister, and E.D.Williams. 1987. Age related reactivation of an X-linked gene. *Nature* 327:725-727.

Weber, K., U.Plessmann, and P.Traub. 1989. Maturation of nuclear lamin A involves a specific carboxy-terminal trimming, which removes the polyisoprenylation site from the precursor; implications for the structure of the nuclear lamina. *FEBS Lett.* 257:411-414.

Weier, H.U., H.D.Kleine, and J.W.Gray. 1991. Labeling of the centromeric region on human chromosome 8 by in situ hybridization. *Hum. Genet.* 87:489-494.

Weierich, C., A.Brero, S.Stein, J.von Hase, C.Cremer, T.Cremer, and I.Solovei. 2003. Three-dimensional arrangements of centromeres and telomeres in nuclei of human and murine lymphocytes. *Chromosome. Res.* 11:485-502.

Widom, J. 1998. Chromatin structure: linking structure to function with histone H1. *Curr. Biol.* 8:R788-R791.

Williams, R.R., S.Broad, D.Sheer, and J.Ragoussis. 2002. Subchromosomal positioning of the epidermal differentiation complex (EDC) in keratinocyte and lymphoblast interphase nuclei. *Exp. Cell Res.* 272:163-175.

Wilson, K.L. 2000. The nuclear envelope, muscular dystrophy and gene expression. *Trends Cell Biol.* 10:125-129.

Winston, F. and C.D.Allis. 1999. The bromodomain: a chromatin-targeting module? *Nat. Struct. Biol.* 6:601-604.

Witt, O., K.Sand, and A.Pekrun. 2000. Butyrate-induced erythroid differentiation of human K562 leukemia cells involves inhibition of ERK and activation of p38 MAP kinase pathways. *Blood* 95:2391-2396.

Wolf, S.F., D.J.Jolly, K.D.Lunnen, T.Friedmann, and B.R.Migeon. 1984. Methylation of the hypoxanthine phosphoribosyltransferase locus on the human X chromosome: implications for X-chromosome inactivation. *Proc. Natl. Acad. Sci U. S. A* 81:2806-2810.

Wolffe,A.P. 1995. Chromatin Structure and Function, Third Edition. London Academic Press.

Wolffe, A.P. and J.J.Hayes. 1999. Chromatin disruption and modification. *Nucleic Acids Res.* 27:711-720.

Worman, H.J., J.Yuan, G.Blobel, and S.D.Georgatos. 1988. A lamin B receptor in the nuclear envelope. *Proc. Natl. Acad. Sci U. S. A* 85:8531-8534.

Wutz, A. and R.Jaenisch. 2000. A shift from reversible to irreversible X inactivation is triggered during ES cell differentiation. *Mol. Cell* 5:695-705.

Xing, Y., C.V.Johnson, P.T.Moen, Jr., J.A.McNeil, and J.Lawrence. 1995. Nonrandom gene organization: structural arrangements of specific pre- mRNA transcription and splicing with SC-35 domains. *J. Cell Biol.* 131:1635-1647.

Xu, G.L., T.H.Bestor, D.Bourc'his, C.L.Hsieh, N.Tommerup, M.Bugge, M.Hulten, X.Qu, J.J.Russo, and E.Viegas-Pequignot. 1999. Chromosome instability and

immunodeficiency syndrome caused by mutations in a DNA methyltransferase gene. *Nature* 402:187-191.

Ye, Q., I.Callebaut, A.Pezhman, J.C.Courvalin, and H.J.Worman. 1997a. Domain-specific interactions of human HP1-type chromodomain proteins and inner nuclear membrane protein LBR. *J. Biol. Chem.* 272:14983-14989.

Ye, Q., I.Callebaut, A.Pezhman, J.C.Courvalin, and H.J.Worman. 1997b. Domain-specific interactions of human HP1-type chromodomain proteins and inner nuclear membrane protein LBR. *J. Biol. Chem.* 272:14983-14989.

Ye, Q. and H.J.Worman. 1996. Interaction between an integral protein of the nuclear envelope inner membrane and human chromodomain proteins homologous to Drosophila HP1. *J. Biol. Chem.* 271:14653-14656.

Yokota, H., M.J.Singer, G.J.van den Engh, and B.J.Trask. 1997. Regional differences in the compaction of chromatin in human G0/G1 interphase nuclei. *Chromosome. Res.* 5:157-166.

Yokota, H., E.G.van den, J.E.Hearst, R.K.Sachs, and B.J.Trask. 1995. Evidence for the organization of chromatin in megabase pair-sized loops arranged along a random walk path in the human G0/G1 interphase nucleus. *J. Cell Biol.* 130:1239-1249.

Yoshida, M., S.Horinouchi, and T.Beppu. 1995. Trichostatin A and trapoxin: novel chemical probes for the role of histone acetylation in chromatin structure and function. *Bioessays* 17:423-430.

Yoshida, M., M.Kijima, M.Akita, and T.Beppu. 1990. Potent and specific inhibition of mammalian histone deacetylase both in vivo and in vitro by trichostatin A. *J. Biol. Chem.* 265:17174-17179.

Zhang, C., H.Jenkins, M.W.Goldberg, T.D.Allen, and C.J.Hutchison. 1996. Nuclear lamina and nuclear matrix organization in sperm pronuclei assembled in Xenopus egg extract. *J. Cell Sci.*

Zhang, K., K.E.Williams, L.Huang, P.Yau, J.S.Siino, E.M.Bradbury, P.R.Jones, M.J.Minch, and A.L.Burlingame. 2002. Histone acetylation and deacetylation: identification of acetylation and methylation sites of HeLa histone H4 by mass spectrometry. *Mol. Cell Proteomics.* 1:500-508.

Zhang, Q., J.N.Skepper, F.Yang, J.D.Davies, L.Hegyi, R.G.Roberts, P.L.Weissberg, J.A.Ellis, and C.M.Shanahan. 2001a. Nesprins: a novel family of spectrin-repeat-containing proteins that localize to the nuclear membrane in multiple tissues. *J. Cell Sci.* 114:4485-4498.

Zhang, W.H., R.Srihari, R.N.Day, and F.Schaufele. 2001b. CCAAT/enhancer-binding protein alpha alters histone H3 acetylation at large subnuclear domains. *J. Biol. Chem.* 276:40373-40376.

Zhang, Y., G.LeRoy, H.P.Seelig, W.S.Lane, and D.Reinberg. 1998. The dermatomyositis-specific autoantigen Mi2 is a component of a complex containing histone deacetylase and nucleosome remodeling activities. *Cell* 95:279-289.

Zhang, Y. and D.Reinberg. 2001. Transcription regulation by histone methylation: interplay between different covalent modifications of the core histone tails. *Genes Dev.* 15:2343-2360.

Zheng, P., Y.Guo, Q.Niu, D.E.Levy, J.A.Dyck, S.Lu, L.A.Sheiman, and Y.Liu. 1998. Proto-oncogene PML controls genes devoted to MHC class I antigen presentation. *Nature* 396:373-376.

Zhong, X.P. and M.S.Krangel. 1997. An enhancer-blocking element between alpha and delta gene segments within the human T cell receptor alpha/delta locus. *Proc. Natl. Acad. Sci U. S. A* 94:5219-5224.

Zilberman, D., X.Cao, and S.E.Jacobsen. 2003. ARGONAUTE4 control of locus-specific siRNA accumulation and DNA and histone methylation. *Science* 299:716-719.

Zink, B. and R.Paro. 1989. In vivo binding pattern of a trans-regulator of homoeotic genes in Drosophila melanogaster. *Nature* 337:468-471.

Zink, D., T.Cremer, R.Saffrich, R.Fischer, M.F.Trendelenburg, W.Ansorge, and E.H.Stelzer. 1998. Structure and dynamics of human interphase chromosome territories in vivo. *Hum. Genet.* 102:241-251.

Zlatanova, J., S.H.Leuba, and K.van Holde. 1999. Chromatin structure revisited. *Crit Rev. Eukaryot. Gene Expr.* 9:245-255.

APPENDIX

COMPARISON OF STATISTICAL ANALYSES OF CHROMOSOME TERRITORY DISTRIBUTION DATA

In chapter 3, I described an analysis method that determines the relative nuclear position (geographical location) of a chromosome territory in 3:1 MAA fixed nuclei defined by chromosome paint FISH. For a series of fluorescent microscope images of individual nuclei (where n>48), the edge of the nucleus was defined (by segmentation of the DAPI signal). The total area of the nucleus in each image was then calculated and divided into 5 concentric shells of equal area (shell 1 includes the nuclear centre and the outer limit of shell 5 is the nuclear edge). Following this, the total pixel intensity of DAPI signal (DNA) and chromosome paint signal was calculated inside each shell. We then used the values obtained to generate a representative histogram demonstrating the relative amount of chromosome paint signal (intensity of chromosome paint/intensity of DNA) in each of the 5 nuclear shells.

This chromosome territory analysis was used to determine the nuclear location of several chromosome paints in primary human fibroblast cells (Figure 1.3). It appeared that the localisation patterns obtained were not identical for each chromosome and this suggested that chromosomes might be preferentially located in the nucleus. To test this hypothesis, I performed simple student *t*-tests on the numerical data generated by the analysis process. For each chromosome in turn, I compared the data set of 48 observations of the relative intensity values for chromosome paint signal in shell number 1, versus the 48 observations of signal intensity for shell number 5. Where the calculated *P* value was <0.05, a chromosome was said to be preferentially located in the nucleus e.g. peripheral chromosomes 13 and X enriched in shell number 1 or internal chromosomes 12, 16 and 21 enriched in shell number 5.

While it was necessary to determine if the observed nuclear localisation pattern was statistically significant for each chromosome in turn, it would also be interesting to compare the localisation of one chromosome compared to another. In this situation, a students *t*-test was used to test the hypothesis that chromosome 'a' was more peripheral or more internal than chromosome 'b'. 48 observations of relative intensity for each nuclear shell in turn (1-5) for chromosome 'a' were tested against the data set for the corresponding shell of

chromosome 'b' analysis (i.e. shell 1 data for 'a' versus shell 1 data for 'b' and so on). This analysis was used to compare the X chromosome territory locations between nuclei harvested from male and female primary fibroblasts. A *P*-value of 0.71 is calculated when the distribution of X paint signal in shell 1 is compared between male (one X chromosome) and female (two X chromosomes) nuclei.

I considered that the student *t*-test might not be a sufficiently robust statistical test to accurately determine if chromosome territories are indeed preferentially distributed. To further analyse the chromosome locations, an additional analysis step was applied to the calculated territory signal distributions for chromosomes 12, 13, 16 and 17, as described in chapter 3. Rather than using the chromosome signal intensity data set for 48 nuclei and comparing the values within each shell in turn, the 'mean shell number' was calculated for each of the 48 nuclei analysed. The mean shell number was calculated as follows:

Nuclear Shell	**Relative Chromosome Intensity**
1	a
2	b
3	c
4	d
5	e

$$\text{Mean Shell Number} = \frac{1*a + 2*b + 3*c + 4*d + 5*e}{a + b + c + d + e}$$

This formula was used to calculate a 'mean shell number' for each nucleus in the chromosome territory analysis data set (n=48 or more). The 'pooled' mean shell number (the mean value in a population of 48 observations) for each of the selected chromosome paint FISH experiments are detailed below.

Chromosome	Mean Shell Number
12	3.282
13	2.616
16	3.466
17	3.243

The distribution of the mean shell number values for a pair of chromosomes was compared by statistical analyses to test the hypothesis that two chromosome territories do not show the same nuclear location in FISH experiments. In this situation, the calculated mean shell numbers for 48 nuclei painted with chromosome 'a' paint were compared with the values for 48 nuclei probed with chromosome 'b' paint (a vs b) in both student *t*-tests (Minitab release 13.31) and the more robust two-sample Kolmogorov-Smirnov (K-S; using SPSS 11.0.1 for Windows) tests. The results of the direct comparisons are as follows:

Comparison	*P* Value (*t*-test)	*P* Value (K-S test)
12 vs 13	0.00022	<0.0005
12 vs 16	0.30	0.37
12 vs 17	0.83	0.85
13 vs 16	<0.00001	<0.0005
13 vs 17	0.0005	0.001
16 vs 17	0.21	0.10

From these direct comparisons it is clear that the two statistical tests give comparable results: a comparison that is found to be statistically significant (where $P < 0.05$) in a *t*-test is also significantly different in two-sample K-S test calculations. These analyses show that the chromosome localisation pattern for chromosome 13 is significantly different from that of chromosomes 12, 16 and 17. This analysis also shows that the calculated nuclear locations for chromosomes 12, 16 and 17 are not significantly different from one another. I therefore conclude that the chromosome territory analysis performed in this thesis is sufficiently accurate to determine if two chromosomes are similarly distributed in the interphase nucleus of cells when analysed by chromosome paint FISH.